

PB 299735

Report No. FRA/ORD-78-16

PREVENTION OF ROLLER BEARING-
INITIATED BURNOFFS IN RAILROAD
FREIGHT CAR JOURNALS

G.E. Allen
J.R. Lucas
F.H. Tomlinson

SKF Industries, Inc.
100 First Avenue
King of Prussia PA 19406



JANUARY 1979
FINAL REPORT

DOCUMENT IS AVAILABLE TO THE PUBLIC
THROUGH THE NATIONAL TECHNICAL
INFORMATION SERVICE, SPRINGFIELD,
VIRGINIA 22161

Prepared for
U.S. DEPARTMENT OF TRANSPORTATION
FEDERAL RAILROAD ADMINISTRATION
Office of Research and Development
Washington DC 20590

NOTICE

This document is disseminated under the sponsorship of the Department of Transportation in the interest of information exchange. The United States Government assumes no liability for its contents or use thereof.

NOTICE

The United States Government does not endorse products or manufacturers. Trade or manufacturers' names appear herein solely because they are considered essential to the object of this report.

1. Report No. FRA/ORD-78-16		2. Government Accession No.		3. Recipient's Catalog No. PB299735	
4. Title and Subtitle PREVENTION OF ROLLER BEARING-INITIATED BURNOFFS IN RAILROAD FREIGHT CAR JOURNALS				5. Report Date January 1979	
7. Author(s) G.E. Allen, J.R. Lucas, F.H. Tomlinson				6. Performing Organization Code	
9. Performing Organization Name and Address SKF Industries, Inc.* Technology Services Center 100 First Avenue King of Prussia PA 19406				8. Performing Organization Report No. DOT-TSC-FRA-79-5	
12. Sponsoring Agency Name and Address U.S. Department of Transportation Federal Railroad Administration Office of Research and Development Washington DC 20590				10. Work Unit No. (TRAIS) RR931/R9326	
				11. Contract or Grant No. DOT-TSC-935	
				13. Type of Report and Period Covered Final Report Dec. 75- Dec. 76	
				14. Sponsoring Agency Code	
15. Supplementary Notes *Under contract to: U.S. Department of Transportation Research and Special Programs Administration Transportation Systems Center Cambridge MA 02142					
16. Abstract The objective of this program was to determine the technical feasibility and cost effectiveness of constructing three separate devices for the prevention of catastrophic roller bearing-initiated, railroad journal failure. 1. Construction of a low cost axle cap bolt which would replace one of the three bolts in a standard bearing assembly, and which would contain a self-powered, maintenance free transmitter to signal a train crew in the event of roller bearing overtemperature, was proven feasible. This is technically and economically superior to current wayside temperature sensing devices, and has the capability of preventing burnoffs associated with bearing failure by any mechanism. 2. The prevention of bearing overlubrication by use of automated ultrasonic test methods was seen to be feasible. Use of such a device in a railroad repair track would prevent regreasing a freshly greased bearing and thereby save the costs of setouts and derailments caused by overlubrication. 3. The early detection of bearing component damage (spalling, brinelling, and particulate contamination) by use of "Shock Pulse Analysis" techniques was also seen to be feasible. Use of an automated device in a railroad wheel shop could save the costs of burnoffs associated with progressive damage, and also of investigative bearing teardown as a result of derailment.					
17. Key Words Railroad Roller Bearing, On-Board Hot Box Detector, Ultrasonic Overlubrication Prevention			18. Distribution Statement DOCUMENT IS AVAILABLE TO THE PUBLIC THROUGH THE NATIONAL TECHNICAL INFORMATION SERVICE, SPRINGFIELD, VIRGINIA 22161		
19. Security Classif. (of this report) Unclassified		20. Security Classif. (of this page) Unclassified		21. No. of Pages 275	22. Price PC A 12 MF A 01

PREFACE

The work reported here was done under Contract No. DOT-TSC-935 Phase II for the Transportation Systems Center (TSC). The present contract is a follow-on to Contract DOT-TSC-935 Phase I.

Phase I established the need for the development of diagnostic techniques aimed at minimizing the economic impact and life threatening effects of "burnoffs" (i.e., heat initiated seizures of railroad freight car journals) as caused by catastrophic failure of railroad journal roller bearings.

Phase II establishes the feasibility of producing an inexpensive, on-board "device" for the prevention of burnoffs and also of two separate maintenance-level devices for the prevention and/or early detection of some major causes of roller bearing-initiated burnoff.

We acknowledge the guidance and assistance provided by R. Ehrenbeck, the TSC Technical Monitor. We also wish to thank W.I. Thompson of TSC for his research into the heat transfer and thermoelectric analyses contained in Chapter 3.

G. Moyer, Vice President of Research and Development, Brenco Bearing Company is acknowledged for his assistance in obtaining in-service failure data for our performance of Task III of this contract.

Also acknowledged are numerous personnel of several major railroads for their guidance in failure mechanism identification, cost benefit identification, and evaluation of the adaptability of developmental systems to railroad maintenance routine.

We would also like to acknowledge the assistance of Robert Martin for his untiring efforts during the final preparations of this report.

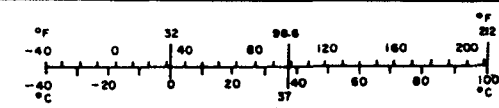
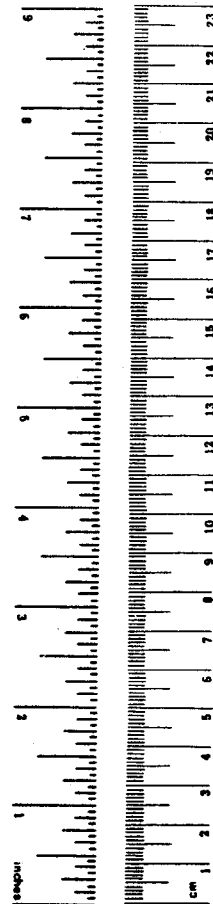
METRIC CONVERSION FACTORS

Approximate Conversions to Metric Measures

Symbol	When You Know	Multiply by	To Find	Symbol
LENGTH				
in	inches	2.5	centimeters	cm
ft	feet	30	centimeters	cm
yd	yards	0.9	meters	m
mi	miles	1.6	kilometers	km
AREA				
in ²	square inches	6.5	square centimeters	cm ²
ft ²	square feet	0.09	square meters	m ²
yd ²	square yards	0.8	square meters	m ²
mi ²	square miles	2.6	square kilometers	km ²
	acres	0.4	hectares	ha
MASS (weight)				
oz	ounces	28	grams	g
lb	pounds	0.45	kilograms	kg
	short tons (2000 lb)	0.9	tonnes	t
VOLUME				
tsp	teaspoons	5	milliliters	ml
Tbsp	tablespoons	15	milliliters	ml
fl oz	fluid ounces	30	milliliters	ml
c	cup	0.24	liters	l
pt	pint	0.47	liters	l
qt	quart	0.95	liters	l
gal	gallon	3.8	liters	l
ft ³	cubic feet	0.03	cubic meters	m ³
yd ³	cubic yards	0.76	cubic meters	m ³
TEMPERATURE (exact)				
°F	Fahrenheit temperature	5/9 (after subtracting 32)	Celsius temperature	°C

Approximate Conversions from Metric Measures

Symbol	When You Know	Multiply by	To Find	Symbol
LENGTH				
mm	millimeters	0.04	inches	in
cm	centimeters	0.4	inches	in
m	meters	3.3	feet	ft
km	kilometers	1.1	yards	yd
		0.6	miles	mi
AREA				
cm ²	square centimeters	0.16	square inches	in ²
m ²	square meters	1.2	square yards	yd ²
km ²	square kilometers	0.4	square miles	mi ²
ha	hectares (10,000 m ²)	2.6	acres	
MASS (weight)				
g	grams	0.035	ounces	oz
kg	kilograms	2.2	pounds	lb
t	tonnes (1000 kg)	1.1	short tons	
VOLUME				
ml	milliliters	0.03	fluid ounces	fl oz
l	liters	2.1	pints	pt
l	liters	1.06	quarts	qt
l	liters	0.26	gallons	gal
m ³	cubic meters	36	cubic feet	ft ³
m ³	cubic meters	1.3	cubic yards	yd ³
TEMPERATURE (exact)				
°C	Celsius temperature	9/5 (then add 32)	Fahrenheit temperature	°F



CONTENTS

<u>Section</u>	<u>Page</u>
1. Introduction	1-1
2. Summary	2-1
3. Task I - Burnoff Prevention Using On-Board Transmitter Bolts	3-1
3.1 Summary	3-1
3.2 Introduction	3-10
3.3 Radio Frequency Transmitter Specification	3-14
3.3.1 Breadboard Transmitter Design	3-14
3.3.2 Breadboard Transmitter Test	3-22
3.3.2.1 Test Equipment and Data Format	3-22
3.3.2.2 Test Data	3-24
3.3.3 Conclusions and Final Transmitter Specifications	3-48
3.4 Thermoelectric Power Source Specification	3-50
3.4.1 Maximum Power Source Operating Temperature	3-51
3.4.2 Determination of Package Size (Volume) Consequential Mechanical Derating of Hollowed Bolt	3-51
3.4.3 Thermal Analysis of Thermoelectric Power Source	3-57
3.4.3.1 Heat Flow Across Thermopile	3-57
3.4.3.2 Heat Exchanger Design	3-58
3.4.4 Laboratory Test of Candidate Thermopile	3-67
3.5 Selection of Temperature and Strain Sensors and Threshold Circuitry	3-70
3.5.1 Temperature Sensor Specifications	3-70
3.5.2 Gage Amplifier and Threshold Circuitry	3-70

CONTENTS (CONT.)

<u>Section</u>	<u>Page</u>
3.5.3 Strain Sensor Selection and Test	3-74
Strain Sensor Test	3-76
3.6 Conclusions	3-83
3.7 Battery Powered Transmitter Bolt - Low Cost Alternative	3-85
3.8 Recommendations	3-89
4. Task II - Bearing Overlubrication Prevention by Ultrasonic Testing	4-1
4.1 Summary	4-1
4.2 Introduction	4-3
4.3 Test Equipment	4-6
4.3.1 Ultrasonic Test Equipment	4-6
4.3.1.1 Background	4-6
4.3.1.2 Test Method	4-6
4.3.1.3 Specific Test Apparatus	4-8
4.3.2 Bearing Test Machine	4-12
4.4 Test Program	4-15
4.4.1 Static Grease Thickness Detectability Tests	4-15
4.4.1.1 Operating Frequency and Echo Selection	4-15
4.4.1.2 Data Presentation	4-16
4.4.1.3 Grease Measurement in Railroad Roller Bearing Seals	4-16
4.4.2 Grease Migration Study	4-21
4.4.2.1 Test Format	4-21
4.4.2.2 Test Results	4-23
4.4.2.2.1 Test I-Normally Greased Bearing Study	4-23

CONTENTS (CONT.)

<u>Section</u>	<u>Page</u>
4.4.2.2.2 Test II-Overgreased Bearing Study	4-35
4.4.2.2.3 Test III-Twice Overgreased Bearing Study	4-35
4.5 Conclusions	4-54
4.6 Recommendations	4-56
5. Task III - Bearing Component Damage Detection by "Shock Pulse" Method	5-1
5.1 Summary	5-1
5.2 Introduction	5-3
5.3 Test Equipment	5-4
5.3.1 Electronic Analysis System	5-4
5.3.2 Bearing Test Machine	5-8
5.3.3 Test Bearings	5-9
5.4 Test Program	5-12
5.5 Test Results	5-14
5.5.1 Test 1 - Baseline Tests	5-14
5.5.2 Test 2 - Inner Ring Spalling	5-14
5.5.3 Test 3 - Roller Spalling	5-21
5.5.4 Test 4 - Outer Ring Spalling	5-21
5.5.5 Test 5 - Brinelling	5-29
5.5.6 Test 6 - Grease Contamination	5-34
5.6 Conclusions	5-38
5.7 Recommendations	5-43
6. Conclusions	6-1
7. Recommendations	7-1
8. References and Bibliography	8-1
Appendix A - Test Plan for On-Board Thermally Powered Transmitter	A-1
Appendix B - Test Plan for Ultrasonic Overlubrication Detector Test Program	B-1
Appendix C - Shock Pulse Meter Instrumentation	C-1

CONTENTS (CONT.)

<u>Section</u>	<u>Page</u>
Appendix D - Test Plan For Shock Pulse Bearing Detection Program	D-1
Appendix E - Glossary	E-1
Appendix F - Report of New Technology	F-1

ILLUSTRATIONS

<u>Figure No.</u>		<u>Page</u>
2-1	Early Concept of Temperature and Strain Sensing Transmitter Bolt	2-2
3-1	Transmitter Bolt Development and Evaluation Program	3-3
3-2	Transmitter Bolt Development and Evaluation Schedule	3-6
3-3	Modified Transmitter Bolt Development and Evaluation Program	3-7
3-4	Modified (Temperature Sensing Only) Transmitter Bolt Development and Evaluation Schedule	3-9
3-5	Temperature and Strain Sensing Transmitter Bolt	3-12
3-6	Breadboard Transmitter Test Circuit	3-15
3-7	Photograph of Breadboard Transmitter Test Circuit	3-16
3-8	AC Equivalent Circuit for Breadboard Transmitter	3-18
3-9	Hybrid - PI Equivalent Circuits for Breadboard Transmitter	3-19
3-10	Transmitter vs. Receiver Antenna Orientations for Field Intensity Data Acquisition	3-25
3-11	Transmitter Test Fixture	3-26
3-12	Transmitter Test Fixture Subassembly for Antenna Encapsulation	3-27

ILLUSTRATIONS (CONT.)

<u>Figure No.</u>		<u>Page</u>
3-13	Field Strength vs. Antenna Orientation for a Modulated, Battery Powered, Horizontally Polarized Breadboard Transmitter at a Distance of 30 Feet	3-31
3-14	Field Strength vs. Antenna Orientation for a Modulated, Battery Powered, Horizontally Polarized, Breadboard Transmitter at a Distance of 1/4 Mile	3-32
3-15	Field Strength vs. Antenna Orientation for a Modulated, Battery Powered, Horizontally Polarized Breadboard Transmitter at a Distance of 1/2 Mile	3-33
3-16	Field Strength vs. Antenna Orientation for a Modulated, Battery Powered, Horizontally Polarized, Breadboard Transmitter with Wheel Simulator at a Distance of 30 Feet	3-35
3-17	Field Strength vs. Antenna Orientation for a Modulated, Battery Powered, Horizontally Polarized, Breadboard Transmitter with Wheel Simulator at a Distance of 1/4 Mile	3-36
3-18	Field Strength vs. Antenna Orientation for a Modulated, Battery Powered, Horizontally Polarized, Breadboard Transmitter with Wheel Simulator at a Distance of 1/2 Mile	3-37
3-19	Field Strength vs. Antenna Orientation for a Modulated, Battery Powered, Horizontally Polarized, Breadboard Transmitter Encapsulated in Wheel Simulator at a Distance of 30 Feet	3-39

ILLUSTRATIONS (CONT.)

<u>Figure No.</u>		<u>Page</u>
3-20	Field Strength vs. Antenna Orientation for a Modulated, Battery Powered, Horizontally Polarized, Breadboard Transmitter Encapsulated in a Wheel Simulator at a Distance of 1/4 Mile	3-40
3-21	Field Strength vs. Antenna Orientation for a Modulated, Battery Powered, Horizontally Polarized, Breadboard Transmitter Encapsulated in Wheel Simulator at a Distance of 1/2 Mile	3-41
3-22	Field Strength vs. Antenna Orientation for a Modulated, Battery Powered, Horizontally Polarized, Breadboard Transmitter Encapsulated in a Hooded Wheel Simulator at a Distance of 30 Feet	3-43
3-23	Field Strength vs. Antenna Orientation for a Modulated, Battery Powered, Horizontally Polarized, Breadboard Transmitter Encapsulated in a Hooded Wheel Simulator at a Distance of 1/4 Mile	3-44
3-24	Field Strength vs. Antenna Orientation for a Modulated, Battery Powered, Horizontally Polarized, Breadboard Transmitter Encapsulated in a Hooded Wheel Simulator at a Distance of 1/2 Mile	3-45
3-25	"GO" - "NO GO" Verification of Transmitted Signal at a Distance of 30 Feet, 1/4 Mile, and 1/2 Mile for Modulated, Horizontally Polarized, Thermally and Battery Powered, Prototype Breadboard Transmitter	3-46
3-26	Temperature Profile of Journal and Cap Screws	3-52

ILLUSTRATIONS (CONT.)

<u>Figure No.</u>		<u>Page</u>
3-27	Thermocouple Locations During Static Tests to Determine Temperature Profile of Standard Railroad Journal and Cap Screws	3-53
3-28	Packaging Proposal for Thermoelectric Power Source of Temperature/Strain Sensing Transmitter Bolt	3-56
3-29	Thermal Model of Proposed Thermopile and Heat Exchanger Assembly	3-59
3-30	Convection Cooler Subassembly	3-60
3-31	Efficiencies of Circumferential Fins of Rectangular Profile	3-62
3-32	Laboratory Test Fixture for Determination Of Internal Resistance of Off-the-Shelf Thermopile Assemblies	3-63
3-33	Gage Amplifier and Threshold Circuit	3-72
3-34	Tabulation of Specifications for a Commercially Available Full Bridge, Metal Foil, 350 SL Strain Gage	3-75
3-35	Torque-Strain Characteristics of a 1 in.-8 Bolt with 17/32 in. Axle Hole	3-78
3-36	Torque-Strain Characteristics of a 1 in.-8 Bolt Having a 5/32 in. Diameter Axial Hole	3-80
3-37	Modified (Temperature Sensing Only) Transmitter Bolt	3-86

ILLUSTRATIONS (CONT.)

<u>Figure No.</u>		<u>Page</u>
4-1	Ultrasonic Method of Grease Detection	4-7
4-2	Ultrasonic Flaw/Thickness Tester	4-10
4-3	Ultrasonic Test Transducers	4-11
4-4	Ultrasonic Transducer Holder	4-13
4-5	Railroad Bearing Test Machine	4-14
4-6	Echo Amplitude Signals from Railroad Bearing Seal Shroud	4-17
4-7	Polar Plot of Grease Distribution in a Seal Shroud; Measured Thickness vs. Ultrasonic Echo Amplitude	4-18
4-8	Grease Thickness Determination by Ultrasonic Echo Amplitude Measurement	4-20
4-9	Typical Grease Distribution in Seals	4-22
4-10	Identification of Bearing Components and Transducer Locations for Ultrasonic Grease Detection	4-25
4-11	Seals of Bearing 063103 with Normal Grease Charge	4-26
4-12	Seals of Bearing 063104 with Normal Grease Charge	4-27
4-13	Echo Amplitudes - Outboard Seal, Bearing 063103 - Normal Grease Charge	4-29
4-14	Echo Amplitudes - Inboard Seal, Bearing 063103 - Normal Grease Charge	4-30
4-15	Echo Amplitudes - Outboard Seal, Bearing 063104 - Normal Grease Charge	4-31
4-16	Echo Amplitudes - Inboard Seal, Bearing 063104 - Normal Grease Charge	4-32
4-17	Echo Amplitudes - Outer Ring, Bearing 063103 - Normal Grease Charge	4-33

ILLUSTRATIONS (CONT.)

<u>Figure No.</u>		<u>Page</u>
4-18	Echo Amplitudes - Outer Ring, Bearing 063104 - Normal Grease Charge	4-34
4-19	Seals of Bearing 063103 with 8 Ounce Grease Recharge	4-36
4-20	Seals of Bearing 063104 with 8 Ounce Grease Recharge	4-37
4-21	Echo Amplitudes - Outboard Seal, Bearing 063103 - 8 Ounce Grease Recharge	4-38
4-22	Echo Amplitudes - Inboard Seal, Bearing 063103 - 8 Ounce Grease Recharge	4-39
4-23	Echo Amplitudes - Outboard Seal, Bearing 063103 - 8 Ounce Grease Recharge	4-40
4-24	Echo Amplitudes - Inboard Seal, Bearing 063103 - 8 Ounce Grease Recharge	4-41
4-25	Echo Amplitudes - Outer Ring, Bearing 063103 - 8 Ounce Grease Recharge	4-42
4-26	Echo Amplitudes - Outer Ring, Bearing 063104 - 8 Ounce Grease Recharge	4-43
4-27	Seals of Bearing 063103 with Additional 8 Ounce Grease Recharge	4-44
4-28	Seals of Bearing 063104 with Additional 8 Ounce Grease Recharge.	4-45
4-29	Echo Amplitudes - Outbound Seal, Bearing 063103 - Additional 8 Ounce Grease Recharge	4-46

ILLUSTRATIONS (CONT.)

<u>Figure No.</u>		<u>Page</u>
4-30	Echo Amplitudes - Inboard Seal, Bearing 063103 - Additional 8 Ounce Grease Recharge	4-47
4-31	Echo Amplitudes - Outboard Seal, Bearing 063104 - Additional 8 Ounce Grease Recharge	4-48
4-32	Echo Amplitudes - Inboard Seal, Bearing 063104 - Additional 8 Ounce Grease Recharge	4-49
4-33	Echo Amplitudes - Outer Ring, Bearing 063103- Additional 8 Ounce Grease Recharge	4-51
4-34	Echo Amplitudes - Outer Ring, Bearing 063104 - Additional 8 Ounce Grease Recharge	4-52
4-35	Proposed Ultrasonic Bearing Lubrication Detector	4-57
4-36	Typical Circumferential Grease Distribution in Outboard Seals	4-58
4-37	Proposed Ultrasonic Lubrication Detector Evaluation Program	4-59
4-38	Proposed Ultrasonic Lubrication Detector Program Schedule	4-60
5-1	Shock Pulse Meter	5-5
5-2	Typical Shock Emission Profiles	5-7
5-3	Modified Railroad Bearing Test Machine	5-10
5-4	Shock Emission Profiles - Baseline Test New 6 in. x 11 in. Tapered Railroad Bearing	5-17
5-5	Shock Emission Profiles - Spalled Inner Rings	5-20
5-6	Lightly Spalled Rollers	5-22
5-7	Shock Emission Profiles - Spalled Rollers	5-24

ILLUSTRATIONS (CONT.)

<u>Figure No.</u>		<u>Page</u>
5-8	Typical Spalled Outer Rings	5-25
5-9	Shock Emission Profiles - Spalled Outer Rings	5-28
5-10	Typical Brinelled Outer Rings	5-30
5-11	Shock Emission Profiles - Brinelled Bearings	5-33
5-12	Shock Emission Profiles - Particulate Contaminant Added	5-37
5-13	Comparison of Shock Emission Profiles of New Bearings vs. Bearings Having Spalled Inner Rings	5-39
5-14	Comparison of Shock Emission Profiles of New Bearings vs. a Bearing Having Spalled Rollers	5-40
5-15	Comparison of Shock Emission Profiles of New Bearings vs. Bearing Having Spalled Outer Rings	5-41
5-16	Comparison of Shock Emission Profiles of New Bearings vs. Brinelled Bearings	5-42
5-17	Proposed Railroad Bearing Shock Emission Analyzer	5-44
5-18	Proposed Railroad Bearing Shock Emission Analyzer Evaluation Program	5-45
5-19	Proposed Railroad Bearing Shock Emission Analyzer Program Schedule	5-47
A-1	Test Plan Schedule	A-3
B-1	Ultrasonic Grease Sensor Detector Locations	B-3
B-2	Ultrasonic Transducer Holder	B-4
C-1	Shock Pulse Generation	C-2
C-2	Shock Emission Profile	C-5
C-3	Shock Pulse Meter Signal Processing Flow	C-8
C-4	Shock Emission Profile Curve Types	C-11

ILLUSTRATIONS (CONT.)

<u>Figure No.</u>		<u>Page</u>
C-5	Tape Roller Bearing Shock Pulse Measurement	C-13
C-6	Shock Level Monitor of Growth of Damaged Area	C-15
C-7	Shock Pulse Meter Ability to Distinguish Shock Emissions of Adjacent Bearings	C-16
C-8	Bearing Condition Indication by Shock Emission as Compared with Vibration	C-18

LIST OF TABLES

<u>Table</u>		<u>Page</u>
1-1	Problem Identification - Results of Phase I Catastrophic Failure Causes in Railroad Roller Bearings	1-3
3-1	Test Program Matrix for Transmitter Broadcast Capabilities	3-23
3-2	Modulated vs. Unmodulated Field Strength Data at 30 Feet	3-28
3-3	Calculated and Observed Field Strength Values	3-29
3-4	Measured Voltage and Electric Field Strength Data as a Function of Antenna Orientation for a Modulated, Battery Powered, Horizontally Polarized Breadboard Transmitter at Distances of 30 Feet, 1/4 Mile and 1/2 Mile	3-30
3-5	Measured Voltage and Electric Field Strength Data as a Function of Antenna Orientation for a Modulated, Battery Powered, Horizontally Polarized, Breadboard Transmitter with Wheel Simulator at Distances of 30 Feet, 1/4 Mile and 1/2 Mile	3-34
3-6	Measured Voltage and Electric Field Strength Data as a Function of Antenna Orientation for a Modulated, Battery Powered, Horizontally Polarized Breadboard Transmitter Encapsulated in Wheel Simulator at Distances of 30 feet, 1/4 Mile, and 1/2 Mile	3-38
3-7	Measured Voltage and Electric Field Strength Data as a Function of Antenna Orientation for a Modulated, Battery Powered, Horizontally Polarized, Breadboard Transmitter Encapsulated in a Hooded Wheel Simulator at Distances of 30 Feet, 1/4 Mile and 1/2 Mile	3-42
3-8	Reynolds Number Tabulation	3-65

LIST OF TABLES

<u>Table</u>		<u>Page</u>
3-9	Tabulation of Test Data for Calculation of Average Internal Resistance of Off-the-Shelf Thermopile Assemblies	3-68
3-10	Tabulation of Resistance Ratio vs. Temperature for a Commercially Available Resistance Thermometer	3-71
3-11A	Tabulation of Torque vs. Base Output Using Commercially Available Strain Gages Attached to Modified Railroad Bearing Axle Cap Bolts (TEST #1)	3-77
3-11B	Tabulation of Torque vs. Base Output Using Commercially Available Strain Gages Attached to Modified Railroad Bearing Axle Cap Bolts (TEST #2)	3-78
3-12	Relative Manufacturing Costs of "Temperature/Strain" and "Temperature Only" Transmitter Bolts	3-88
4-1	Data Reference for Grease Migration Study	4-24
4-2	Tabulation of Bearing Operating Temperatures and Visual Observations of Grease Migration Study	4-53
5-1A	Shock Pulse Data - Baseline Test - 20 MPH New 6 in. x 11 in. Tapered Railroad Bearings	5-15
5-1B	Shock Pulse Data - Baseline Test - 10 MPH New 6 in. x 11 in. Tapered Railroad Bearings	5-16
5-2A	Shock Pulse Data - Moderately Spalled Inner Ring - Bearing 063201	5-18
5-2B	Shock Pulse Data - Heavily Spalled Inner Ring - Bearing 063202	5-19
5-3	Shock Pulse Data - Lightly Spalled Rollers - Bearing 063301	5-23
5-4A	Shock Pulse Data - Moderately Spalled Outer Ring - Bearing 063401	5-26

LIST OF TABLES (CONT'D)

<u>Table</u>		<u>Page</u>
5-4B	Shock Pulse Data - Heavily Spalled Outer Ring - Bearing 063402	5-27
5-5A	Shock Pulse Data - Moderately Brinelled Bearing - Bearing 063502	5-31
5-5B	Shock Pulse Data - Heavily Brinelled Bearing - Bearing 063501	5-32
5-6A	Shock Pulse Data - Particulate Contaminant Added to One Bearing Cone Assembly - Bearing 063101	5-35
5-6B	Shock Pulse Data - Particulate Contaminant Added to Both Bearing Cone Assemblies - Bearing 063102	5-36
A-1	Program One Test Matrix	A-2
B-1	Ultrasonic Overlubrication Detector Test Program	B-7
D-1	Shock Pulse Damage Detection Test Program	D-5

LIST OF ABBREVIATIONS AND SYMBOLS

A	- tensile strength area (sq in.); amperes; cross-sectional area (sq in.)
A_H	- area of hole (sq in)
A_M	- fin area
A_T	- tensile strength area (sq in.)
AAR	- Association of American Railroads
ac	- alternating current
AGC	- automatic gain control
AISI	- American Iron and Steel Institute
ant	- antenna
ARO	- after receipt of order
B	- base connection terminal
brg	- bearing
BTU	- British thermal unit
C	- collector connection terminal
c	- speed of light (meters/sec)
$C_{b,c}$	- base-to-collector capacitance (farads)
$C_{b,e}$	- base-to-emitter capacitance (farads)
C_f	- feedback capacitance (farads)
C_N	- capacitance ($N = 1, 2, 3...$)
CRT	- cathode ray tube
C_x	- capacitance of tapered line section (farads)
D	- nominal bolt diameter (in.); variable capacitance diode
d	- tube diameter
dB	- decibels
dc	- direct current
dia	- diameter

LIST OF ABBREVIATIONS AND SYMBOLS (CONT)

ds	- strain
E	- modulus of elasticity tension (psi); emitter connecting terminal
E_m	- electric field strength
E_{mod}	- input terminal
E_o	- output voltage
F_a	- axial load
F_r	- radial load
freq	- frequency
ft	- feet
g	- heat transfer (BTU/hr)
g_m	transconductance of transistor
gnd	- ground
h	- heat transfer coefficient (Btu/hr-ft- ^o F)
HORZ	- horizontal
hp	- heat pipe
hr	- hour
ht	- heat
i_{ant}	- ac antenna current (amperes)
i_c	- collector current (amperes)
i_e	- ac emitter current (amperes)
i_{EQ}	- i equivalent
i_{in}	- input current (amperes)
i_{out}	- output current
i_l	- output current (amperes)
in.	- inches

LIST OF ABBREVIATIONS AND SYMBOLS (CONT)

j	-	$\sqrt{-1}$
K	-	thermal conductivity (Btu/hr-ft-°F); one thousand ohms
K _A	-	thermal conductivity of air
K _f	-	thermal conductivity of each element (BTU/in.-hr °F)
K _{TF}	-	torque friction coefficient
kHz	-	one thousand hertz
L	-	length of each element in thermocouple (in.); inductance; loop of transistor head
L _{ant}	-	equivalent antenna length (radians)
L _C	-	inductance of coil (henrys)
lb	-	pound
m	-	meter
mA	-	one thousandth of an ampere
mi	-	miles
MHz	-	one million hertz
mph	-	miles per hour
mV	-	millivolt
mW	-	milliwatt
N	-	index number; number of thermocouples
no.	-	number
OD	-	outside diameter
OUT	-	output connection terminal
oz	-	ounce
P	-	bolt clamping load development by tightening (lb)
PC	-	printed circuit

LIST OF ABBREVIATIONS AND SYMBOLS (CONT)

P_{in}	-	input power
P_o	-	power output (watts)
P_T	-	tension strength (lb)
pF	-	pico farad
P - P	-	peak to peak
psi	-	pounds per square inch
pt	-	point
PWR	-	power
q	-	heat transfer rate (Btu/hr)
q_{actual}	-	actual heat loss
q_{hp}	-	thermal capacity heat pipe
q_{max}	-	maximum heat loss
QZ	-	power length product
r	-	distance (meters)
$R_{b'e/\beta}$	-	base emitter resistance
R_d	-	resistance
R_{in}	-	input resistance
R_L	-	resistor
R_N	-	resistor (N = 1,2,3...)
R_o	-	resistance
R_r	-	antenna radiation resistance (ohms)
R_S	-	electrical resistance proportional to strain; discreet resistor
R_T	-	electrical resistance proportional to temperature
r_1	-	tube surface radius (ft)
R_2	-	resistor; fin surface radius

LIST OF ABBREVIATIONS AND SYMBOLS (CONT)

R_{δ}	-	various resistances
Re	-	Reynolds number
RF	-	radio frequency
RFC	-	radio frequency choke
Rg	-	resistance thermometer
RMS	-	root mean square
RPM	-	revolutions per minute
RS	-	resistor
SAE	-	Society of Automotive Engineers
sec	-	seconds
sq	-	square
T	-	tightening torque (lb-in.)
t	-	fin thickness
T_A	-	temperature of air
T_C	-	cold side temperature
T_H	-	hot side temperature
T_T	-	tensile strength (psi)
TTL	-	transistor - transistor logic
V	-	volts
ν	-	kinematic viscosity of air (ft ² /sec)
V_A	-	velocity of air (ft/sec)
V_{cb}	-	collector to base voltage
V_{cc}	-	supply voltage
V_f	-	feedback voltage; emitter to base ac voltage
V_{oc}	-	open circuit voltage
V_{out}	-	output voltage
V/m	-	volts/meter

LIST OF ABBREVIATIONS AND SYMBOLS (CONT)

W	- watt
W_R	- upper cutoff frequency of transistor
W_T	- transconductance of transmitter
X_A	- dummy reactance variable
$X_{(ant)}$	- antenna reactance at 450 MHz (ohms)
$X_{b'c}$	- base-to-collector capacitive reactance at 450 MHz (ohms)
$X_{b'e}$	- base-to-collector capacitive reactance at 450 MHz (ohms)
X_f	- feedback capacitive reactance at 450 MHz (ohms)
X_1	- circuit board
yr	- year
Z	- electrical impedance (ohms)
$Z_{(ant)}$	- antenna impedance (ohms)

GREEK LETTERS

α	- voltage amplification factor, common base circuit
β	- voltage amplification factor, common emitter circuit
δ	- index number (0,1,2,3...)
Δ	- elongation of bolt (in)
ΔT	- difference in temperature ($^{\circ}F$)
η	- fin efficiency (%)
μ_o	- permeability of transmission medium
μin	- micro inch
μV	- microvolt
Ω	- ohms

1. INTRODUCTION

SKF Industries, Inc., under the sponsorship of the U.S. Department of Transportation, has developed techniques which, if translated to maintenance-level hardware, could provide solutions for the following major problems associated with freight car roller bearings:

1. Costly and life-threatening derailments caused by journal burnoffs associated with catastrophic roller bearing failure.
2. Hot box setouts caused by inadvertent overlubrication.
3. Excessive inspection costs associated with investigative bearing teardown after derailment.

The importance and urgency of developing techniques, in order to prevent thermal destruction of bearings (burnoffs) and subsequent train derailments caused by catastrophic journal roller bearing failure, was established in Phase I of Contract DOT-TSC-935. Roller bearing-initiated burnoffs currently cost North American railroads approximately \$12 million/yr.

Two factors make the elimination of roller bearing-initiated derailments imperative:

1. The frequency (and annual cost) of such derailments is certain to rise as the freight car fleet is continuously converted from plain to roller bearings and as a greater number of "older" roller bearings approach fatigue. (Conversion to roller journal bearings was started in the late 1950's and will continue until completion in the 1980's; about half of the 2 million car fleet is now converted.)
2. The potential of dangerous cargo derailments in a populated area is a constant threat to increase the annual costs of derailments far beyond the \$12 million average experience to date.

Results of the "Problem Identification" task of Phase I are compiled in Table 1-1. Identifiable railroad roller bearing failure causes, and their average annual costs are listed in decreasing order of importance.

As a result of Phase I, three separate diagnostic tools were proposed by SKF as candidates for development as derailment prevention devices. Contract DOT-TSC-935 Phase II was awarded to determine the feasibility of developing the devices listed below:

Task I - A "Transmitter Bolt" which, when substituted for a standard axle cap bolt, would sense excessive bearing operating temperature (or loss of bolt tension) and signal the train crew in time to prevent derailment. Since all types of bearing failures ultimately result in excessive operating temperature, the temperature sensing function of this device would prevent catastrophic failure by any failure mechanism. The tension sensing function would detect loosening of the bearing assembly, as evidenced by reduced tension on the axle cap bolt, and thereby act as an early warning device for failures of this type.

Task II - An "Ultrasonic Overlubrication Detector" which, when used at a Railroad Repair Track, would prevent overgreasing, a condition considered by many to be a major cause of catastrophic failure and known to be a major cause of costly hot box setout.

Task III - A "Shock Emission Analyzer" which, when used in a Railroad Wheel Shop, would detect physical damage (such as spalling or brinelling) without bearing disassembly.

TABLE 1-1. PROBLEM IDENTIFICATION - RESULTS OF PHASE I
CATASTROPHIC FAILURE CAUSES IN RAILROAD ROLLER BEARINGS

Generalized Sequence of Failure						
Failure Cause	% Failure Attributable to this cause	Derailment Cost Savings (Millions of Dollars/Yr.)	Manufacturing or Maintenance Defect	Service Initiated Defect	Early Symptom of Defect	Catastrophic Failure (Burn-off)
Loose Inner Rings	27	3.24	*	*	I	I
Overlubrication	21	2.52	II			I
Loose Seals (lubricant Contamination)	14	1.68		*	III	I
Worn or Misplaced Adaptor	15	1.8	*	*		I
Loose Axle Cap Bolts	7	.84	*		I	I
Spalling/Brinelling	5	.6	*	*	III	I
Miscellaneous	11	1.52	*	*		I

*The feasibility of developing techniques to detect or prevent catastrophic failure from the above causes has been demonstrated by SKF Industries, Inc.

*Three separate techniques will obviate these failure modes.

*The Ultrasonic Overlubrication Detector will prevent overgreasing. (II)

*The Shock Emission Analyzer will detect spalling, brinelling, particulate contaminant and other physical bearing damage (III)

*Loose inners and loose bolts can be detected before causing substantial thermal excursions by the strain sensing function of the "Transmitter Bolt". (I)

*Since all failure modes ultimately cause overheating, all can be detected at that stage by the "Transmitter Bolt". (I)

2. SUMMARY

A summary of activity performed to demonstrate the feasibility of each of the three techniques follows. (Details of the development of each technique are presented in Sections 3, 4, and 5, each of which includes excisable, self-contained reports relative to their specific topics.)

A. Imminent Catastrophic Failure Detection by Implantation of a Miniaturized Transmitter in an Axle Cap Bolt.

Task I of Contract DOT-TSC-935 Phase II consisted of tests and analyses to determine the feasibility of implanting (in one of the three standard axle cap bolts) a self-powered transmitter, capable of sensing bearing overheating and bolt loosening.

Tests and analyses concluded that implantation of a temperature and strain sensing bolt is feasible but not clearly cost effective. As a result, a modified battery-operated bolt, which would sense temperature only, has been recommended for further development and test.

An early conceptualization of the Transmitter Bolt (Figure 2-1) was presented to several major railroads and attained unanimous approval as having technical superiority (relative to currently used devices), enormous cost and life saving potential, and adaptability to railroad operational environments and procedures.

A schedule and work plan for development of both "temperature sensing only" and "temperature/strain sensing" bolts are presented in the body of this report. Further development of the temperature sensing transmitter bolt is strongly recommended.

2-2

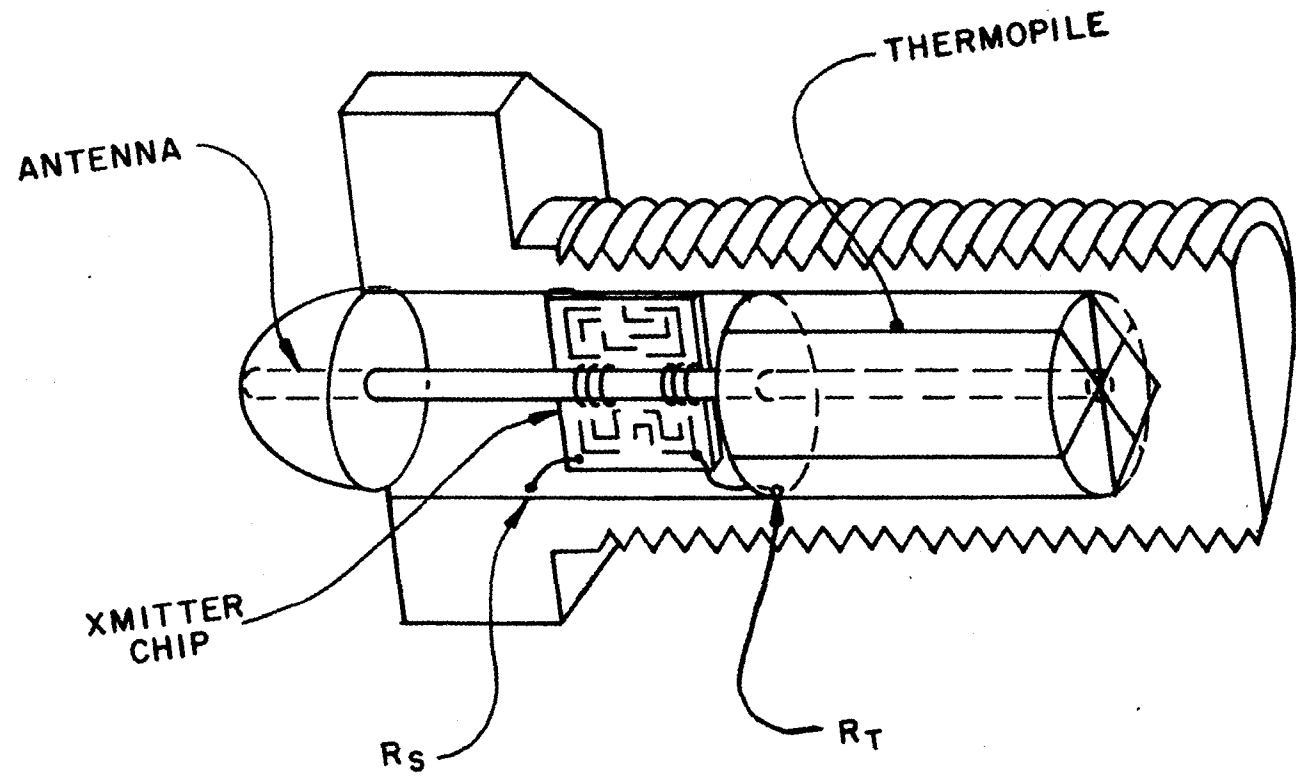


FIGURE 2-1. EARLY CONCEPT OF TEMPERATURE AND STRAIN SENSING TRANSMITTER BOLT

B. Overlubrication Prevention by Ultrasonic Test Methods

Task II of Contract DOT-TSC-935 Phase II consisted of tests to demonstrate the feasibility of detecting the presence of lubricating grease through the outboard seal of a railroad journal roller bearing, and to show that such detection is useful in determining the greasing history of a bearing. Determination of greasing history in a railroad repair track would prevent regreasing a freshly greased bearing and thus eliminate overgreasing at its source.

Tests performed demonstrated the feasibility of such grease detection. The equipment and techniques used, however, were not intended for railroad maintenance-level operation and for that reason, an automated system was conceptualized and proposed to several major railroads. They unanimously agreed that the proposed system would eliminate a major problem, save the substantial costs of overgreasing-initiated catastrophic failure and hot box setouts, and be adaptable to Railroad Repair Track maintenance environments.

A schedule and work plan for evaluation and test of such a device is presented in the body of this report. Because of the substantial cost and lifesaving potential of this device, follow-up work on this task is strongly urged.

C. Bearing Component Damage Determination by Shock Pulse Analysis Techniques

The shock pulse analysis task of contract DOT TSC-935 Phase II consisted of tests to determine the feasibility of detecting bearing component damage such as spalling, brinelling, grease contamination, etc.

The capability of a commercially available analog instrument to detect brinelling, spalling, and contaminated lubricant was investigated.

Bearings having known defects were investigated. These bearings, which were run at two speeds under relatively light load, were used to acquire "shock pulse" data. Data acquired were plotted to obtain "shock pulse profiles." These profiles, when compared to those produced from data obtained from running new bearings, demonstrated the feasibility of detecting the various defects by Shock Pulse Analysis methods.

More specifically, the results of Shock Pulse Analysis testing are as follows:

1. Spalling on inner rings, rollers, and outer rings is readily detectable. The Shock Pulse Meter could be used to eliminate disassembly and visual inspection for spalling damage.
2. Brinelling on inner rings and outer rings is readily detectable. The Shock Pulse Meter could be used to eliminate disassembly and visual inspection for brinelling damage as caused by derailment.
3. Particulate contamination is readily detectable. The Shock Pulse Meter could be used to eliminate disassembly and visual examination for particulate contamination.

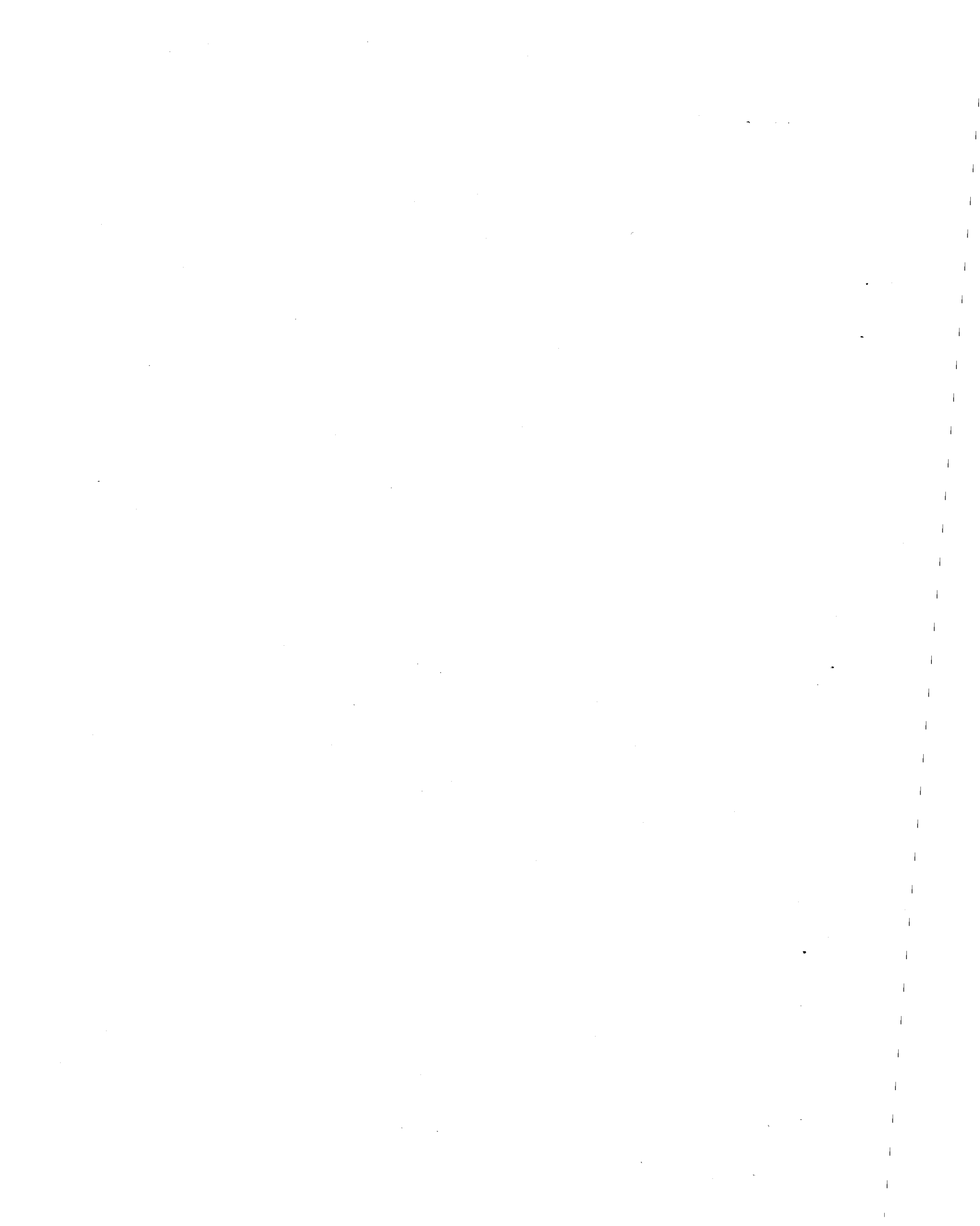
Use of the Shock Pulse Meter could preclude progressive catastrophic failure, as caused by the above defects.

Use of the Shock Pulse Meter in a railroad maintenance facility, however, is not cost effective since it requires significant operator interpretation, including the plotting of profiles. For this reason, the development of a "Shock Emission Analyzer" that would provide (go)-(no-go) indications of bearing condition was conceptualized as a follow-on to this feasibility study.

An automatic "Shock Emission Analyzer" concept was presented to several major railroads in order to obtain their reaction to such a device. They unanimously agreed that the "Shock Emission Analyzer" addresses a major problem, has substantial cost and lifesavings potential regarding avoidance of derailments, and has the potential of offsetting its annual operating cost in less than two months operation by avoiding unnecessary bearing teardown.

It is therefore recommended that a program be established to produce hardware which will automatically cull out bearings having component damage or contaminated grease.

A packaging and evaluation program to produce an operating system is presented in the body of this report.



3. TASK I

BURNOFF PREVENTION USING ON-BOARD TRANSMITTER BOLTS

3.1 SUMMARY

The feasibility of developing an onboard system for the detection of overheating in railroad journal roller bearings has been established by the work described and the data presented herein. Such feasibility is possible because of recent advances in the fields of thermoelectric power generation and electronic miniaturization.

Work performed under Contract DOT TSC-935 Phase II established the feasibility of implanting a self-powered radio frequency transmitter in one of the three standard axle cap bolts used for bearing mounting. This transmitter, in combination with implanted temperature transducers, will alert the train crew if the bearing in which it is installed experiences abnormal operating temperatures. Having been alerted, the train crew will halt the train and then use a portable radio receiver to identify the roller bearing which has been identified by the transmitter bolt.

The bolt, currently under development, will also sense bolt strain, and thus provide an early warning for the loss of bolt torque. Its major subsystems include a transmitter, thermoelectric power source, temperature sensor, strain sensor, two integrated circuits for signal conditioning, a heat exchanger consisting of a "heat pipe" and cooling fins, and an antenna.

Inclusion of the necessary subsystems (in particular, the thermal power source and strain sensors), however, increases the cost of this version of the transmitter bolt.

For that reason a low-cost, modified bolt which will sense temperature (but not strain) is being recommended for further development. This bolt will be battery operated and will contain a temperature sensitive switch to activate the transmitter. The battery will have capacity to operate the transmitter for a period sufficient for the train crew to complete the required pull-by inspection.

A work plan and schedule for development and test of both versions of the transmitter bolt are found in Figures 3-1, 3-2, 3-3, and 3-4. For cost effectiveness, the program of Figures 3-3 and 3-4 is more highly recommended for further development.

TASK I. Systems Development

A. Packaging

- (a) Design and breadboard sensor amplifier and discriminator circuits for use in final integration process.
- (b) Place and monitor bolt component subcontract.
 - 1. Transmitter hybrid package
 - 2. Thermal power source
 - 3. Sensor amplifier and discriminator circuit integration
 - 4. Strain sensor packaging
 - 5. Heat pipe and heat exchanger packaging
- (c) Measure bolt package thermal characteristics.
- (d) Conduct Design Review

- (e) Design and fabricate laboratory bolt test fixture.

B. Prototype Fabrication

- (a) Procure bolt components: functionally and environmentally test.
 - 1. Transmitter hybrid package
 - 2. Thermal power source
 - 3. Sensor amplifier and discriminator circuit
 - 4. Strain sensor
 - 5. Heat pipe and heat exchanger package
- (b) Design and build (1) portable transmitter bolt test unit.
- (c) Fabricate (3) prototype axle cap bolts with transmitter, power source, and antenna: functionally and environmentally test.

FIGURE 3-1. TRANSMITTER BOLT DEVELOPMENT AND EVALUATION PROGRAM

- (d) Develop transmitter design specification and drawing data package.

TASK II. Systems Evaluation

A. Laboratory

- (a) Evaluate overtemperature and lost-strain sensing capability of prototype bolts on test fixture.
- (b) Evaluate overtemperature and loss of strain capability of prototype bolts in bearings tested on standard railroad test machine.
- (c) Measure field strength versus range of an installed prototype bolt in an actual stub shaft/end cap.

B. Field

- (a) With cooperation of railroads, verify setpoint selection by measurement of operating bearing temperatures.
- (b) Fabricate (9) additional bolt units and functionally test.
- (c) Install (12) transmitter bolts on 3 cars used in unit train service. Determine servicability of the bolts over a 6-month period. Remove each bolt after 500 accumulated miles and verify performance using the portable transmitter bolt test unit.
- (d) At the conclusion of the unit train test, submit each of the 12 bolts to testing defined above in Task II, Section A(a).

FIGURE 3-1 (CONT.)

- (e) Provide (1) bolt for installation on a DOT furnished train (at the Transportation Test Center) having an intentionally faulty wheel bearing to generate an operational over temperature condition. Support test and demonstration of the bolt sensing capability during this test.
- (f) Generate Final Test Report.

FIGURE 3-1 (CONT.)

MONTHS ARO

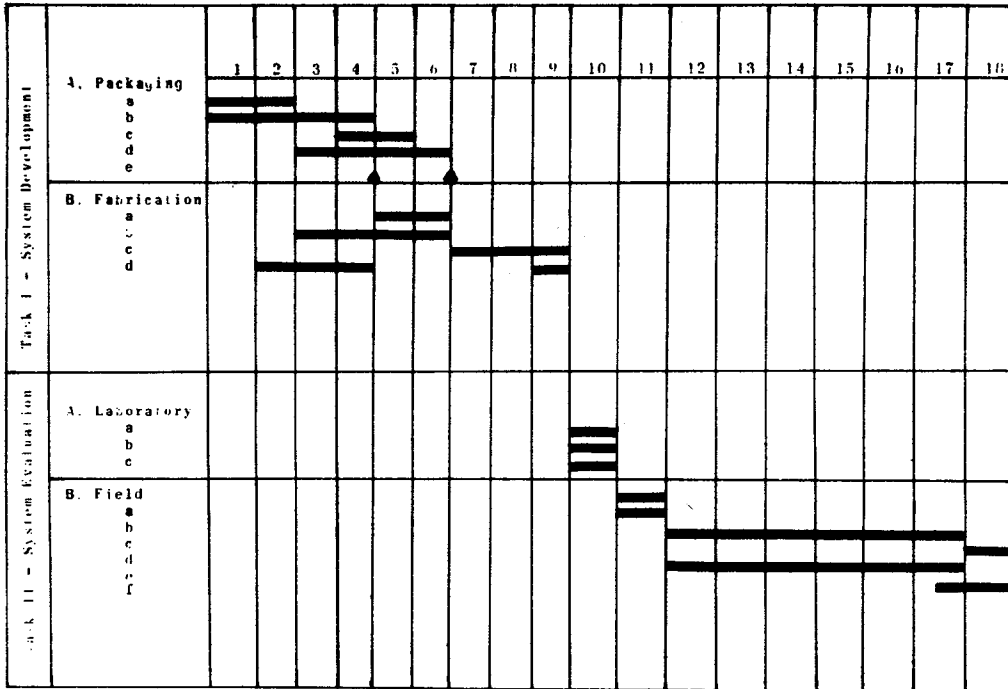


FIGURE 3-2. TRANSMITTER BOLT DEVELOPMENT AND EVALUATION SCHEDULE

Task I. Systems Development

A. Packaging

- (a) Design physical layout of transmitter bolt.(ie. transmitter, antenna, battery, switch)
- (b) Place and monitor transmitter hybrid package subcontract
- (c) Design and fabricate laboratory bolt test fixture.

B. Prototype Fabrication

- (a) Procure bolt components: functionally and environmentally test.
 - 1. Transmitter hybrid package
 - 2. Battery power source
 - 3. Thermal switch
- (b) Design and build (1) portable transmitter bolt test unit.
- (c) Fabricate (3) prototype axle cap bolts with transmitter, power source, and antenna: functionally and environmentally test.
- (d) Develop transmitter design specification and drawing data package.

Task II. Systems Evaluation

A. Laboratory

- (a) Evaluate overtemperature sensing capability of prototype bolts on test fixture.

FIGURE 3-3. MODIFIED TRANSMITTER BOLT DEVELOPMENT AND EVALUATION PROGRAM

- (b) Evaluate overtemperature capability of prototype bolts in bearing tested on standard railroad test machine and verify temperature set point.
- (c) Measure field strength versus range of an installed prototype bolt in an actual stub shaft/end cap.

B. Field

- (a) With cooperation of railroad, verify set point selection by measurement of operating bearing temperatures.
- (b) Fabricate (9) additional bolt units and functionally test.
- (c) Install (12) transmitter bolts on 3 cars used in unit train service. Determine serviceability of the bolts over a 6-month period. Remove each bolt after 500 accumulated miles and verify performance using the portable transmitter bolt test unit.
- (d) At the conclusion of the unit train test, submit each of the 12 bolts to testing defined in Task II, Section A (a).
- (e) Provide (1) bolt for installation on a DOT furnished train (at the Transportation Test Center) having an intentionally faulty wheel bearing to generate an operational over temperature condition. Support test and demonstration of the bolt sensing capability during this test.
- (f) Generate Final Test Report.

FIGURE 3-3. (CONT.)

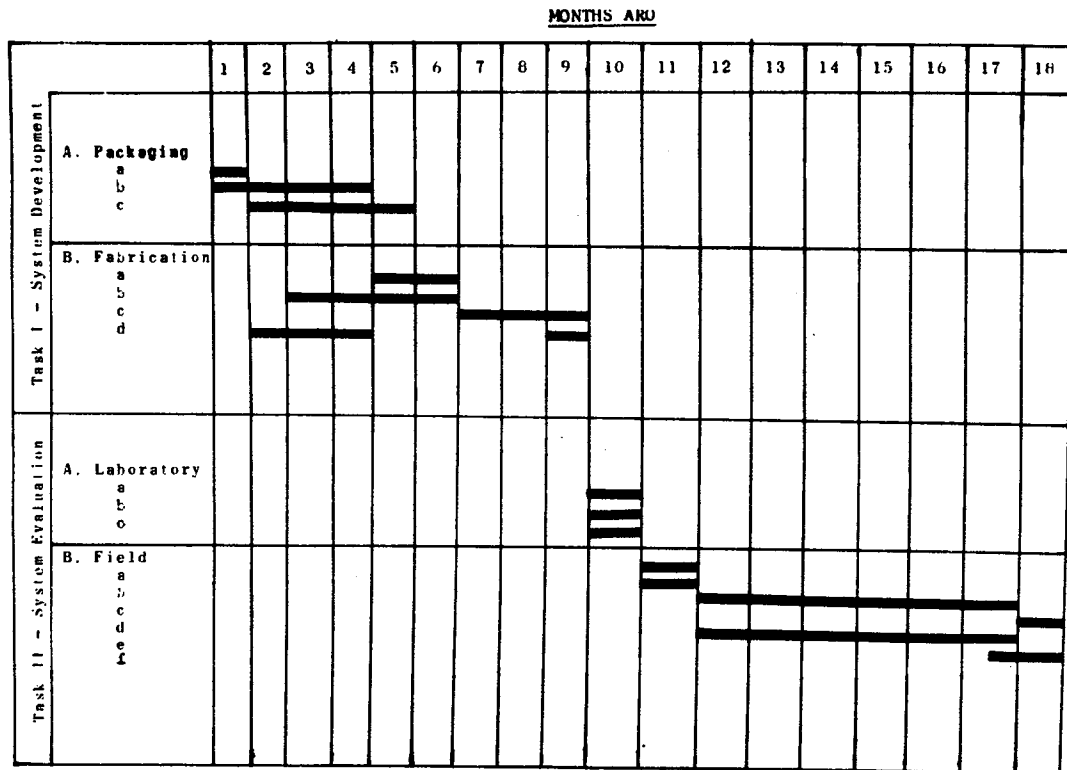


FIGURE 3-4. MODIFIED (TEMPERATURE SENSING ONLY)
TRANSMITTER BOLT DEVELOPMENT AND EVALUATION SCHEDULE

3.2 INTRODUCTION

The development of a device for the detection of imminent catastrophic railroad journal roller bearing failure has been the subject of much research and development effort. Such devices have attempted to sense the occurrence of abnormally high temperatures associated with incipient catastrophic failure.

The most successful device, to date, has been the hot box detection system which consists of a "wayside" infrared heat detector and data transmission system. These detectors and their associated transmission apparatus are placed at track intervals of approximately 30 miles, depending on traffic. They measure temperatures by remotely sensing the infrared energy emanating from each bearing of a passing train, and in the event of an abnormally high temperature, signal the train crew via wayside instrumentation to stop the train. Although these systems have been quite successful, there are a number of disadvantages:

1. Initial capital outlays are on the order of \$40,000, and each requires an annual maintenance cost.
2. Monitoring of bearings is a sampling process and thus, the possibility of missing failures exists.
3. Local weather conditions, such as blowing snow or sand, often render the infrared detectors ineffective.

The development of a continuous monitoring device is the only sure way of overcoming the statistical and meteorological uncertainties associated with hot box detection systems.

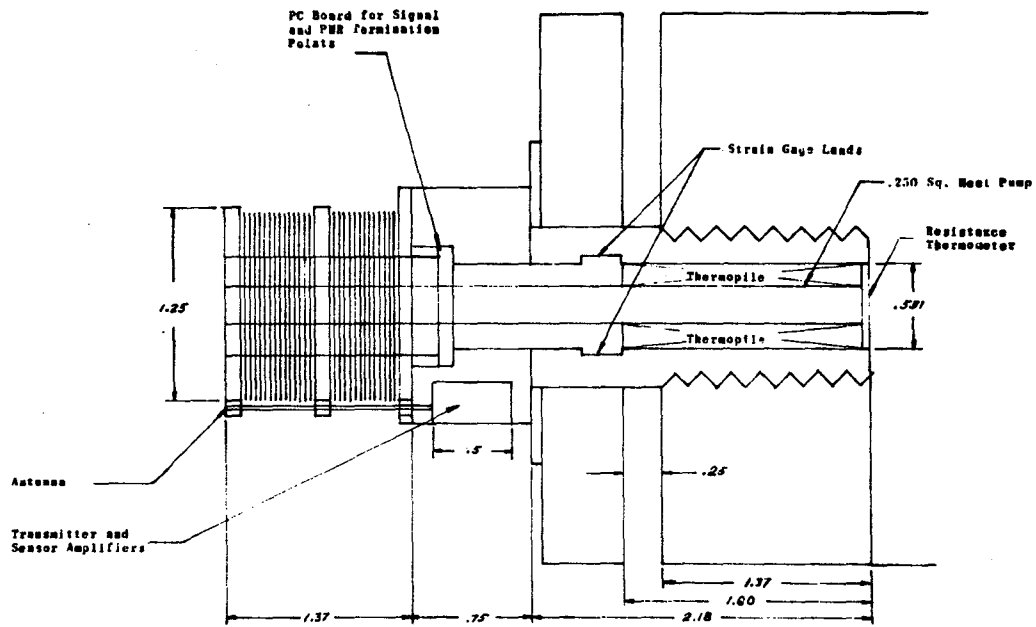
A detailed drawing of an on-board transmitter bolt capable of overcoming the deficiencies of wayside diagnostics is shown in Figure 3-5. It is composed of a power source, a transmitter and antenna, temperature and strain sensing transducers, and a heat exchanger system composed of a heat pipe and convection cooler. The transmitter, designed to operate at 450 MHz, is composed of a specially designed "hybrid" electronic circuit. (A hybrid circuit is one composed of both integrated and discrete devices.)

The self-contained power source is composed of a number of commercially available "thermopiles" connected in series. A thermopile is a series combination of thermocouples. (Thermocouples convert thermal energy into electrical energy in proportion to the temperature differential across their terminals.)

Temperature is sensed by a commercially available nickel/phenolic resistance thermometer whose electrical resistance changes in proportion to temperature. Strain sensing is accomplished by a commercially available strain gage whose resistance changes in proportion to elongation (strain).

Calculation based on the thermal characteristics of operating bearings and thermopiles have determined the necessity of including a specially designed heat exchanger to provide the temperature differential necessary for thermoelectrical power production. The heat exchanger is composed of a heat pipe and cooling fins.

Feasibility studies associated with the development of this system fell into three major categories:



ALL DIMENSIONS IN INCHES

FIGURE 3-5. TEMPERATURE AND STRAIN SENSING TRANSMITTER BOLT

1. Identification of physical and electrical specifications for the encapsulated transmitter. This includes the design, test and evaluation of a specific bread-board transmitter along with a vendor survey for eventual large-scale transmitter production to the specifications determined here. Transmitter design and evaluation is the subject of Section 3.3.
2. Identification of physical, thermal, and electrical specifications for the implantable power source. Included is an analysis of electrical power capacities of a candidate "thermopile" operating in the expected thermal environment of a bearing axle. These are the subjects of Section 3.4.
3. Identification of the thermal, physical and electrical specifications of implantable temperature and strain sensors is the subject of Section 3.5.

These studies were performed chronologically in the order described above, and for that reason the probable production costs of a thermally powered, strain and temperature sensing bolt were not identified until late in the program. The more highly recommended battery operated, temperature sensing bolt will utilize the transmitter identified in Section 3.3 below but, for cost effectiveness, will not utilize the thermal power source or the sensors described in Section 3.4 and 3.5.

3.3 RADIO FREQUENCY TRANSMITTER SPECIFICATION

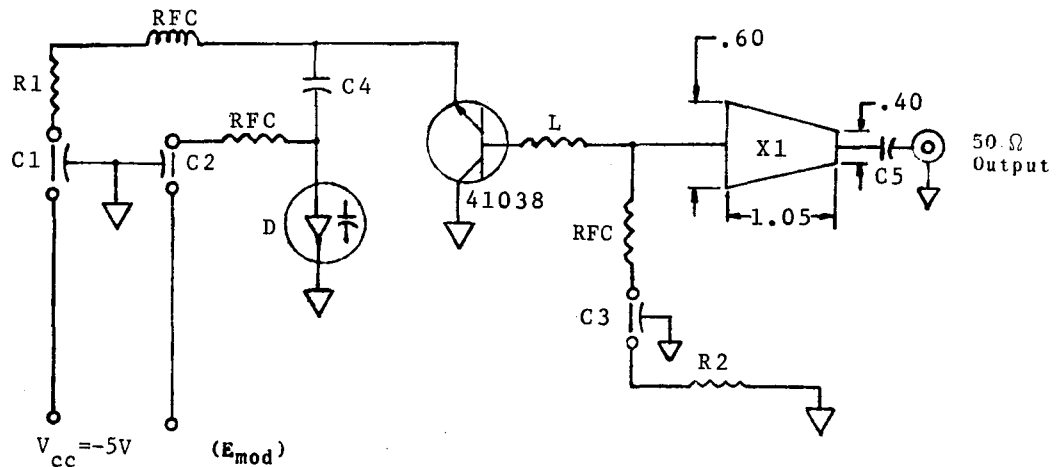
The establishment of transmitter specifications was accomplished in the following sequence:

1. A 450 MHz transmitter was designed, breadboard tested, and analyzed.
2. Field strength vs. transmitter input power data were collected and used to establish the dc input power requirements of a finalized encapsulated unit.
3. A modulated breadboard transmitter, in conjunction with a commercially available RF receiver, was used to verify transmission capabilities (range and directivity) when operated in a reflective environment similar to that of a railroad wheel set.

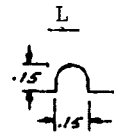
3.3.1 Breadboard Transmitter Design

The transmitter used for developing specifications and determining the reflective characteristics of a railroad wheel set is analyzed below.

The circuit used is an adaptation of a common base Clapp oscillator as shown in Figure 3-6 [1]. It was fabricated on a double sided, copper clad, glass epoxy circuit board and is shown in the photograph of Figure 3-7. The trapezoidal copper section shown in the schematic of Figure 3-6 and the photo of Figure 3-7 is unique to oscillators of this type. Its capacitance forms part of the tuned circuit which, for this application, is tuned to 450 MHz. Capacitors C_1 , C_2



- C1,C2,C3: 1000 F Feedthrough
- C4: 4.7 pF
- C5: 0.3-3.5 pF
- R1: 10 Ω , 1/4 W carbon
- R2: 0-100, 1/4 W
- D: Variable Capacitance Diode-
7-15 pF Range
- L: Loop of Transistor Lead -
- X1: 1732 Teflon-Fiberglass Board -
Double-Clad Board, one side gnd



ALL DIMENSIONS IN INCHES

FIGURE 3-6. BREADBOARD TRANSMITTER TEST CIRCUIT

Reproduced from
best available copy.

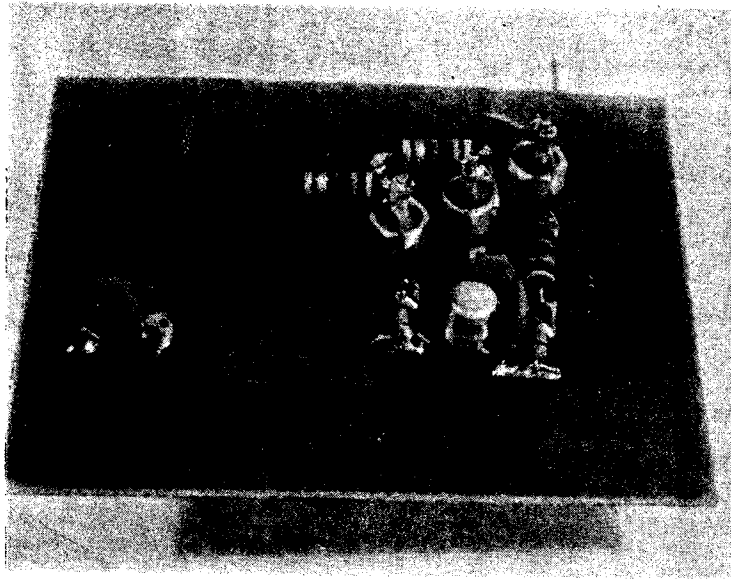


FIGURE 5-7. PHOTOGRAPH OF BREADBOARD TRANSMITTER TEST CIRCUIT

and C_3 are commercially available feedthrough capacitors especially designed for radio frequency applications. A high frequency transistor (41038) was used as the active element.

To determine the maximum output available from this transmitter as used with a proposed antenna of 1 in. length and 1/8 in. dia, the input impedance of such an antenna is calculated from [2]:

$$Z(\text{ant}) = 138 \log_{10} \frac{2 (\text{antenna length})}{(\text{antenna dia})} \quad (1)$$

$$Z(\text{ant}) = 166\Omega$$

Figures 3-8 and 3-9 show the hybrid pi ac equivalent circuits of the oscillator [1]. The emitter current (i_e) flowing in the circuit of Figures 3-8 and 3-9 is calculated from [3]:

$$i_e = \frac{V_f}{X_f} \cdot \frac{X_A}{X_A + R_{b'e}/\beta} \quad (2)$$

Where

β = Voltage amplification factor, 150
 V_f = Feedback voltage, V_{cb} , 5 V P to P
 X_f = Feedback capacitive reactance at 450 MHz

$$X_f = X_4 + X_o = j 125 \Omega$$

$$\text{where } X_4 = \frac{1}{\omega C_4} \text{ and } X_o = \frac{1}{\omega C_o}$$

$X_{b'e}$ = base/emitter capacitive reactance at

$$450 \text{ MHz, } X_{b'e} = \frac{\omega_T}{\omega_R g_m} = j 2.5 \omega$$

where ω_T = upper cutoff frequency of transistor = 1680 MHz

g_m = transconductance of transistor = 1.48 mhos

ω_R = resonant frequency of transmitter

$$X_A = (X_f) (X_{b'e}) / X_f + X_{b'e} = j 2.45 \Omega$$

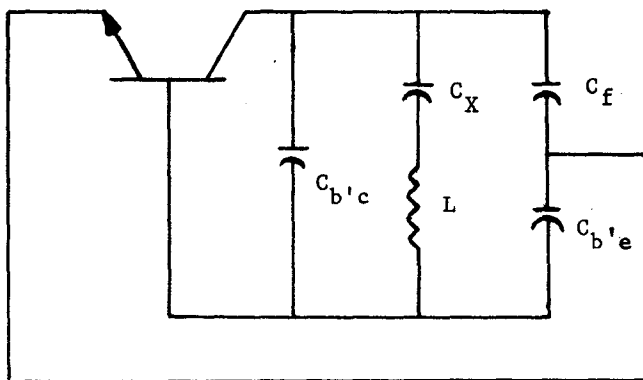


FIGURE 3-8. AC EQUIVALENT CIRCUIT FOR BREADBOARD TRANSMITTER

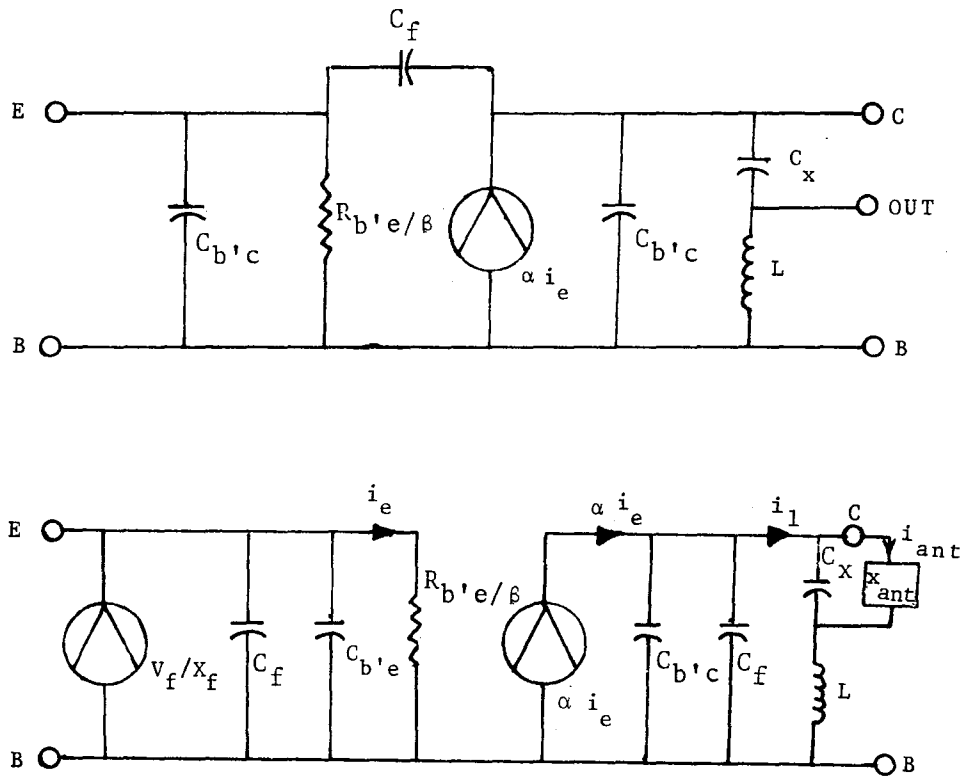


FIGURE 3-9. HYBRID - PI EQUIVALENT CIRCUITS FOR BREADBOARD TRANSMITTER

$$R_{b'e} = \text{base/emitter resistance} = \beta/40 i_{EQ} = 101\Omega$$

Where $i_{EQ} = 37 \text{ mA}$ (measured)

Substituting, $i_e = 31.1 \text{ mA P to P (max)}$

The collector current (i_c) flowing in the circuit is given by

$$i_c = \alpha i_e = 30.9 \text{ mA, P to P where } \alpha \quad (3)$$

is taken from published manufacturers' specifications.

At resonance, assuming proper impedance matching, the antenna current (i_{ant}) is equal to one-half the output current (i_1). This is depicted in Figure 3-9. The output current (i_1) is given by

$$i_1 = \alpha i_e \frac{X_b X_c}{X_b + X_c} \quad (4)$$

$$\text{where } X_b = \frac{X_{b'c} X_f}{X_{b'c} + X_f} \quad \text{and} \quad X_c = \frac{X_{c_x} X_{ant}}{X_{c_x} + X_{ant}} X_L$$

Since the output current (i_1) approaches i_e at resonance, the antenna current thus approaches

$$1/2 \alpha i_e = 15.45 \text{ mA P to P} = 5.46 \text{ mA, (RMS)}$$

To calculate the radiated antenna power associated with this antenna current, the antenna radiation resistance (R_r) is calculated by the following equation from [2].

$$R_r \approx 10 L^2 \quad (5)$$

where $L_{(ant)}$ = equivalent antenna length in radians

Since the wavelength radiated $\lambda = c/f$ where, c = velocity of light, and $f = 450$ MHz, the radiated wavelength is 0.66 meter. Since 0.66 meters is equivalent to 2 radians, the equivalent antenna length of a 1 in. (0.25 meters) antenna is 0.239.

$$\text{Substituting, } R_r = 0.574 \text{ ohms.} \quad (5)$$

The radiated antenna power output from [2] is given by

$$\begin{aligned} P_o &= R_r [i_{ant} \text{ (RMS)}]^2 \\ &= (0.574) (5.46)^2 = 17.1 \mu \text{ W.} \end{aligned} \quad (6)$$

With the radiated output power known, the electric field strength (E_m) at a given distance (r) from a point source radiator is from [4] given by

$$E_m = \frac{1}{r} \left[\frac{P_o \mu c}{2} \right]^{1/2} \quad (7)$$

where

- P_o = output power (watts)
- r = distance (meters)
- μ = permeability of transmission medium
- c = velocity of light (meters/sec)

Substituting, the radiated power, E_m , at distances of 1 mile and 30 feet is given below:

$$\begin{aligned} E_m \text{ (1 mile)} &= 19.8 \mu \text{V/meter} \\ E_m \text{ (30 ft)} &= 3484 \mu \text{V/meter..} \end{aligned}$$

3.3.2 Breadboard Transmitter Test

3.3.2.1 Test Equipment and Data Format

The breadboard transmitter described in Section 3.3.1 above was operated at 450 MHz in order to determine signal reception characteristics under the transmission conditions expected in actual use. Field strength (detectability of transmitter output) as functions of distance, antenna orientation, and transmitter environment were measured. The transmitter was operated with 250 mW maximum input power, i.e. 5 Vdc about 50 mA maximum input current.

The test matrix of Table 3-1 was followed as the basic test plan. The formal test plan for this program is reproduced in Appendix A. Vertical polarization is defined as operation with the antenna axis vertical, and horizontal polarization (as would occur in actual service) refers to horizontal orientation of the antenna axis. An antenna length of one inch was used for all tests.

Signal strengths were measured by use of a rented signal strength meter for modulated and unmodulated (where practical) transmitter operation. A commercially available RF receiver was used to verify modulated signal reception. Frequency modulation was provided by a laboratory signal generator. Its output was applied at input terminals E_{mod} , as was shown in Figure 3-6.

Field strength data were accumulated for transmission distances of 30 feet, one-quarter mile, and one-half mile. Polar plots of measured field strengths (in μ V/meter) are presented for all data acquired using the field strength meter. Polar signal strength data were acquired by rotation of the

TABLE 3-1. TEST PROGRAM MATRIX FOR TRANSMITTER BROADCAST CAPABILITIES

ADDED AFTER TEST PLAN APPROVED

Conditions		Vertically polarized	Horizontally polarized	Horizontally polarized with wheel simulator as ground plane	Horizontally polarized with transmitter encapsulated in wheel simulator	Horizontally polarized with transmitter encapsulated in hooded wheel simulator
		A	B	C	D	E
Bread Board Transmitter Battery Powered Unmodulated	1	1A	1B	1C	1D	1E
Bread Board Transmitter Battery Powered Modulated	2	2A	2B	2C	2D	2E
Bread Board Transmitter Thermally Powered Modulated	3	3A	3B	3C	3D	3E
Prototype Bread Board Transmitter Battery Powered Modulated (w/ temp. & strain sensing)	4	4A	4B	4C	4D	4E
Prototype Bread Board Transmitter Thermally Powered Modulated (w/ temp. & strain sensing)	5	5A	5B	5C	5D	5E

transmitter antenna relative to the field strength meter antenna as depicted in Figure 3-10.

For tests requiring a thermoelectric power source, a series combination of commercially available thermopiles was used to power the transmitter. Their operation is described in detail in Section 3.4.

The test fixture shown in Figures 3-11 and 3-12 was used for tests C, D and E in order to simulate the expected in-service transmission environment.

To determine the effect of an on-the-ground or electrically grounded railroad wheel which, in actual service, will be perpendicular to and in close proximity to the antenna axis, the test fixture of Figure 3-11 was used without the container and hood for tests (C). For tests (D) of Table 3-1, a metal container was added to the wheel simulator and placed over the transmitter as shown in Figure 3-11. Placement of this container in the manner shown allowed a one-inch maximum antenna protrusion. For tests (E), the hood was attached to the fixture to simulate the undercarriage of a railroad car.

3.3.2.2 Test Data

Tests 1A through 1E, using an unmodulated carrier were not conducted for distances over 30 feet. Radio traffic rendered the unmodulated carrier virtually imperceptible over larger distances. Using a modulated signal over short distances, it was determined, however, (See Table 3-2) that there was negligible variation in signal strength between a modulated and unmodulated carrier. For this reason, Tests 1A

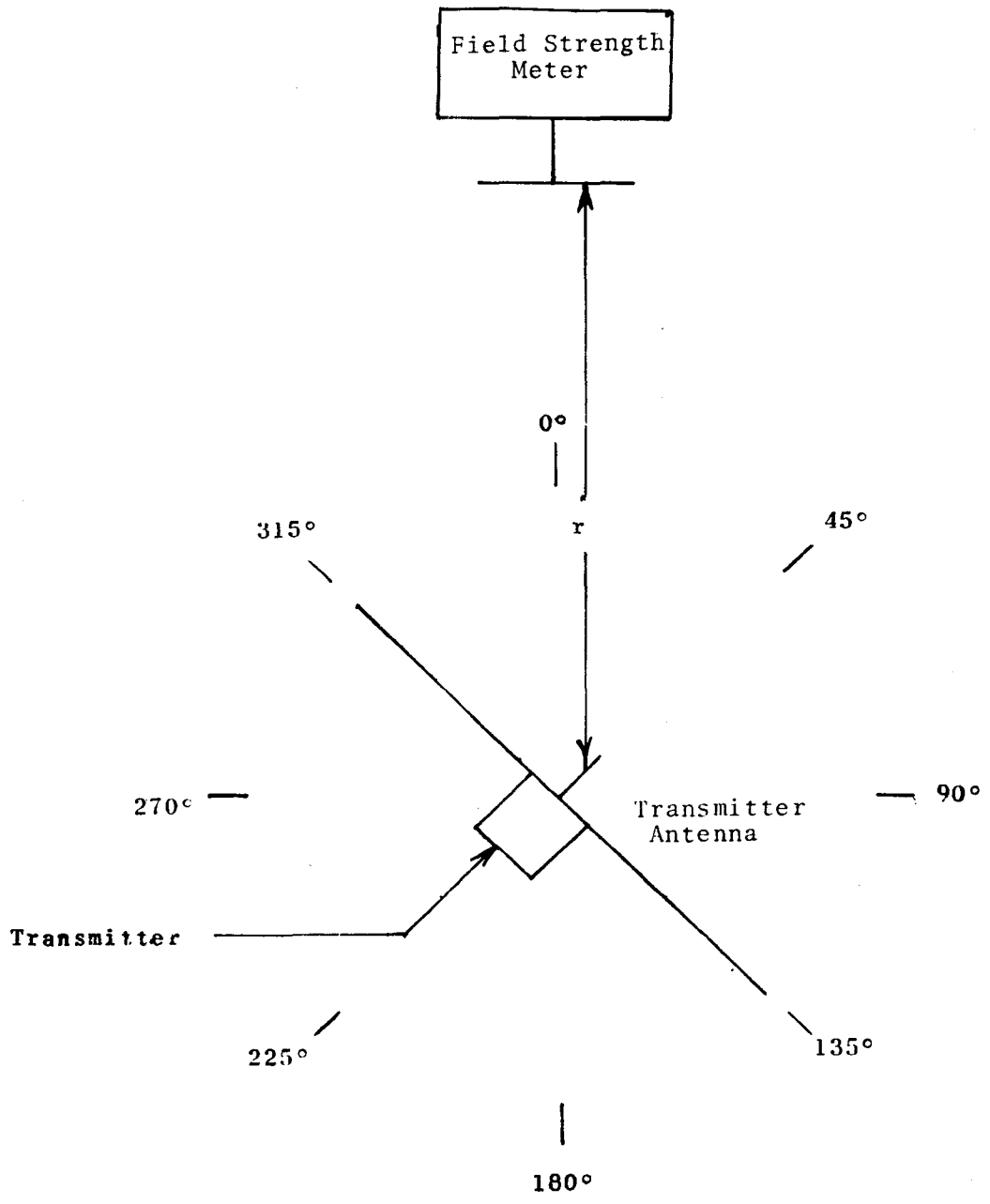


FIGURE 3-10. TRANSMITTER VS. RECEIVER ANTENNA ORIENTATIONS FOR FIELD INTENSITY DATA ACQUISITION

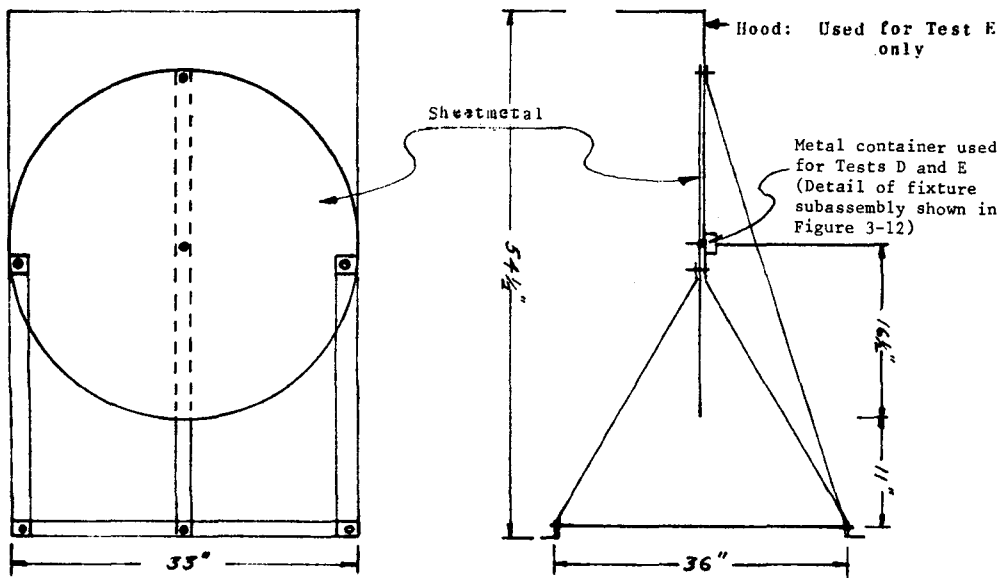


FIGURE 3-11. TRANSMITTER TEST FIXTURE

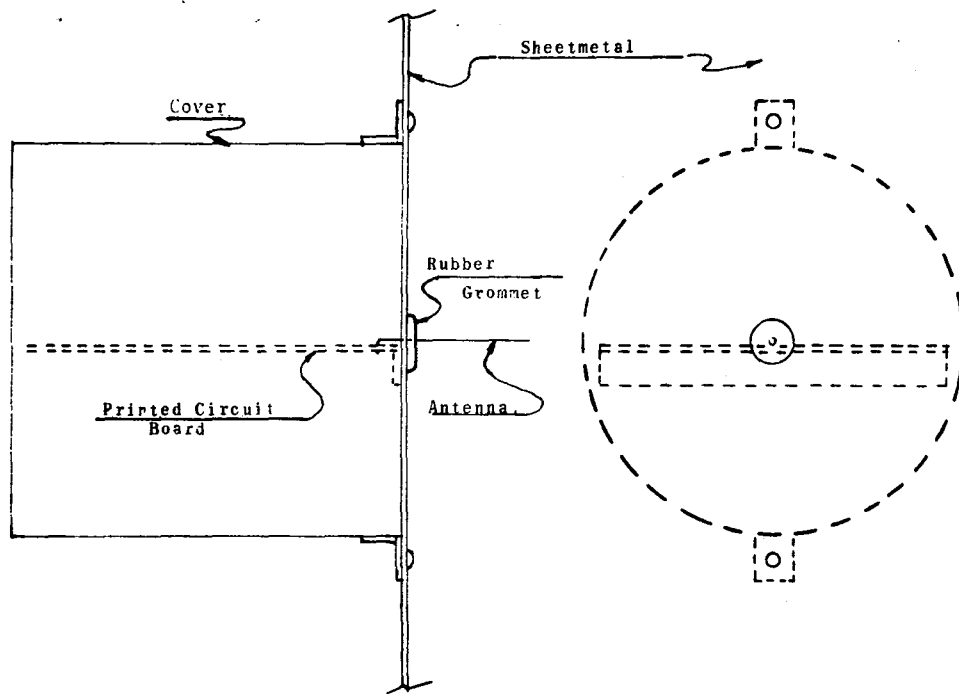


FIGURE 3-12. TRANSMITTER TEST FIXTURE SUBASSEMBLY FOR ANTENNA ENCAPSULATION

TABLE 3-2. MODULATED VS. UNMODULATED FIELD STRENGTH
DATA AT 30 FEET (expressed in dB above 1 MV/m)

TEST NO	TEST 1B (Unmodulated)	TEST 2B (Modulated)	TEST 1D (Unmodulated)	TEST 2D (Modulated)
1	48	53	50	51
2	44	48	50	50
3	58	52	60	60
4	58	52	60	50
5	58	51	58	51

through 1E were considered nonessential in determining transmitter output potential and were suspended.

Tests conducted using a vertically polarized antenna yielded signal strengths equivalent to those using a horizontally polarized antenna. As a result, and in light of the fact that vertical polarization is unfeasible in actual service, tests 2A, 3A, 4A, and 5A are not reported.

Data acquired in the performance of tests 2B through 2E are presented in Tables 3-4 - 3-7 and in Figures 3-13 - 3-25. The modulation signal consisted of a 160 mV (P to P), 1 kHz, square wave. Ambient noise levels for these tests averaged 16 μ V/m.

It is seen that the modulated signal (tests 2B through 2E) was detectable above background noise at distances up to one-half mile. The observed signal strengths as compared to calculated values (by methods of Section 3.3.1) appears in Table 3-3 below:

TABLE 3-3. CALCULATED AND OBSERVED FIELD STRENGTH VALUES

TRANSMISSION DISTANCE	(Free space) CALCULATED (μ V/m)	(Actual ground plane) OBSERVED VALUES* (μ V/m)
30 Feet	3484	332
1/4 Mile	79	26
1/2 Mile	18	39

*with ground plane

where building reflections were severe, observed signal strengths correlated well with calculated free-space field intensities.

TABLE 3-4. MEASURED VOLTAGE AND ELECTRIC FIELD STRENGTH DATA AS A FUNCTION OF ANTENNA ORIENTATION FOR A MODULATED, BATTERY POWERED, HORIZONTALLY POLARIZED, BREADBOARD TRANSMITTER AT DISTANCES OF 30 FEET, 1/4 MILE, AND 1/2 MILE

Antenna Rotation Angle (deg)	TRANSMISSION DISTANCE					
	30 FEET		1/4 MILE		1/2 MILE	
	Voltage (dB*)	Field Strength (μ V/m)	Voltage (dB*)	Field Strength (μ V/m)	Voltage (dB*)	Field Strength (μ V/m)
0	50	332	13	20.5	8	18
15	52	414	10	19	8	18
30	53	463	12	20	8	18
45	54	517	12	20	8	18
60	55	578	14	21	8	18
75	55	578	16	22	10	19
90	55	578	18	24	9	18
105	54	517	19	25	11	19
120	53	463	16	22	8	18
135	51	371	14	21	8	18
150	48	267	11	19	9	18
165	46	216	12	20	8	18
180	44	174	16	22	8	18
195	47	240	18	24	8	18
210	50	332	18	24	8	18
225	52	414	19	25	8	18
240	52	414	19	25	8	18
255	52	414	20	16	8	18
270	52	414	19	15	8	18
285	51	371	19	15	8	18
300	51	371	19	15	8	18
315	49	298	17	23	8	18
330	46	216	16	22	8	18
345	46	216	13	20	8	18

*Decibels relative to 1μ V.

TEST - 2B

DATE-5-76

Transmitter Test Conditions:

Test Fixture:

V_{cc} - 5 V

(1) Free space - X

I_{in} - 37 mA

(2) Wheel simulator

P_{in} - 185 mW

(3) Other -

$I_c(ac)$

Transmitter ant polarization - HORZ

$I_c(dc)$ 20 mA

Transmitter ant height - 36 in.

Ant length - 1 in.

Receiving ant polarization - HORZ

Carrier freq - 450 MHz

Receiving ant ht - 36 in.

Modulation freq - 1000 Hz

Receiving ant length - 14 in.

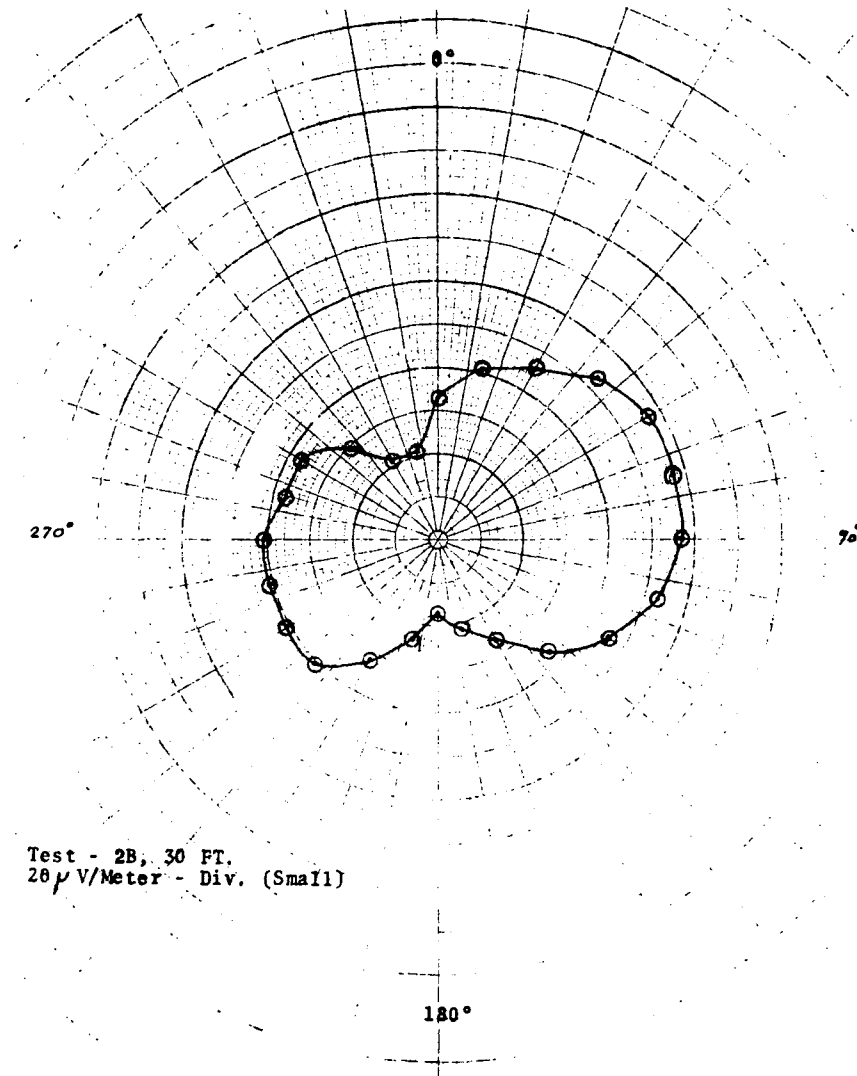


FIGURE 3-13. FIELD STRENGTH VS. ANTENNA ORIENTATION FOR A MODULATED, BATTERY POWERED, HORIZONATLLY POLARIZED, BREADBOARD TRANSMITTER AT A DISTANCE OF 30 FEET

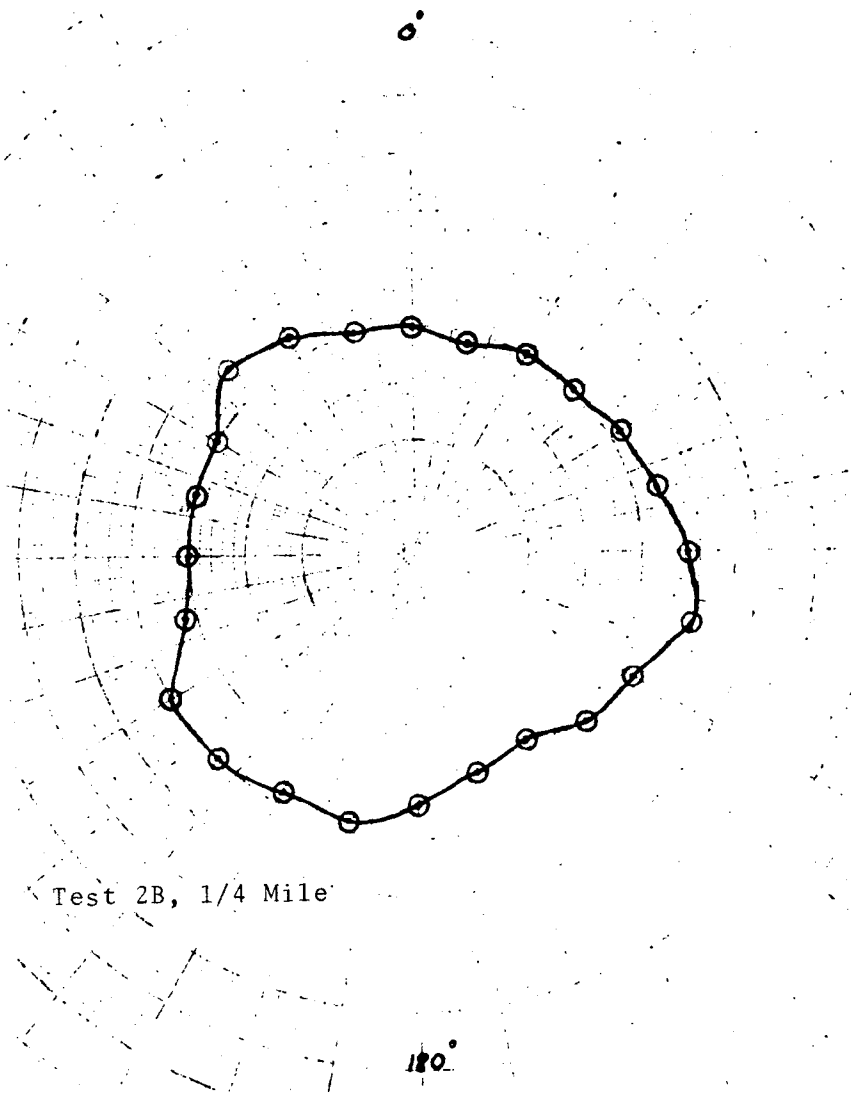


FIGURE 3-14. FIELD STRENGTH VS. ANTENNA ORIENTATION FOR A MODULATED, BATTERY POWERED, HORIZONTALLY POLARIZED, BREADBOARD TRANSMITTER AT A DISTANCE OF 1/4 MILE

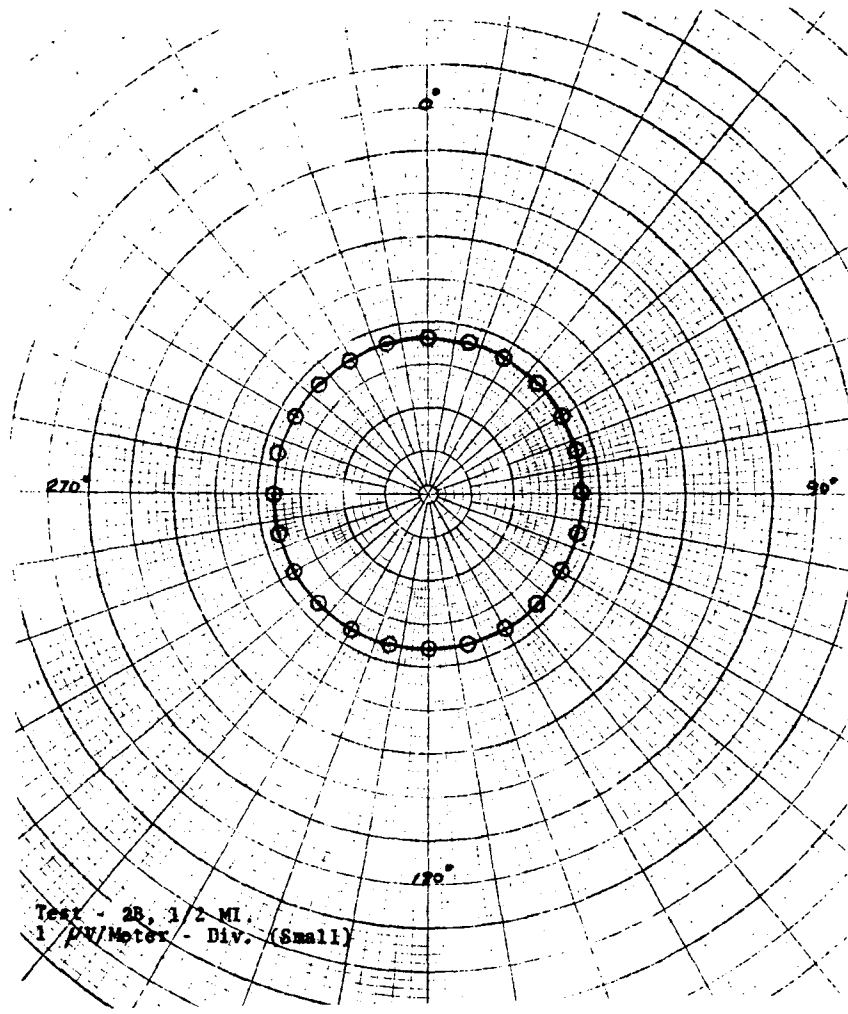


FIGURE 3-15. FIELD STRENGTH VS. ANTENNA ORIENTATION FOR A MODULATED, BATTERY POWERED, HORIZONTALLY POLARIZED, BREADBOARD TRANSMITTER AT A DISTANCE OF 1/2 MILE

TABLE 3-5. MEASURED VOLTAGE AND ELECTRIC FIELD STRENGTH DATA AS A FUNCTION OF ANTENNA ORIENTATION FOR A MODULATED, BATTERY POWERED HORIZONTALLY POLARIZED BREADBOARD TRANSMITTER WITH WHEEL SIMULATOR AT DISTANCES OF 30 FEET, 1/4 MILE, AND 1/2 MILE

Antenna Rotation Angle (deg)	TRANSMISSION DISTANCE					
	30 FEET		1/4 MILE		1/2 MILE	
	Voltage (dB*)	Field Strength (μ V/m)	Voltage (dB*)	Field Strength (μ V/m)	Voltage (dB*)	Field Strength (μ V/m)
0	48	267	32	56	12	20
15	56	647	32	56	12	20
30	58	810	32	56	14	21
45	60	1016	32	56	13	20
60	58	810	31	51	15	21
75	56	647	31	51	15	21
90	57	724	30	47	16	22
105	60	1016	30	47	16	22
120	60	1016	30	47	18	24
135	66	2016	30	47	18	24
150	65	1796	32	56	18	24
165	63	1426	34	66	12	20
180	64	1596	35	72	16	22
195	66	2016	34	66	18	24
210	66	2016	34	66	19	25
225	67	2256	34	66	18	24
240	66	2016	33	61	17	23
255	62	1276	30	47	16	22
270	60	1016	30	47	16	22
285	53	463	29	44	15	21
300	57	724	28	41	15	21
315	58	810	28	41	16	22
330	58	810	29	44	16	22
345	50	332	30	47	16	22

*Decibels relative to 1 μ V.

TEST 2C

Transmitter Test Conditions:

V_{cc} - 5V
 I_{cc} - 37 mA
 P_{in} - 185 mW
 I_{c(ac)} -
 I_{c(dc)} - 20 mA
 Ant length - 1 in.
 Carrier freq - 450 MHz
 Modulation freq - 1000 Hz

DATE - 5-76

Test Fixtures:

(1) Free Space -
 (2) Wheel simulator - X
 (3) Other -
 Transmitter ant polarization- HORZ
 Transmitter ant height - 36 in.
 Receiving ant polarization - HORZ
 Receiving ant ht 36 in.
 Receiving ant length - 14 in.

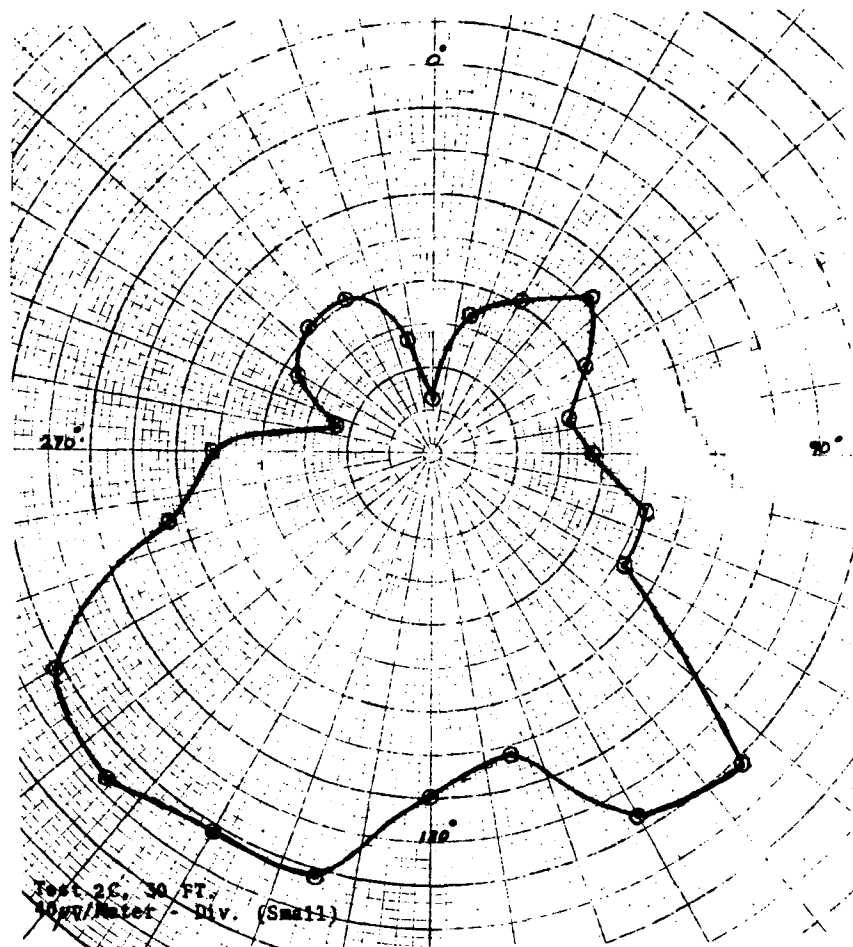


FIGURE 3-16. FIELD STRENGTH VS. ANTENNA ORIENTATION FOR A MODULATED, BATTERY POWERED, HORIZONTALLY POLARIZED, BREADBOARD TRANSMITTER WITH WHEEL SIMULATOR AT A DISTANCE OF 30 FEET

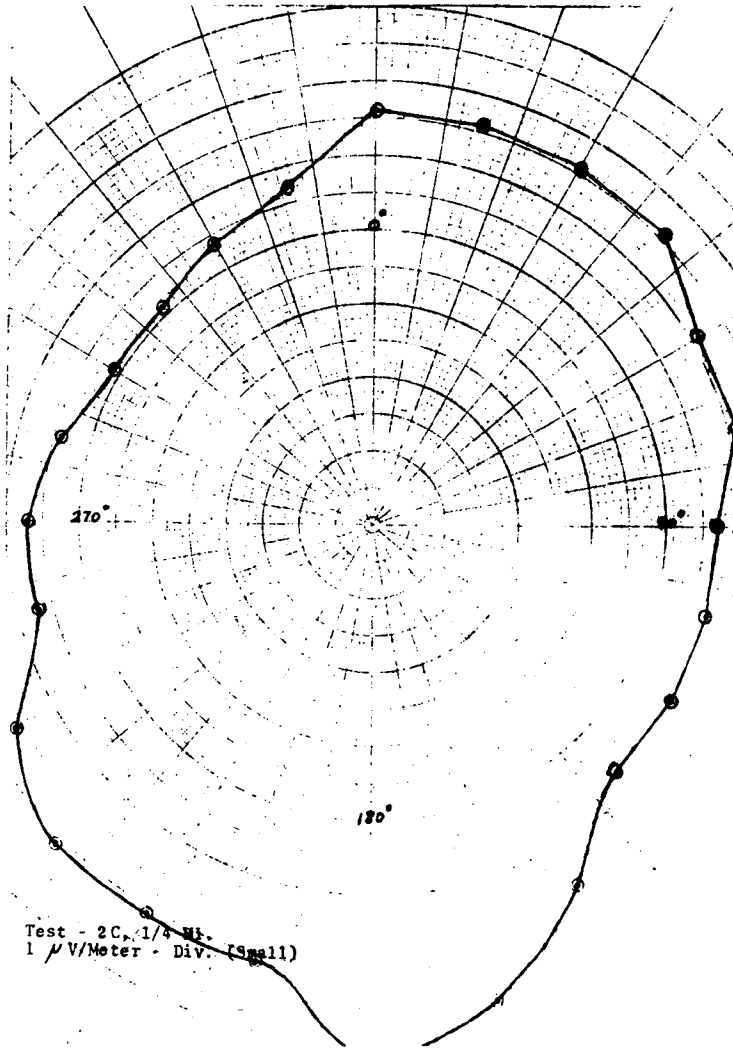


FIGURE 3-17. FIELD STRENGTH VS. ANTENNA ORIENTATION FOR A MODULATED, BATTERY POWERED, HORIZONTALLY POLARIZED, BREADBOARD TRANSMITTER WITH WHEEL SIMULATOR AT A DISTANCE OF 1/4 MILE

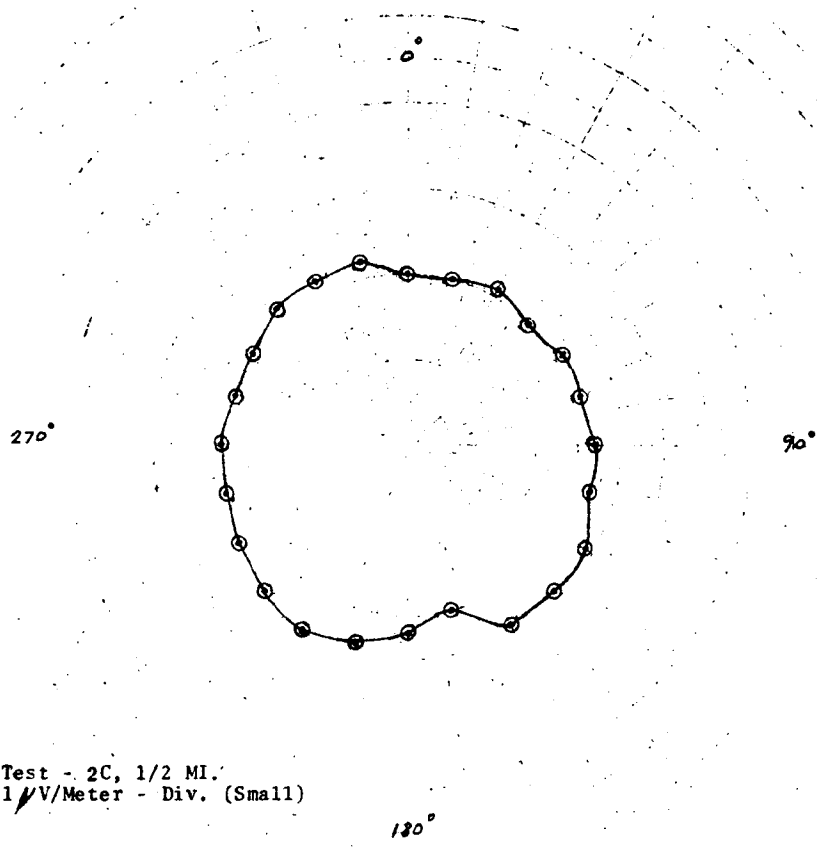


FIGURE 3-18. FIELD STRENGTH VS. ANTENNA ORIENTATION FOR A MODULATED, BATTERY POWERED, HORIZONTALLY POLARIZED, BREADBOARD TRANSMITTER WITH WHEEL SIMULATOR AT A DISTANCE OF 1/2 MILE

TABLE 3-6. MEASURED VOLTAGE AND ELECTRIC FIELD STRENGTH DATA AS A FUNCTION OF ANTENNA ORIENTATION FOR A MODULATED BATTERY POWERED, HORIZONTALLY POLARIZED, BREADBOARD TRANSMITTER ENCAPSULATED IN WHEEL SIMULATOR AT DISTANCES OF 30 FEET, 1/4 MILE, AND 1/2 MILE

Antenna Rotation Angle (deg)	TRANSMISSION DISTANCE					
	30 FEET		1/4 MILE		1/2 MILE	
	Voltage (dB*)	Field Strength (μ V/m)	Voltage (dB*)	Field Strength (μ V/m)	Voltage (dB*)	Field Strength (μ V/m)
0	48	267	20	26	10	19
15	51	371	24	32	10	19
30	52	414	27	38	10	19
45	52	414	22	28	10	19
60	51	371	24	32	10	19
75	44	174	25	34	10	19
90	50	332	23	30	14	21
105	55	578	23	30	13	20
120	60	1016	23	30	14	21
135	60	1016	23	30	14	21
150	64	1596	22	28	15	21
165	64	1596	21	27	13	20
180	63	1426	20	26	10	19
195	62	1276	20	26	10	19
210	72	1276	20	26	12	20
225	61	1136	20	26	12	20
240	60	1016	19	25	10	19
255	51	371	19	25	10	19
270	50	332	19	25	12	20
285	48	267	19	25	12	20
300	51	371	19	25	12	20
315	53	463	19	25	12	20
330	54	517	19	25	12	20
345	50	332	19	25	10	19

*decibels relative to 1μ V.

TEST - 2D

Transmitter Test Conditions:

V_{cc} - 5 V

I_{in} - 37 mA

P_{in} - 185 mW

$I_c(ac)$

$I_c(dc)$ 20 mA

Ant length - 1 in.

Carrier freq - 450 MHz

Modulation freq - 1000 Hz

DATE-5-76

Test Fixture:

(1) Free space -

(2) Wheel simulator - X

(3) Other -

Transmitter ant polarization - HORZ

Transmitter ant height - 36 in.

Receiving ant polarization - HORZ

Receiving ant ht - 36 in.

Receiving ant length - 14 in.

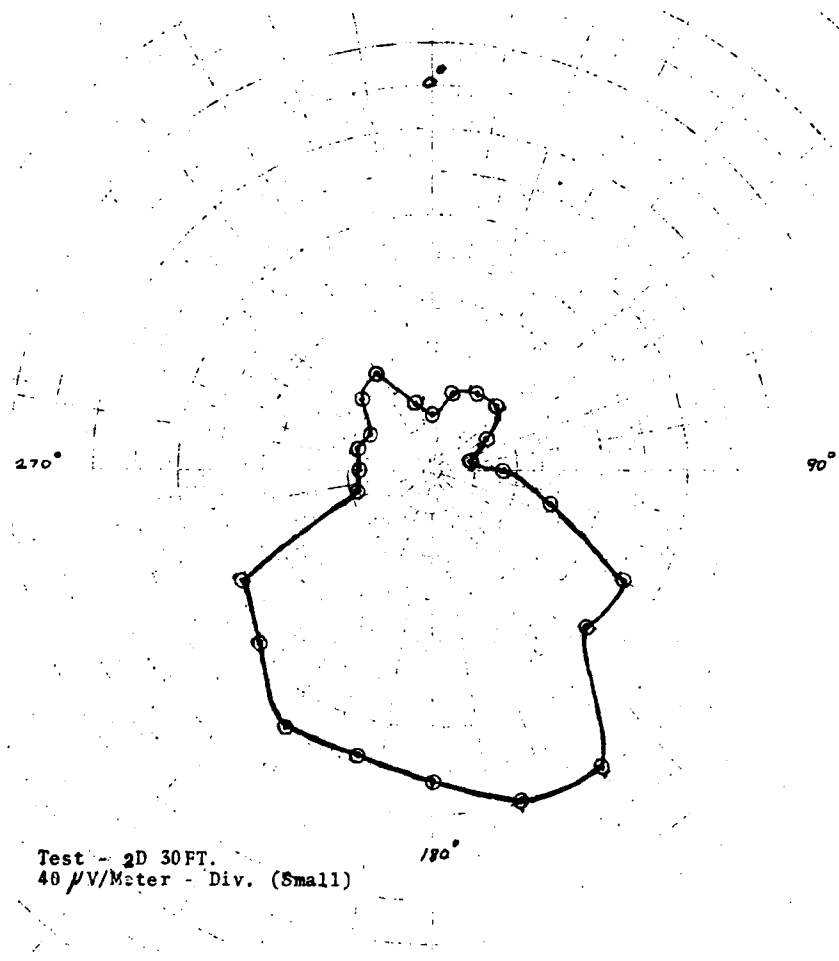


FIGURE 3-19. FIELD STRENGTH VS. ANTENNA ORIENTATION FOR A MODULATED, BATTERY POWERED, HORIZONTALLY POLARIZED, BREADBOARD TRANSMITTER ENCAPSULATED IN WHEEL SIMULATOR AT A DISTANCE OF 30 FEET

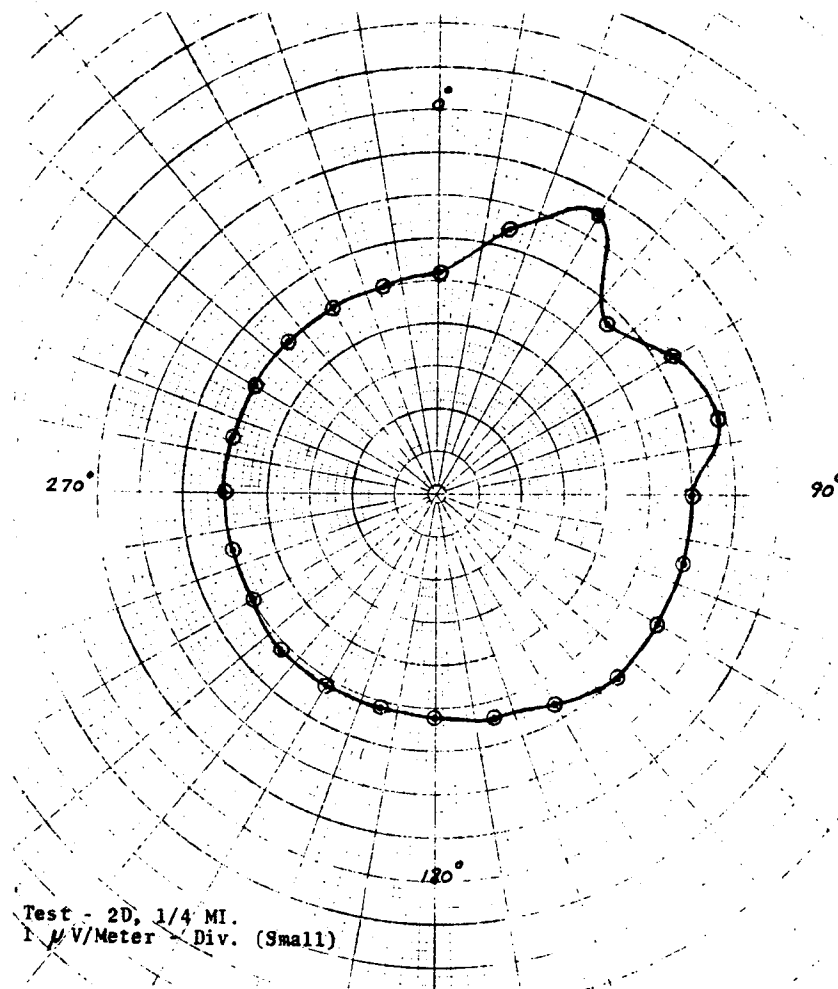


FIGURE 3-20. FIELD STRENGTH VS. ANTENNA ORIENTATION FOR A MODULATED, BATTERY POWERED, HORIZONTALLY POLARIZED, BREADBOARD TRANSMITTER ENCAPSULATED IN A WHEEL SIMULATOR AT A DISTANCE OF 1/4 MILE

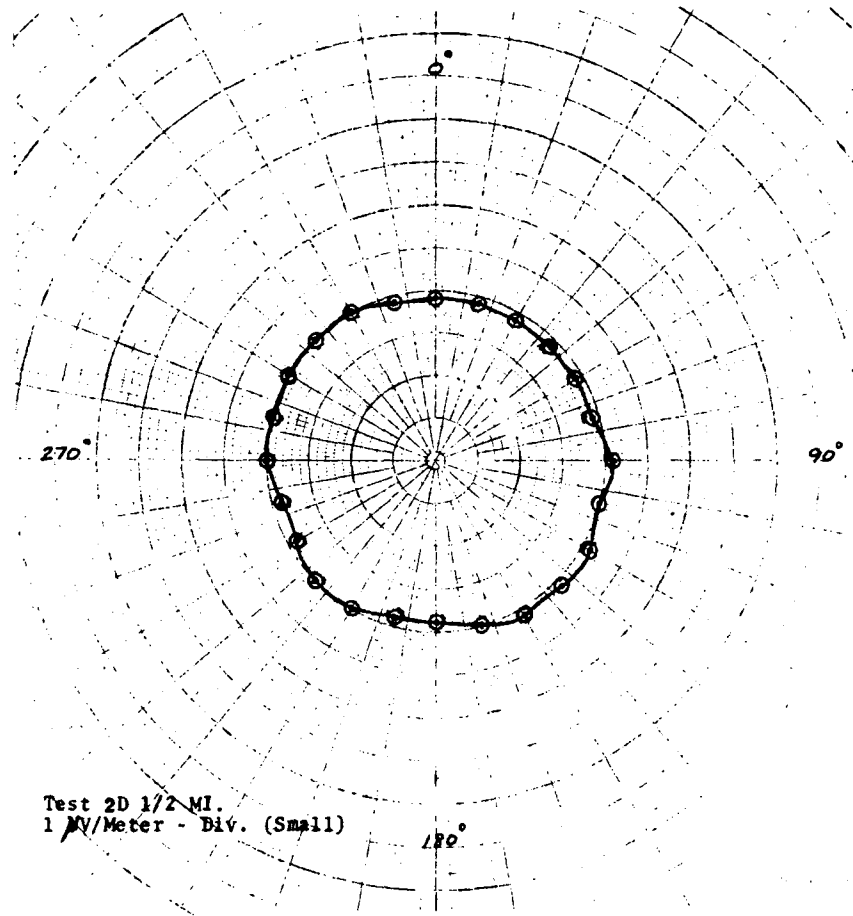


FIGURE 3-21. FIELD STRENGTH VS. ANTENNA ORIENTATION FOR A MODULATED, BATTERY POWERED, HORIZONTALLY POLARIZED, BREADBOARD TRANSMITTER ENCAPSULATED IN A WHEEL SIMULATOR AT A DISTANCE OF 1/2 MILE

TABLE 3-7. MEASURED VOLTAGE AND ELECTRIC FIELD STRENGTH DATA AS A FUNCTION OF ANTENNA ORIENTATION FOR A MODULATED, BATTERY POWERED, HORIZONTALLY POLARIZED, BREADBOARD TRANSMITTER ENCAPSULATED IN A HOODED WHEEL SIMULATOR AT DISTANCES OF 30 FEET, 1/4 MILE, AND 1/2 MILE

Antenna Rotation Angle (deg)	TRANSMISSION DISTANCE					
	30 FEET		1/4 MILE		1/2 MILE	
	Voltage (dB*)	Field Strength (μ V/m)	Voltage (dB*)	Field Strength (μ V/m)	Voltage (dB*)	Field Strength (μ V/m)
0	46	216	17	23	8	18
15	46	216	15	21	8	18
30	46	216	14	21	9	19
45	48	267	14	21	8	18
60	52	414	17	23	9	19
75	52	414	18	24	8	18
90	46	216	15	21	9	19
105	57	724	16	22	12	20
120	64	1596	26	36	12	20
135	64	1596	29	44	14	21
150	63	1426	29	44	14	21
165	63	1426	26	36	12	20
180	64	1596	25	44	12	20
195	63	1426	26	44	12	20
210	62	1276	27	38	12	20
225	60	1016	24	32	12	20
240	60	1016	16	22	9	19
255	52	414	9	19	8	18
270	50	332	9	19	9	19
285	55	578	14	21	10	19
300	55	578	11	19	9	19
315	55	578	18	24	8	18
330	47	240	16	22	8	18
345	50	332	18	24	8	18

*decibels relative to 1μ V.

TEST - 2E

Transmitter Test Conditions:

V_{cc} - 5 V

I_{in} - 37 mA

P_{in} - 185 mW

$I_c(ac)$

$I_c(dc)$ 20 mA

Ant length - 1 in.

Carrier freq - 450 MHz

Modulation freq - 1000 Hz

DATE-5-76

Test Fixture:

(1) Free space

(2) Wheel simulator - X

(3) Other -

Transmitter ant polarization - HORZ

Transmitter ant height - 36 in.

Receiving ant polarization - HORZ

Receiving ant ht - 36 in.

Receiving ant length - 14 in.

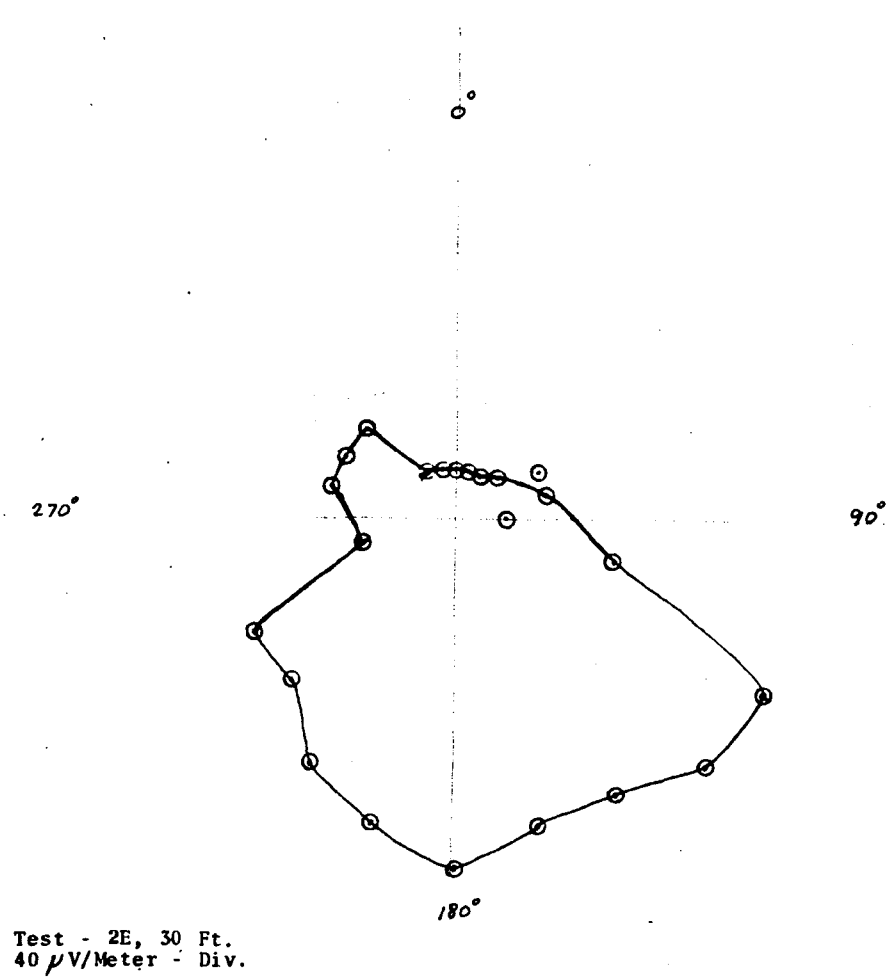


FIGURE 3-22. FIELD STRENGTH VS. ANTENNA ORIENTATION FOR A MODULATED, BATTERY POWERED, HORIZONTALLY POLARIZED, BREAD-BOARD TRANSMITTER ENCAPSULATED IN A HOODED WHEEL SIMULATOR AT A DISTANCE OF 30 FEET

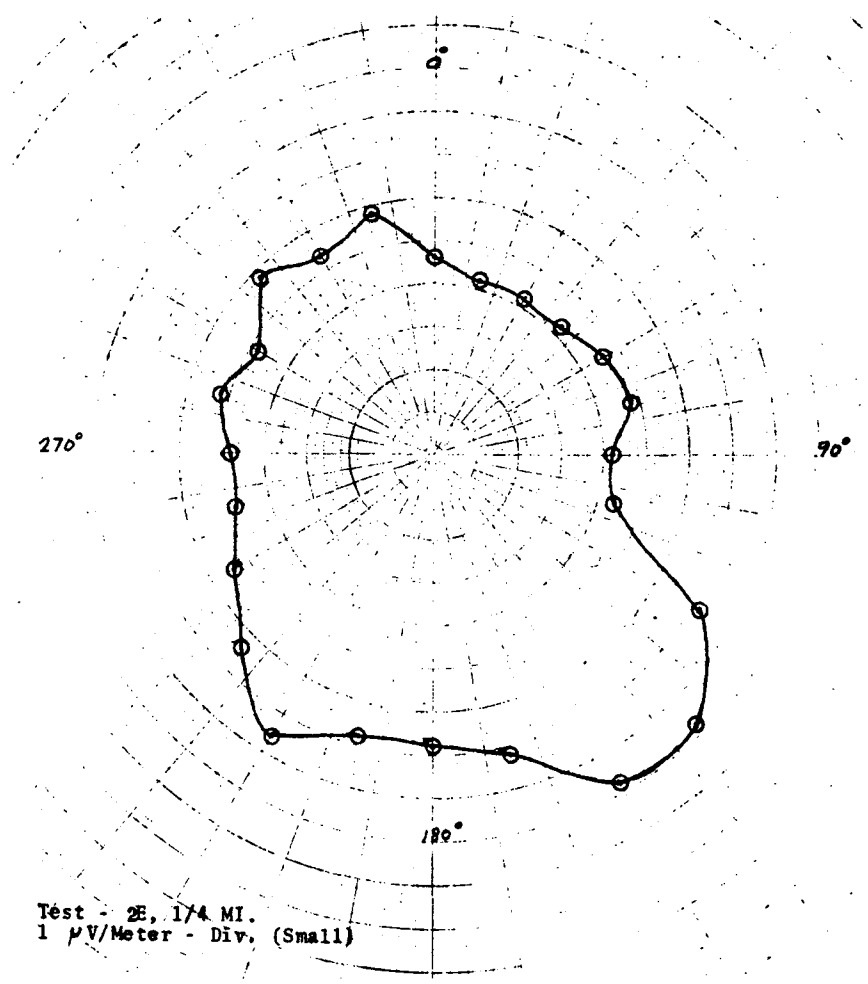


FIGURE 3-23. FIELD STRENGTH VS. ANTENNA ORIENTATION FOR A MODULATED, BATTERY POWERED, HORIZONTALLY POLARIZED, BREAD-BOARD TRANSMITTER ENCAPSULATED IN A HOODED WHEEL SIMULATOR AT A DISTANCE OF 1/4 MILE

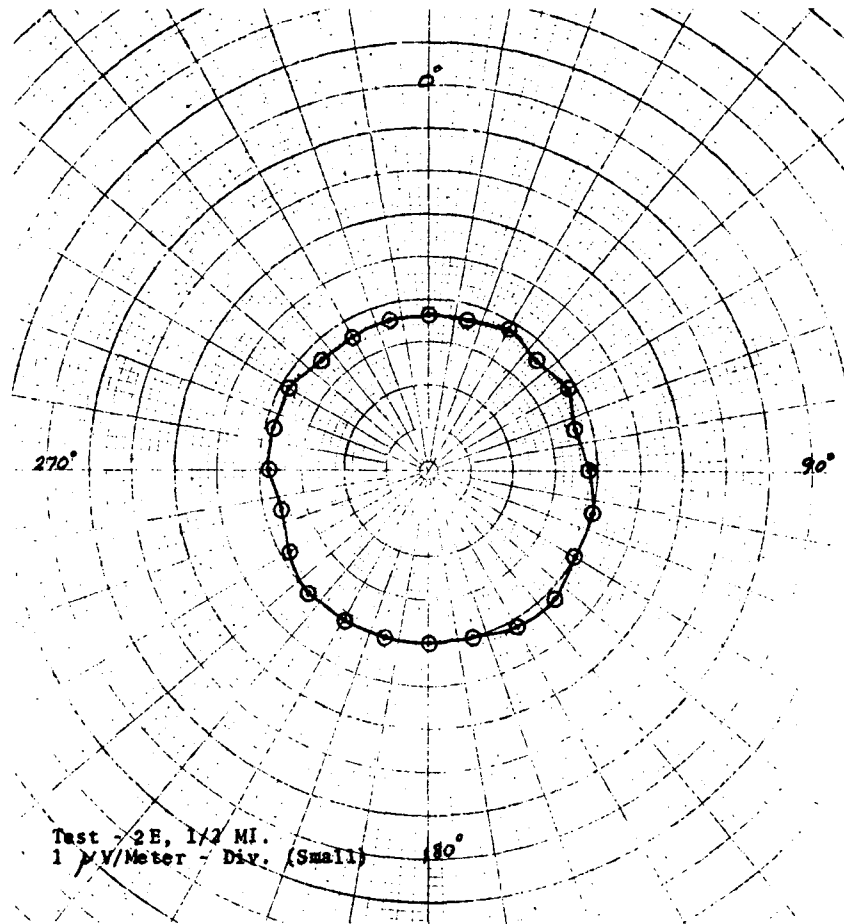


FIGURE 3-24. FIELD STRENGTH VS. ANTENNA ORIENTATION FOR A MODULATED, BATTERY POWERED, HORIZONTALLY POLARIZED, BREADBOARD TRANSMITTER ENCAPSULATED IN A HOODED WHEEL SIMULATOR AT A DISTANCE OF 1/2 MILE

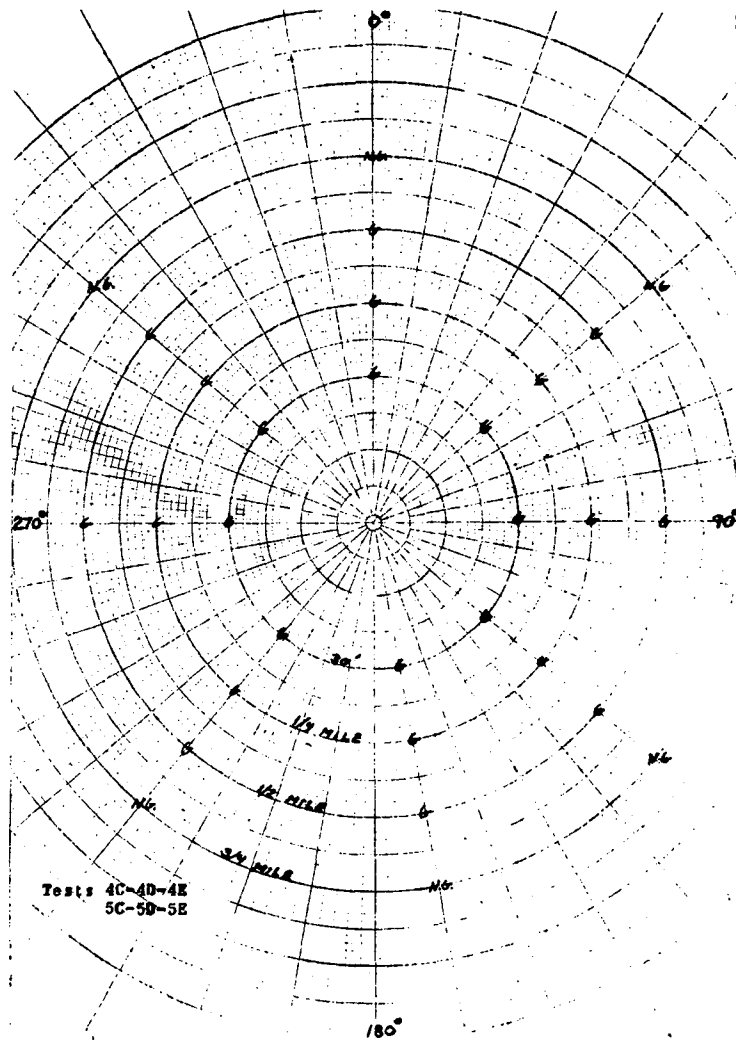


FIGURE 3-25. "GO" - "NO GO" VERIFICATION OF TRANSMITTED SIGNAL AT A DISTANCE OF 30 FEET, 1/4 MILE, AND 1/2 MILE FOR MODULATED, HORIZONTALLY POLARIZED, THERMALLY AND BATTERY POWERED, PROTOTYPE BREADBOARD TRANSMITTER

Comparison of the results of tests 2C and 2D with those of 2B indicate that reflection characteristics of a wheel simulator yield a marked overall increase in measured field intensity.

It thus appears that the proximity of a grounded circular reflector such as a railroad wheel will serve to aid rather than hinder the implanted transmitter, and therefore, data acquired for the "free-space" tests of 3B, 4B, 5B are not reported.

At the request of the sponsor, the tests of 2D above were augmented by placing a sheet metal "roof" over the wheel simulator in order to approximate the reflective and/or absorptive effects of the underside of a railroad car. Data accumulated for these tests (2E) were shown in Table 3-7 and in Figures 3-22 through 3-25, and it is seen that only slight attenuation in transmitted power was observable under this condition.

For further augmentation the results of test 2E were duplicated along the length of a train stopped at a local railroad siding. Although field strength measurements were unattainable, use of a battery powered receiver capable of "picking up" (but not quantitatively evaluating) the modulated carrier, verified that the transmitter signal was observable at distances up to one-half mile.

For performance of tests 4C, 4D and 4E, the sensor circuits described in Section 3.5 were utilized as transmitter activation switches. Field strength measurements were not accumulated, but verification of signal detectability vs. distance and antenna orientation was determined by use of an RF receiver. The plots of Figure 3-25 show go (g) and no-go (ng) data accumu-

lated for these tests. The transmitter was activated for these tests by applying heat to a proposed resistance thermometer and by relieving the strain on the proposed strain gage. Threshold settings for these devices were $210^{\circ}\text{F} \pm 10^{\circ}\text{F}$ and 200 ft-lb respectively.

Tests 5C, 5D, and 5E demonstrated that transmitter operation with a thermoelectric power source, is feasible. (go) - (no-go) data for these tests were coincident with those of tests 4C, 4D, and 4E. Since tests 5 and 3 are identically related to tests 4 and 2 respectively, the results of tests 3C, 3D, and 3E are omitted.

3.3.3 Conclusions and Final Transmitter Specifications

The results of tests reported in Section 3.3.2 above indicate that a horizontally polarized, 450 MHz transmitter, implanted in a railroad axle cap bolt, will be perceptible by an "off-the-shelf" receiver at a distance of up to one-half mile from the point of transmission. This will permit train crew perception of signals emanating from any bearing of a one-mile-long train having receivers in the engine and caboose.

A potential vendor for eventual supply of such transmitters in large quantity was found. This vendor has agreed to supply (for further tests as part of a follow-on effort) implantable, 450 MHz, transmitters having the following specifications:

V_{cc}	5 V
Power Output	20 mW, 50 Ω load
Stability	< 7 MHz 0° to 65°C

Modulation	1 kHz Square wave (TTL compatible)
Deviation	>10 MHz for 5V modulation input
Size	.05 in. dia x .156 in. ht.

The feasibility of implanting a transmitter with proper output characteristics in an axle cap bolt is thus established.

3.4 THERMOELECTRIC POWER SOURCE SPECIFICATION

Establishment of the feasibility of constructing and implanting of a source of electrical power capable of operating the transmitter described in Section 3.3 is described below.

It was established by the tests of Section 3.3.2 that 250 mW (5 V dc) is sufficient to drive an implanted transmitter. The electrical power source must be small enough to be implanted within an axle cap bolt without destroying or seriously derating the mechanical properties of the axle cap bolt itself.

There are, of course, several sources of energy available in an operating railroad bearing. Rotational energy, vibratory energy, and thermal energy are abundant in and around an operating bearing. To be useful, however, any of these must be convertible to electrical energy and easily transferable from the point of conversion to the transmitter. In addition, there is a storage requirement, since, in order to conduct a pull-by inspection for the purpose of isolating a transmitting bearing, the power source must be available for some time after the train has been stopped or its speed reduced.

Thermal energy, by virtue of its proximity to the implanted transmitter and its "inertia," is considered the prime conversion candidate.

The feasibility of using commercially available thermoelectric power sources (thermopiles) for energy conversion is established below.

3.4.1 Maximum Power Source Operating Temperature

Work performed at the laboratory of Norfolk and Western Railway [7] has established temperature profiles in heated static bearings to be as depicted in Figure 3-26. These data were accumulated by implantation of thermocouples at the location depicted in Figure 3-27. From these data, expected temperature profiles to be experienced by a thermopile package implanted in an axle bolt cap can be extracted.

It can be seen from Figure 3-26 that the maximum inner race temperature that can be safely experienced is 220°F, and that at this temperature the axle cap bolt temperature is 200°F. This was determined to be the maximum operating temperature for the thermoelectric power source, since bearing operation yielding an interior temperature above this limit would have produced inner race temperatures in excess of 210°F and, thus, would have damaged the bearing itself.

3.4.2 Determination of Package Size (Volume)

The power source under consideration must be implantable and have minimal deleterious effects on the mechanical properties of the bolt itself. The volume required of a given thermopile is directly related to the output power requirement. The requirement of 250 mW at 5V has been determined in Section 3.3.

Norfolk and Western Railway Company

Temp. Sensitive Cap Screws
 For Journal Roller Bearings
 Project No. 4-69
 Temp. Profile of Journal and Cap Screws

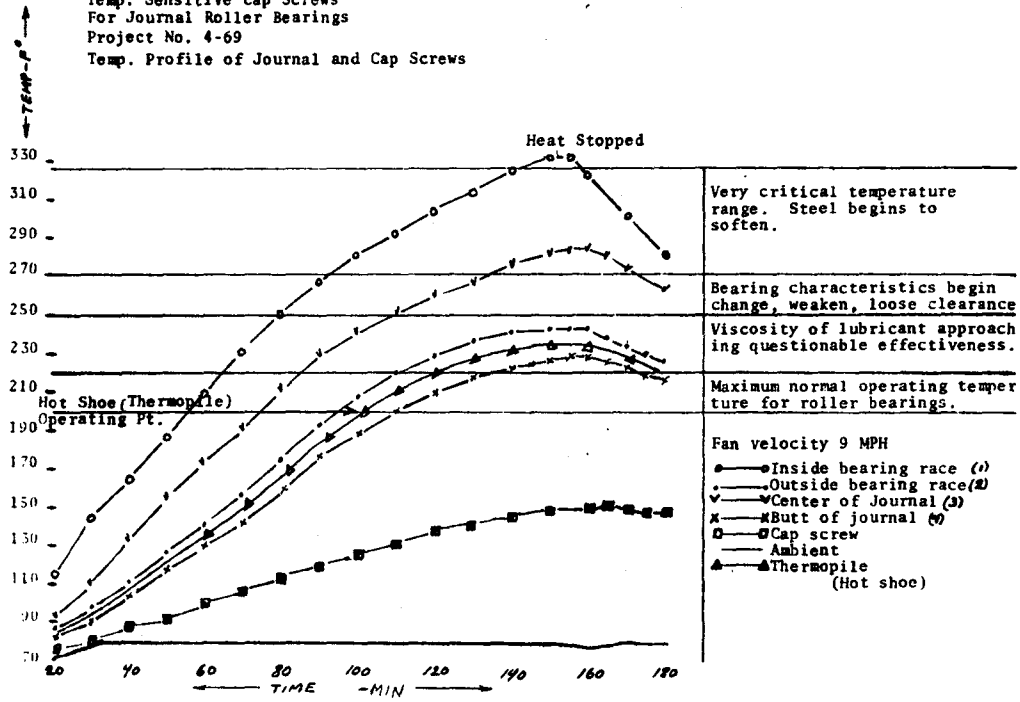


FIGURE 3-26. TEMPERATURE PROFILE OF JOURNAL AND CAP SCREWS

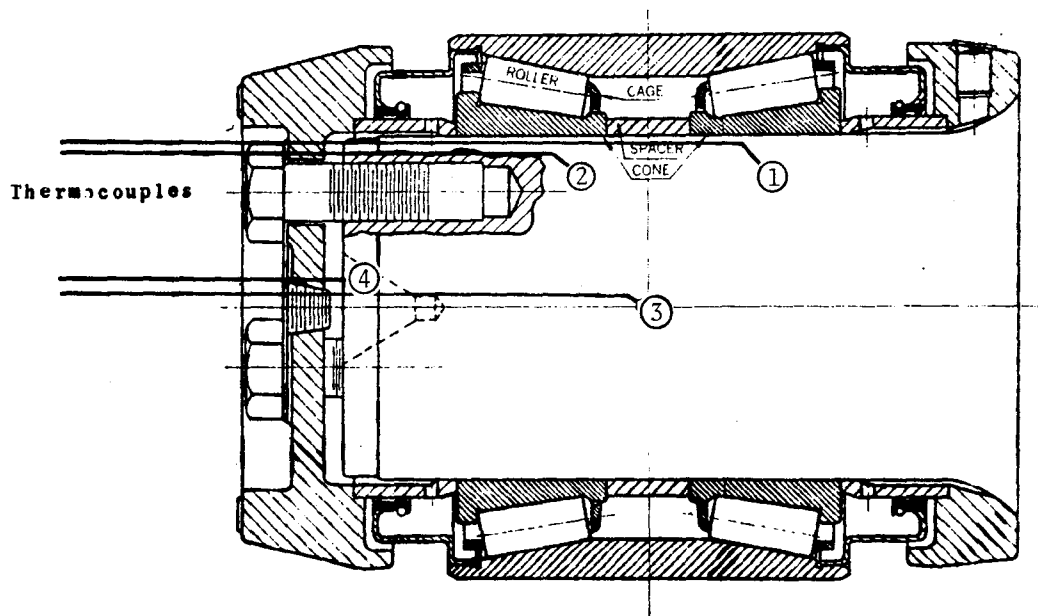
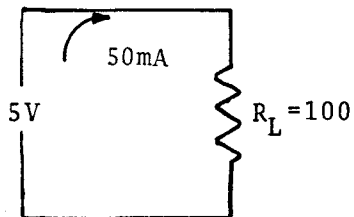


FIGURE 3-27. THERMOCOUPLE LOCATIONS DURING STATIC TESTS TO DETERMINE TEMPERATURE PROFILE OF STANDARD RAILROAD JOURNAL AND CAP SCREWS

Commercially available thermopiles (which are a series connection of many thermocouples) are routinely used for the conversion of thermal to electrical energy. A typical thermocouple element available as an off-the-shelf item measures .027 in. long x .027 in. wide x .05 in. high. Calculation of the number of thermocouples needed for transmitter power proceeds as follows:

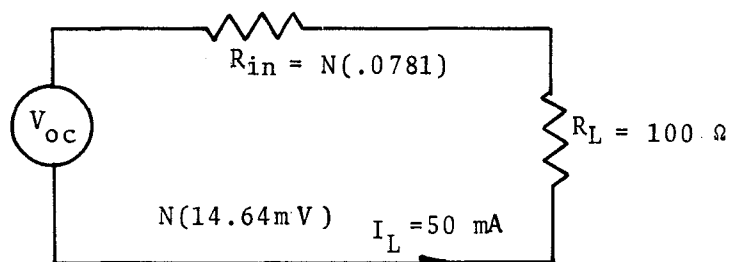
Assuming a differential temperature of 66°F across each element, the electrical specification of the total system are as listed below:

$$\begin{aligned} V_{\text{out}} &= 5 \text{ V} \\ I_{\text{out}} &= 50 \text{ mA} \\ R_L &= 100 \cdot \Omega \end{aligned}$$



From laboratory measurements described later, the internal resistance of each thermocouple is $.0781\Omega$. The open circuit thermoelectric voltage available is $400 \mu\text{V}/\text{C}^\circ$.

At a differential temperature of 36°C , each thermocouple supplies 14.64 mV . The thermopile equivalent circuit for thermocouples of this type is:



The number of thermocouples (N) necessary to power the required load is given by

$$N = \frac{I_L (R_L)}{V_{oc} - I_L R_{in}} \quad (8)$$

Substituting the appropriate quantities,

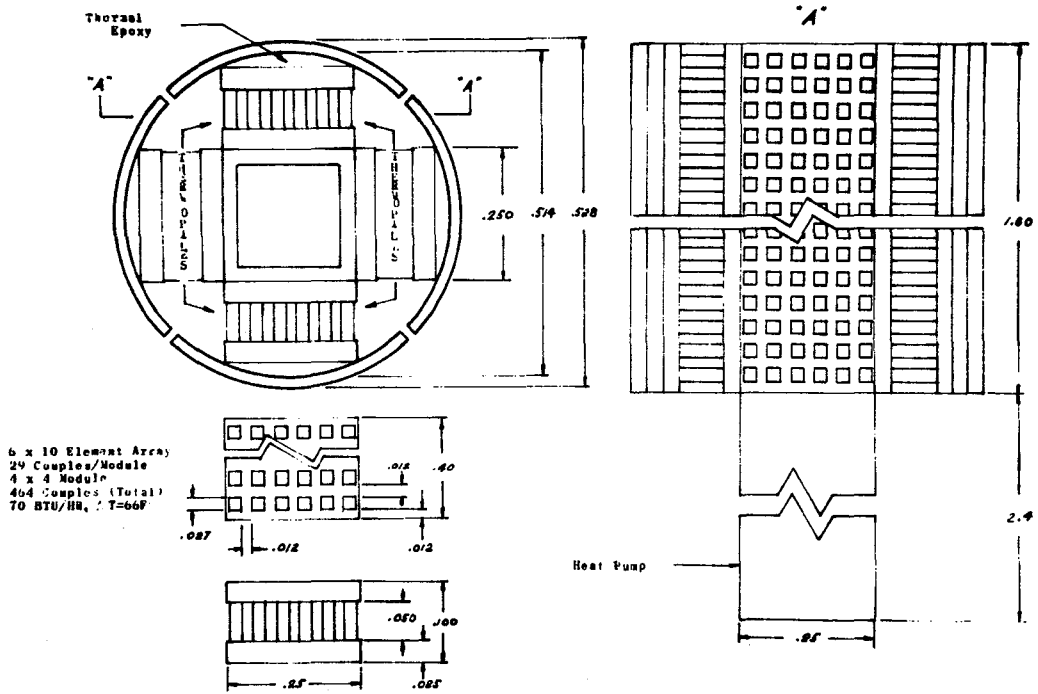
$$N = 466 \text{ thermocouples}$$

A sketch of a proposed arrangement of commercially available thermoelectric elements is shown in Figure 3-28. Sixteen separate thermoelectric modules will be utilized. The overall thermopile package dimensions are 1.60 in. length and .528 OD. Each thermoelectric module will contain 29 thermocouples (i.e. 58 thermocouple elements arranged in a 6 x 10 matrix with two corner elements missing for interconnection.) The dimensions of each element are 0.1 in. long, 0.25 in. wide and 0.4 in. high.

To accommodate the required thermopile, therefore, it is necessary to drill a hole of 0.528 diameter in the center of the transmitter bolt.

Consequential Mechanical Derating of Hollowed Bolt

The mechanical derating of a modified axle cap bolt as a result of its hollow center is detailed in Section 3.5. It is seen that a 17/32" diameter hole will reduce tensile strength by 36 percent and, as a consequence, the transmitter bolt must be manufactured from an alloy having tensile strength sufficient to overcome such mechanical derating.



ALL DIMENSIONS SHOWN IN INCHES

FIGURE 3-28. PACKAGING PROPOSAL FOR THERMOELECTRIC POWER SOURCE OF TEMPERATURE/STRAIN SENSING TRANSMITTER BOLT

3.4.3 Thermal Analysis of Thermoelectric Power Source

3.4.3.1 Heat Flow Across Thermopile

Assumed in the calculation of Section 3.4.2 is the ability to continuously maintain 36°C differential across each thermocouple element. The amount of heat transferred across each thermocouple element from [5] is given by:

$$q = \frac{kA}{L} (T_C - T_H) \quad (9)$$

where

$$\begin{aligned} q &= \text{heat transfer - BTU hr} \\ k_f &= \text{Thermal conductivity of each} \\ &\quad \text{element BTU/in-hr } ^\circ\text{F} \\ A &= \text{cross sectional area (in}^2\text{)} \\ L &= \text{length of each element (in)} \\ T_C &= \text{cold side temperature } ^\circ\text{F} \\ T_H &= \text{hot side temperature } ^\circ\text{F.} \end{aligned}$$

From manufacturer supplied literature,

$$k_f = 7.703 \times 10^{-2} \text{ BTU/in-hr-}^\circ\text{F and substituting,}$$

$$q = 7.41 \times 10^{-2} \text{ BTU/hr/element.}$$

Since there are 930 elements needed, 68.9 BTU/hr must be transferred across the requisite thermopile package.

3.4.3.2 Heat Exchanger Design

The dissipation of 70 BTU/hr is the subject of this section. Calculations have shown that a solid copper insert in contact with the cold "shoes" of the proposed thermopile package, as shown in Figure 3-28 would be unable to carry 70 BTU/hr away from the thermopile with the differential temperature environment expected. For that reason, a heat exchanger assembly shown in Figure 3-29 composed of a "heat pipe" and forced convection cooling fins is a necessary adjunct to the generation of thermoelectric power.

The function of the heat pipe is to transfer large amounts of thermal energy from the interior of the axle cap bolt to the bolt head. The heat pipe is composed of a hollow evacuated rod containing an evaporative liquid (such as water). It operates by absorbing thermal energy of the entrapped fluid at its "hot" end and releasing this energy at its opposite end by condensation. This process can continue ad infinitum if the energy lost to the "cold" end can be continuously carried away, i.e., if the cold end can be considered an infinite heat sink.

Such heat dissipation is the function of the forced convection cooler (fins) of Figure 3-30. Heat carried away from the cold side of the thermopile (after being transferred by the heat pipe) is lost to the atmosphere by the convective action of the fins.

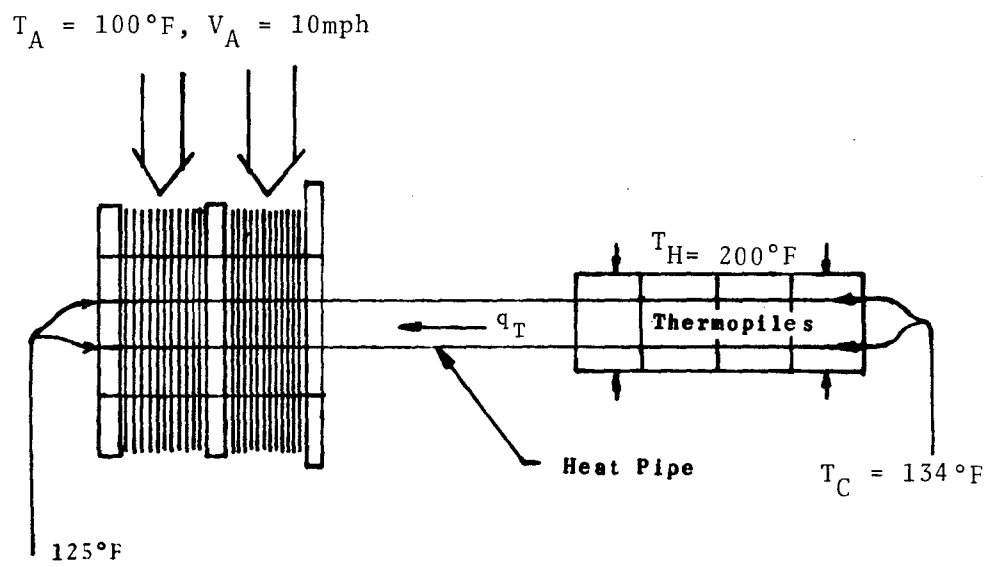


FIGURE 3-29. THERMAL MODEL OF PROPOSED THERMOPILE AND HEAT EXCHANGER ASSEMBLY

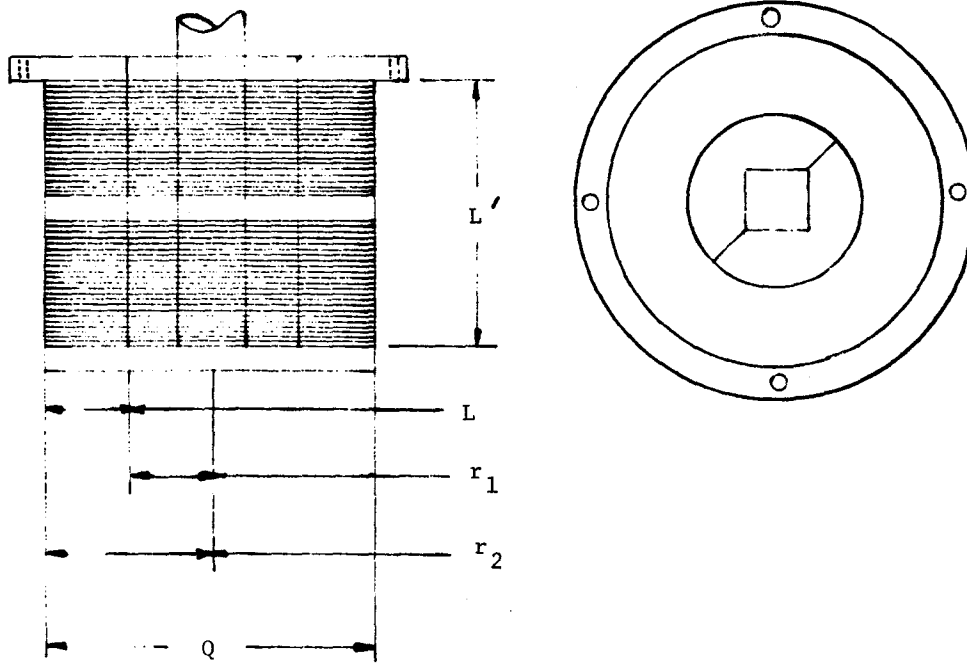


FIGURE 3-30. CONVECTION COOLER SUBASSEMBLY

Heat pipe capacity is calculated by use of the following equation from [6]:

$$q_{hp} = \frac{(QZ)}{L} \left[\frac{T_H - T_C}{18^\circ\text{C}} \right] \quad (10)$$

where the power-length product, (QZ), as taken from manufacturer's specifications is 600 W-in, and a $\Delta T (=T_H - T_C)$ of 18°C is assumed. A 1/4 in. heat pipe of 4 in. length is capable of transferring roughly four times the thermal energy required to operate the proposed power source, i.e. from Eq. (10).

$$q_{hp} = 283 \text{ BTU/hr @ } 5^\circ\text{C } \Delta T, \text{ i.e. } (T_H - T_C) = 5^\circ\text{C}.$$

Calculation for heat dissipation capabilities for the fin arrangement of Figure 3-31 proceeds as follows. (Refer to Figure 3-32 for physical parameter description.) An equation used to approximate maximum heat loss for a finned heat exchanger from [5] given by

$$q_{\max} = 2h\pi \left[r_{2c}^2 - r_1^2 \right] \Delta T \quad (11)$$

where

- h = average heat transfer coefficient
BTU/hr - ft - F°
- ΔT - difference in temperature existing
between the tube surface temperature
and the ambient gas, F°
- r_{2c} = $r_1 + L_c$ (ft)
- r_1 - tube surface radius (ft).

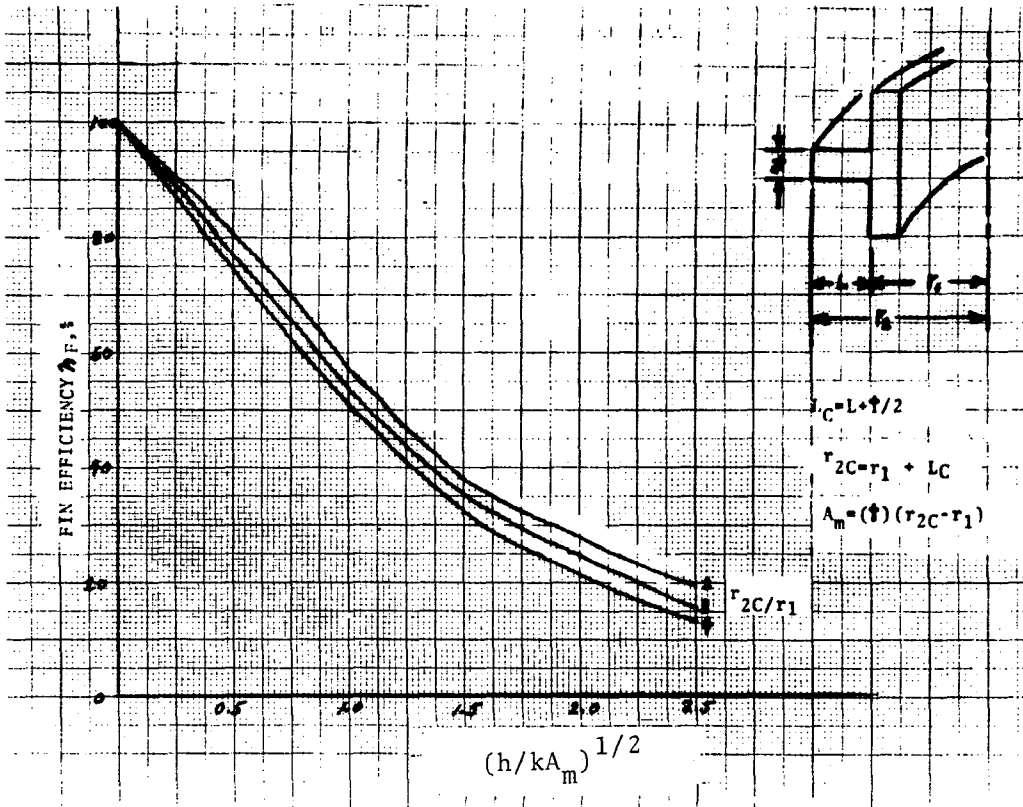


FIGURE 3-31. EFFICIENCIES OF CIRCUMFERENTIAL FINS OF RECTANGULAR PROFILE (AFTER HOLMON, [5])

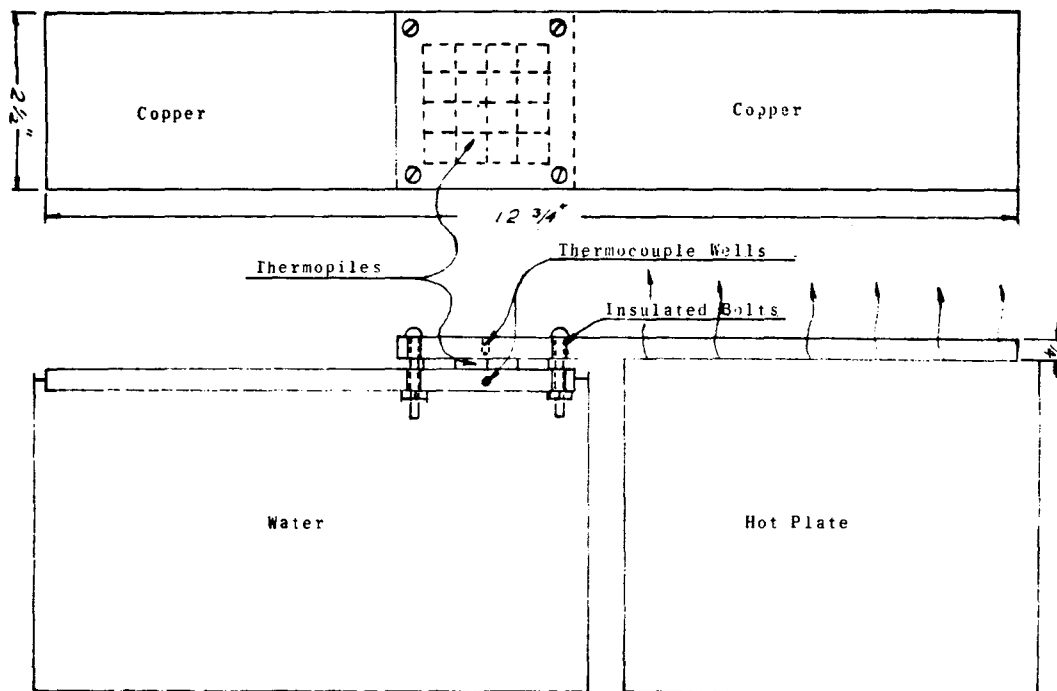


FIGURE 3-52. LABORATORY TEST FIXTURE FOR DETERMINATION OF INTERNAL RESISTANCE OF OFF-THE-SHELF THERMOPILE ASSEMBLIES

The actual heat transfer rate is then the product of heat flow (q_{\max}) and fin efficiency, i.e.:

$$q_{\text{actual}} = \eta (q_{\max}) \quad (12)$$

where η = fin efficiency (%).

Fin efficiency is a function of fin geometry and can be determined by using the equations and graph found in Figure 3-31.

Because of the complicated nature of the flow-separation process, it is not possible to calculate analytically the average heat-transfer coefficients in cross flow; however, correlations of the experimental data (reference [7]) indicate that the average heat-transfer coefficients for gases for use in Eq. (11) may be calculated with

$$h = \frac{Ck_f}{d} \left[\frac{V_A d}{\nu} \right]^n \quad (13)$$

where ν - kinematic viscosity of air, ft²/sec
 d - tube diameter (ft)
 V_A - air velocity (ft/sec)
 k_A - thermal conductivity of air (BTU/hr-ft-°F)

and the constants C and n are tabulated in Table 3-8 as functions of the Reynolds number (5).

TABLE 3-8. REYNOLDS NUMBER TABULATION (FROM HOLMAN [5])

Re_{df}	C, for gases	n
0.4-4	0.891	0.330
4-40	0.821	0.385
40-4,000	0.615	0.466
4,000-40,000	0.174	0.618
40,000-400,000	0.0239	0.805

The Reynold's number needed to determine the constants (C) and (n) in Table 3-8 above can be calculated using the following equation from [5]:

$$Re = \frac{V_A d}{\nu} \quad (14)$$

where, ν - kinematic viscosity of air
 d - tube diameter (OD) (ft)
 V_a - air velocity (ft/sec)

Substituting,

$$Re_{df} = \frac{V_A d}{\nu}$$

$$V_A = 10 \text{ mph} = 14.66 \text{ ft/sec}$$

$$d = 0.864 \text{ in.} = 0.072 \text{ ft}$$

$$\nu = 0.23 \times 10^{-3} \text{ ft}^2/\text{sec}$$

Thus,

$$Re_{df} = 4589.$$

Returning to Eq. (13), $h = \left[\frac{Ck_A}{d} \right] \left[\frac{V_A d}{v} \right]^n$

where

C	=	0.174	}	from Table 3-8
n	=	0.618		
k_A	=	0.0157 BTU/hr-ft-° F @ 100°F		
d	=	0.875/12 = .072 ft		
V_A	=	14.66 ft/sec , 10 mph		
v	=	0.23 x 10 ⁻³ ft ² /sec and thus,		
$h_{(10 \text{ mph})}$	=	6.94 BTU/hr-ft ² -F° @ 10 mph		
$h_{(30 \text{ mph})}$	=	13.6 BTU/hr-ft ² -F° @ 30 mph		

for wind (train) speeds of 10 and 30 mph.

The maximum for heat transfer (q_{\max}) at train speeds of 10 mph is calculated from Eq. (11).

$$q_{\max} = 2 \pi h [r_{2c}^2 - r_1^2] \Delta T$$

where

$h_{(10 \text{ mph})}$	=	6.94 BTU/hr-ft ² -F° from Eq. (13)
r_{2c}	=	$r_1 + L + t/2$
	=	0.053 ft, when $r_1 = 0.026$ ft. and
		$\Delta T = 25^\circ\text{F}$.

Substituting,

$$q_{\max} (10 \text{ mph}) = 2.46 \text{ BTU/hr/fin.}$$

Next, the fin efficiency is determined From Figure 3-31 by first calculating,

L_c	=	$L + t/2$
	=	0.027 ft.

Now, also from Figure 3-31,

$$\begin{aligned} r_{2c} &= r_1 + L_c \\ &= .53', \\ A_m &= (t) (r_{2c} - r_1) \\ &= 2.70 \times 10^{-5} \end{aligned}$$

$$\text{and } L_c \frac{3}{2} (h/kA_m)^{1/2} = .410 \quad (\text{for } k = 30).$$

Since $\frac{r_{2c}}{r_1} = 2$, we determine from the graph of Figure (3-37) that $\eta = 85\%$. Therefore Eq. (12) yields
 $q(\text{actual}) = (q_{\text{max}}) \eta = (2.46) (.85) = 2.09 \text{ BTU/hr/fin}$

It is therefore seen that 35 fins of 1.25 in. diameter and .012 in. spacing are therefore needed to dissipate 70 BTU/hr.

The analytical feasibility of providing thermoelectric power sufficient to operate the transmitter bolt is thus established. Package dimensions was shown in Figure 3-28. A thermal model showing the "temperature drops" calculated across each thermal subsystem was shown in Figure 3-29.

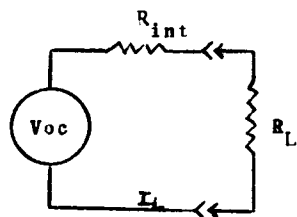
3.4.4 Laboratory Test of Candidate Thermopile

The success of the thermoelectric power system described above is dependent on the fact that output power and elemental internal resistances can be repeatably supplied. For that reason, three off-the-shelf thermopile units were tested on the fixture shown in Figure 3-32. Heat was supplied to the "hot" side of the thermopile by a hotplate and extracted from the cold side by the "infinite" heat sink of the water filled container. The thermopile elements were affixed to the copper plates with a tightening

TABLE 3-9. TABULATION OF TEST DATA FOR CALCULATION OF AVERAGE INTERNAL RESISTANCE OF OFF-THE-SHELF THERMOPILE ASSEMBLIES

Open Circuit Voltage (mV)			Load Resistance	Load Voltage	Load Current	R_{INT}
Before Test	After Test	Avg.	ohms	mV	mA	ohms
1. 308	302	305	10.51	248	23.5	2.42
2. 301	293	297	10.51	240	22.8	2.50
3. 286	278	282	10.51	229	21.7	2.44
4. 336	330	333	10.51	270	25.6	2.40
5. 330	322	326	10.51	264	25.1	2.47
6. 320	312	316	10.51	256	24.3	2.46
1. 333	324	328.5	1.34	122	91.0	2.26
2. 322	314	318	1.34	118	88.0	2.27
3. 312	304	308	1.34	115	85.8	2.24
4. 302	292	297	1.34	111	82.8	2.24
5. 291	282	286	1.34	107	79.8	2.24
6. 281	272	276	1.34	103	76.3	2.25
1. 270	266	268	23.18	243	10.4	2.40
2. 340	337	339	23.18	306	13.2	2.50
3. 335	330	332	23.18	301	12.9	2.05
4. 326	321	323	23.18	293	12.6	2.42
5. 319	313	316	23.18	286	12.3	2.43
6. 312	307	309	23.18	280	12.0	2.45

EQUIVALENT CIRCUIT USED IN ABOVE TESTS



torque of 14 in-lb and their interfaces were coated with thermal grease. External thermocouples were used for hot and cold side temperature monitoring.

Output voltage as a function of load resistance for the circuit of Table 3-9 is tabulated in the same Table. Internal resistance was calculated for each of three load resistances. All data were accumulated with a thermopile differential temperature of $26^{\circ}\text{C} \pm 2^{\circ}\text{C}$.

The average internal resistance for these couples is seen to be 2.44Ω . Since this is the average of 32 couples, an average internal resistance of 0.076Ω per couple was determined. This value was used in the calculations of Section 3.4.2 above. It differs from the published specification by 63 percent. The manufacturer, however, has stated that, even though these particular units did not conform to his published specifications, future conformance is attainable with tightened quality control methods.

The feasibility of obtaining parts and building the necessary power and heat exchanger subsystems has been analytically established. Further empirical verification of their feasibility, although beyond the scope of the current contract, is a necessary first step toward the continued development of this Transmitter Bolt.

3.5 SELECTION OF TEMPERATURE AND STRAIN SENSORS AND THRESHOLD CIRCUITRY

3.5.1 Temperature Sensor Specifications

From the work performed at Norfolk and Western Railroad [8] (Figure 3-26), it is seen that the maximum allowable bearing temperature as sensed at the maximum penetration depth of an axle cap bolt is approximately 200°F. The target threshold temperature for activation of the transmitter is, therefore, defined as 200°F.

To accomplish this, a temperature sensitive element will be placed within the bolt as was shown in Figure 3-5.

A commercially available nickel/phenolic resistance thermometer has been chosen as the candidate temperature sensor.

Table 3-10 shows a compilation of published manufacturers specifications. From Figure 3-26, it is seen that resistance variation as a function of temperature is relatively constant over the proposed operating range of the device i.e. 70-200°F. A gage having a basic resistance of 50 Ω at 70°F and a temperature coefficient of .19 Ω /°F. will be used. A vendor survey indicates that gages having this specification can be repeatably produced in high volume.

3.5.2 Gage Amplifier and Threshold Circuitry

The resistance thermometer (R_G) described above will be used in the integratable circuit shown in Figure 3-33. This circuit consists of a full bridge, a unity gain differential amplifier, a noninverting amplifier and a threshold level discriminator.

TABLE 3-10. TABULATION OF RESISTANCE RATIO VS. TEMPERATURE FOR A COMMERCIALY AVAILABLE RESISTANCE THERMOMETER

Temp °F	R/R _{70°F}	Δ/o _F	Temp. °F	R/R _{70°F}	Δ/o _F
70	1.000	.0031	155	1.277	"
75	1.016	"	160	1.295	.0035
80	1.031	"	165	1.312	"
85	1.047	"	170	1.329	"
90	1.063	.0032	175	1.347	"
95	1.079	"	180	1.365	.0036
100	1.095	"	185	1.383	"
105	1.111	"	190	1.401	"
110	1.127	"	195	1.419	"
115	1.144	"	200	1.437	.0037
120	1.160	.0033	205	1.456	"
125	1.176	" * - - -	210	1.474	"
130	1.193	"	215	1.493	"
135	1.209	"	220	1.511	"
140	1.226	.0034	225	1.530	.0038
145	1.243	"	230	1.549	"
150	1.260	"	235	1.568	"

*Alarm temperature of transmitter bolt. Gage resistance at this temperature is 73.7 ohms.

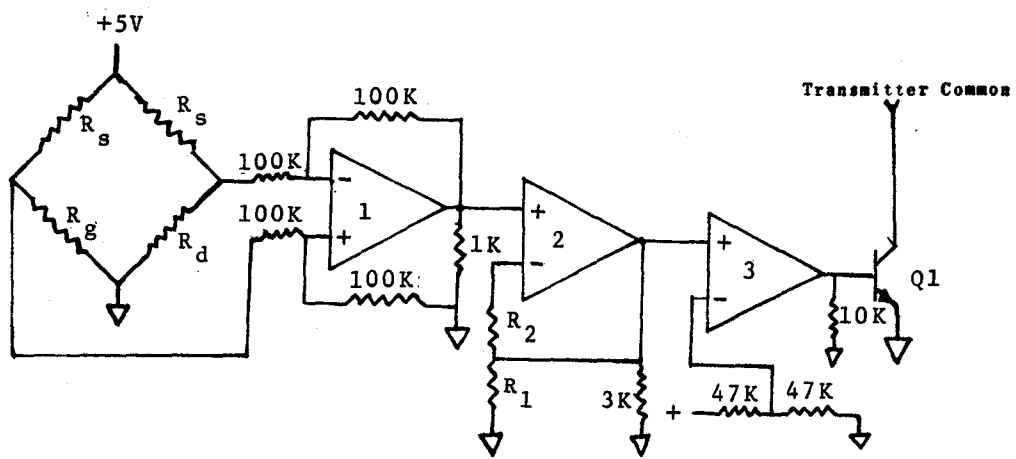


FIGURE 3-33. GAGE AMPLIFIER AND THRESHOLD CIRCUIT

A vendor survey has established the reproducibility of this circuit on an integrated circuit "chip" of 2 mm x 2 mm (0.079 in. x 0.079 in.).

A small circuit board containing discrete resistors R_S and R_D will be incorporated into each bolt at manufacture to ensure known bridge imbalance at the threshold temperature. (The integrated circuit "chip" will be fastened to the small circuit card containing the discrete components.) The use of integrated circuits in the temperature and vibration environment to be experienced inside an axle cap bolt is not novel.

The ground lead of the transmitter of Figure 3-6 is connected to the collector of output transistor (T_1) and is thus activated when the threshold set by combination R_3 and R_4 is exceeded. Actual fabrication of the integrated circuit shown in Figure 3-33 was beyond the scope of this task and thus manufacturing limits for the circuit parameters of the "chip" are unknown.

It was for that reason, that feedback amplifiers (having gains dependent on resistance ratios rather than absolute values) and discrete components (R_S and R_D) were included in the amplifier and threshold circuit design.

The overall threshold temperature accuracy for a mass-produced device is estimated to be approximately $\pm 5^\circ\text{F}$, since the basic gage resistance, which is expected to be the least repeatable component, is reproducible to within ± 2 percent.

3.5.3 Strain Sensor Selection and Test

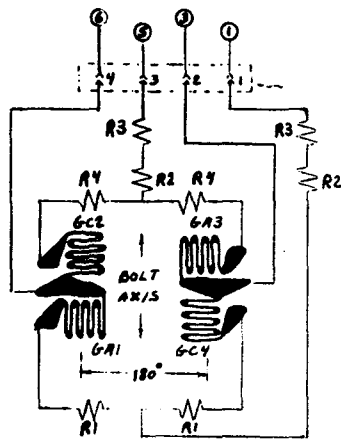
A candidate full bridge, metal foil, 350 Ω strain gage circuit is depicted in Figure 3-34. Excitation voltage will be supplied by the encapsulated thermal power source.

A vendor for supplying gages of this type has been determined. This manufacturer has expertise in the implantation of strain gage bridges in bolts, and in fact, offers instrumented bolts as a product line. Their service could be utilized for gage implantation and bridge balancing of prototype bolts.

The bridge output will be amplified and bridge imbalance will be detected by an integrated circuit analagous to that described in Section 3.5.2 above.

As seen from the specifications listed in Figure 3-34, extreme threshold accuracy is attainable with the gage proposed. Such accuracy is probably not required, however, since a 50 ft - lb degradation of torque (from 250 to 200 ft - lb) will provide a sufficiently early warning of bearing assembly loosening. Tests on prototype bolts (beyond the scope of this contract) will better establish the sensitivity requirements, and it is possible that such tests will dictate the use of a less accurate (and less expensive) strain gage system.

For the establishment of feasibility, however, the gage of Figure 3-34 was used for the tests described in the following section.



Full-Bridge
(FB)

LEGEND

Ga: Active Gage
 Gc: Complementary Gage
 Excitation: +1 and -5 (Number correspond to Model)
 Signal: +3 and -0 (HW1-D Strain Indicator terminals).

BRIDGE TRIM RESISTORS

Initial Zero Load Balance: R1a or R1b
 Signal Trims: R2
 Modulus Trims: R3
 Zero Load Temp. Compensation: R4a or R4b

ELECTRICAL SPECIFICATIONS

Item	Characteristic
Gages	Metal Foil
Gage Factor	2.00
Service Temp.	-50°F or 300°F
Linearity	+1% of Allowable Load
Repetition	±0.1%
Resistance	120 + 2 or + 5 ohms
Configuration	Quarter-(QB), Double Quarter-(QB), or Full Bridge (FB).
Excitation	120-ohm QB: 6V Across Gage 350-ohm QB: 12V Across Gage 120-ohm DQB: 6V Across Bridge 350-ohm DQB: 12V Across Bridge 120-ohm FB: 6V Across Bridge 350-ohm FB: 12 V Across Bridge

FIGURE 3-34. TABULATION OF SPECIFICATIONS FOR A COMMERCIALY AVAILABLE FULL BRIDGE, METAL FOIL, 350 SL STRAIN GAGE

Strain Sensor Test

The following tests were conducted to verify the accuracy of published strain gage specifications. Two standard railroad axle cap bolts were used for this test. "Flats" were ground on their OD's and holes drilled through their centers. Strain gages were mounted on the "flats" and the strain gage outputs were monitored with a digital voltmeter as torque was applied with a calibrated torque wrench.

Tables 3-11A and 3-11B show data accumulated for three separate "tightenings" of each bolt. Plots of strain vs. torque are shown in Figures 3-35 and 3-36. (These data show an apparent resistance to elongation after the bolts have been tightened. This is most likely due to the "seating" of the strain sensor and not to any mechanical properties of the bolts themselves.)

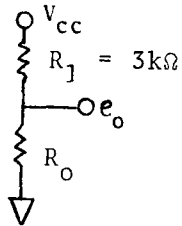
Calculation of the loads induced in the bolts is possible from [8] given by

$$\begin{array}{ll} \text{Eq.} & P = T/K_{TF} \qquad (15) \\ \text{where} & P = \text{bolt clamping load developed} \\ & \qquad \text{by tightening, lb} \\ & T = \text{tightening torque, in-lb} \\ & K_{TF} = \text{torque friction coefficient} \\ & D = \text{nominal bolt diameter, in.} \end{array}$$

At 250 ft - lb, which is the specified tightening torque for railroad bearing axle cap bolts, the tightening load (from

TABLE 3-11A. TABULATION OF TORQUE VS. BASE OUTPUT USING
 COMMERCIALY AVAILABLE STRAIN GAGES ATTACHED TO MODIFIED
 RAILROAD BEARING AXLE CAP BOLTS (TEST # 1)

CIRCUIT



- V_{cc} - 5V
- R - $3K\Omega$
- R_o - Test #1 - 17/32 hole - 364 ohms
- R_o - Test #2 - 5/32 hole - 359 ohms
- K - -103

Test #1 - 17/32 hole

Trial	#1		#2		#3	
Torque (ft - lb)	e_o (mV)	d_s (μ in/in)	e_o (mV)	d_s (μ in/in)	e_o (mV)	d_s (μ in/in)
0	530	0	531	20.4	524	122
25	526	81.6	526	81.6	523	142
50	525	102	523	142	520	204
75	519	224	518	245	515	306
100	512	367	512	367	511	387
125	506	489	508	449	505	510
150	496	693	496	693	502	571
175	480	1020	493	755	495	693
200	477	1081	490	816	407	877
225	471	1202	484	938	487	877
250	469	1244	482	979	479	1040
275	458	1469	473	1163	473	1163
300	451	1612	470	1224	472	1185

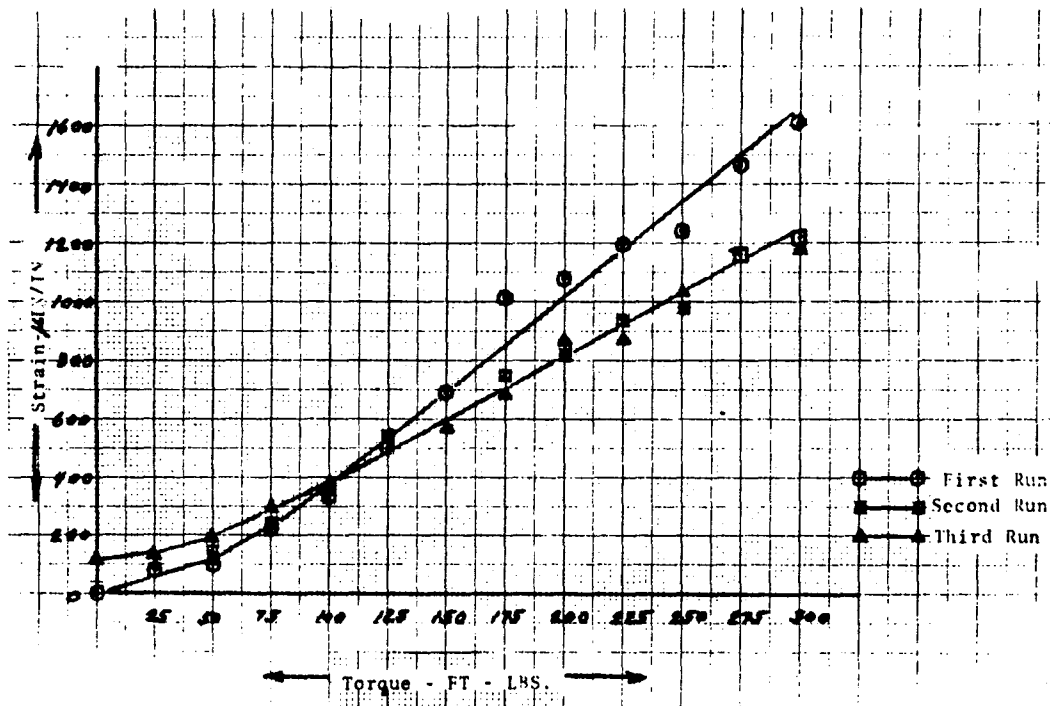


FIGURE 3-35. TORQUE-STRAIN CHARACTERISTICS OF A 1 IN.-8 BOLT WITH 17/32 IN. AXIAL HOLE

TABLE 3.11B. TABULATION OF TORQUE VS. BASE OUTPUT USING
 COMMERCIALY AVAILABLE STRAIN GAGES ATTACHED TO MODIFIED
 RAILROAD BEARING AXLE CAP BOLTS (TEST #2)

Test #2 - 5/32 in. diameter hole

Trial	#1		#2		#3	
Torque (ft - lbs)	e_o (mV)	ds (μ in/in.)	e_o (mV)	ds (μ in/in.)	e_o (mV)	ds (μ in/in.)
0	520	0	520	0	520	0
25	516	81.6	515	102	515	102
50	507	265	509	224	511	183
75	502	367	506	285	508	244
100	501	387	503	346	505	306
125	495	510	501	387	502	367
150	491	591	499	428	500	408
175	487	673	497	469	499	428
200	485	714	492	571	495	510
225	483	754	489	632	492	571
250	483	754	486	693	490	612
275	482	775	484	734	486	693
300	480	816	484	734	487	796

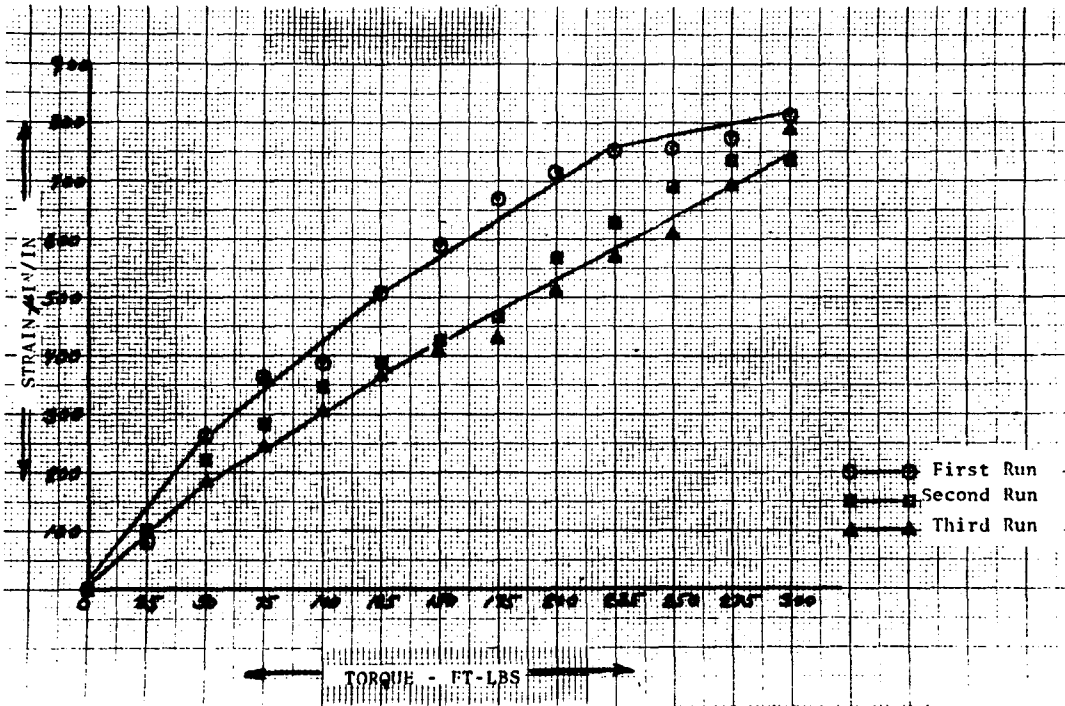


FIGURE 3-36. TORQUE-STRAIN CHARACTERISTICS OF A 1 IN.-8 BOLT HAVING A 5/32 IN. DIAMETER AXIAL HOLE

Eq. (15) is 20,000 lb. Calculation of the total elongation of the bolt under load follows from [9]:

$$\Delta = \frac{PL}{AE} \quad (16)$$

where Δ = elongation of bolt (in.)
 L = length of bolt segment (in.)
 A = tensile strength area (varies with hole diameter) (in.²)
 E = modulus of elasticity in. tension (psi).

Substitution in Eq (15) where $L = 1''$ yields the following

$$\begin{array}{l} ds = 1343 \mu \text{ in/in. (17/32 in. diam. hole) } \\ ds = 881 \mu \text{ in/in. (5/32 in. diam. hole) } \\ ds = 853 \mu \text{ in/in. (solid) } \end{array} \left. \begin{array}{l} \\ \\ \end{array} \right\} \text{--at 250 ft - lb. torque}$$

These calculated values compare favorably with the measured results (i.e. from Tables 3-11A and 3-11B: $ds = 1040 \mu \text{ in/in.}$ for a 17/32 hole; and $612 \mu \text{ in.}$ for a 5/32 hole).

The tensile strength of a bolt can be approximated using from [8]:

$$\text{Eq. } P_T = (A_T - A_H) T_T \quad (17)$$

where P_T = tension strength, (lbs)
 A_T = tension area, (in.²)
 T_T = tensile strength (psi)
 A_H = area of hole, (in.²).

Substituting yields,

$$P_T = 51,484 \text{ lb}$$

for the solid bolt and

$$P_T = 32,648 \text{ lb}$$

for a bolt having a $17/32$ in. diameter hole.

Since the hole size needed for the thermoelectric power system of Section 3.4 is $17/32$ in. in diameter, a 36 percent degradation in tensile strength for the transmitter bolt is indicated.

For that reason, the material for the candidate transmitter bolt must be changed, for example, to AISI - 4340 alloy steel or equivalent. The tensile strength of a bolt of this material having a hole diameter of $17/32$ in. is 77,000 lbs, which is considerably higher than the solid bolt currently in use. The use of such bolt will not degrade the torque handling characteristics of the axle cap assembly.

3.6 CONCLUSIONS

Data and analyses reported herein have established the feasibility of producing a transmitter bolt capable of signalling a train crew in the event a journal roller bearing overheats or has loosened.

Specifically, three separate studies have shown:

1. Transmitters small enough for implantation, and with range enough to be sensed at distances of 0.5 miles, can be mass-produced and that the power requirements for continuous operation of such transmitters is 5 Vdc about 50 μ A.
2. Thermoelectric devices, capable of delivering the required transmitter power, can be implanted and mass-produced, and that specialized thermal transfer devices necessary to operate the power source can be incorporated into a bolt without significantly altering its size or mechanical effectiveness.
3. Temperature and strain sensors, and their associated transmitter activation circuits are implantable and mass-produceable and that their production specifications are repeatable enough to obviate sophisticated electronic "trimming" of the final bolt assembly.

An early conceptualization of the final bolt assembly (shown in Figure 2-1) was presented to four major railroads. They unanimously agree that:

1. The transmitter bolt was technically superior to any currently used technique; and

2. It has enormous cost and life saving potential, as a preventor of both catastrophic failures and "false hot box setouts," and has also a freedom from periodic maintenance costs; and
3. The requisite "pull-by" inspection, necessitated when a warning signal is transmitted and received, is compatible with normal train crew routine in the event of suspected malfunction.

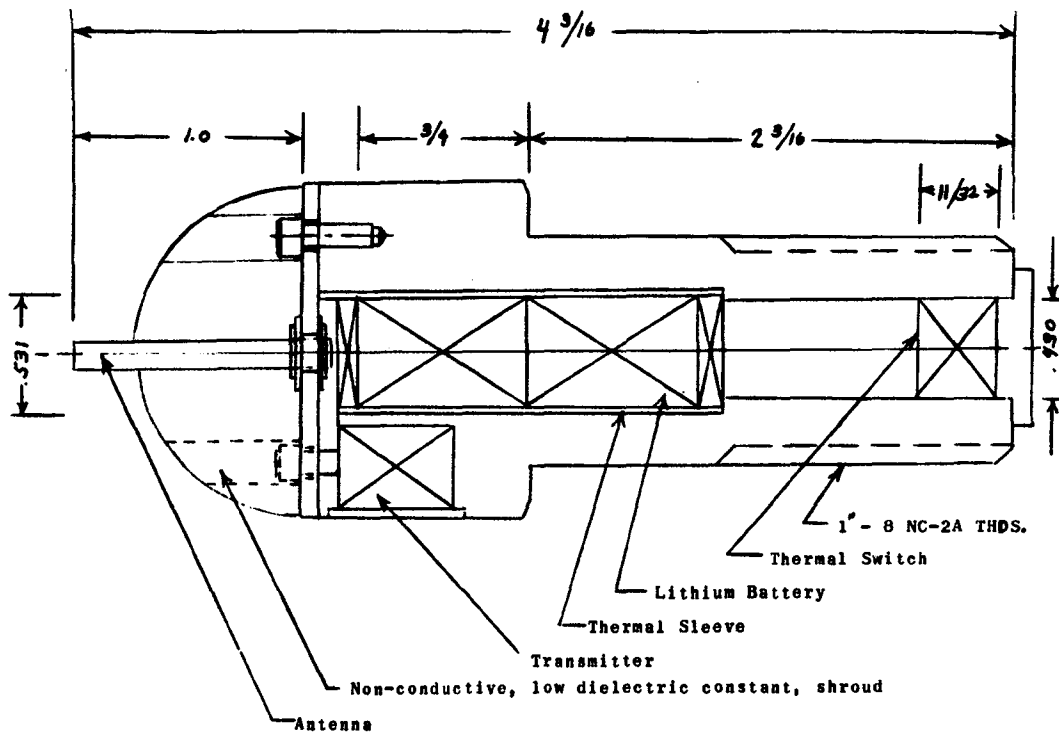
3.7 BATTERY POWERED TRANSMITTER BOLT - LOW COST ALTERNATIVE

As stated earlier, analysis of the probable production costs of the bolt described in the previous sections was unidentifiable until after the technical feasibility and configuration of its major subsystems had been established. As shown in Section 3.8 below, the cost of producing a modified bolt of essentially similar function is an order of magnitude lower than that of the thermally powered bolt.

This modified bolt is shown in Figure 3-37. It compares to the original concept in the following manner:

1. Power Source - The thermoelectric power source (and its requisite heat transfer subsystems) is replaced by a battery. This battery will deliver power only while transmitting and would require replacement at the normal bearing lubrication interval, or after each transmitter activation in service
2. Thermal Sensor - The nickel phenolic resistance thermometer (and its electronic amplifier) is replaced by a temperature sensitive switch
3. Strain Sensor - Deleted
4. Transmitter and Antenna - No change.

From the above it is seen that this bolt will be capable of sensing bearing overtemperature, but not loss of bolt tension. Although the early warning capability for failures which first manifest themselves as loosened bolts is lost, reference to Table 1-1 shows that such failures are relatively infrequent, always result in excessive operating temperatures, and are therefore detectable.



ALL DIMENSIONS SHOWN IN INCHES

FIGURE 3-37. MODIFIED (TEMPERATURE SENSING ONLY) TRANSMITTER BOLT

For that reason, as an alternative, the temperature sensing bolt of Table 3-12 has been conceptualized. It contains transmitter and antenna of the type described in Section 3.3 along with a state-of-the art, sealed, lithium battery and a simple nonreversible thermochemical or bimetallic temperature switch. This bolt, the cost of which would almost certainly meet the target (in large quantity production), would provide a "one-time" switch closure when the interior temperature exceeds 210°F, and activate the transmitter (powered by the battery shown) for a period sufficient to conduct the required "pull-by" inspection.

A bolt of this type would provide the overtemperature device capability similar to the more sophisticated bolt described previously. It would not provide the less important "loss-of-bolt-torque" sensing capability.

A work plan and schedule for development and test of this modified bolt are found in Figures 3-3 and 3-4 respectively. Estimated large and small scale production costs are shown in Part 2 of Table 3-17.

As is seen from Table 3-12, the "modified" bolt is more cost effective than the "unmodified" bolt. For this reason, and because a bolt of this type will eliminate the uncertainties inherent in wayside hot box detection, further development and evaluation of the temperature sensing Transmitter Bolt is considered urgent.

TABLE 3-12. RELATIVE MANUFACTURING COSTS OF "TEMPERATURE/STRAIN"
AND "TEMPERATURE ONLY" TRANSMITTER BOLTS

RELATIVE MANUFACTURINGS COSTS OF
"TEMPERATURE/STRAIN" AND "TEMPERATURE ONLY" TRANSMITTER BOLTS

1. Temperature and Strain Transmitter Bolt		
<u>Component</u>	<u>Prototype</u>	<u>Large Scale Production Estimate (1000 Pcs.)</u>
1. Transmitter	500.00	10.00
2. Thermopile	960.00	192.00
3. Heat Pipe	100.00	20.00
4. Fins	250.00	20.00
5. Bolt, Strain Gage and Mounting	450.00	40.00
6. Amplifier and Threshold Circuitry	180.00	1.50
7. Resistance Thermometer	11.00	5.00
8. Assembly and Test		25.00
Total	\$2451.00	\$313.50

2. Modified (Temperature Only) Transmitter Bolt		
<u>Component</u>	<u>Prototype</u>	<u>Large Scale Production Estimate (1000 Pcs.)</u>
1. Transmitter	500.00	10.00
2. Batteries	8.00	5.00
3. Thermal Switch	12.00	3.00
4. Bolt Manufacture	25.00	5.00
5. Assembly and Test		5.00
Total	\$545.00	\$28.00

3.8 RECOMMENDATIONS

Large scale production of a temperature and strain sensing bolt, configured as in Figure 3-5, is a feasible system for protection against catastrophic roller bearing failure.

A work plan and schedule for further development and test of such system is shown in Figures 3-1 and 3-2 respectively.

Final (per bolt) cost of this system is at this time difficult to estimate accurately. Work done in this program, however, indicates that the thermoelectric power source (and its attendant heat transferral subsystems) and implantation of the strain sensors, will constitute about 80 percent of the total cost of the developed bolt.

Part 1 of Table 3-12 shows estimated large and small scale manufacturing costs for bolts of this type; tooling costs are not shown. Although large scale cost benefit analyses have not been performed, a cost of \$25 per bolt (\$200 per rail car) has been indicated by canvassed railroads as a workable target cost for incorporation of a transmitter bolt on inservice equipment. It has become apparent during the latter stages of performance of this contract that incorporation of the rather sophisticated subsystems of Sections 3.4 and 3.5 will almost certainly cause production costs to exceed this figure. And for that reason, the modified bolt of the preceding section is more highly recommended for further development.

A work plan and schedule for development of the modified bolt are shown in Figures 3-3 and 3-4. Although cursory vendor contact has elicited positive reaction, the question of surviveability and longevity of the major subsystems (battery, thermal switch and transmitter) will be addressed as a first major subtask of follow-on work.

4. TASK II BEARING OVERLUBRICATION PREVENTION BY ULTRASONIC TESTING

4.1 SUMMARY

Overgreasing of railroad journal roller bearings is a frequent cause of catastrophic failure (burnoff) and "hot box" setouts. It was the purpose of this task to demonstrate the feasibility of developing a system which would prevent overgreasing and thus save the costs of derailment and unnecessary setouts.

Data presented herein establishes the feasibility of using an ultrasonic pulse-echo technique to determine the amount of grease in a bearing seal shroud by examining the seal for the presence of grease at specific locations around its circumference.

Use of such a device in a railroad repair track would preclude the greasing of a freshly greased bearing (the prime cause of overgreasing) and thus eliminate overgreasing at its source.

Use of the specific commercially available device evaluated in this task requires more operator attention than can be expected in a railroad repair track without disrupting maintenance schedules, and is therefore not recommended as a maintenance level system.

For this reason, an automatic ultrasonic inspection device for use at the maintenance level has been conceptualized. This concept has been presented to several major railroads. They all agreed that:

1. Such a device addresses a major problem.
2. It would be useable by railroad maintenance personnel.

3. It would have great cost and human life saving potential by reducing the occurrence of overgreasing-initiated derailments and "hot box" setouts.

All railroads visited offered their manpower and facility to help evaluate prototypes of such a device when it becomes available.

4.2 INTRODUCTION

It was determined in Phase I of Contract DOT-TSC-935 that overgreasing is a major cause of premature, and sometimes catastrophic, roller bearing failure. Catastrophic roller bearing failures (which cause derailments) carry an extremely high price tag in terms of lost revenues and potential personal safety hazards. It is estimated that North American railroads spend upwards of \$12 million per annum as a consequence of roller bearing-initiated derailments.

Overgreasing a railroad roller bearing causes abnormally high heat generation in the bearing. Heat generation tends to reduce internal clearances. This can have the affect (under certain circumstances) of further increasing operating temperatures and eventually creating thermal instability, thus leading to catastrophic failure.

A more common failure mode, however, progresses as abnormal bearing temperatures causes lubricating grease to liquify. Such liquification allows outflow of lubricant and influx of particulate and liquid contaminants, either of which can lead directly to catastrophic failure. This failure mode predominates in older seals where grease retention characteristics have degraded through normal wear.

An example of how overgreasing can occur is as follows: Overgreasing generally occurs in a railroad repair track (the repair track is an integral part of a "hump yard"). Maintenance mechanics visually examine each car entering a hump yard for "time up" regarding regreasing intervals. (Regreasing occurs

every three to four years depending on service; a regreasing date is printed on the side of each car.) Any car due for regreasing goes to the repair track in the hump yard. All four wheel sets on each car are regreased, (8 oz is a typical regrease charge). Unavailable to the mechanic applying grease, however, is specific knowledge regarding the maintenance history of each wheel set of any particular car. If one wheel set had been recently out of service (for any of a number of reasons) and is thus freshly greased, both bearings on that particular wheel set will be given an "extra" charge of grease by the repair track mechanic. These bearings are, at this point, "overgreased" by 8 oz.

When the car returns to service, it is quite common that the elevated temperatures in the overgreased bearings cause failure as described above. A well intentioned wayside maintenance mechanic, noticing the outflow of grease assumes that the bearing needs a booster charge. He gives the bearing an additional 8 oz charge. That bearing is now overgreased by 16 oz. If the car is not soon taken out of service, operating temperature increases, bringing with it the distinct possibility of setout or worse: catastrophic bearing failure and derailment.

It was the purpose of this investigation to determine the feasibility of developing a device, for use by railroad maintenance personnel, which would prevent initial overlubrication. It would do so by segregating all recently regreased bearings from those which actually need regreasing.

Critical to such an investigation is the ability of a test instrument to measure the amount of grease in an outboard seal cavity without disassembly.

Data presented herein establishes the feasibility of using an ultrasonic pulse-echo technique to determine the amount of grease in an outboard seal cavity. This device examines the outboard seal shroud for presence of grease at specific locations around its interior. The success of this device depends on two conditions:

1. The ultrasonic device is capable of determining the presence of grease adhering to the interior wall of a seal.
2. The circumferential distribution of grease in the outboard seal is related to the "greasing history" of an in-service bearing.

Section 4.3 describes the test equipment used for establishing detectability of grease in a seal. Section 4.4.2 describes grease distribution in the seals of two bearings having normal and excessive grease. Section 4.5 and 4.6 discuss the results and indicates follow-on work, ie., the packaging and evaluation of a system useable by railroad personnel in a railroad repair track.

4.3 TEST EQUIPMENT

4.3.1 Ultrasonic Test Equipment

4.3.1.1 Background

Ultrasonic techniques have long been used as valuable non-destructive testing tools for the integrity of various components. Previous experience has indicated that when an ultrasonic pulse-echo transducer is coupled to the outer surface of a thin-walled ring (such as a bearing seal or outer race) ultrasonic echos reflecting from the interior wall vary perceptibly as a function of grease layer thickness adhering to that wall. By proper selection of the time elapsed between the original ultrasonic pulse, and measurement of the amplitude of an echo returning at that particular time, grease layer thickness can be determined.

4.3.1.2. Test Method

For the tests reported herein the following ultrasonic method was used.

A transducer was held firmly against the outer circumference of a bearing seal (or outer race), see Figure 4-1. This transducer was ultrasonically coupled (via a viscous fluid, i.e. couplant) to the surface on which it rests. (The transducer oscillates at a specific frequency in the ultrasonic range, usually between 1-20 MHz, when pulses of electrical energy are impressed across a face.)

An electronic pulser sends an impluse to the transducer,

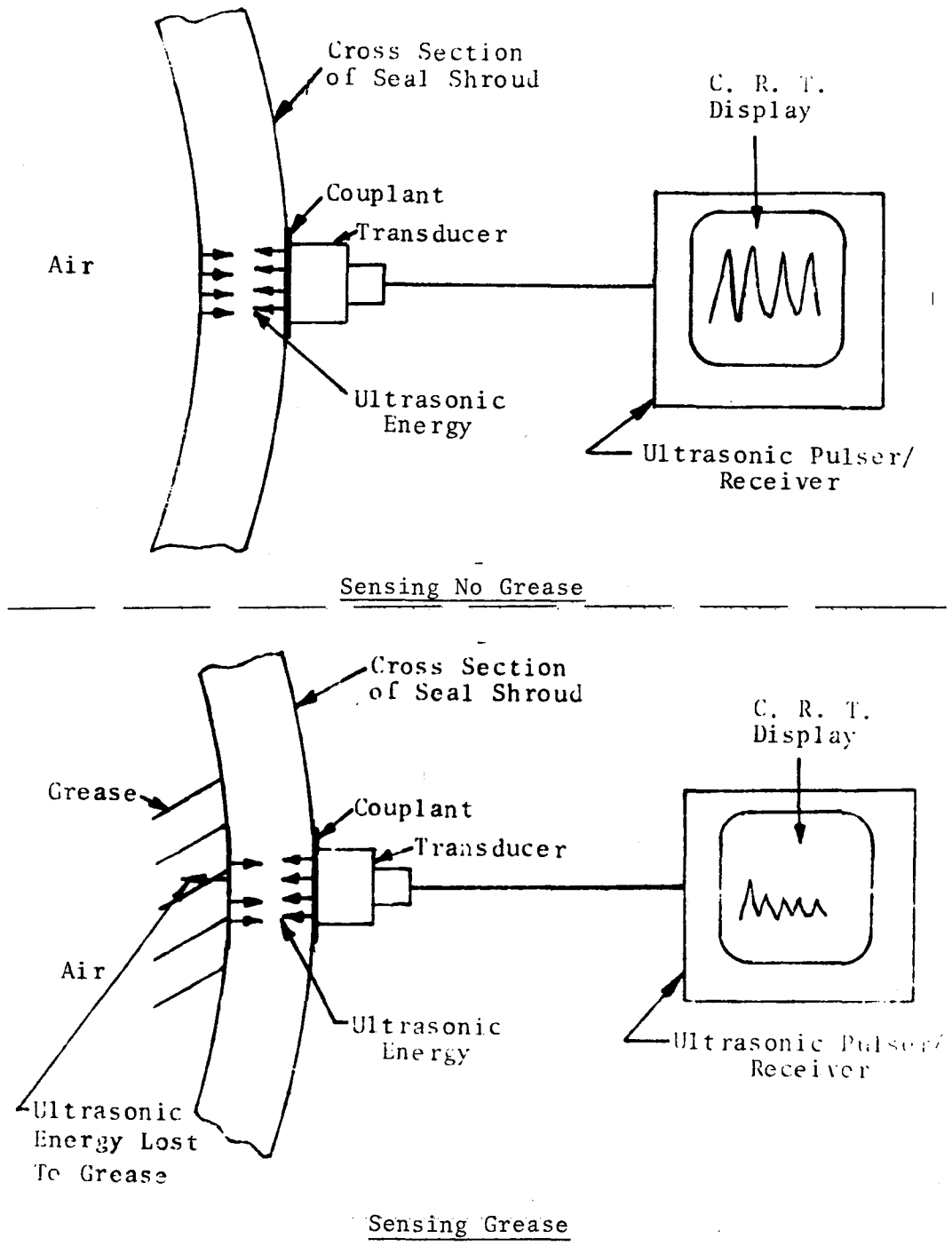


FIGURE 4-1. ULTRASONIC METHOD OF GREASE DETECTION

causing it to oscillate. These oscillations (mechanical vibrations) travel through the couplant and into the bearing seal. They reflect from the inside face of the seal and return to the transducer. The returning echo vibrates the transducer, which produces an electrical signal at the time of receipt. The amplitude of such a signal is proportional to the amount of energy returning to the transducer; the time at which it is seen (on a cathode ray tube display) is linearly related to total distance travelled. Many echos will return to the transducer as a result of each initial impulse as the wave travels repeatedly between the transducer and reflecting surface. The number and amplitude of such echos are dependent on the acoustical impedance of the material(s) in which the vibration travels.

If the inside face of the seal is coated with grease, some energy will be absorbed by the grease each time the ultrasonic vibrations strike the interior surface of the seal. The difference in the amount of energy returning to the transducer (and in the echo amplitude displayed) from greased, vs. nongreased surfaces is accentuated with each succeeding echo.

The electronic device which pulses the transducer, also receives and displays each echo returning to the transducer on a cathode ray tube. By examination of the amplitude of returning echos (in practice one particular echo is chosen) it is possible to determine the presence and (over a certain range) the layer thickness of grease beneath the transducer.

4.3.1.3. Specific Test Apparatus

A literature survey was conducted to determine the most suitable ultrasonic device for grease detection. Some pre-

liminary empirical investigations of the grease detection capabilities of several instruments were then conducted. As a result, a rugged, portable ultrasonic flaw/thickness tester was chosen over several candidates. A photograph of the pulser/receiver apparatus is shown in Figure 4-2. It is a laboratory/industrial instrument, combining readability and ruggedness with a relatively broad range of front-panel-selectable operating parameters (pulser frequency, damping and tuning, etc). It weighs approximately 16 lbs, and is powered by 12 nickel-cadmium rechargeable batteries. The case is constructed of high impact plastic with rubber bezels, making it suitable for field evaluation in a wheel shop or repair track.

Two candidate ultrasonic transducers (1/4 in.-dia.) were tested. A 10 MHz single element transducer was found slightly superior to a 5 MHz dual element transducer for grease thickness determination. The addition of a plexiglass "delay line" of 3/8" length (which is an in-line transducer extension used to prevent interferences caused by echos emanating from the outside surface of the seal shroud) was found necessary for CRT display clarity. Both transducers, and the delay line, are shown in Figure 4-3.

A relatively new synthetic couplant fluid was tested and found satisfactory. It has a viscosity equivalent to SAE 90 weight oil and low acoustic impedance, two highly desirable characteristics for ultrasonic testing. (Outdoor application of this couplant (-30 to 130°F) is a subject still to be investigated.)

Reproduced from
best available copy.

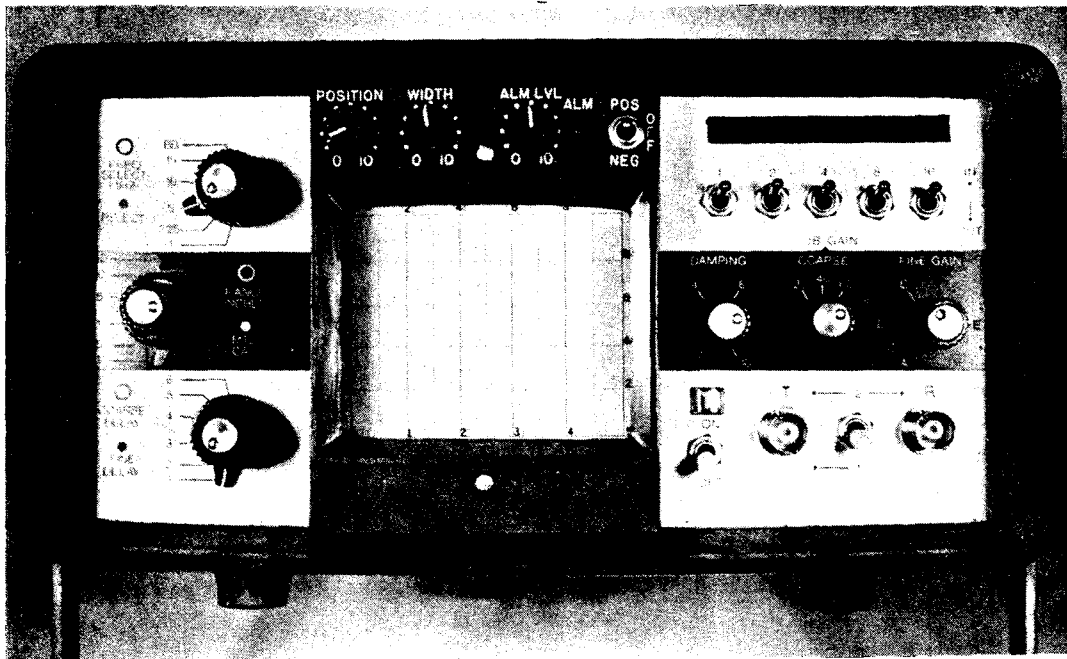
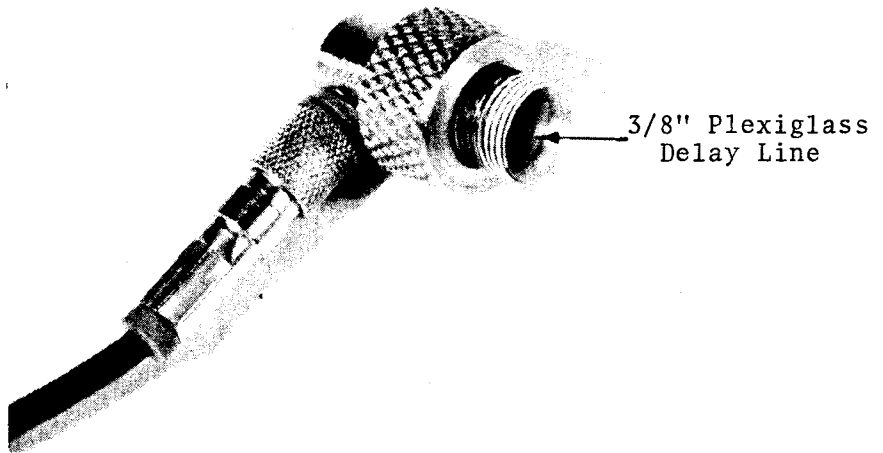
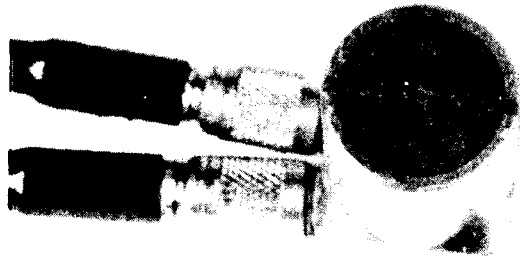


FIGURE 4-2. ULTRASONIC FLAW/THICKNESS TESTER



Fingertip Removeable Delay Thickness Gaging Transducer



Dual Element Transducer

FIGURE 4-3. ULTRASONIC TEST TRANSDUCERS

A plexiglass transducer holder for proper orientation of the transducer with respect to the seal OD was designed, built and tested. This hand held adapter, which also provides a couplant reservoir during the inspection process, is shown in Figure 4-4

4.3.2 Bearing Test Machine

A test machine for operating railroad bearings for the "Grease Migration" tests of Section 4.4 is described below.

A laboratory railroad bearing test machine, consisting of two large load carrying pillow blocks on a casting frame, is shown in Figure 4-5. The pillow blocks support a rotating shaft which is driven by pulleys and "V" belts from an electric motor. Both outboard shaft ends are machined and ground to 6 in. x 11 in. axle shaft bearing seat dimensions, and contain the required axle cap bolt holes. Test bearings are mounted on the outboard ends of the shaft. Loads are applied to the test bearing via a load beam and yoke type arrangement, coupled to a railroad bearing adapter, which rests on the outer ring of the bearing.

A No. 1 1/2 grade grease which meets AAR specifications M-917 for grease type railroad roller bearings, was used for all tests.

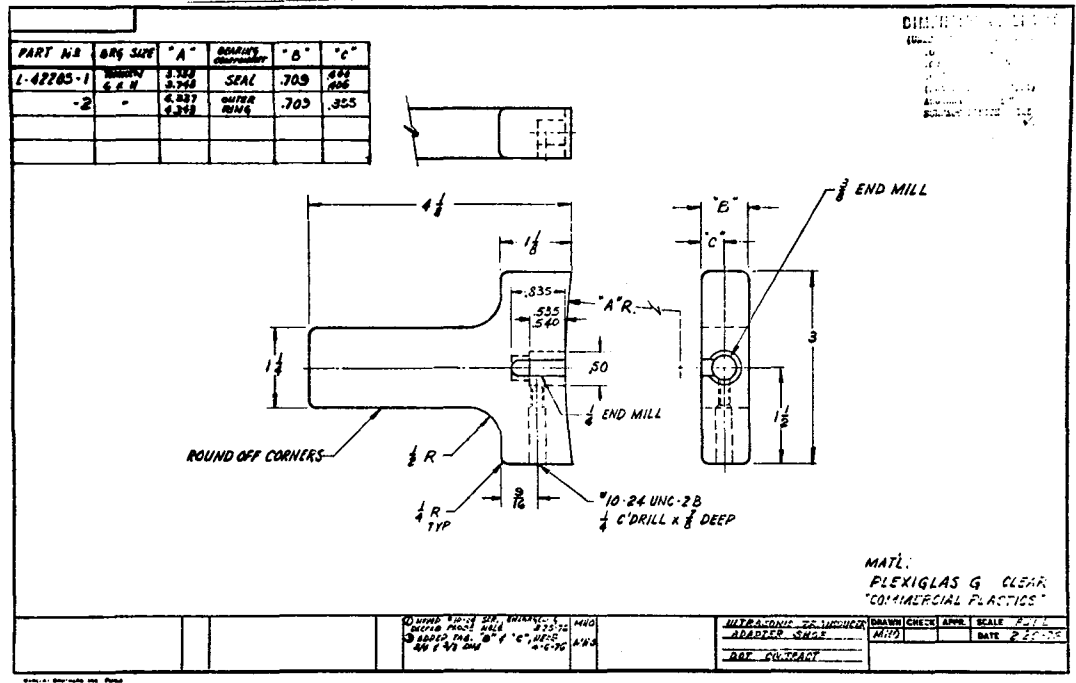


FIGURE 4-4. ULTRASONIC TRANSDUCER HOLDER

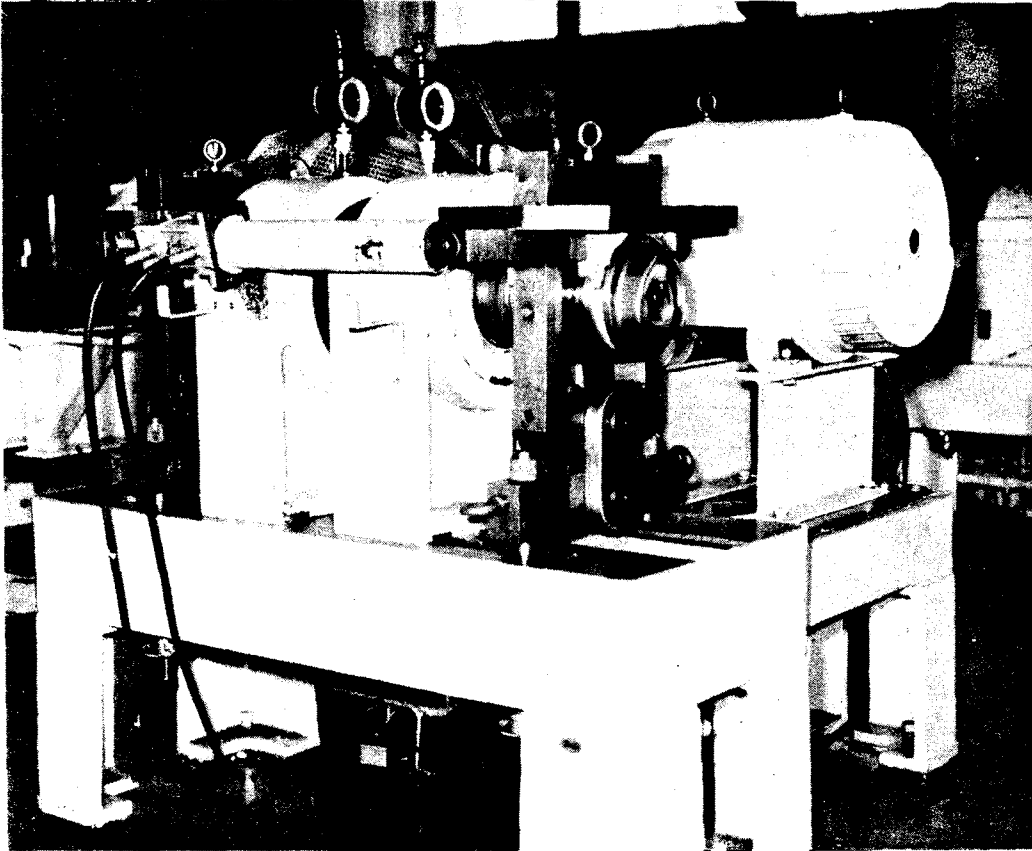


FIGURE 4-5. RAILROAD BEARING TEST MACHINE

4.4 TEST PROGRAM

The Ultrasonic Overlubrication Detector Test Program as submitted to DOT under Contract DOT-TSC-935 Phase II, Task II is reproduced in Appendix B.

4.4.1 Static Grease Detectability Tests

4.4.1.1 Operating Frequency and Echo Selection

The purpose of these tests was to optimize the subject parameters for measurement of grease layer thickness on the interior surfaces of seals and outer races.

Grease layers of varying thickness were applied to the interior surface of a seal and outer race. A single element 10 MHz transducer with a 3/8-in. delay line was used for all tests. Grease thickness detectability was investigated as a function of pulser frequency. Previous experience has shown that optimum pulser frequency is dependent, to a large extent, on the physical characteristics of individual transducers, and therefore data taken to optimize detection capabilities of this transducer are not presented. It should be noted, however, that the best grease thickness discrimination was obtained with the 10 MHz transducer operated at 5 MHz for seals, and at 2.25 MHz for outer races. These operating frequencies were chosen for accumulation of all data to follow.

Since the difference in echo amplitude (grease vs. no-grease) is accentuated with each successive reflection from the interior face (where a percentage energy loss to grease occurs), it is desirable to investigate the amplitude of one of the lattermost

distinguishable interior face echos for grease discrimination. For that reason the ultrasonic analyzer was operated at maximum gain, in order to view the lattermost echos. (In automatic operation, a small time increment (in which a particular echo falls) will be "gated" into an amplitude discriminator circuit for (go)-(no-go) grease recognition).

Figure 4-6 shows echos returning from seals with and without grease. Note that echo amplitudes (which are a function of energy content returning to the transducer) are lower when sensing grease.

4.4.1.2 Data Presentation

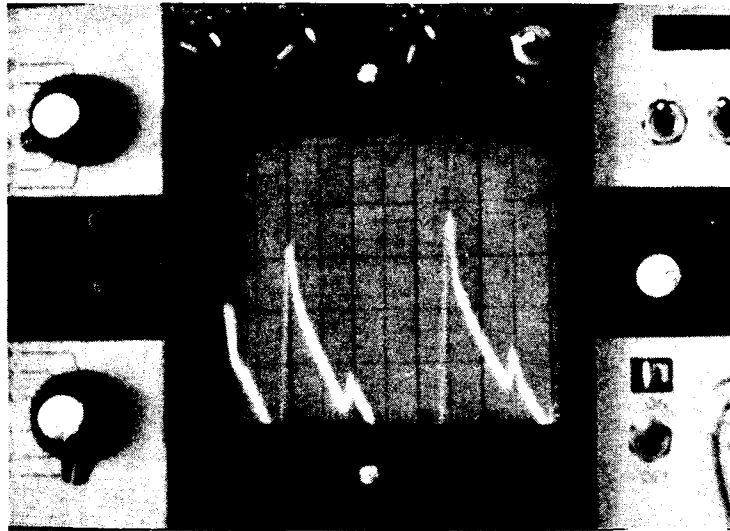
All data reported here show echo amplitudes, determined by manual measurement of echos displayed on a CRT. The presence, absence, and thickness of grease layers manifest themselves as variations in the amplitude of particular ultrasonic echos.

Data are presented in polar graph form. Their format is detailed in 4.4.1.3 below, and used throughout this report.

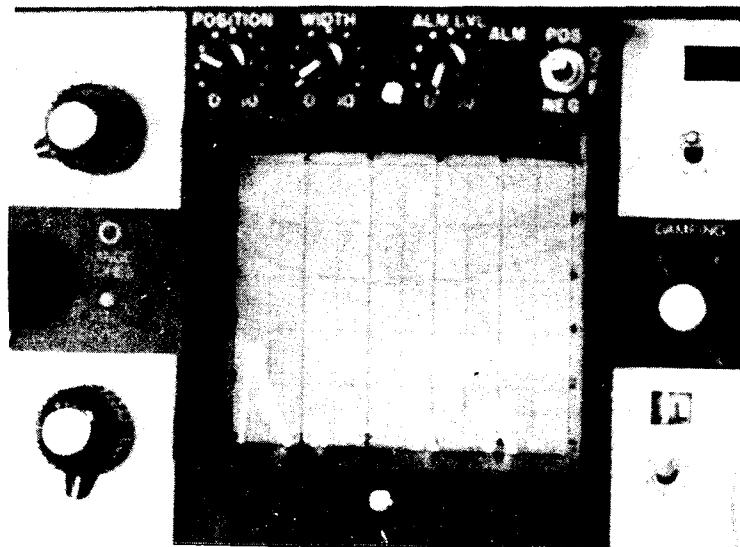
Each echo amplitude data point reported here, represents the average of two separate acquisitions. Individual data points were within ± 10 percent of those shown.

4.4.1.3 Grease Measurement in Railroad Roller Bearing Seals

The interior surface of a roller bearing seal was coated with grease as depicted in the shaded portion of Figure 4-7.



Sensing No Grease



Sensing Grease

FIGURE 4-6. ECHO AMPLITUDE SIGNALS FROM RAILROAD BEARING SEAL SHROUD

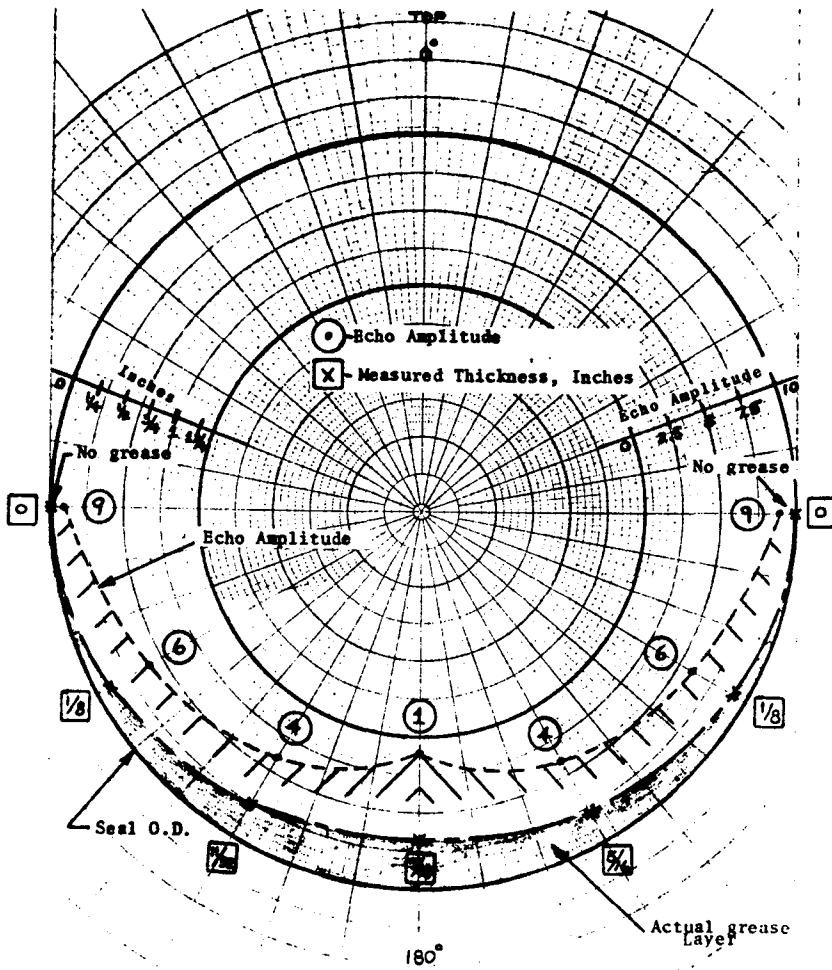


FIGURE 4-7. POLAR PLOT OF GREASE DISTRIBUTION IN A SEAL SHROUD: MEASURED THICKNESS VS. ULTRASONIC ECHO AMPLITUDE

Measured layer depths (in.) at 30° intervals (from 90°-270°) are tabulated in Figure 4-8 and plotted in Figure 4-7. (The grease distribution of Figure 4-7 is representative of that in an outboard seal of a properly greased bearing after a short period of railroad service.) Echo amplitudes in arbitrary units at the same locations are tabulated in Figure 4-8, and plotted in Figure 4-7. Note that zero echo amplitude (which corresponds to a layer thickness in excess of 7/16 in.) is located 6 major divisions from center and is accentuated by a darkened line. Note also that "no grease" (occurring at 90° and 270°) yields an echo amplitude of 9.

Echo amplitudes vs. grease layer thickness are plotted in Figure 4-8, (note the inversion of units on the abscissa). Figure 4-8 shows that ultrasonic echo amplitude is a recognizable, nearly linear, function of grease layer thickness over the range tested. Physical explanation of the detectability of grease vs. no grease is, as stated earlier, rather straight forward, i.e. the interior grease/metal interface provides a low impedance path for ultrasonic energy yielding a net energy loss each time that interface is struck. Grease thickness detectability is not as easily explained. The fact that grease thickness is detectable implies that, over a certain range, the grease/air interface also reflects energy and that such reflections return to the transducer "out of phase" with some of those from the grease/seal interface. Such interference could serve to diminish certain echos, thus yielding information regarding grease thickness. As grease thickness increases beyond about 7/16 in. ultrasonic scatter associated with the basic inhomogeneity of grease reduces the directivity of reflections and thus the further effect of such reflections is imperceptible.

<u>Seal Measurement Location</u>	<u>Echo Amplitude</u>	<u>Depth, Inches</u>
90°	9	0
120°	6	1/8
150°	4	5/16
180°bottom	1	7/16
210°	4	11/32
240°	6	1/8
270°	9	0

Graph of Grease Thickness Versus Echo Amplitude

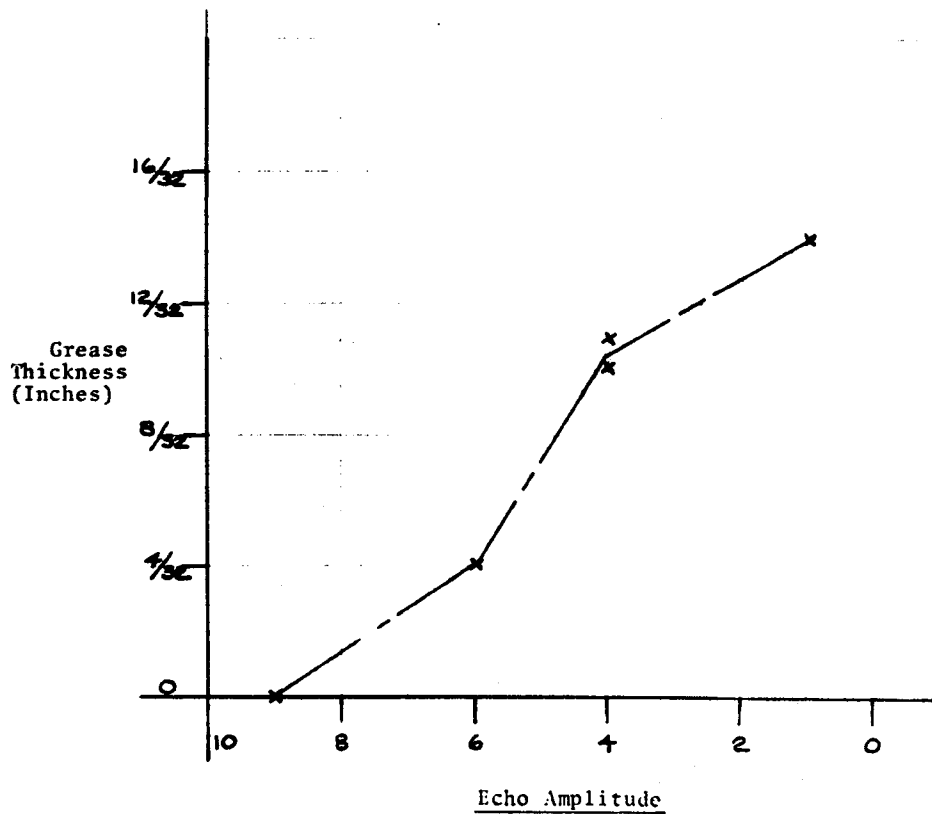


FIGURE 4-8. GREASE THICKNESS DETERMINATION BY ULTRASONIC ECHO AMPLITUDE MEASUREMENT

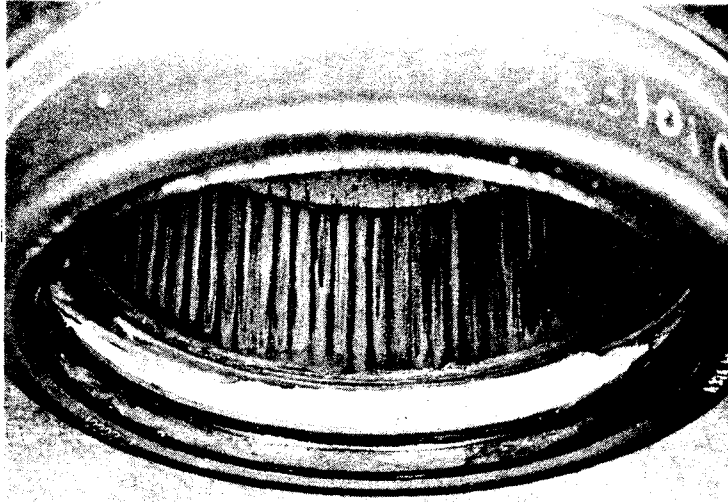
Detailed examination of the physical mechanism(s) involved in this phenomenon would require empirical and computational methods beyond the scope of this task. (It should be pointed out, however, that the eventual success of the device being tested here relies only on the existence of observable differences between grease and no grease and not on the quantitative measurement of absolute grease thickness. It is for this reason also that investigation of grease parameters such as temperature, grease type, microscopic grease contamination, etc. were considered irrelevant as part of this feasibility study.)

4.4.2 Grease Migration Study

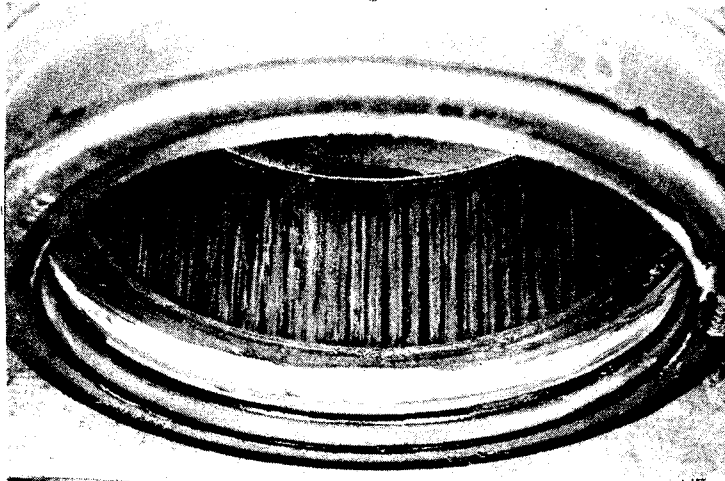
4.4.2.1 Test Format

The purpose of these tests was to verify the feasibility of using knowledge of the circumferential distribution of grease in the bearing seals or outer races, in assessing the total volume of available grease in a 6 in. x 11 in. tapered railroad roller bearing. The circumferential distribution depicted in Figure 4-9 is representative of those found in the outboard seals of operating railroad roller bearings.

Two standard 6 in. x 11 in. railroad journal bearings were operated, on the test machine of Section 4.3.2 at equivalent train speeds of 60 MPH and radial loads of 25,000 lb. A 16 in. diameter fan operating at 1700 RPM was used to simulate windage. Bearing operating temperatures were sensed by thermocouples and recorded for all tests.



6" x 11" Outboard Railroad
Bearing Seal



6" x 11" Inboard Railroad
Bearing Seal

FIGURE 4-9. TYPICAL GREASE DISTRIBUTION IN SEALS

These bearings were run three times (for 24-hour periods) with successively increased amounts of grease. Prior to Test I, each bearing was provided an 18 oz grease charge, (4.5 oz in each cone assembly and 9 oz in the area between cone assemblies per AAR new and rebuilt greasing specification). Prior to Test II, an additional 8 oz. charge was applied at the grease fitting - per AAR regreasing specifications. Prior to Test III, another 8 oz charge was applied at the grease fitting.

After each test, the seals and outer races of both bearings were ultrasonically tested at 45° intervals around their outer circumferences. Echo amplitudes were plotted in polar form. The bearings were disassembled and grease distributions on their circumferences were visually examined, photographed, and correlated with ultrasonic echo amplitude plots.

4.4.2.2 Test Results

A reference for data described in this section is shown in Table 4-1. The outboard seal, inboard seal and outer race of each bearing was inspected after each of three tests. Use of Table 4-1 permits analysis of the effect of progressive over-greasing on each individual component, without repeated reference to the text. A sketch depicting the locations of each component, and placement of ultrasonic transducers for their inspection, is shown in Figure 4-10.

4.4.2.2.1 Test I - Normally Greased Bearing Study

Photographs of seal grease distributions after Test I are shown in Figures 4-11 and 4-12 for bearings 063103 and 063104 respectively. Outboard and inboard seals of each bearing are shown. Ultrasonic echo amplitudes measured from the OD of

TABLE 4-1. DATA REFERENCE FOR GREASE MIGRATION STUDY

Bearing No.	Grease Amount	Echo Amplitude Polar Plot	Seal Grease Distribution Photographs
<u>Outboard Seal</u>			
063103	Normal charge	Figure 4-13	Figure 4-11
	8 oz recharge	Figure 4-21	Figure 4-19
	16 oz recharge	Figure 4-29	Figure 4-27
063104	Normal charge	Figure 4-15	Figure 4-12
	8 oz recharge	Figure 4-23	Figure 4-20
	16 oz recharge	Figure 4-31	Figure 4-28
<u>Inboard Seal</u>			
063103	Normal charge	Figure 4-14	Figure 4-11
	8 oz recharge	Figure 4-22	Figure 4-19
	16 oz recharge	Figure 4-30	Figure 4-27
063104	Normal charge	Figure 4-16	Figure 4-12
	8 oz recharge	Figure 4-24	Figure 4-20
	16 oz recharge	Figure 4-32	Figure 4-28
<u>Outer Ring</u>			
063103	Normal charge	Figure 4-17	
	8 oz recharge	Figure 4-25	
	16 oz recharge	Figure 4-33	
063104	Normal charge	Figure 4-18	
	8 oz recharge	Figure 4-26	
	16 oz recharge	Figure 4-34	

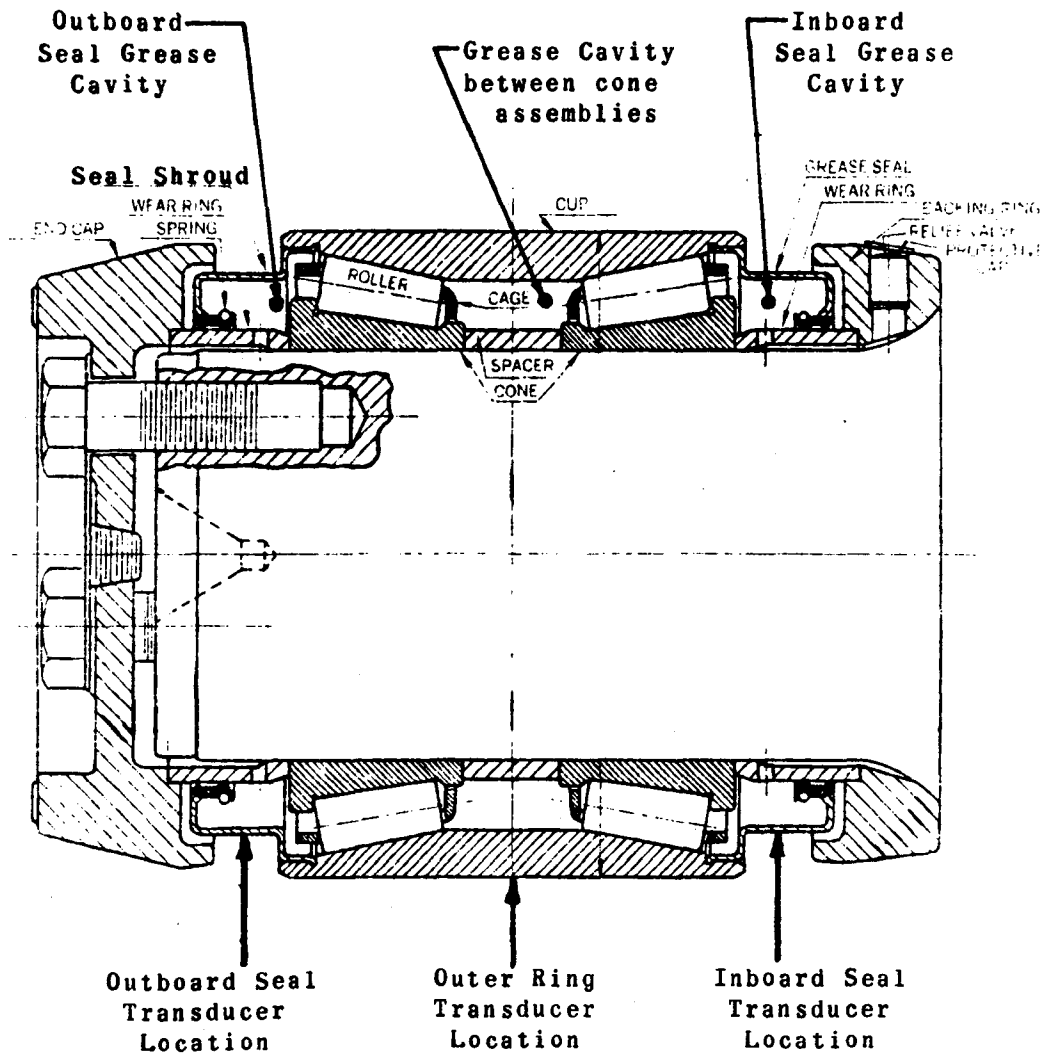
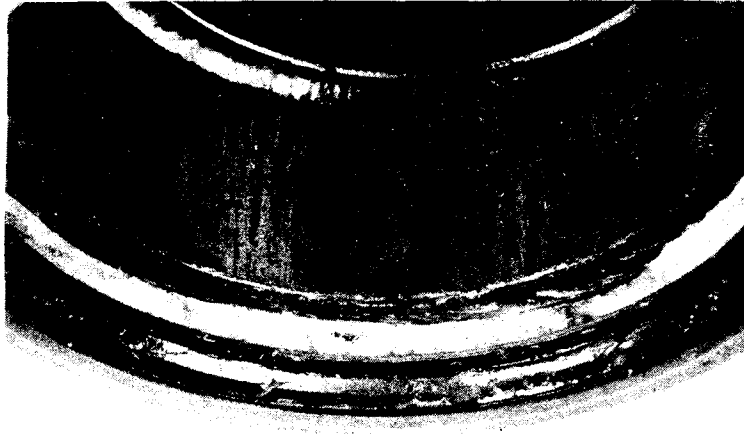


FIGURE 4-10. IDENTIFICATION OF BEARING COMPONENTS AND TRANSDUCER LOCATIONS FOR ULTRASONIC GREASE DETECTION



Grease Distribution in Outboard Seal

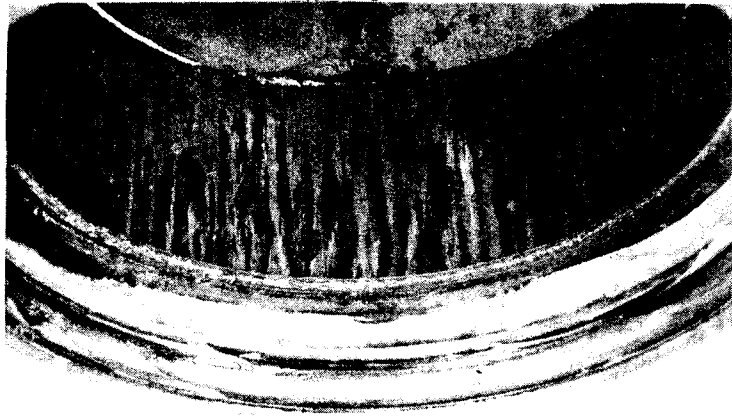


Grease Distribution in Inboard Seal

FIGURE 4-11. SEALS OF BEARING 063103 WITH NORMAL GREASE CHARGE



Grease Distribution in Outboard Seal



Grease Distribution in Inboard Seal

FIGURE 4-12. SEALS OF BEARING 063104 WITH NORMAL GREASE CHARGE

the seal shrouds of these bearings are plotted in Figures 4-13, 4-14, 4-15, and 4-16 respectively.

As is seen from Figures 4-13 through 4-16, ultrasonic inspection suggested that each seal had grease around its entire inner circumference. Visual examination of the seals verified that such was their condition. Grease color was unchanged relative to startup, but there was some local oil separation visible in both bearings.

The 360° circumferential grease distribution observed in the seal shrouds of these normally greased bearings is seemingly incongruous with field experience regarding in-service grease migration (where distributions as in Figure 4-9 are observed). Such distributions occur because the present test machine differs from actual service in many respects. High centrifugal forces associated with rapid test machine startup, and constant vibration-free operation are never experienced in actual service. Lower starting speeds, rail joint/wheel impact loads, and "humping" impact loads cause grease located in seals to "slump" into the lower portion of the interior seal cavities. The start of such "slumping" was ultrasonically detected and visually confirmed in these tests. Careful inspection of Figures 4-13 through 4-16 reveal echo amplitudes significantly higher in the upper portions of the seal. In fact the distribution of Figure 4-9 is a result of running a new bearing in the laboratory, for 20 hours at 20 MPH and 1300 lb radial load, during performance of Task III of this contract. (A few hundred miles of actual railroad service is more than sufficient to produce such slumping.)

Figures 4-17 and 4-18 show plots of grease distributions in the area between the cone assemblies as observed from the outside of the outer rings of both test bearings. There was no change in grease distribution relative to original packing.

Grease Distribution Outboard Seal

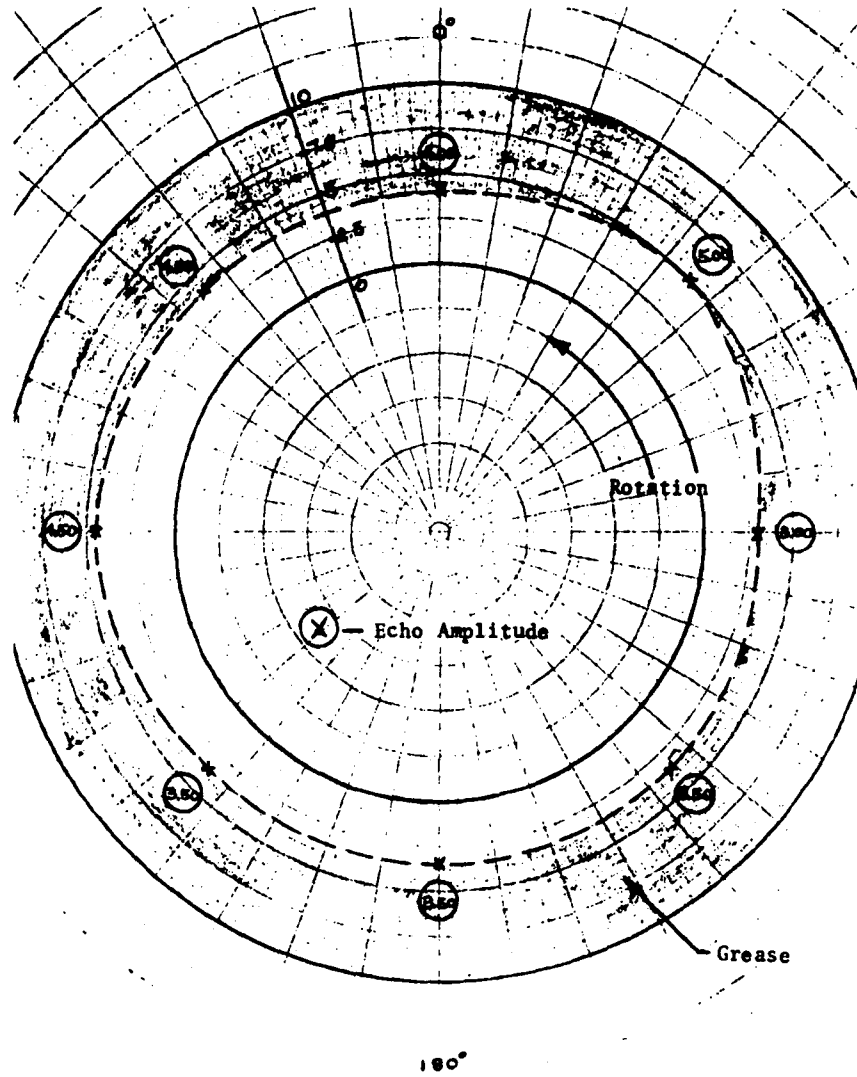


FIGURE 4-13. ECHO AMPLITUDES - OUTBOARD SEAL,
BEARING 063103 - NORMAL GREASE CHARGE

Grease Distribution Inboard Seal

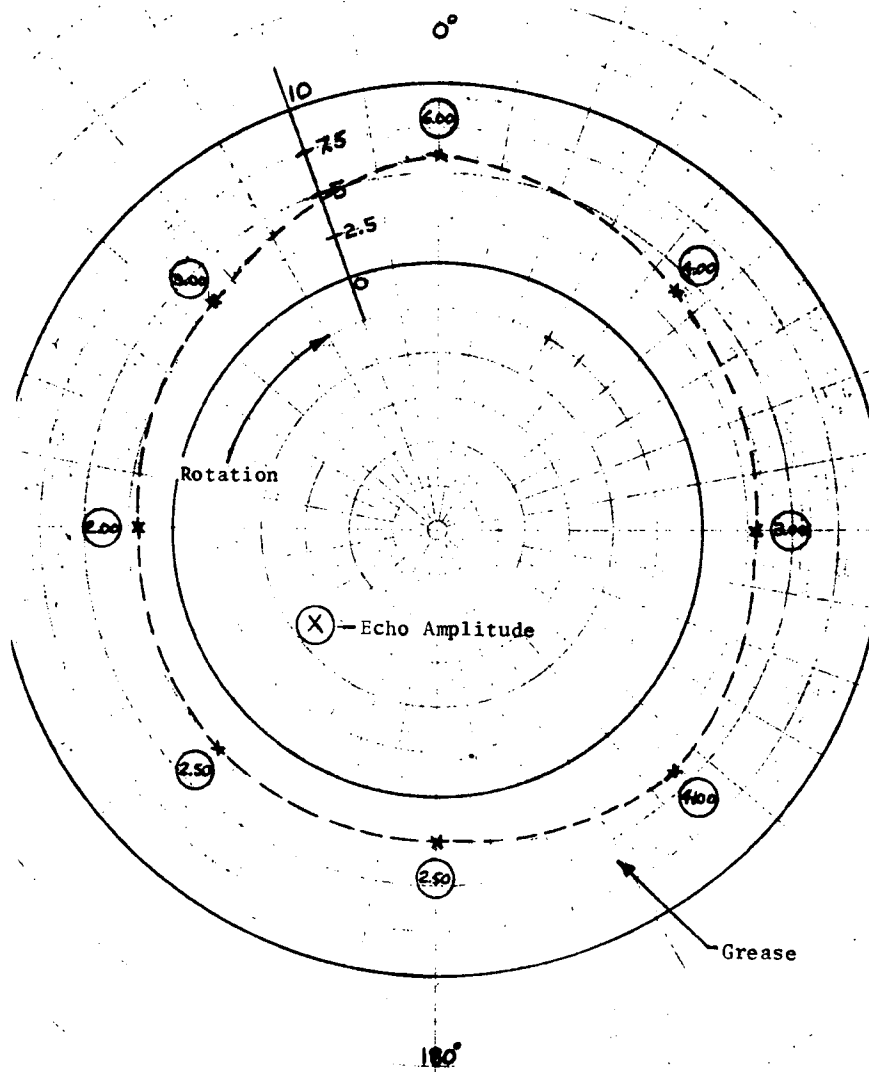


FIGURE 4-14. ECHO AMPLITUDES - INBOARD SEAL, BEARING 063103 - NORMAL GREASE CHARGE

Grease Distribution Outboard Seal

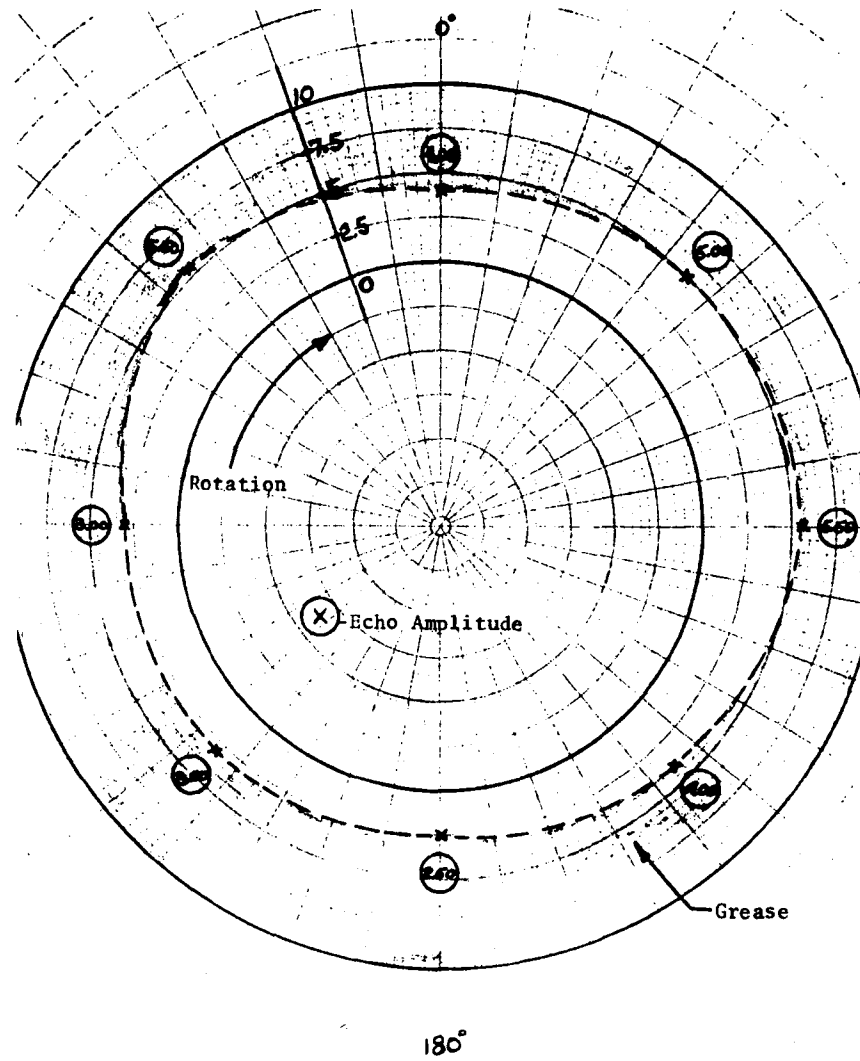


FIGURE 4-15. ECHO AMPLITUDES - OUTBOARD SEAL, BEARING 063104 - NORMAL GREASE CHARGE

Grease Distribution Inboard Seal

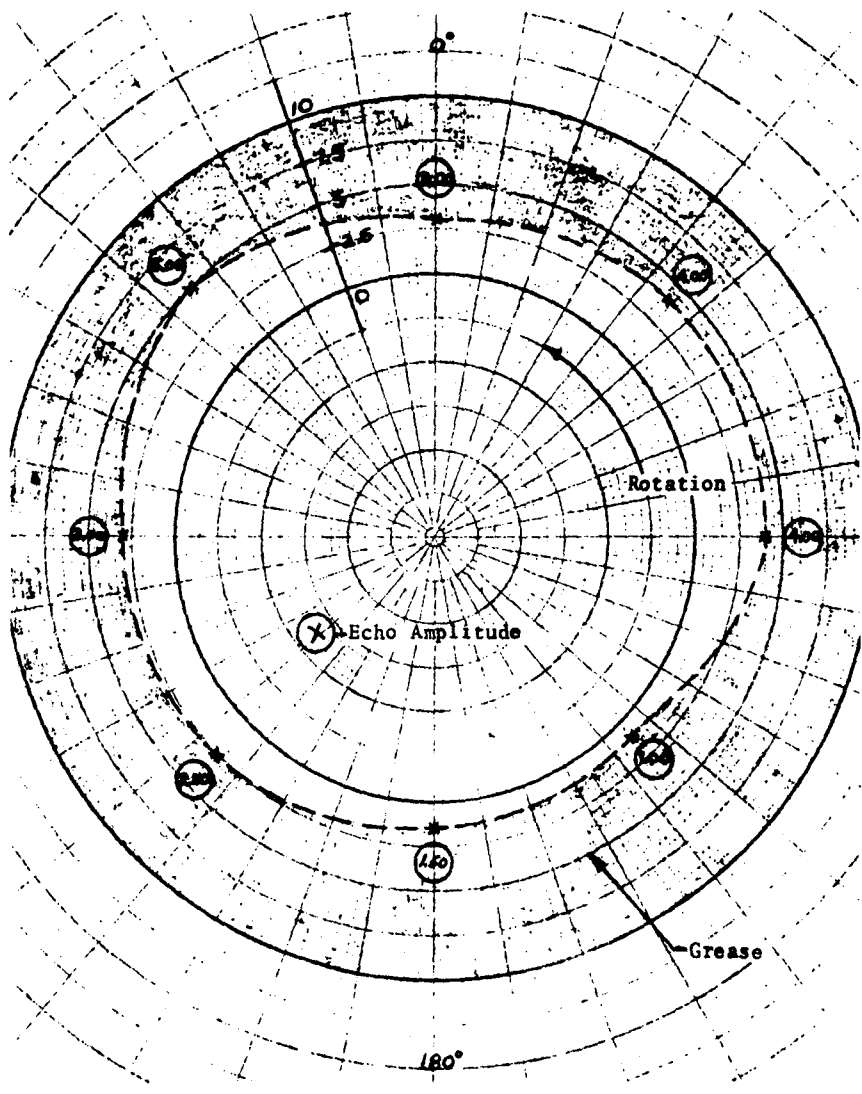


FIGURE 4-16. ECHO AMPLITUDES - INBOARD SEAL, BEARING 063104 - NORMAL GREASE CHARGE

Grease Distribution Outer Ring

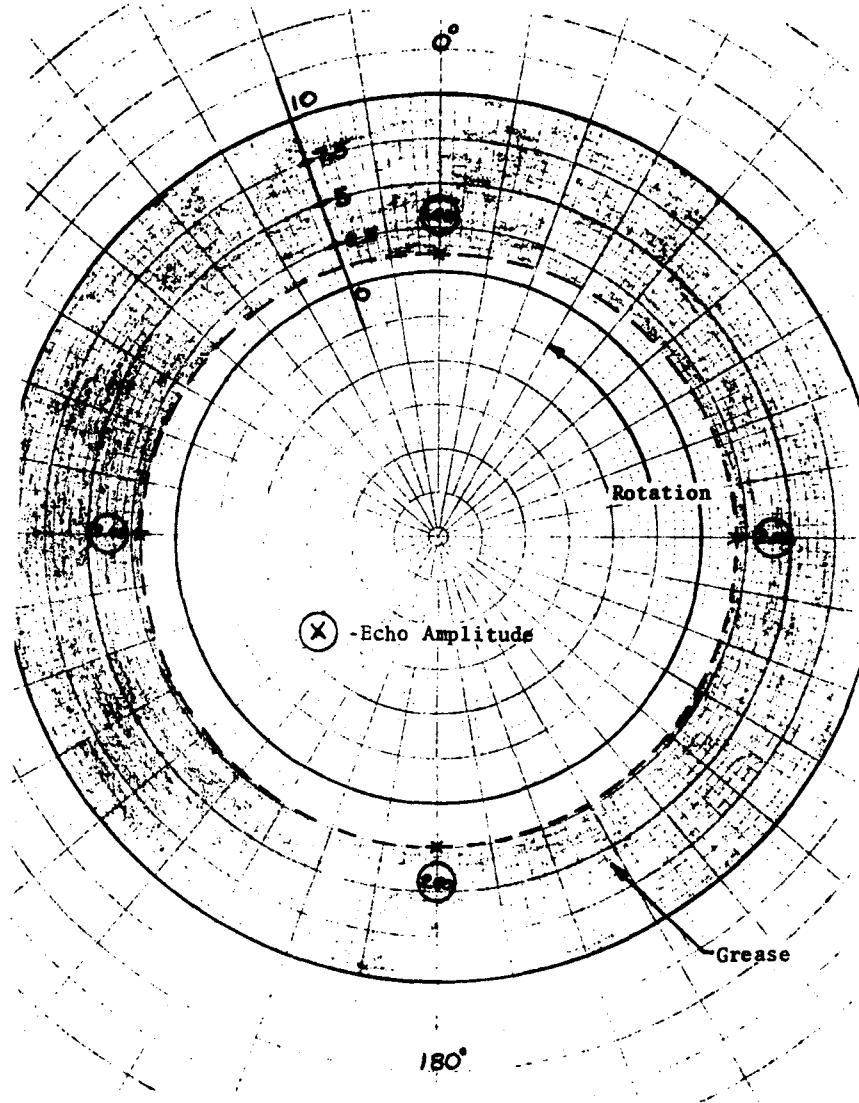


FIGURE 4-17. ECHO AMPLITUDES - OUTER RING,
BEARING 063103 - NORMAL GREASE CHARGE

Grease Distribution Outer Ring

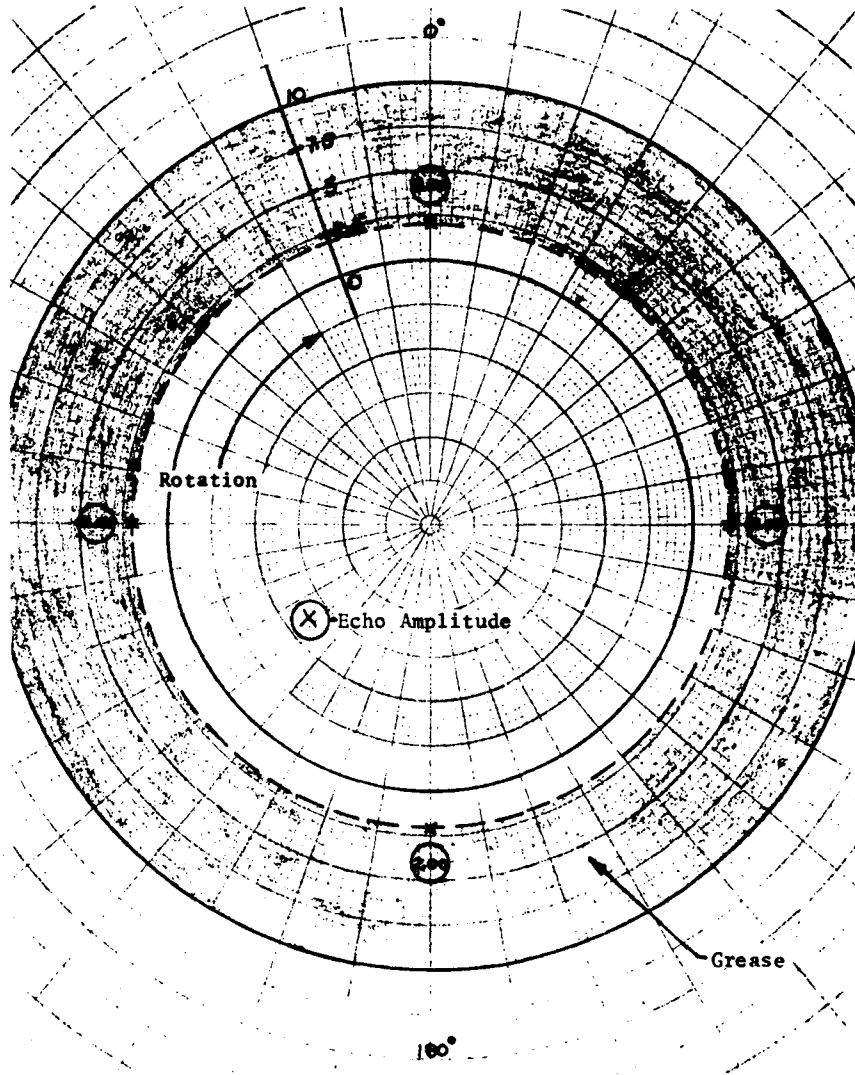


FIGURE 4-18. ECHO AMPLITUDES - OUTER RING,
BEARING 063104 - NORMAL GREASE CHARGE

4.4.2.2.2 Test II - Overgreased Bearing Study

Photographs of seal grease distributions after Test II are shown in Figures 4-19 and 4-20, for bearings 063103 and 063104 respectively. Ultrasonic echo amplitudes measured from the outside of the seal shrouds are plotted in Figures 4-21 through 4-24.

As expected, ultrasonic echo amplitudes show the outboard seals (into which the grease charge is directed by the grease fitting) to be entirely full.

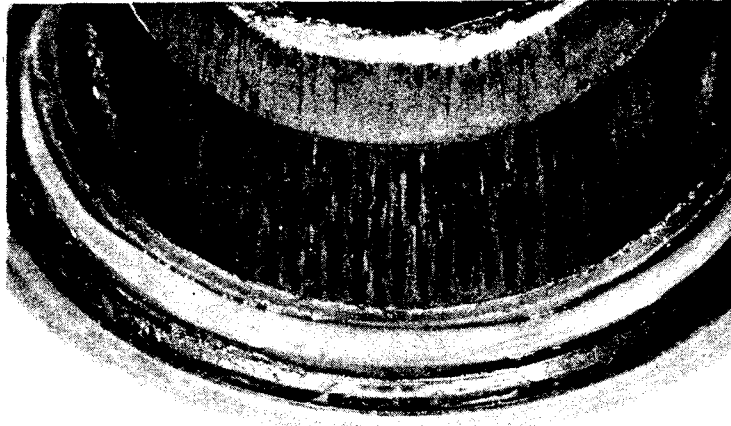
Grease distributions in the inboard seals and the area between cone assemblies (as shown in Figures 4-25 and 4-26) remained virtually unchanged.

Visual observation confirmed these data. The additional 8 oz charge had been distributed to the outboard seal, the outboard cone assembly and, to some extent, to the space beneath the end cap. Grease located between the cone assemblies and in the inboard seals was unchanged.

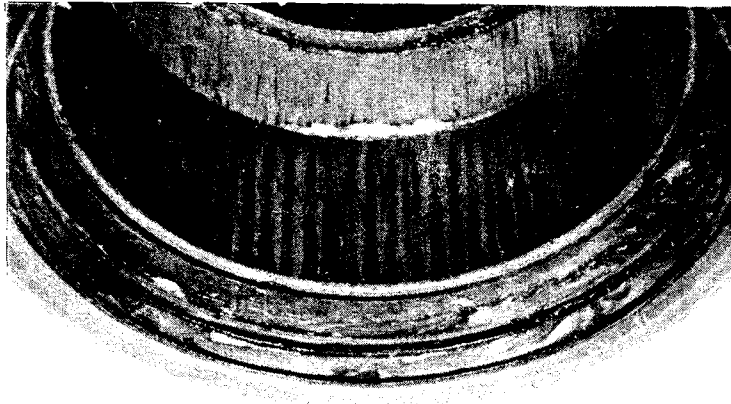
Grease in the outboard seal had darkened somewhat and there was evidence of local oil separation and churning. Bearing operating temperatures had risen 3°C relative to Test 1. The seals of both bearings remained intact.

4.4.2.2.3 Test III - Twice Overgreased Bearing Study

Photographs of seal grease distributions after Test III are shown in Figures 4-27 and 4-28. Figures 4-29 through 4-32 show



Grease Distribution in Outboard Seal

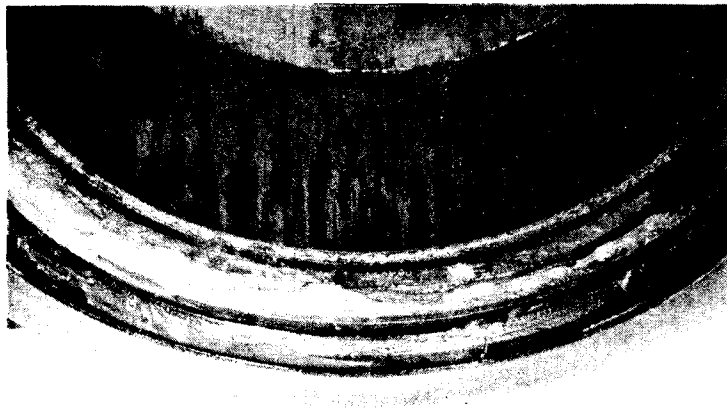


Grease Distribution in Inboard Seal

FIGURE 4-19. SEALS OF BEARING 063103 WITH 8 OUNCE GREASE RECHARGE



Grease Distribution in Outboard Seal



Grease Distribution in Inboard Seal

FIGURE 4-20

FIGURE 4-20. SEALS OF BEARING 063104 WITH 8 OUNCE GREASE RECHARGE

Grease Distribution Outboard Seal

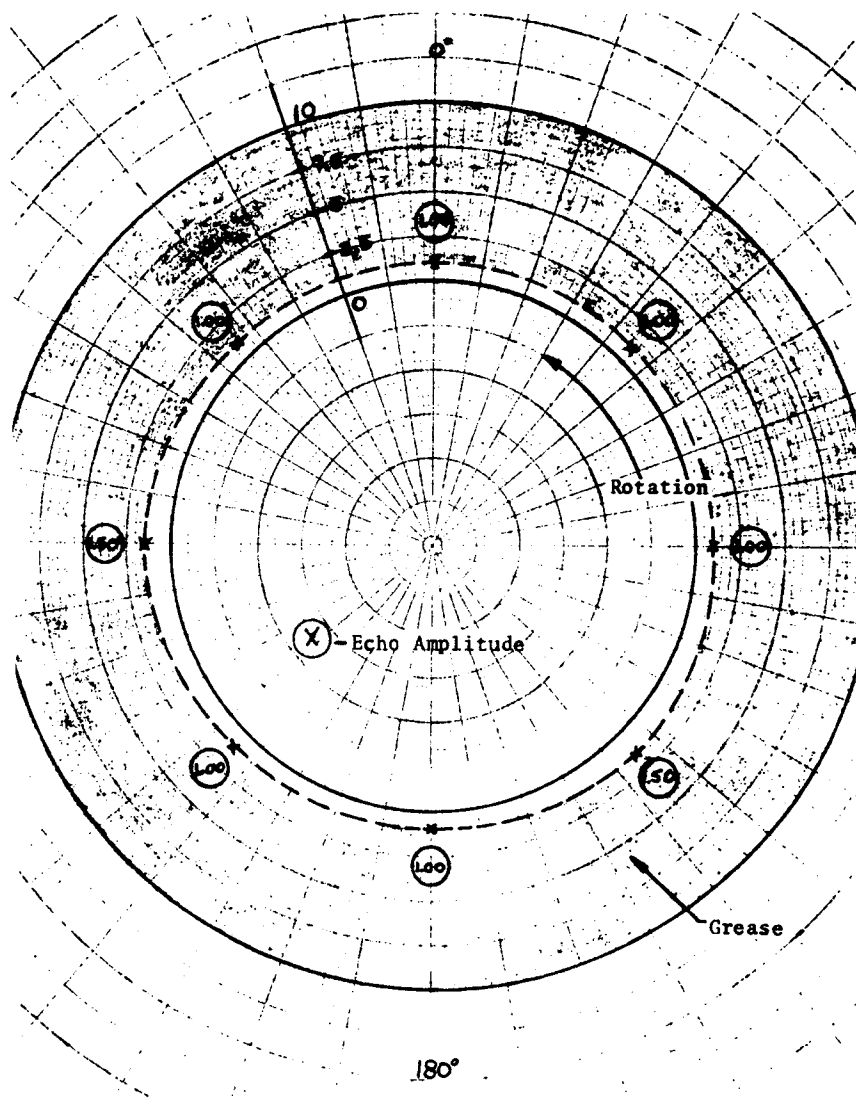


FIGURE 4-21. ECHO AMPLITUDES - OUTBOARD SEAL,
BEARING 063103 - 8 OUNCE GREASE RECHARGE

Grease Distribution Inboard Seal

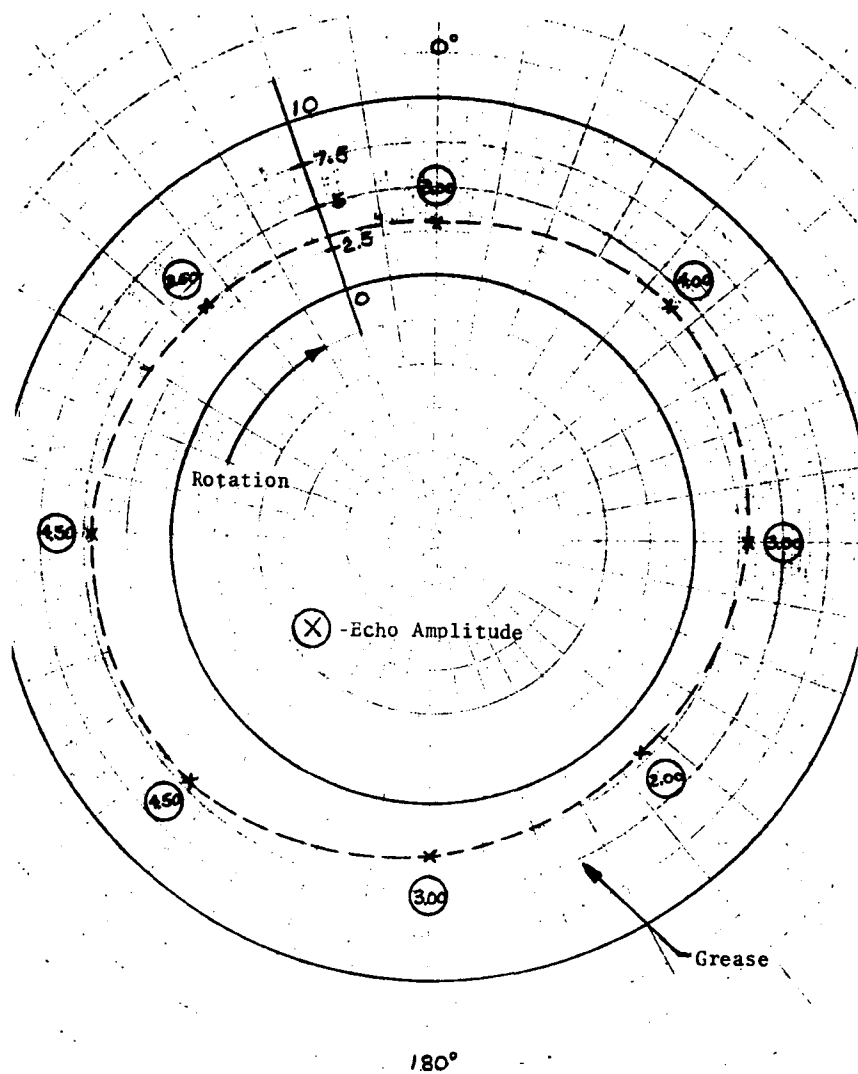


FIGURE 4-22. ECHO AMPLITUDES - INBOARD SEAL, BEARING 063103 - 8 OUNCE GREASE RECHARGE

Grease Distribution Outboard Seal

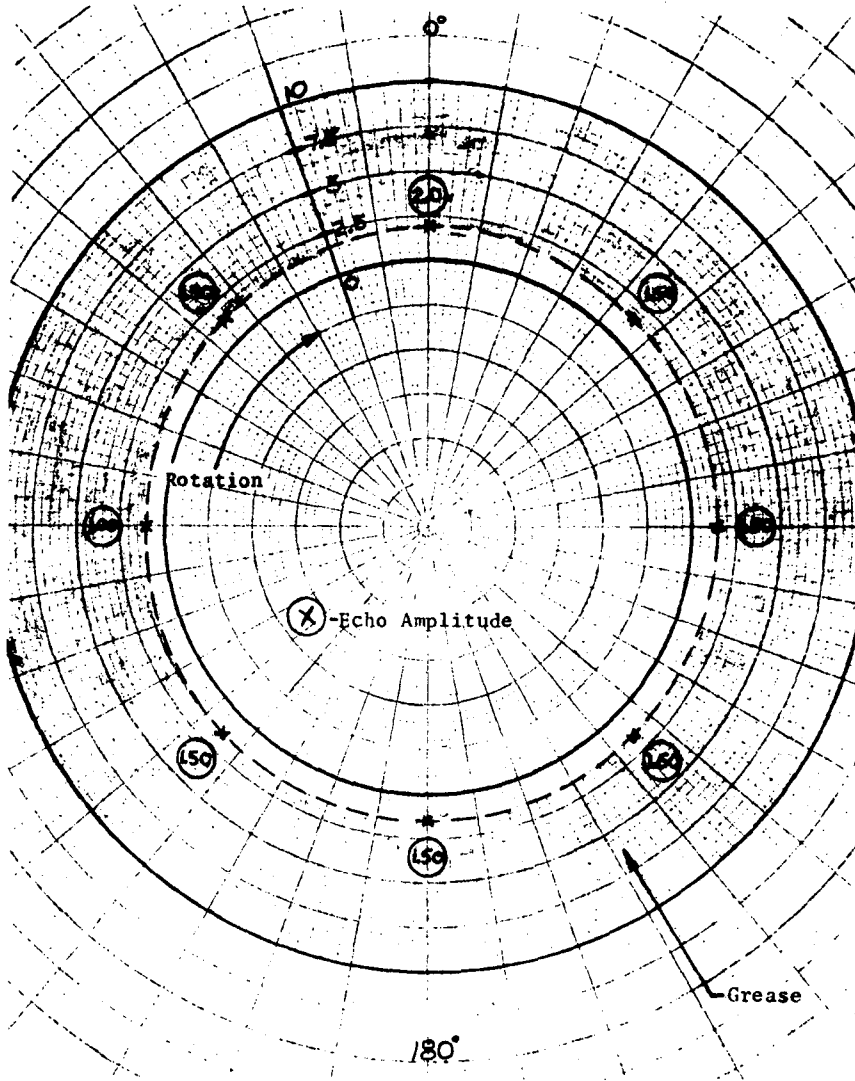


FIGURE 4-23. ECHO AMPLITUDES - OUTBOARD SEAL,
BEARING 063103 - 8 OUNCE GREASE RECHARGE

Grease Distribution Inboard Seal

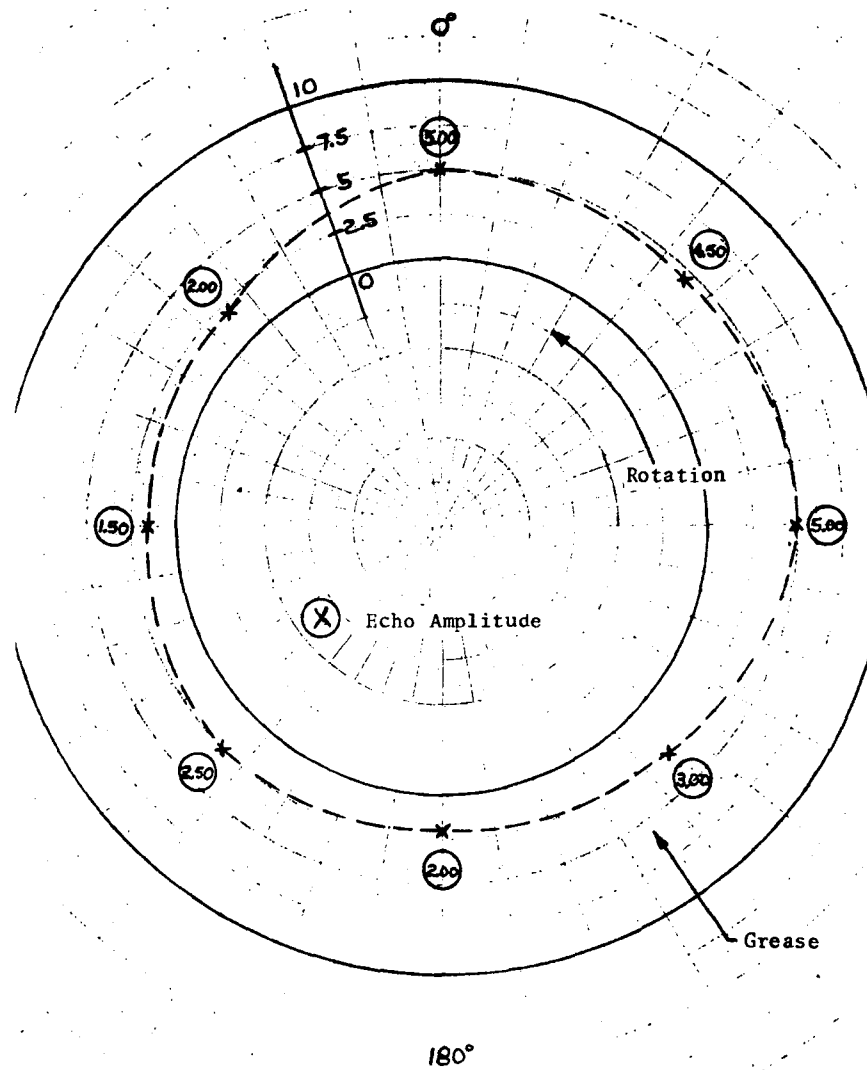


FIGURE 4-24. ECHO AMPLITUDES - INBOARD SEAL, BEARING 063104 - 8 OUNCE GREASE RECHARGE

Grease Distribution Outer Ring

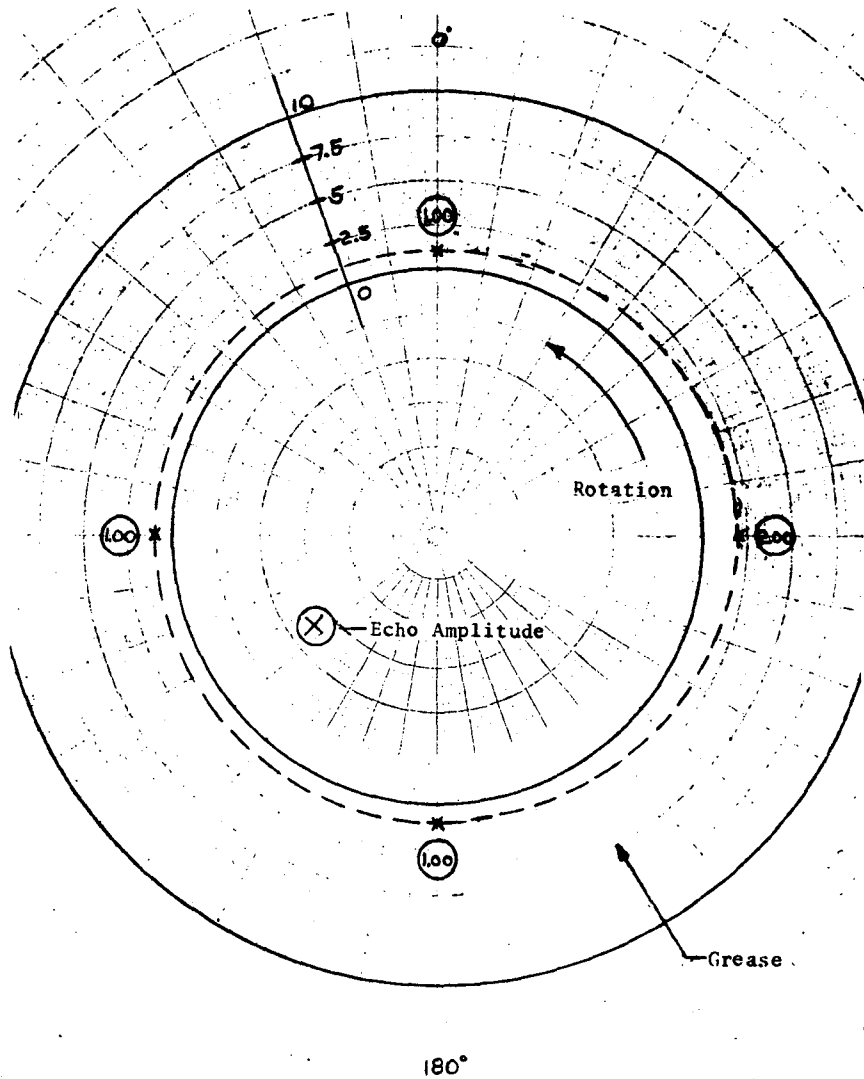


FIGURE 4-25. ECHO AMPLITUDES - OUTER RING,
BEARING 063103 - 8 OUNCE GREASE RECHARGE

Grease Distribution Outer Ring

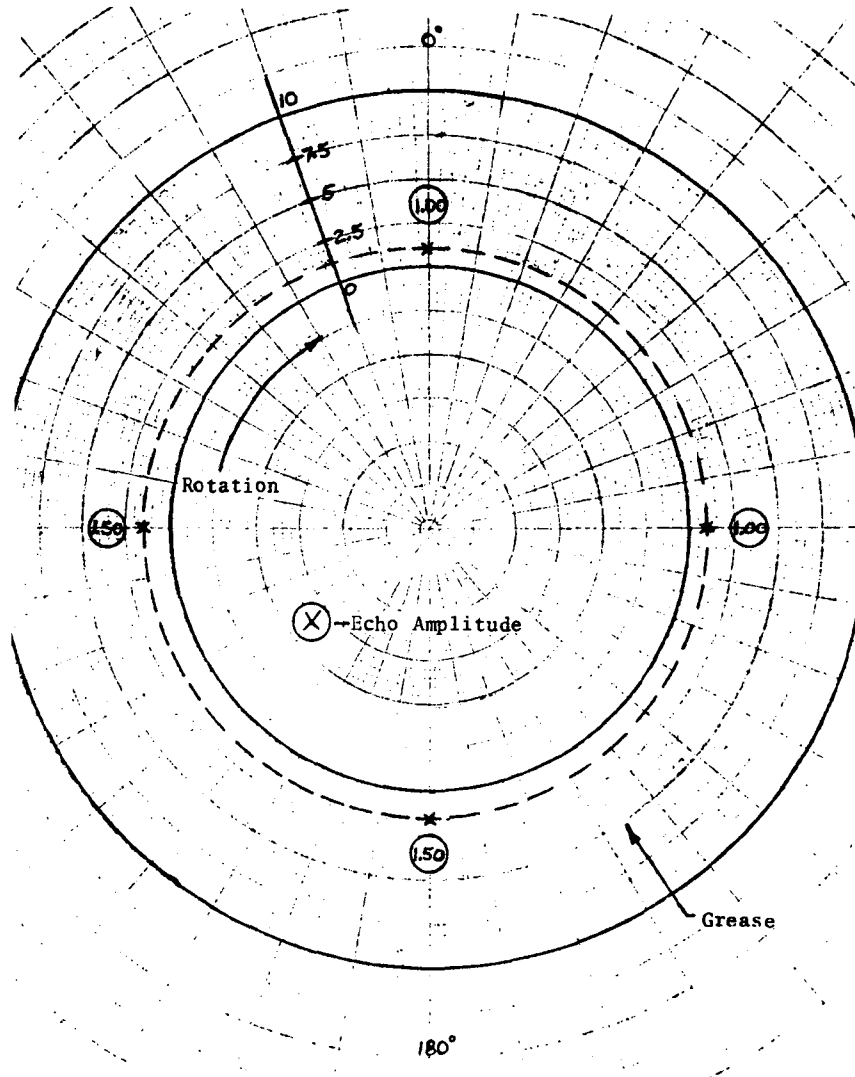


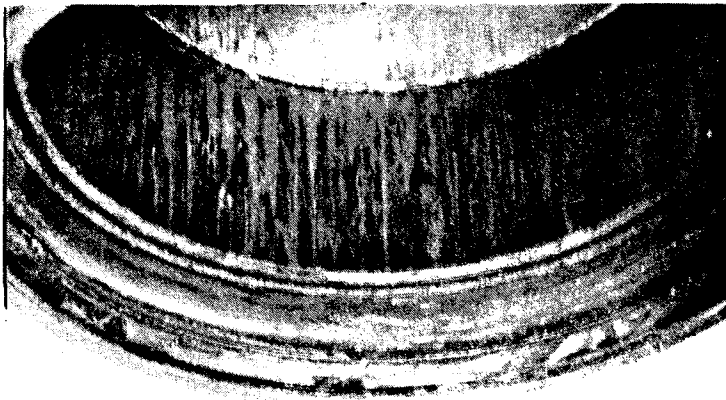
FIGURE 4-26

FIGURE 4-26. ECHO AMPLITUDES - OUTER RING,
BEARING 063104 - 8 OUNCE GREASE RECHARGE

Reproduced from
best available copy. 




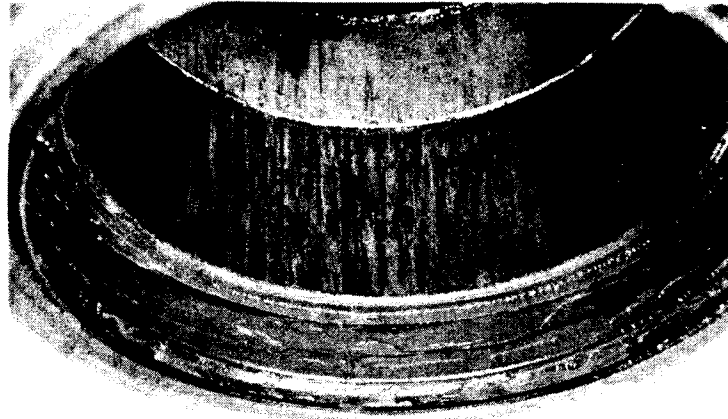
Grease Distribution in Outboard Seal



Grease Distribution in Inboard Seal

FIGURE 4-27. SEALS OF BEARING 065103 WITH
ADDITIONAL 3 OUNCE GREASE RECHARGE.

Reproduced from
best available copy. 



Grease Distribution in Outboard Seal



Grease Distribution in Inboard Seal

FIGURE 4-28. SEALS OF BEARING 063104 WITH
ADDITIONAL 8 OUNCE GREASE RECHARGE

Grease Distribution Outboard Seal

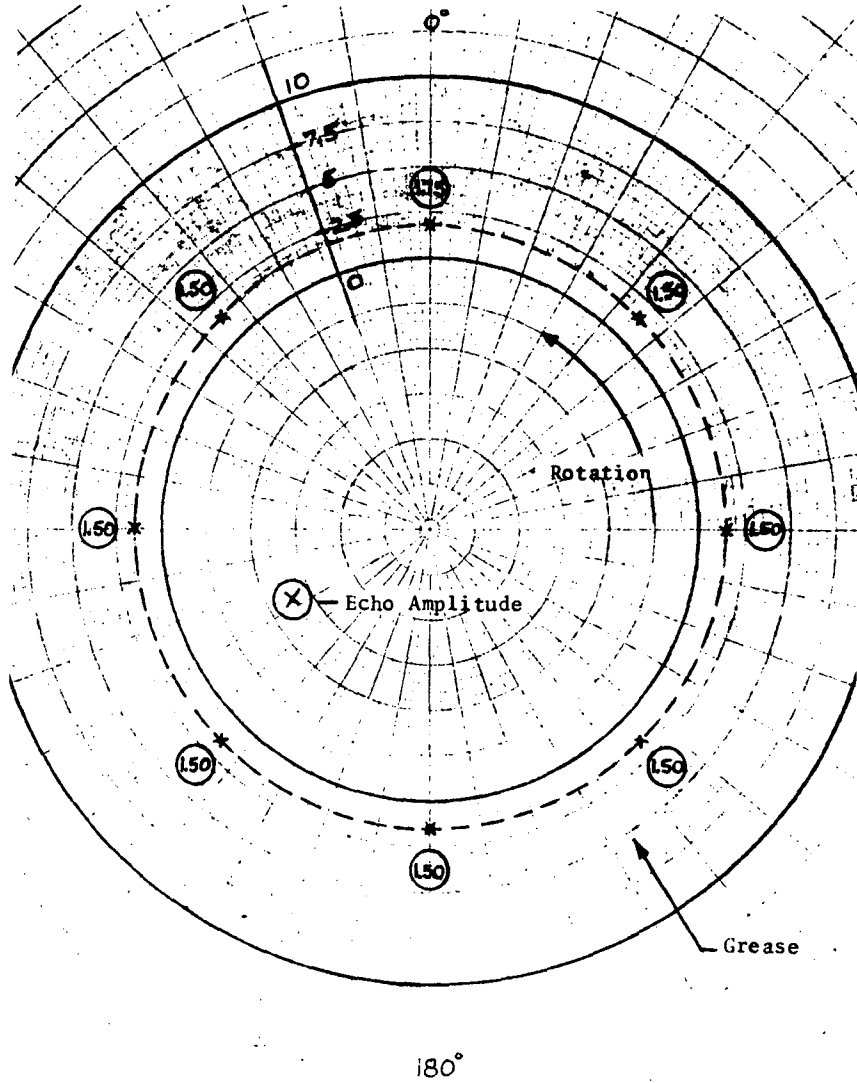


FIGURE 4-29. ECHO AMPLITUDES - OUTBOARD SEAL, BEARING 063103 - ADDITIONAL 8 OUNCE GREASE RECHARGE

Grease Distribution Inboard Seal

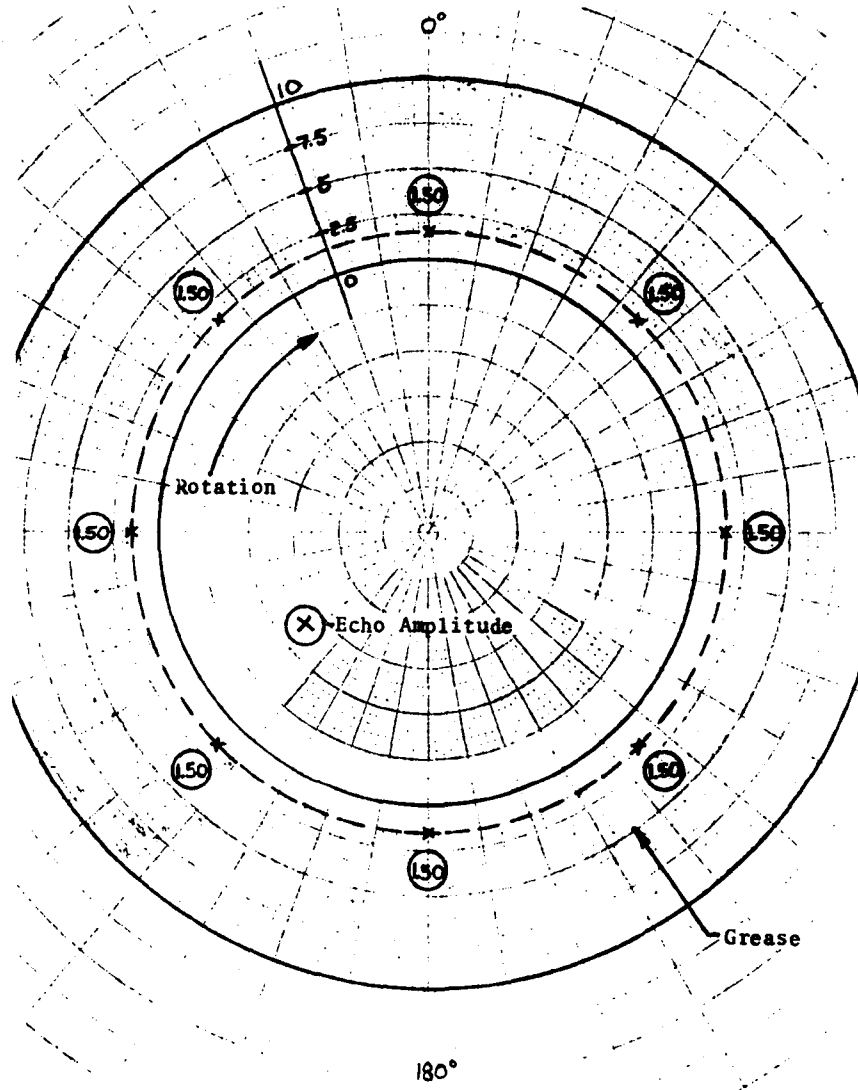


FIGURE 4-30. ECHO AMPLITUDES - INBOARD SEAL, BEARING 063103 - ADDITIONAL 8 OUNCE GREASE RECHARGE

Grease Distribution Outboard Seal

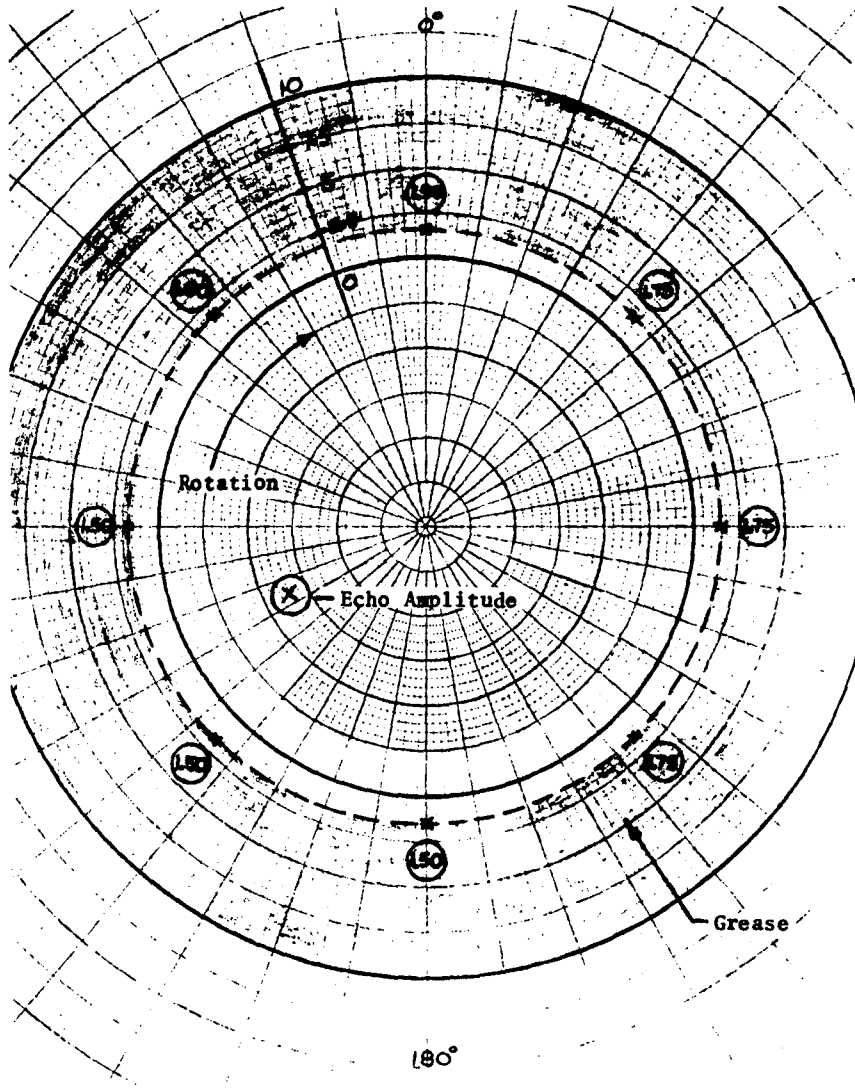


FIGURE 4-31. ECHO AMPLITUDES - OUTBOARD SEAL, BEARING 063104 - ADDITIONAL 8 OUNCE GREASE RECHARGE

Grease Distribution Inboard Seal

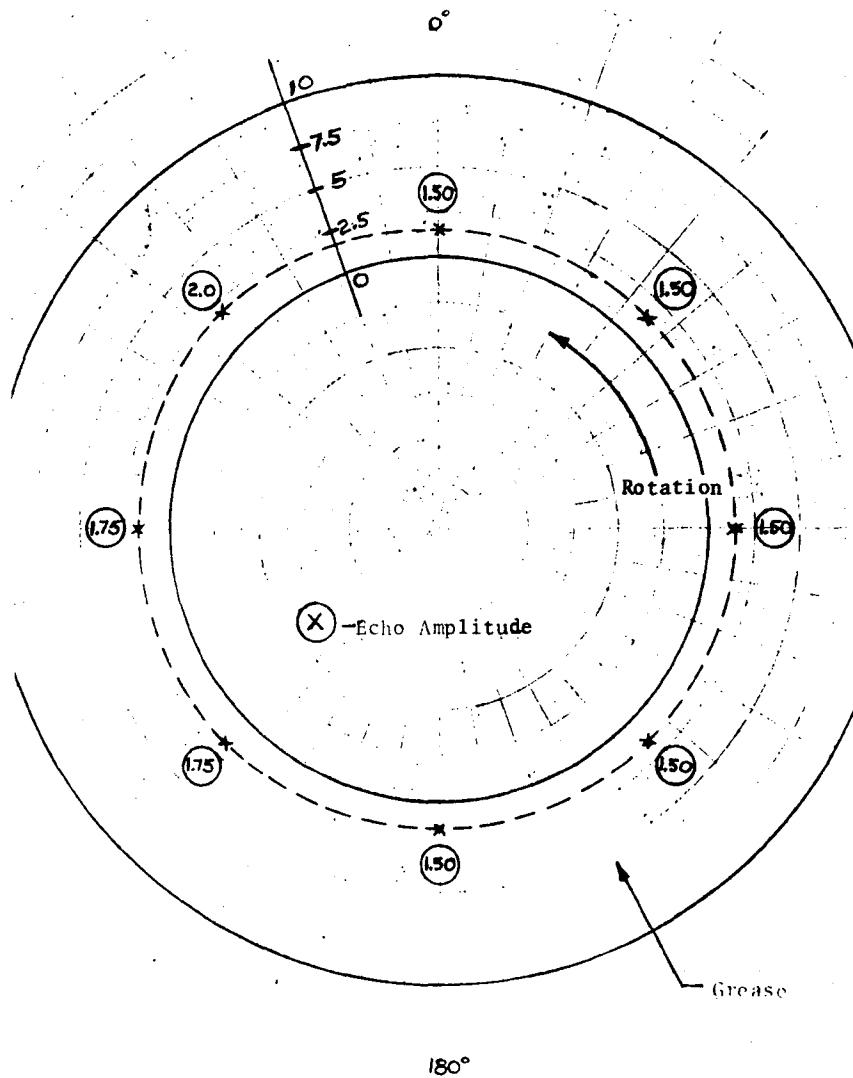


FIGURE 4-32. ECHO AMPLITUDES - INBOARD SEAL, BEARING 063104 - ADDITIONAL 8 OUNCE GREASE RECHARGE

echo amplitudes measured from the outside of the seal shrouds and Figures 4-33 and 4-34 those measured from the outer race OD. (Total overgreasing of these bearings for this test was 16 oz , a condition not uncommon in railroad service - see Section 4-2.

Ultrasonic echo amplitudes showed, and visual observation confirmed, that both seals (of each bearing) and area between the cone assemblies were totally full. The additional 8 oz charge (relative to Test II) had migrated through the bearing and served to completely fill the cone assemblies, the area between the cone assemblies, the inboard seals, and to a larger extent (relative to Test II) the space beneath the end caps.

Grease had darkened considerably throughout the bearing and oil separation was extensive. Bearing operating temperatures had risen 13°C relative to Test I. There was no discernible grease leakage throughout this test.

Table 4-2 shows a tabulation of bearing operating temperatures and visual observations for all tests. It is seen that operating temperatures stabilized, and that seals remained intact, i.e. there was no grease leakage, for all tests. It should be noted that these tests were run with new bearings (having new seals) and were of extremely short duration. Field service bearings having normal seal wear would have almost certainly lost grease if operated under similar conditions. Detailed metrological examination of the individual bearing assemblies (beyond the scope of this task) would most likely explain the observed variation in operating temperatures of the two bearings tested.

Grease Distribution Outer Ring

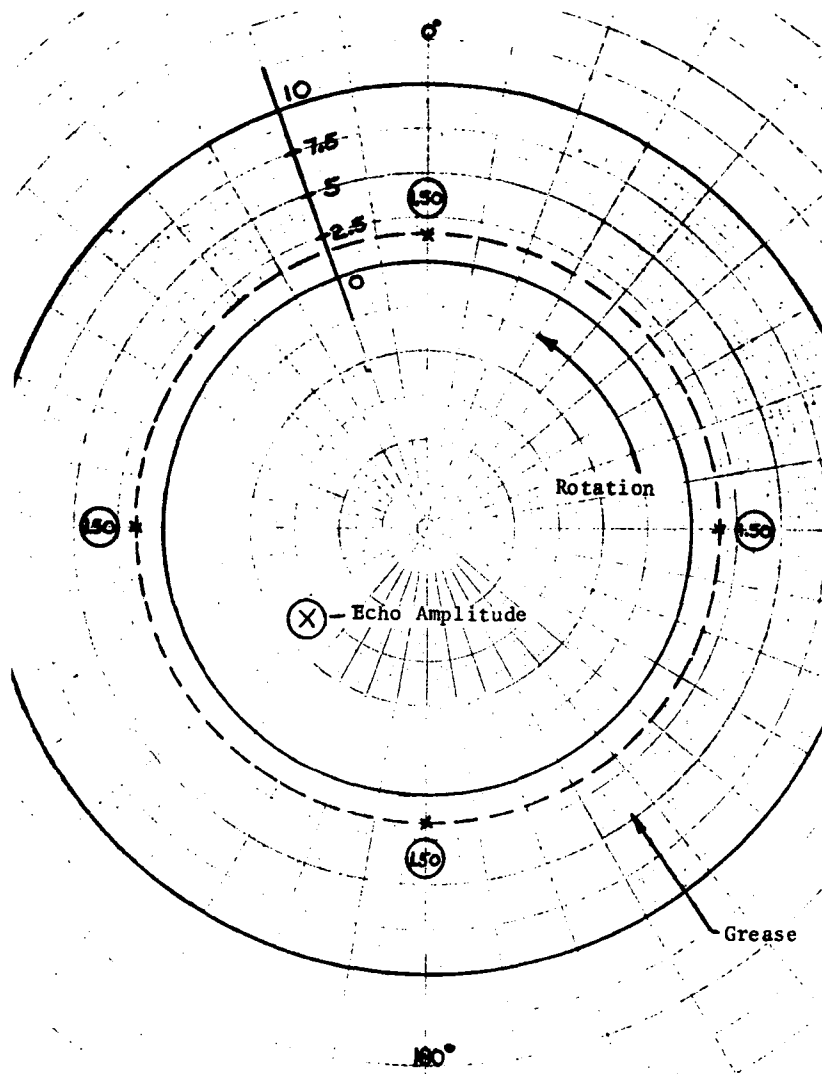


FIGURE 4-33. ECHO AMPLITUDES - OUTER RING, BEARING 063103 - ADDITIONAL 8 OUNCE GREASE RECHARGE

Grease Distribution Outer Ring

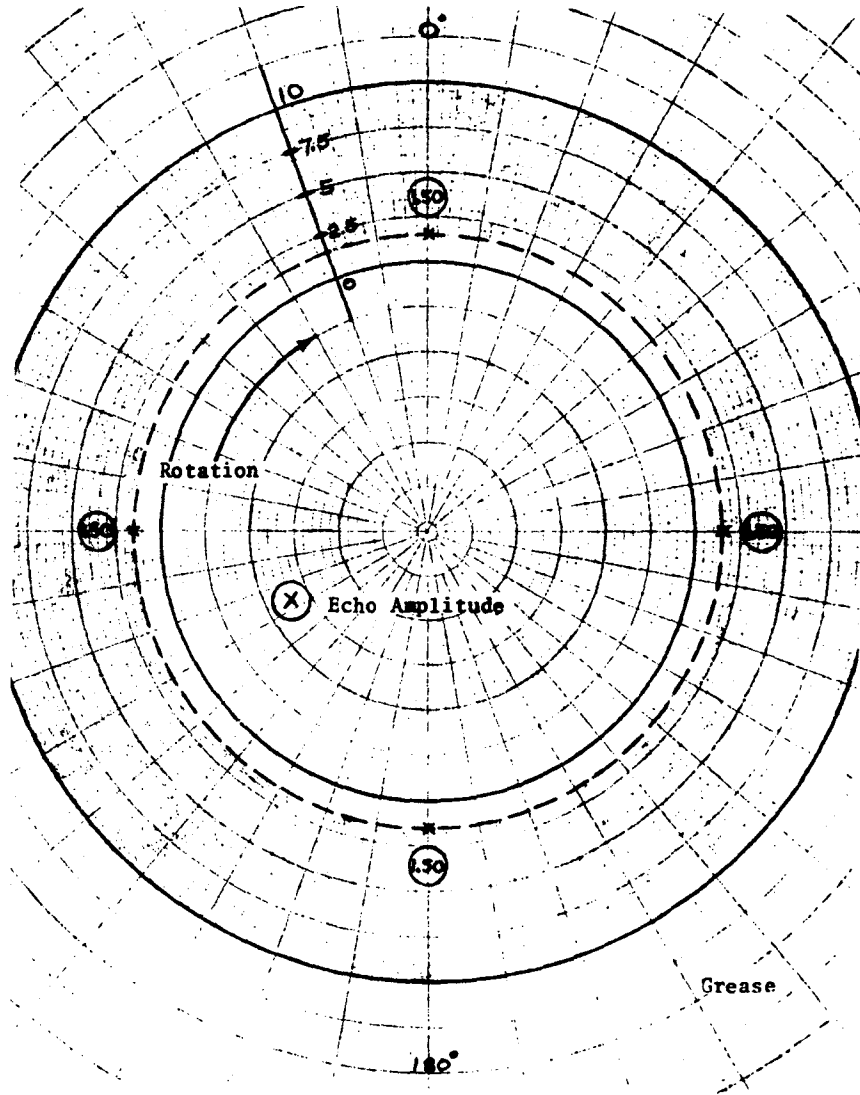


FIGURE 4-34. ECHO AMPLITUDES - OUTER RING, BEARING 063104 - ADDITIONAL 8 OUNCE GREASE RECHARGE

TABLE 4-2. TABULATION OF BEARING OPERATING TEMPERATURES AND VISUAL OBSERVATIONS OF GREASE MIGRATION STUDY

Operating Temperature °C					
Test No.	Grease Charge	Bearing 063103	Bearing 063104	Room Ambient °C	Remarks
I	Normal Pack (18 Ounces)	67	58	30	No visible grease leakage at seals
II	Normal Pack with 8 Ounce Recharge (Total 26 ounces)	67	58	27	No visible grease leakage at seals
III	Normal Pack with 8 Ounce Additional Recharge (Total 34 Ounces)	81	72	28	No visible grease leakage at seals

Test Conditions:

$F_r = 25,000 \text{ lb}$

$F_a = 0 \text{ lb}$

Speed - 60 MPH

Fans: one per bearing

Note: (a) All temperatures stabilized during 24 hour test.

(b) Normal Grease Charge:

4.5 oz in each cone assembly

9.0 oz center area between cone assemblies

4.5 CONCLUSIONS

The feasibility of using ultrasonic pulse echo techniques for determining grease layer thickness on the interior surfaces of railroad bearing seals and outer races has been demonstrated.

It was shown that visual observation of ultrasonic echo amplitudes on a cathode ray tube provides a measure of grease layer thickness adhering to the interior surfaces of seals and outer races.

Data acquired indicates:

1. That the outboard seal of a railroad bearing is the recipient of most of the 8 oz grease charge applied at the grease fitting and that, as a consequence, the circumferential distribution of grease adhering to the interior surface of the outboard seal is a reliable indicator of recent regreasing "history." See Figures 4-13, 4-15, 4-21 and 4-23.

2. That the circumferential grease distributions observed from inboard seals and outer races of a railroad bearing are poor indicators of recent regreasing history. This condition exists because the grease fitting does not direct grease specifically into the inboard seal and the space between the cone assemblies, and thus, there is little variation at these locations between normal and recently regreased bearings.

Since a regrease charge, applied at the grease fitting per current AAR standards, is almost totally absorbed by the outboard seal cavity, and since approximately 210°F of the outer seal shroud is accessible without bearing disassembly, ultrasonic inspection could eliminate overgreasing. A maintenance

mechanic in a railroad repair track would be able to determine the presence of a regrease charge beneath the outboard seal cavity before he regreases a recently regreased wheel set. This would eliminate overgreasing at its source.

Alternatively, a wayside mechanic seeing an outflow of grease from a bearing seal, could determine (with a portable ultrasonic tester) if such outflow was the result of inadvertent repair track overgreasing (in which case the seal would be full) or seal failure by some other cause (in which case the seal would be nearly empty). This would eliminate regreasing an already overgreased bearing.

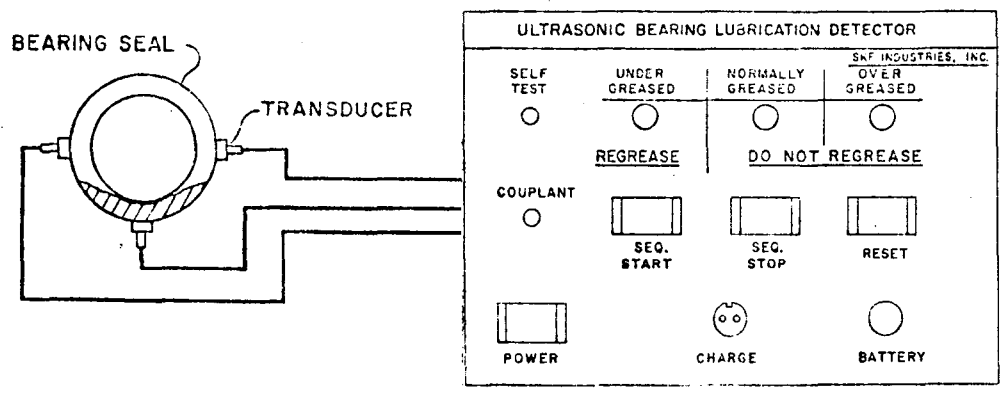
4.6 RECOMMENDATIONS

Use of the commercially available ultrasonic tester described here is not recommended as a maintenance level device. (Railroad personnel would have to slide a transducer along the OD of the outboard seal shroud and visually interpret CRT displays in order to determine bearing grease content.)

Instead, the device, depicted in Figure 4-35, containing a number of strategically located transducers is recommended as a maintenance level system. Each transducer would sense only the presence or absence of grease at a particular location (a task of minimal complexity from the results reported here). Electronic logic circuitry would automatically compute circumferential grease distributions and indicate whether regreasing is necessary. The instructions "Regrease" or "Do Not Regrease" would be indicated to the repair track mechanic. Figure 4-36 depicts the approximate total grease volumes vs. circumferential seal distributions for bearings arriving at Repair Track. (Recently regreased bearings have distributions similar to the middle sketch of Figure 4-36.

A work statement and schedule for a multiphase packaging and evaluation program, to produce prototypes of a maintenance level device are shown in Figures 4-37 and 4-38 respectively.

Reproduced from best available copy.



Ultrasonically detects grease distribution in roller bearing seal and indicates:

- Undergreased bearing "Regrease"
- Normally greased bearing "Do not Regrease"
- Overgreased bearing "Do not Regrease"

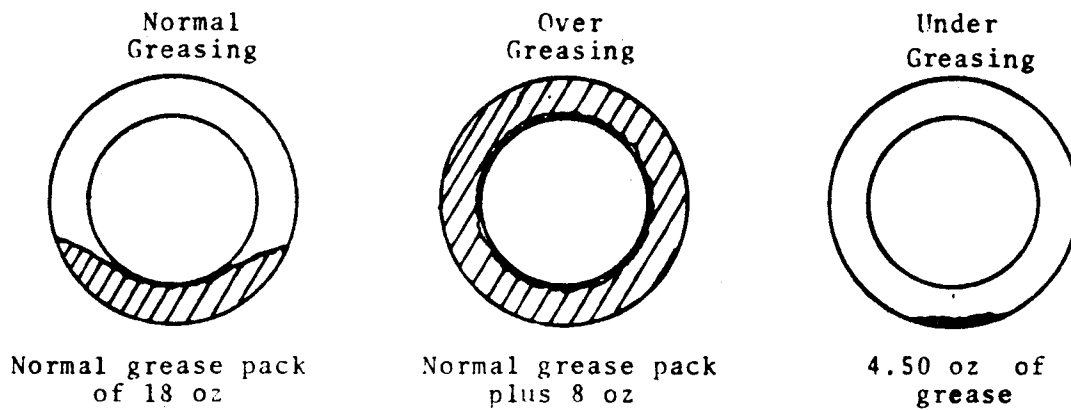
To be used by Maintenance Personnel, who now regrease based on calendar time alone.

Prevents overgreasing by indicating if a bearing actually needs grease, regardless of its recorded "date code".

Visited railroads have indicated that this device would be easily adaptable to their maintenance environment and that it would save very substantial derailment costs.

Railroads also indicated that, as a bonus, it would offset its operating cost by eliminating "hot box" setouts caused by overlubrication.

FIGURE 4-35. PROPOSED ULTRASONIC BEARING LUBRICATION DETECTOR



Illustrations of outboard seals showing normally, over, and undergreased bearings.

These illustrations show representative grease distributions for bearings having at least several hours of running time.

FIGURE 4-36. TYPICAL CIRCUMFERENTIAL GREASE DISTRIBUTION IN OUTBOARD SEALS

Phase I - Prototype System Fabrication and Packaging

- (a) Field - Visually and ultrasonically inspect (100) outboard seals of 6 in. x 11 in. railroad bearings from three major manufacturers at two railroad wheel shops to verify locations and operating limits of the outboard seal sensors.
- (b) Fabricate and package (2) prototype instrumentation systems.
- (c) Fabricate and package (2) transducer shoe assemblies (2 separate designs).
- (d) Fabricate and package (2) couplant supply systems (2 designs).
- (e) Laboratory "bench test" transducer shoe assemblies, couplant assemblies and instrumentation systems.
- (f) Update specifications for production prototypes.

Phase II - Evaluation of Two Engineering Prototype Systems

- (a) Laboratory - Evaluate two complete systems using (4) 6 in. x 11 in. railroad bearings run under endurance test conditions, and correlate ultrasonic data with visual examination for over, under and properly greased bearings.
- (b) Field Tests - (at two railroad wheel shops)
 - 1. Ultrasonically inspect incoming outboard bearing seals using systems fabricated and packaged in Phase I above.
 - 2. Visually inspect seals at disassembly, document inspection data, and correlate data with that obtained in (1b) above.
 - 3. Verify serviceability at repair track on incoming operational condition seals.

FIGURE 4-37. PROPOSED ULTRASONIC LUBRICATION DETECTOR EVALUATION PROGRAM

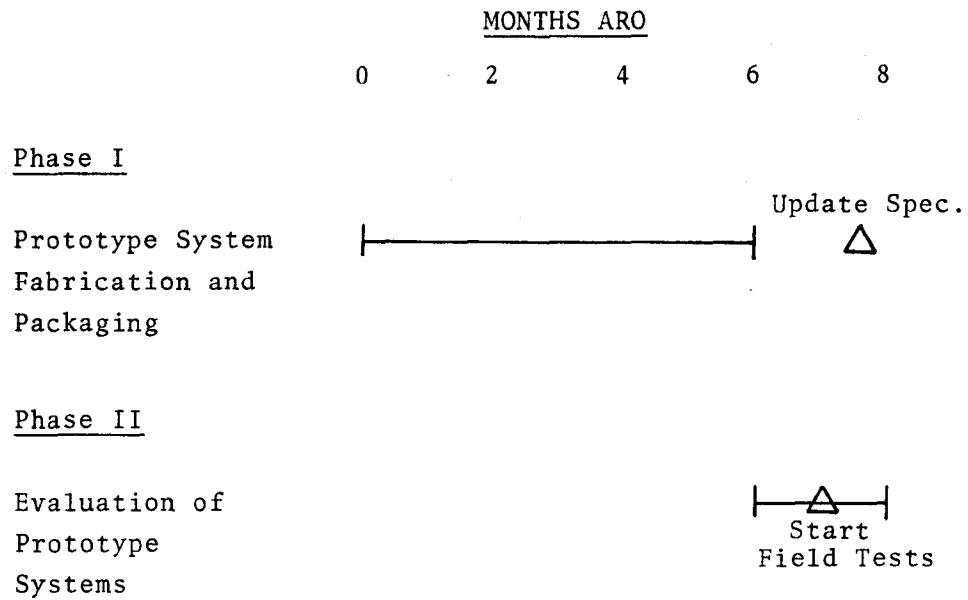


FIGURE 4-38. PROPOSED ULTRASONIC LUBRICATION DETECTOR PROGRAM SCHEDULE.

5. TASK III

BEARING COMPONENT DAMAGE DETECTION BY "SHOCK PULSE" METHOD

5.1 SUMMARY

The object of the Shock Pulse Program is to determine the feasibility of detecting certain predominant railroad roller bearing failure modes by using the principle of Shock Pulse Analysis.

The capability of the "Shock Pulse Meter," a commercially available analog instrument, to detect brinelling, spalling, and contaminated lubricant was investigated.

Railroad bearings having known defects were investigated. These bearings, which were run at two speeds under relatively light load, were used to acquire shock pulse data. Data acquired (by Shock Pulse Meter) were plotted to obtain shock pulse profiles. These profiles, were compared to those produced from data obtained from running new bearings, demonstrate the feasibility of detecting the various defects by Shock Pulse Analysis methods.

The Shock Pulse Technique has demonstrated its ability to:

1. Detect spalling, brinelling, and lubricant contamination in railroad roller bearings without disassembly.
2. Indicate progressive mechanical damage, thereby precluding catastrophic failures (derailments).

Use of an analog instrument in a railroad maintenance facility, however, is not cost effective since it requires significant operator interpretation, (including the plotting of profiles). For this reason, the development of a "Shock Emission Analyzer" that would provide (go)-(no-go) indications of bearing

condition was conceptualized as a logical follow-on to this feasibility study.

The "Shock Emission Analyzer" concept was presented to the engineering and maintenance staffs of several major railroads in order to obtain their reactions to such a device. They unanimously agreed that the "Shock Emission Analyzer:"

1. Addresses a major problem area.
2. Has substantial cost and life savings potential, regarding avoidance of derailments.
3. Has the potential of offsetting its annual operating cost in less than two months operation by avoiding unnecessary bearing teardown.

Two railroads specifically offered to use their manpower and facility to assist in evaluating prototypes of this device.

5.2 INTRODUCTION

It was shown in Phase I of Contract DOT-TSC-935 that spalling, brinelling other miscellaneous mechanical damages and grease contamination in railroad roller bearings play a major causative role in catastrophic roller bearing failure in freight service. Analysis of reported failure data indicates that catastrophic failures of roller bearings cost North American Railroads at least \$12 million per annum. The potential cost in human life resulting from roller bearing failure could be astronomical in the case of a dangerous cargo derailment in a heavily populated area.

This project consists of tests to determine the feasibility of detecting spalling, brinelling, grease contamination, etc. by use of a device employing a "Shock Pulse Analysis" technique. The Test Equipment Section describes the Shock Pulse Analysis device, the test machinery, and the test bearings used for this feasibility study. The Test Program Section outlines the tests, and the Test Results Section describes the data. The Conclusions Section summarizes the data and the Recommendations Section comments on the follow-on work.

5.3 TEST EQUIPMENT

5.3.1 Electronic Analysis System

The shock pulse principle of operation is described in Appendix C. An abbreviated discussion follows:

A damaged bearing in operation generates mechanical shocks at each encounter of a damaged surface with its contacting element. This causes short duration, sharp rise-time pulses of mechanical energy to emanate from the point of impact. The pulse of energy is governed in its travel by the speed of sound in the structural material, and not by the spring-mass characteristics of the mounting structure. Therefore, detectability is less dependent on detailed knowledge of specific mechanical transfer functions than with vibration signature analysis systems. The pulse is attenuated at each mechanical interface and decays in amplitude in proportion to the distance travelled and the damping characteristics of the material through which it is travelling. A resonant accelerometer is used as the pulse sensor, and its output is fed into an amplifier tuned to the accelerometer's resonant frequency. After signal processing, the output may be analyzed in terms of shock pulse "rate of occurrence" and "amplitude."

The Shock Pulse Meter (Figure 5-1), a commercially available unit is used as the shock pulse analyzer. It is composed of two distinct parts: (1) an accelerometer having a resonance of approximately 38 kHz and (2) a tuned amplifier and discriminator.

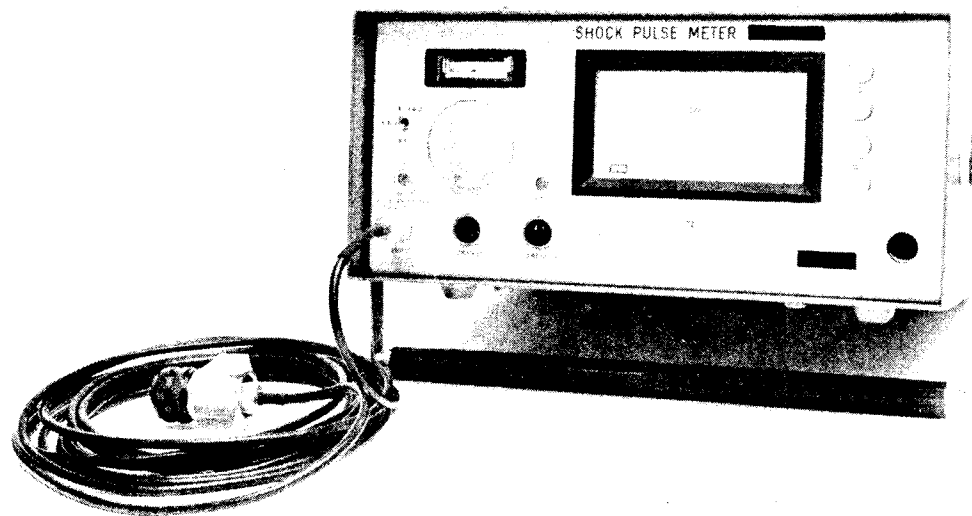


FIGURE 5-1. SHOCK PULSE METER

The accelerometer and electronic unit are used in a tuned mode. The shock pulse resonates the accelerometer while the amplifier is tuned to the accelerometer resonance. In this manner, the background vibration is completely ignored and the results of the impressed shock pulses are passed into the electronic unit.

The input signal is amplified and then passed to a peak sample and hold circuit. The peak determined is used for gain control of the amplifier and is sent to the rate threshold detector and meter circuit. The peak sample-and-hold circuit presents a pulse amplitude proportional to the input signal and is thus a quantization of the shock pulse.

The unit was used in the "Rate" mode for this test program. An analog meter displays rate (pulses per second) that are of a magnitude greater than the threshold set by a potentiometer dial on the front panel of the unit. Setting this dial, and measurements of rate, provide the data required to construct the shock emission profiles generated in these tests.

The shock emission profile shape reveals bearing condition and can be used to separate damaged and undamaged bearings, regardless of whether damage is a result of faulty installation, poor lubrication, progressive wear, and/or spalling.

Shock emission profile shapes are typically one of three types, shown as curves "A", "B", and "C" in Figure 5-2.

Curve shape "A" indicates a high rate of very small shocks

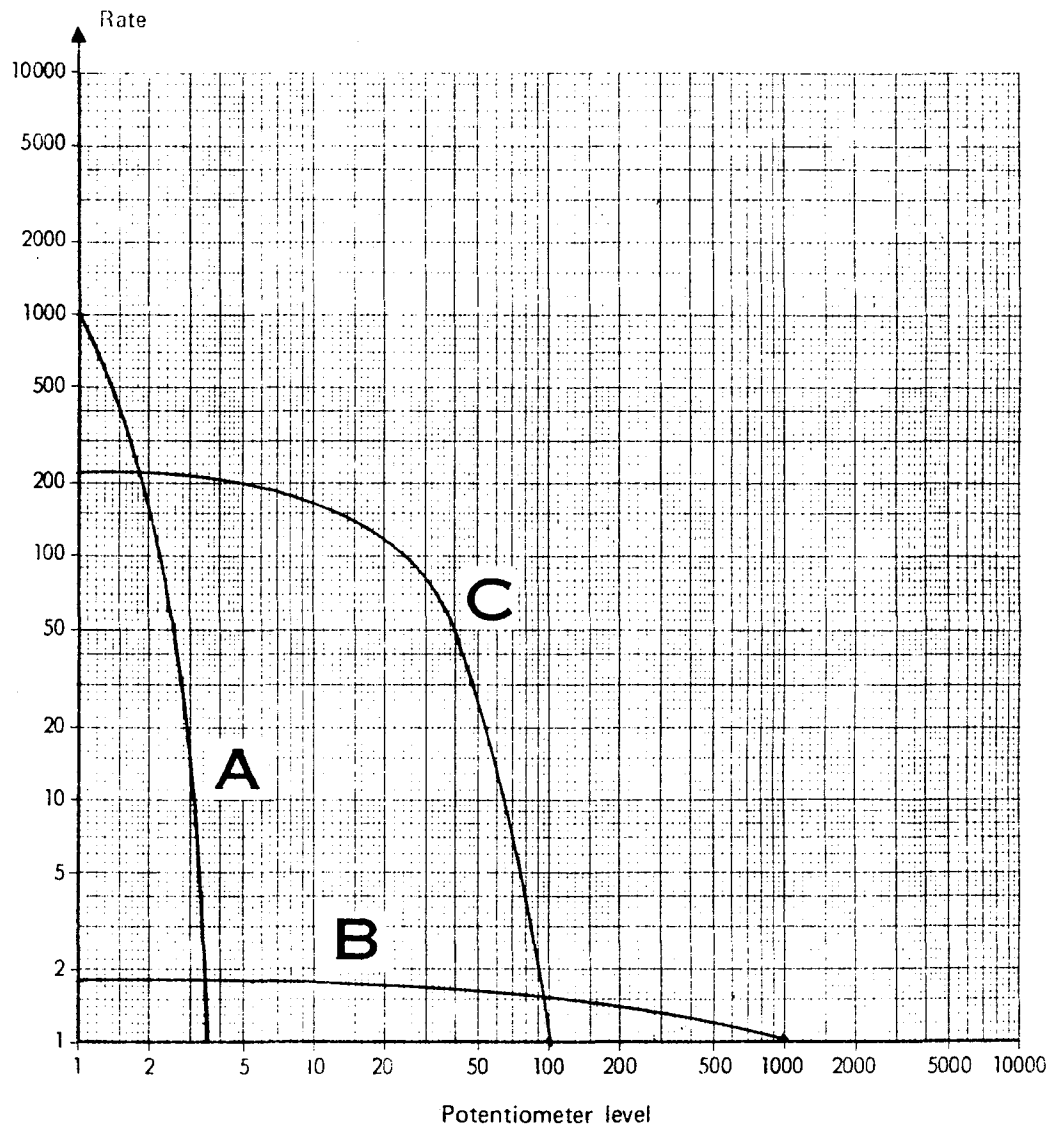


FIGURE 5-2. TYPICAL SHOCK EMISSION PROFILES

and the absence of shocks of high magnitude. It is characterized by its decrease in rate of occurrence with increasing shock level. This shock emission profile is characteristic of solid particles in the lubricant.

Curve shape "B" indicates the existence of large shock levels at low shock rate levels. This curve is prevalent in marginally lubricated bearings.

Curve shape "C" indicates the existence of a nearly constant rate of shock occurrence over a wide range of shock levels. It is an indicator of component damage.

An increase in the level of shocks occurring at a specific rate is indicative of component damage growth. Early damage is seen to yield minor "squaring out" of the shock emission profile whereas advanced damage results in a nearly rectangular shaped profile.

5.3.2 Bearing Test Machine

An endurance tester, adapted for railroad bearing testing, was employed. The railroad bearing test machine was shown in Figure 4-5 and was described in Section 4.3.2.

For this program, two test rig modifications (shown in Figure 5-3) were necessary:

1. The railroad bearing adaptor was drilled and tapped in the bearing load zone to accept the accelerometer sensor stud.
2. The bearing loading system was changed from load beams to dead weights because of the relatively light bearing test loads.

5.3.3 Test Bearings

Standard 6 in. x 11 in. tapered railroad bearings were used for testing. They consisted of two new bearings and several service failures.

The new bearings were representative of unfailed bearings with uncontaminated grease. They were run to provide baseline data for the tests to follow.

Service failures were obtained from a railroad bearing rebuild shop.

All "service failure" bearings were deemed failures in accordance with the AAR Roller Bearing Manual and had been removed from service. These failures consisted of two different levels of spalling severity on inner rings exclusively; one roller spalling failure; two different levels of spalling on outer races exclusively; and two with different levels of brinelling damage.

The new bearings used initially for baseline testing were subsequently utilized in grease contamination tests.

Contamination, in the form of Grade 33 sandblasting sand, was added to the lubricated cone assemblies at bearing assembly. This was done to simulate the ingress of particulate contaminant which could occur when a bearing with a failed seal is exposed to a sandy environment.

Reproduced from
best available copy.

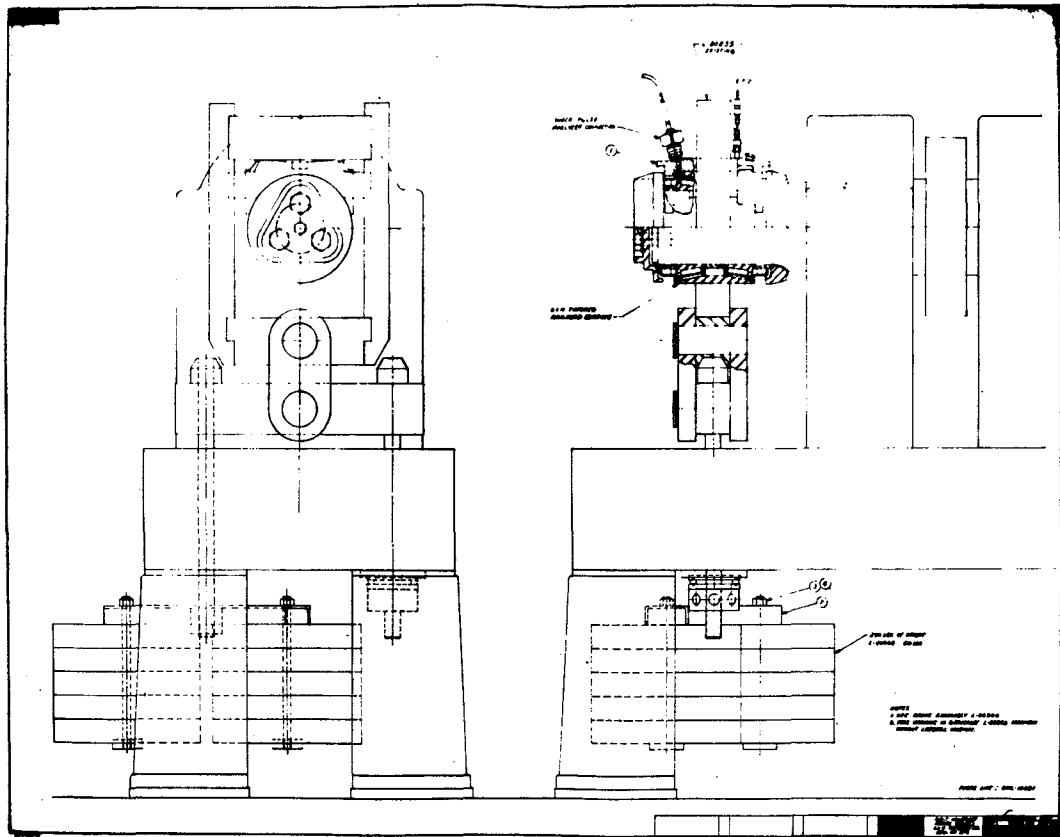


FIGURE 5-3. MODIFIED RAILROAD BEARING TEST MACHINE

All test bearings were lubricated to AAR lubrication specification. Each cone assembly was packed with 4.5 oz of lubricant and the center area of the bearing between the cone assemblies was packed with 9 oz of the same lubricant. This provided a total grease pack of 18 oz. All bearings were checked for lateral clearance at assembly and met the specified .021 in. to 0.27 in. lateral play.

5.4 TEST PROGRAM

The Shock Pulse Bearing Damage Detection Test Plan, Contract DOT-TSC-935 Phase II, Task III, is reproduced in Appendix D. An abbreviated discussion follows.

All bearings were tested under an applied radial load of 1300 lbs and at speeds of 100 to 200 RPM (equivalent to train speeds of 10 to 20 miles per hour). This light bearing load represents the approximate weight of a railroad wheel set and the slow speeds are representative of the cutting speeds of a wheel turning machine. (These test conditions simulate conditions in a wheel shop where the shock pulse technique may ultimately be applied).

All test bearings were first run for 20 hours at 20 mph, and then for another 4 hours at 10 mph. Data were accumulated at the ends of each phase.

Data were accumulated from the Shock Pulse Meter for the five different test bearing groups using "rate" mode. In this mode, the front panel meter displays the occurrence rate (pulse/sec) of pulses greater in magnitude than a predetermined dialable level. The rates of occurrence at each of several dialed-in magnitudes were recorded for each test. From this, a graph of shock rate versus shock level (shock emission profile) was plotted. Bearing condition was interpreted by the shape of the shock emission profile. Shapes of the profiles will be referred to as "A," "B," or "C" curves as described previously in the discussion of the Shock Pulse Meter in the Test Equipment Section.

For all tests shock rate data reported, represent averages of three separate data acquisitions. Individual data points were within +5 percent of those shown in the tables of Section 6.6.

To verify bearing condition, photographs of the failed bearing components were taken wherever possible and are presented along with the shock pulse data.

5.5 TEST RESULTS

5.5.1 Test I - Baseline Tests

Two new 6 in. x 11 in. tapered roller bearings were tested under the aforementioned test conditions to establish a baseline, simulating unfailed bearings with uncontaminated grease. Data taken from these bearings on the Shock Pulse Meter are presented in Tables 5-1A and 5-1B. From these data, the shock emission profile (Figure 5-4) was generated. The profiles revealed "A" curves of log magnitude which are indicative of unfailed bearings with little or no contaminant present. The average shock level for the two new bearings at a speed of 20 mph was 21 with low shock rates of 7.5 pulses per second. At the 10 mph speed the shock level was 6.0 with low-shock rates of 4.5 pulses per second.

5.5.2 Test 2 - Inner Ring Spalling

This test consisted of running two bearings with different degrees of spalling on the inner ring roller paths. Data taken on these bearings at the two different speeds are presented in Tables 5-2A and 5-2B. Shock emission profiles plotted from these readings are shown in Figure 5-5. The profiles revealed "C" curves having significant shock levels and high shock rates for the heavily spalled inner ring at the two test speeds. Shock rates of 12 pulses per second with shock levels of 10 to 50 were recorded for the moderately spalled inner ring at the two speeds.

The appearance of "C" curves in three of the four test runs indicates the presence of rolling element damage in the bearings, as compared to the low profile "A" curve which are indicative of unfailed bearings run in the baseline tests. At the test speed of 10 mph, the moderately spalled inner ring was not detectable.

TABLE 5-1A. SHOCK PULSE DATA - BASELINE TEST -
 20 MPH NEW 6 IN. x 11 IN. TAPERED RAILROAD BEARINGS

SHOCK PULSE DATA			
Potentiometer Level (Shock Level)	Brg. No. 063101	Brg. No. 063102	Average
1	8.0	9.0	8.5
2	7.0	8.5	7.75
5	5.0	4.0	4.5
10	2.5	1.2	1.85
20	1.5	1.0	1.25
50	1.0		

Test Conditions

Load F_r = 1300 lb

F_a = 0 lb

Speed 20 mph for 20 hr

TABLE 5-1B. SHOCK PULSE DATA - BASELINE TEST -
 10 MPH NEW 6 IN. x 11 IN. TAPERED RAILROAD BEARINGS

<u>SHOCK PULSE DATA</u>			
<u>Potentiometer Level (Shock Level)</u>	<u>Brg. No. 063101</u>	<u>Brg. No. 063102</u>	<u>Average</u>
1	6.0	3.5	4.75
2	1.9	1.5	1.7
5	1.2	1.5	1.35

Test Conditions

Load $F_r = 1300$ lb

$F_a = 0$ lb

Speed 10 mph for 4 hr

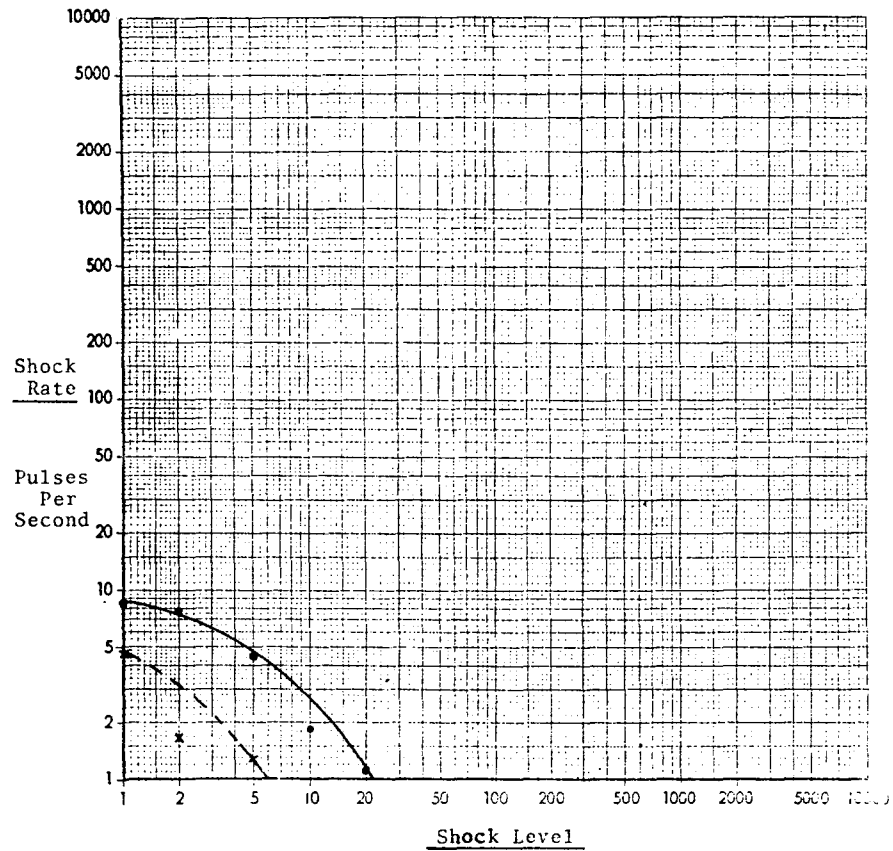


FIGURE 5-4. SHOCK EMISSION PROFILES - BASELINE
 TEST NEW 6 IN. X 11 IN. TAPERED RAILROAD BEARINGS

TABLE 5-2A. SHOCK PULSE DATA - MODERATELY SPALLED
INNER RING-BEARING 063201

SHOCK PULSE DATA		
Shock Rate - Pulses per Second		
Potentiometer Level (Shock Level)	Speed-20 mph	Speed-10 mph
1	12.0	12.0
2	12.0	6.5
5	12.0	3.5
10	3.8	1.0
20	1.5	—
50	1.0	

Test Conditions

Load $F_r = 1300$ lb

$F_a = 0$ lb

Speed 20 mph for 20 hours

10 mph for 4 hours

TABLE 5-2B. SHOCK PULSE DATA - HEAVILY SPALLED
INNER RING - BEARING 063202

SHOCK PULSE DATA		
Potentiometer Level (Shock Level)	<u>Shock Rate - Pulses per Second</u>	
	Speed- 20 mph	Speed-10 mph
1	170.0	160.0
2	170.0	130.0
5	150.0	130.0
10	150.0	90.0
20	150.0	55.0
50	95.0	17.0
100	50.0	4.5
200	12.0	2.0
500	3.0	1.0
1000	1.5	—
2000	1.0	

Test Conditions

Load - $F_r = 1300 \text{ lb}$

$F_a = 0 \text{ lb}$

Speed - 20 mph for 20 hours

10 mph for 4 hours

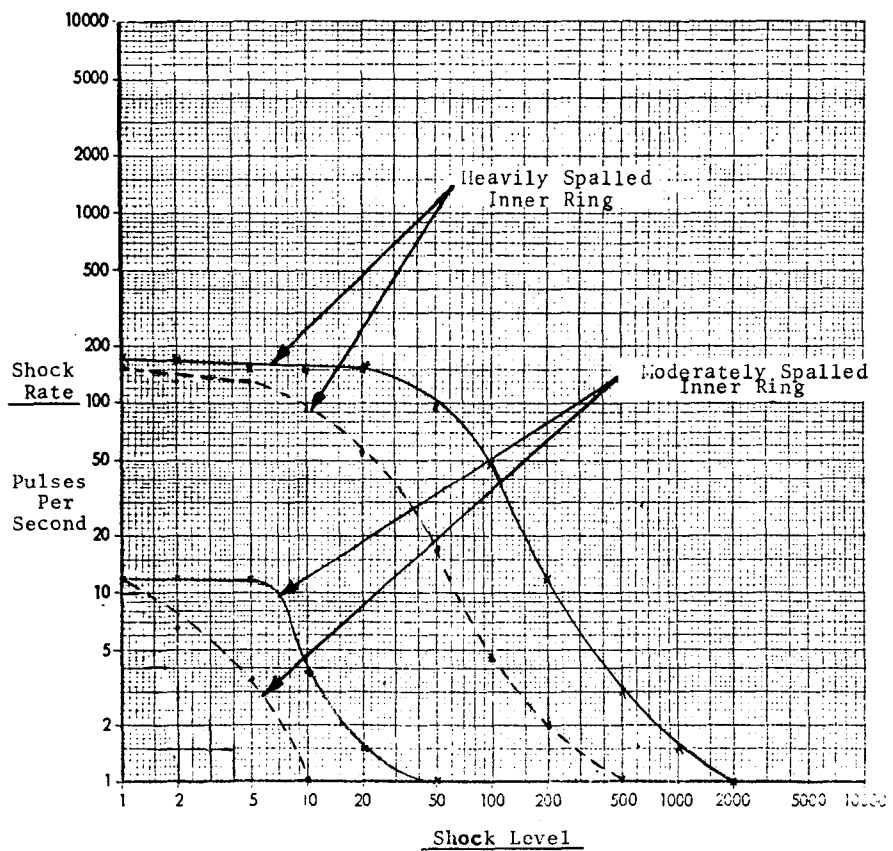


FIGURE 5-5. SHOCK EMISSION PROFILES - SPALLED INNER RINGS

5.5.3 Test 3 - Roller Spalling

This test consisted of running one bearing with lightly spalled rollers as shown in Figure 5-6. Data taken on this bearing at two different speeds by the Shock Pulse Meter are presented in Table 5-3. A shock emission profile plotted from these readings is shown in Figure 5-7. The profiles revealed "C" and "A" curves having significant shock levels in the magnitude of 4 to 25 and low shock rates of 15 to 20 pulses per second at the two speeds.

The appearance of a "C" curve at the 20 mph speed indicates the presence of rolling element damage in the bearing, as compared to the low profile "A" curve which was indicative of unfailed bearings run in the baseline test. At a test speed of 10 mph, the lightly spalled rollers were not detectable.

5.5.4 Test 4 - Outer Ring Spalling

This test consisted of running two bearings with different degrees of spalling on one outer ring roller path. One outer ring was moderately spalled and one was heavily spalled as shown in Figure 5-8. Data taken on these bearings at the two speeds by the Shock Pulse Meter are presented in Tables 5-4A and 5-4B. Shock emission profiles plotted from this data is shown in Figure 5-9. The heavily spalled outer ring at 20 mph speed revealed a "C" curve having a significant shock level of 80 with a shock rate of 90 pulses per second. The moderately spalled outer ring at 20 mph also revealed a "C" curve having a shock level of 50 with a shock rate of 45 pulses per second.

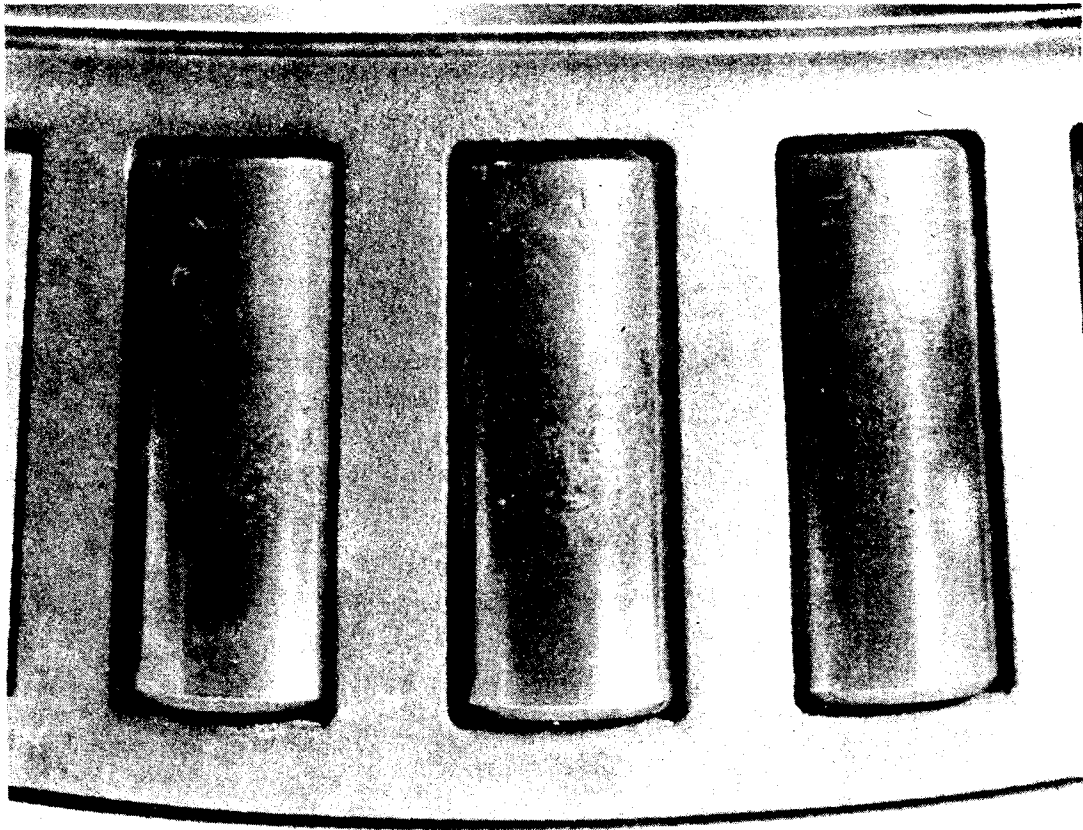


FIGURE 5-6. LIGHTLY SPALLED ROLLERS

TABLE 5-3
 TABLE 5-3. SHOCK PULSE DATA - LIGHTLY SPALLED
 ROLLERS - BEARING 063301

SHOCK PULSE DATA		
Potentiometer Level (Shock Level)	Shock Rate - Pulses Per Second	
	Speed - 20 mph	Speed - 10 mph
1	20.0	15.0
2	20.0	6.5
3	-	1.5
4	-	1.0
5	20.0	-
10	10.0	
15	4.0	
20	1.5	
25	1.0	

Test Conditions

Load F_r = 1300 lb

F_a = 0 lb

Speed - 20 mph for 20 hours

10 mph for 4 hours

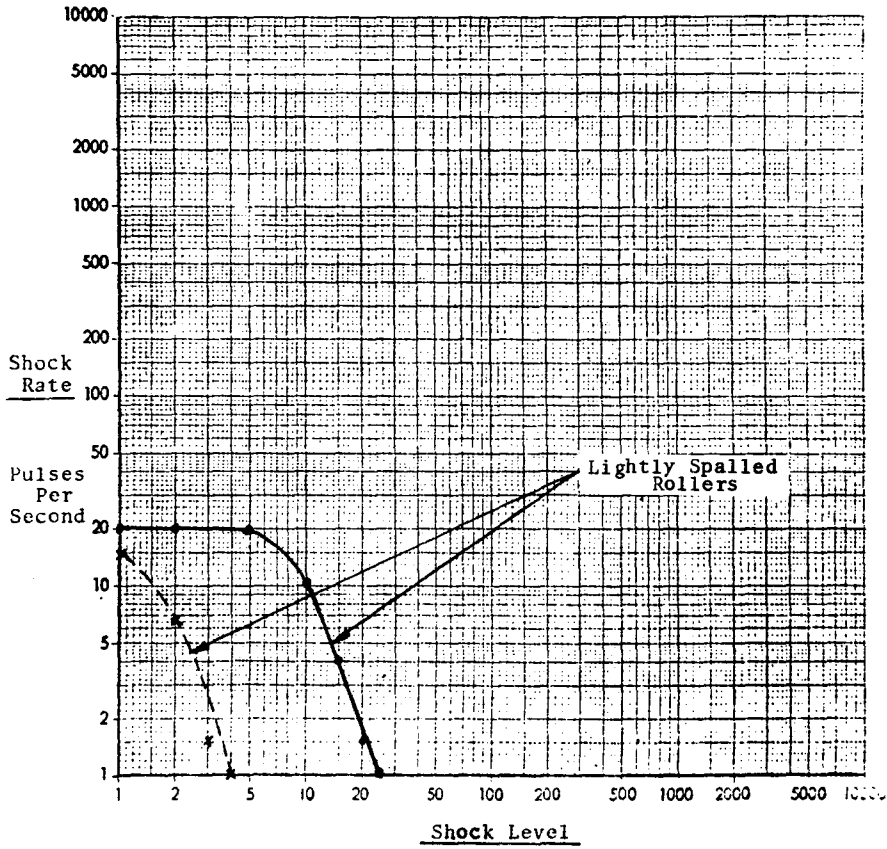
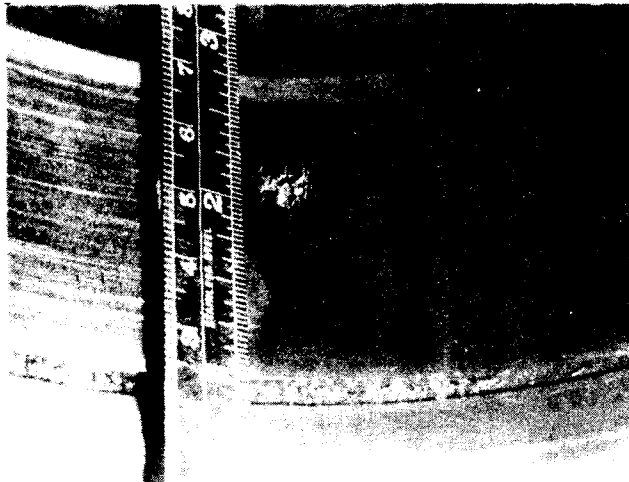
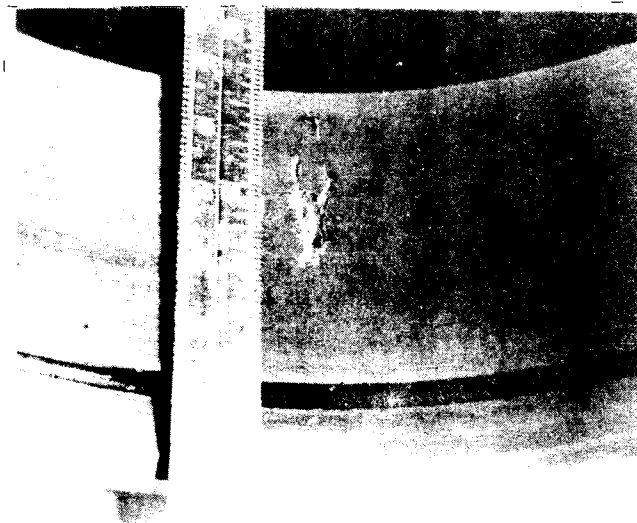


FIGURE 5-7. SHOCK EMISSION PROFILES - SPALLED ROLLERS



Moderately Spalled Outer Ring



Heavily Spalled Outer Ring

FIGURE 5-8. TYPICAL SPALLED OUTER RINGS

TABLE 5-4A. SHOCK PULSE DATA - MODERATELY SPALLED
 OUTER RING - BEARING 063401

SHOCK PULSE DATA

<u>Potentiometer Level</u> <u>(Shock Level)</u>	<u>Shock Rate - Pulses Per Second</u>	
	<u>Speed - 20 mph</u>	<u>Speed - 10 mph</u>
1	45.0	45.0
2	45.0	15.0
3	-	8.0
4	-	4.5
5	25.0	3.0
6	-	1.8
7	-	1.5
8	-	1.0
10	12.0	-
20	5.0	
30	2.5	
40	1.5	
50	1.0	

Test Conditions

Load $F_r = 1300$ lb

$F_a = 0$ lb

Speed 20 mph for 20 hours
 10 mph for 4 hours

TABLE 5-4B. SHOCK PULSE DATA - HEAVILY SPALLED
 OUTER RING - BEARING 063402

SHOCK PULSE DATA		
Potentiometer Level (Shock Level)	Shock Rate - Pulses Per Second	
	Speed - 20 mph	Speed - 10 mph
1	90.0	90.0
2	90.0	75.0
5	90.0	40.0
10	45.0	17.0
20	15.0	4.0
30	-	1.8
40	-	1.0
50	4.0	-
60	2.5	
70	1.5	
80	1.0	

Test Conditions

Load F_r = 1300 lb

F_a = 0 lb.

Speed 20 mph for 20 hours

10 mph for 4 hours

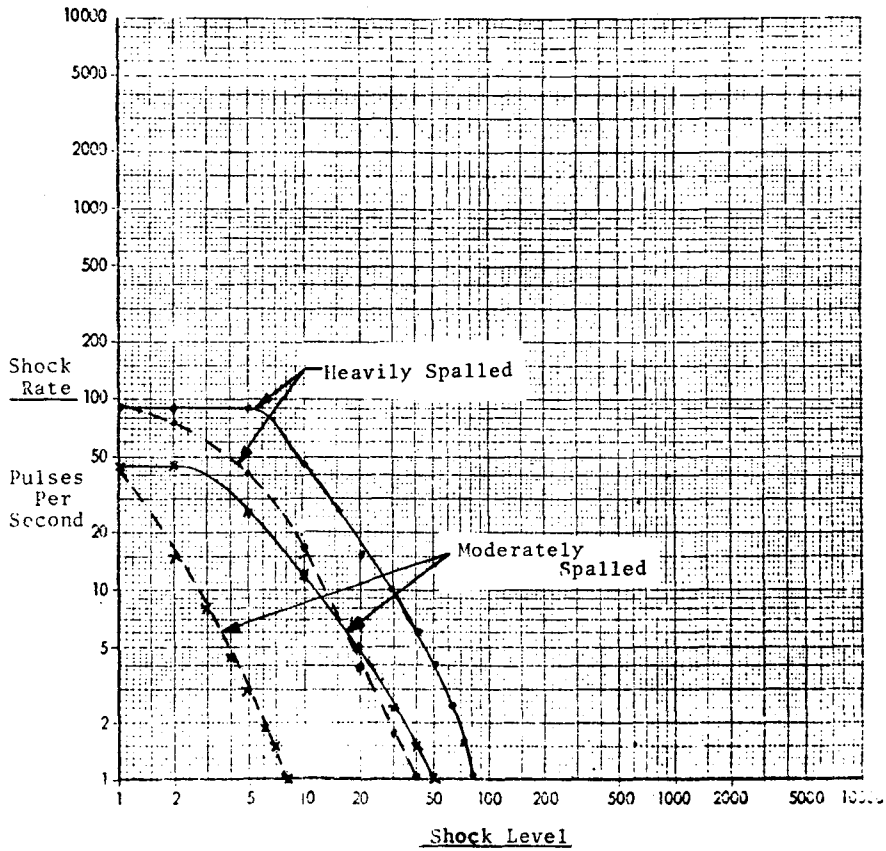


FIGURE 5-9. SHOCK EMISSION PROFILES - SPALLED OUTER RINGS

The appearance of "C" curves in two of the four test runs indicates the presence of rolling element damage in the bearings, as compared to low profile "A" curves which were indicative of unfailed bearings run in the baseline tests. At the test speed of 10 mph, neither spalling failure was detectable.

5.5.5 Test 5 - Brinelling

This test consisted of running two bearings with different degrees of brinelling on the inner and outer rings. One was moderately brinelled and one heavily brinelled. Photographs of the brinell marks in the outer rings of the bearings are shown in Figure 5-10. Data taken on these bearings at two different speeds are presented in Tables 5-5A and 5-5B. A shock emission profile plotted from this data is shown in Figure 5-11. The profiles produced "C" curves having significant shock levels of 90 to 1000 with high shock rates of 240 to 250 pulses per second for the heavily brinelled bearing. Shock levels of 30 to 110 with a shock rate of 110 pulses per second were recorded for the moderately brinelled bearing.

The appearance of "C" curves in all the test runs indicates the presence of rolling element damage in the bearing as compared to the low profile "A" curves which were indicative of unfailed bearing in the baseline tests.

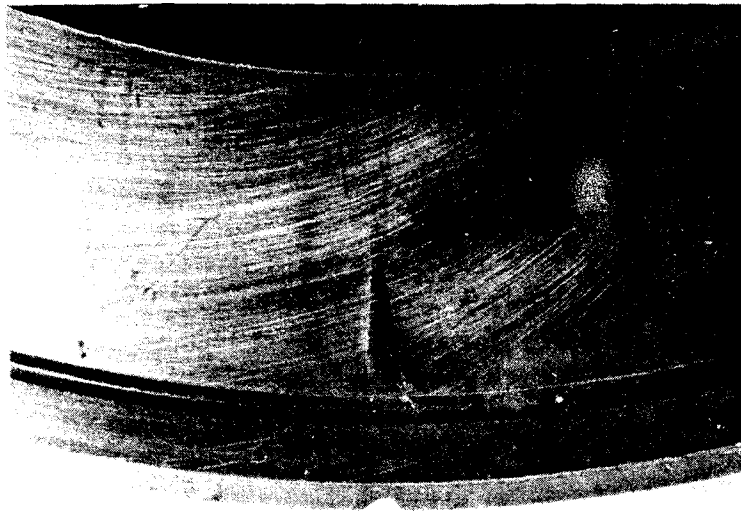
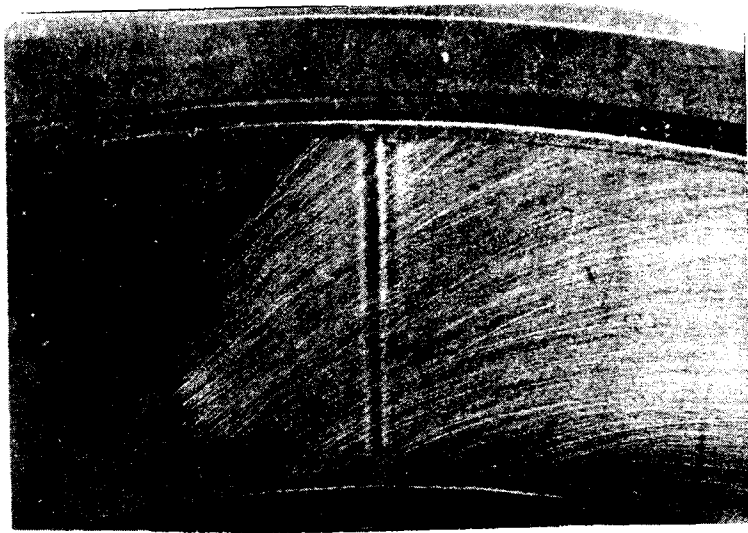


FIGURE 5-10. TYPICAL BRINELLED OUTER RINGS

TABLE 5-5A. SHOCK PULSE DATA - MODERATELY BRINELLED
BEARING - BEARING 063502

SHOCK PULSE DATA

<u>Potentiometer Level (Shock Level)</u>	<u>Shock Rate - Pulses Per Second</u>	
	<u>Speed - 20 mph</u>	<u>Speed - 10 mph</u>
1	110.0	110.0
2	100.0	100.0
5	95.0	30.0
7	-	10.0
10	90.0	5.5
20	55.0	1.5
30	-	1.0
50	12.0	-
60	5.5	
70	4.0	
80	2.0	
90	1.8	
100	1.5	
110	1.0	

Test Conditions

Load F_r = 1300 lb

F_a = 0 lb

Speed - 20 mph for 20 hours
10 mph for 4 hours

TABLE 5-5B. SHOCK PULSE DATA - HEAVILY
BRINELLED BEARING - BEARING 063501

SHOCK PULSE DATA		
Potentiometer Level (Shock Level)	Shock Rate - Pulses Per Second	
	Speed - 20 mph	Speed - 10 mph
1	250.0	240.0
2	240.0	210.0
5	220.0	180.0
10	220.0	130.0
20	200.0	45.0
30	-	15.0
40	-	10.0
50	190.0	6.5
60	-	3.0
90	-	1.0
100	100.0	-
200	10.0	
500	3.0	
1000	1.0	

Test Conditions

Load $F_r = 1300 \text{ lb}$

$F_a = 0 \text{ lb}$

Speed 20 mph for 20 hours
10 mph for 4 hours

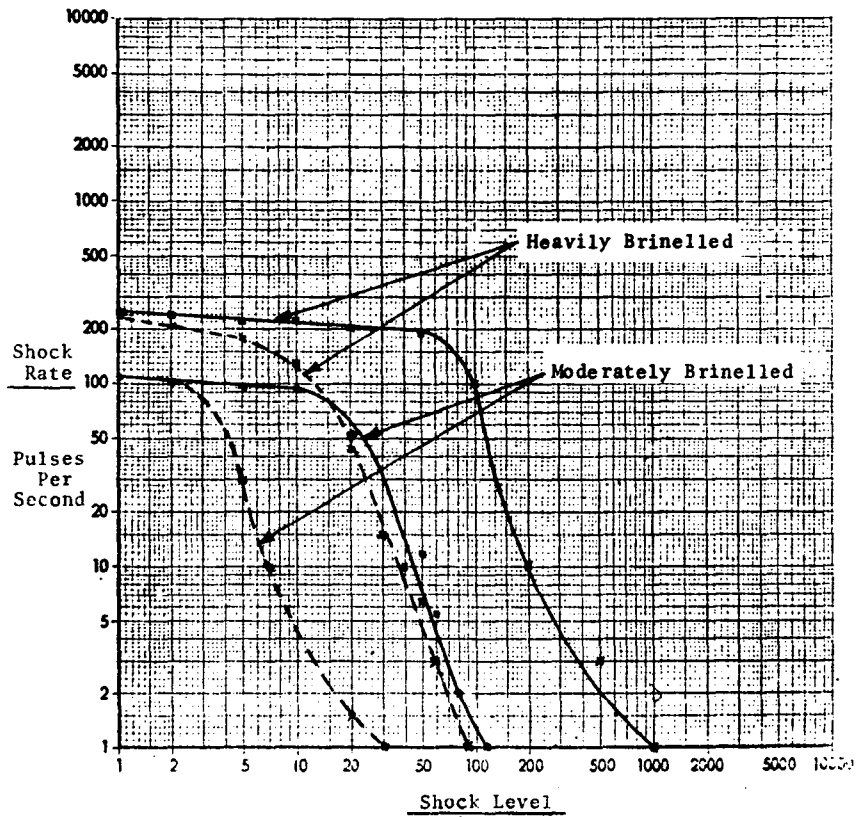


FIGURE 5-11. SHOCK EMISSION PROFILES - BRINELLED BEARINGS

5.5.6 Test 6 - Grease Contamination

This test consisted of running two new bearings with particulate contaminant added to the grease. The contaminant used was Grade 33 sandblasting sand (30-35 mesh) which is representative of abrasives found along railroad roadbeds. In one test bearing, one gram of sand was added to the grease in one cone assembly. In the other test bearing, one gram of sand was added to the grease in both cone assemblies. Data taken on these bearings at the two speeds by the Shock Pulse Meter are presented in Tables 5-6A and 5-6B. A shock emission profile plotted from these data is shown in Figure 5-12. The profiles produced "A" curves having significant shock levels combined with high shock rates.

The appearance of "A" curves with high shock rates in all the tests indicates the presence of contaminant in the lubricant as compared to the low profile "A" curves (low shock rates) which were indicative of unfailed bearings with noncontaminated lubricant run in the baseline tests.

TABLE 5-6A. SHOCK PULSE DATA - PARTICULATE CONTAMINANT
 ADDED TO ONE BEARING CONE ASSEMBLY - BEARING 063101

<u>SHOCK PULSE DATA</u>		
<u>Shock Rate - Pulses Per Second</u>		
<u>Potentiometer Level (Shock Level)</u>	<u>Speed - 20 mph</u>	<u>Speed - 10 mph</u>
1	400.0	50.0
2	300.0	30.0
5	200.0	4.0
6	-	3.0
7	-	2.0
8	-	1.0
10	60.0	-
20	6.0	
50	1.75	
70	1.0	

Test Conditions

Load F_r = 1300 lb

F_a = 0 lb

Speed 20 mph for 20 hours
 10 mph for 4 hours

TABLE 5-6B. SHOCK PULSE DATA - PARTICULATE CONTAMINANT
 ADDED TO BOTH BEARING CONE ASSEMBLIES - BEARING 063102

SHOCK PULSE DATA		
Potentiometer Level (Shock Level)	Shock Rate - Pulses Per Second	
	Speed - 20 mph	Speed - 10 mph
1	500.0	60.0
2	300.0	40.0
5	100.0	8.0
8	25.0	-
10	9.0	2.5
15	-	1.0
20	3.0	-
40	1.0	

Test Conditions

Load $F_r = 1300$ lb

$F_a = 0$ lb

Speed 20 mph for 20 hours
 10 mph for 4 hours

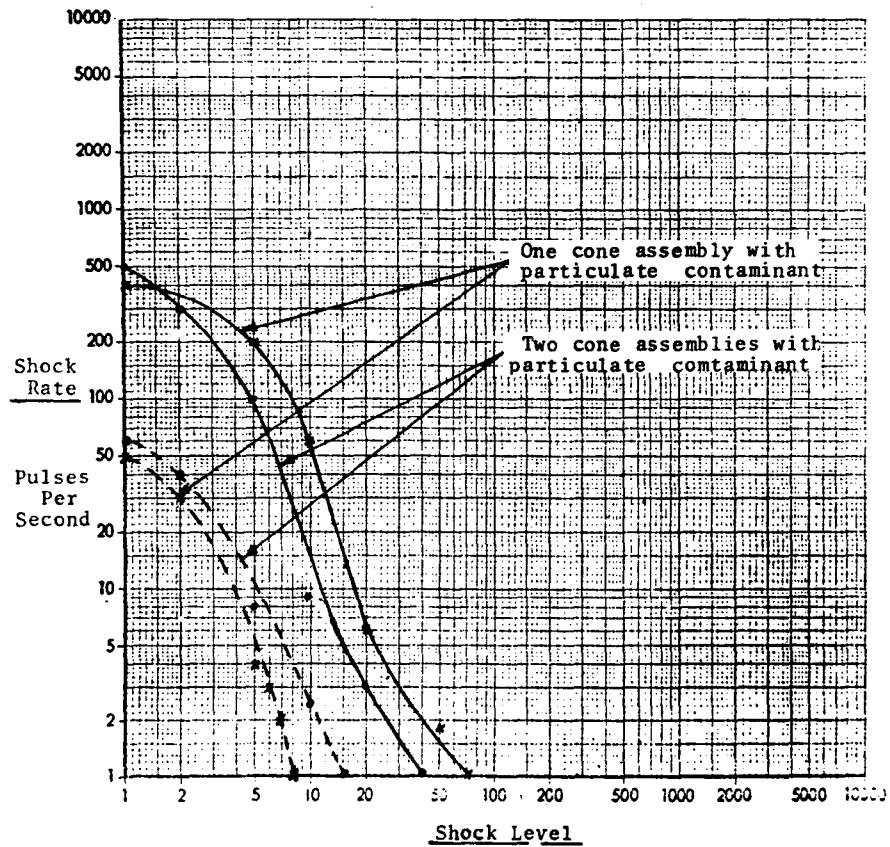


FIGURE 5-12. SHOCK EMISSION PROFILES - PARTICULATE CONTAMINANT ADDED

5.6 CONCLUSIONS

Data summary graphs are shown in Figures 5-13, 5-14, 5-15, and 5-16. The difference in profiles between new and defective bearings is evident.

Spalling on inner rings, rollers, and outers was readily detected. The Shock Pulse Meter could be used to eliminate disassembly and visual inspection for spalling damage.

Brinelling on inner rings and outer rings readily was detected. The Shock Pulse Meter could be used to eliminate disassembly and visual inspection for brinelling damage caused by derailment.

Particulate contamination was readily detected. The Shock Pulse Meter could be used to eliminate disassembly and visual examination for particulate contamination.

Use of the Shock Pulse Meter would preclude progressive catastrophic failures, as caused by the above defects.

Reproduced from
best available copy.

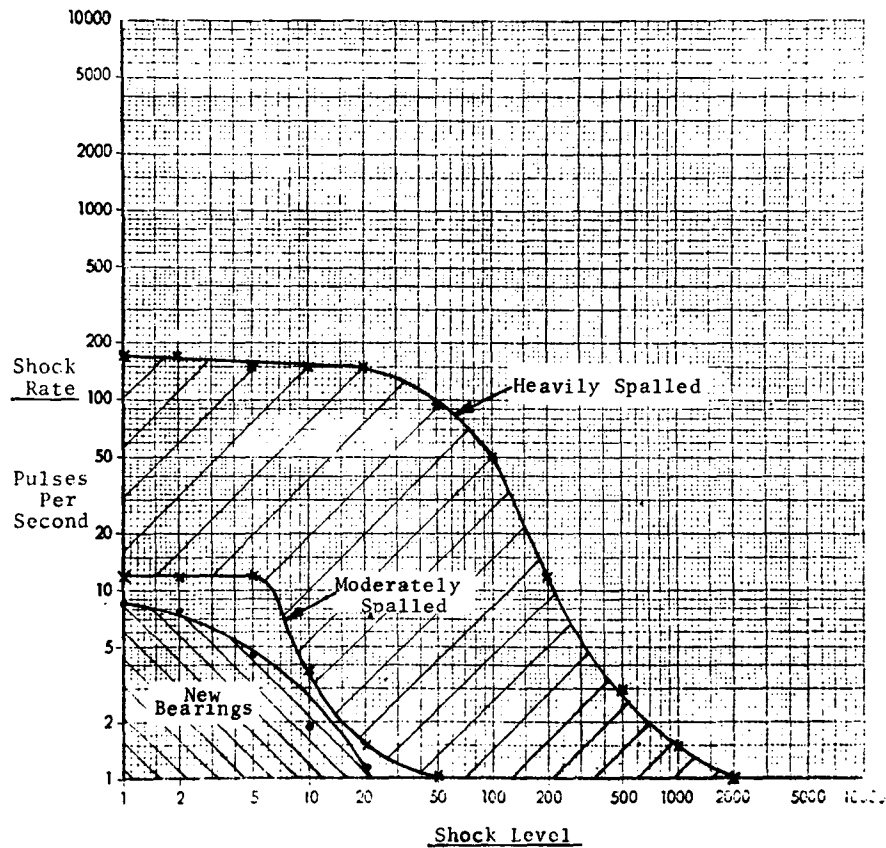


FIGURE 5-13. COMPARISON OF SHOCK EMISSION PROFILES OF NEW BEARINGS VS. BEARINGS HAVING SPALLED INNER RINGS

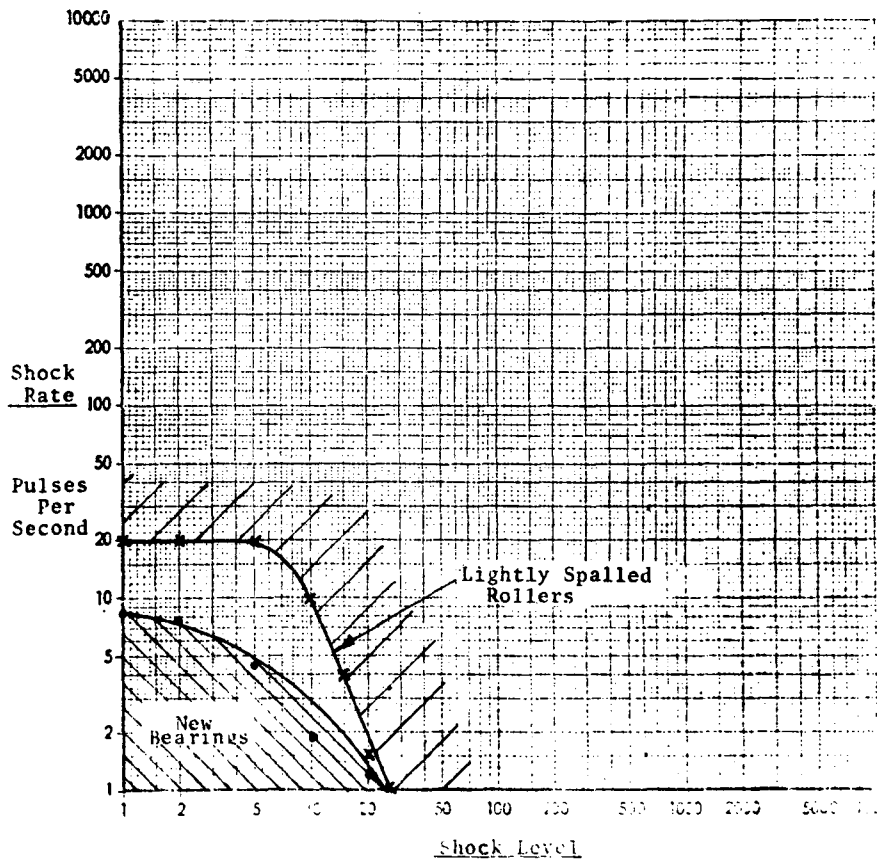


FIGURE 5-14. COMPARISON OF SHOCK EMISSION PROFILES OF NEW BEARINGS VS. A BEARING HAVING SPALLED ROLLERS

Reproduced from
best available copy.

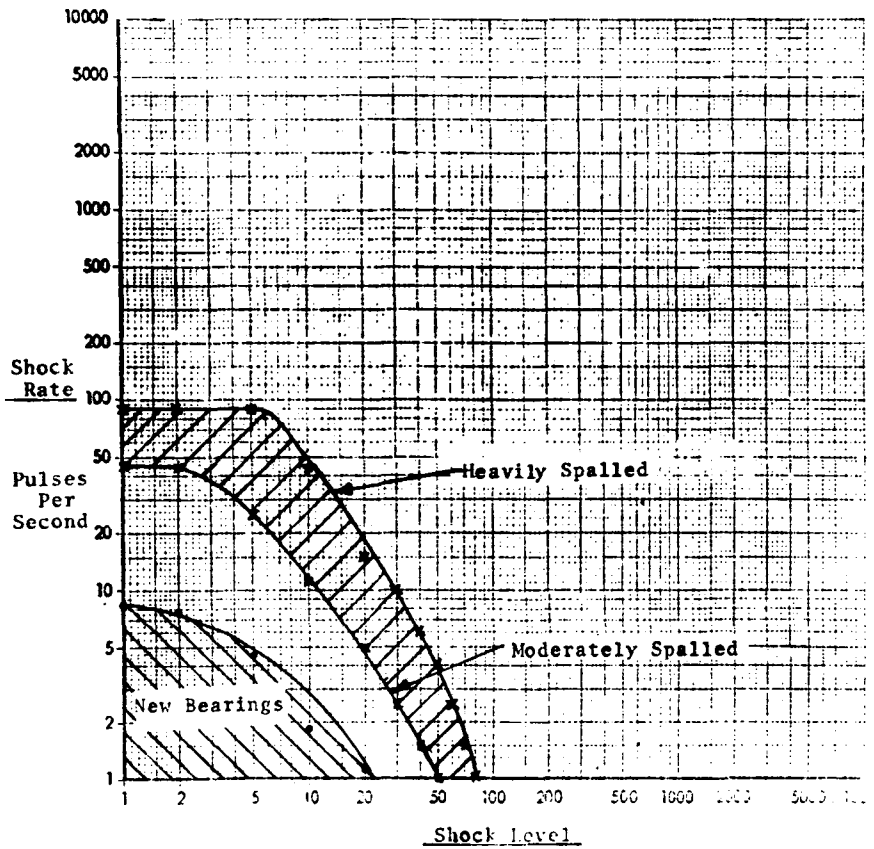


FIGURE 5-15. COMPARISON OF SHOCK EMISSION PROFILES OF NEW BEARINGS VS. BEARING HAVING SPALLED OUTER RINGS

Reproduced from
best available copy.

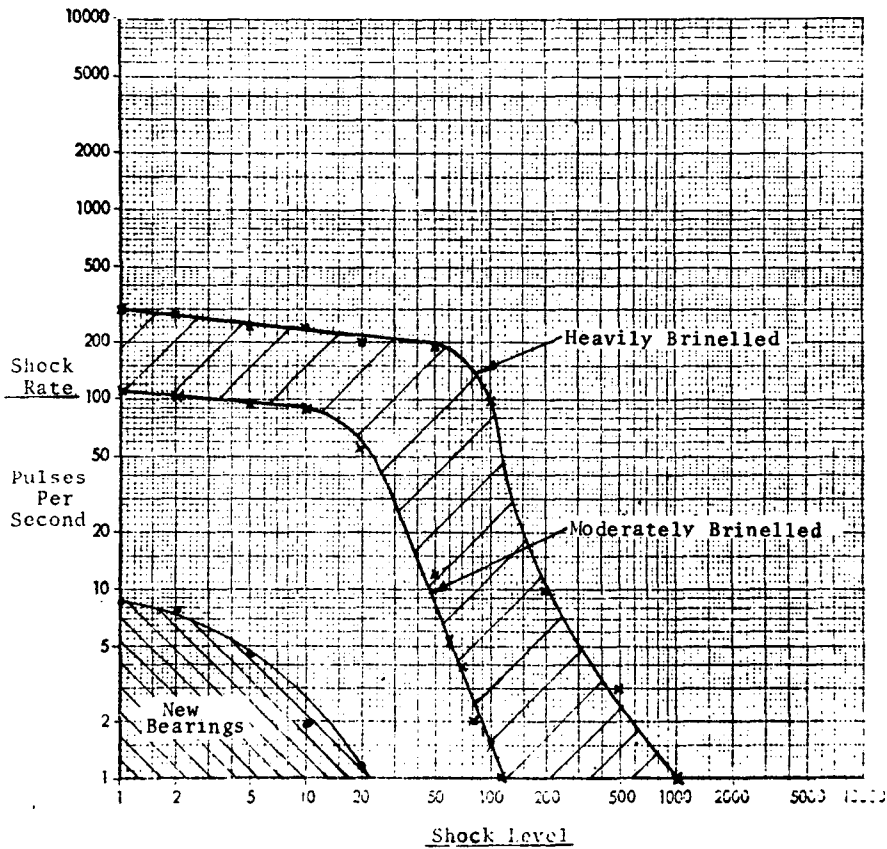


FIGURE 5-16. COMPARISON OF SHOCK EMISSION PROFILES OF NEW BEARINGS VS. BRINELLED BEARINGS

5.7 RECOMMENDATIONS

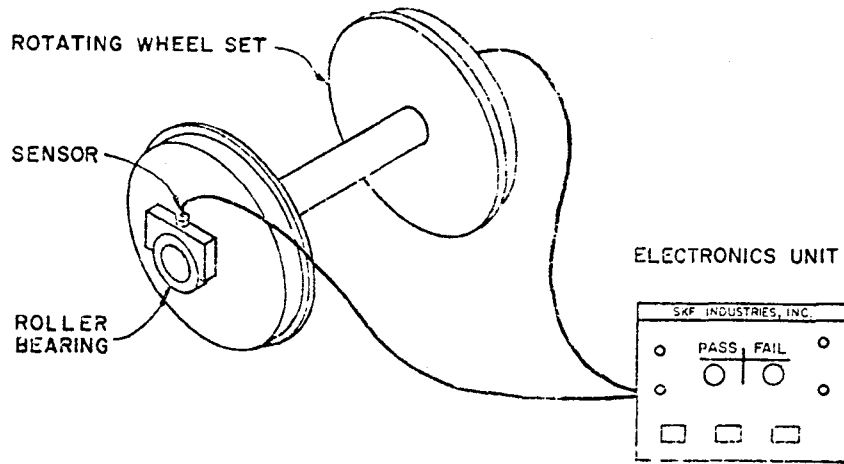
It is seen, from Figures 5-13 through 5-16, that no single parameter (e.g. maximum shock value) can be used in determining bearing condition. An interpretation of "area under the curve," axis intercepts, and other parameters associated with curve shape is needed to successfully discriminate between good and defective bearings.

Since the Shock Pulse Meter does not have the capacity to perform automatically such analysis, a follow-on program to package and evaluate an automatic Shock Emission Analyzer has been proposed. This device would analyze data as they are being gathered and provide (go)-(no-go) indication of bearing condition.

It is recommended that a program be established to produce hardware which will set apart bearings having mechanical damage or contaminated grease. Such a system, and its salient features, is shown conceptually in Figure 5-17.

This concept was presented to four major railroads. It gained unanimous approval from the railroads because of its cost and life-saving potential, and its adaptability to a railroad maintenance environment.

A polyphase packaging and evaluation program to produce two operating systems is shown in Figure 5-18. A proposed program schedule is shown in Figure 5-19.



- Testing is done at a Railroad Wheel Shop by Maintenance Personnel.
- Detects spalling, brinelling, broken components, and contamination in railroad roller bearings before catastrophic failure occurs.
- Gained unanimous approval from railroads because of its cost and life saving potential, and its adaptability to a railroad maintenance environment.
- It was recognized as having substantial cost savings potential, regarding derailments.
- As a bonus, it has the potential of offsetting its annual operating cost in several months operation by avoiding unnecessary bearing teardown. (Based on preliminary operating cost versus derailed bearing inspection costs).
- Two railroads enthusiastically offered to assist in field evaluation of the device.

FIGURE 5-17. PROPOSED RAILROAD BEARING SHOCK EMISSION ANALYZER

Phase I - Systems Fabrication and Packaging

- (A) Fabricate and Package Portable Railroad Wheel Set Rotating Device
- (a) Fabricate and package (2) portable rotating devices compatible with Railroad Wheel Shop environment for rotating, loading, and precessing outer rings of bearings under test.
 - (b) Evaluate portable rotating device in laboratory by running (6) tests varying speed and load to optimize Shock Emission Profiles on failed bearings.
 - (c) Install rotating mechanics at wheel shops of two different railroads.
 - (d) Final Data Acquisition and Analysis Report.
- (B) Fabricate and Package Automated Shock Emission Analysis System
- (a) Establish (go)-(no-go) limits for prototype tester in conformance with established A.A.R. standards.
 - (b) Fabricate, Package and Checkout two engineering prototypes.
 - (c) Generate Performance Specification and Drawing Data Package.

Phase II - Evaluation of Engineering Prototype Systems (2)

- (a) Laboratory Evaluation - Verify defect discriminating ability of Shock Emission Analyzer by testing 12 bearings (six passable and six rejectable), and correlating results with Shock Pulse Meter profiles previously generated in Contract DOT TSC-935.
- (b) Install rotating mechanics (Fabricated in Phase I) and automated Shock Emission Analyzer (Fabricated in Phase I) at two Railroad Wheel Shops.

FIGURE 5-18. PROPOSED RAILROAD BEARING SHOCK EMISSION ANALYZER EVALUATION PROGRAM

- (c) Collect (go)-(no-go) data for incoming bearings at each shop: Collect (go)-(no-go) data for all (minimum 12 bearings) known or suspected service failures at each shop: verify operability by visual examination of all bearings after teardown.
- (d) Final Evaluation and Data Analysis Report.

FIGURE 5-18 (CONT.)

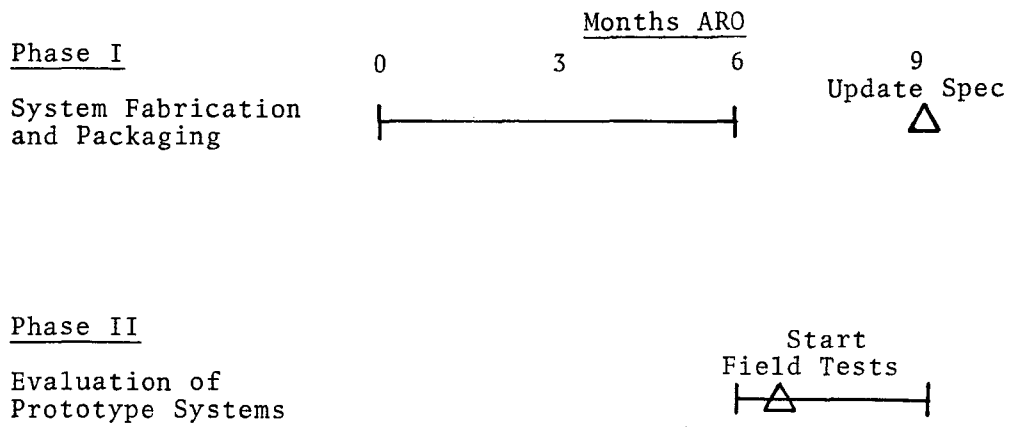


FIGURE 5-19. PROPOSED RAILROAD BEARING SHOCK EMISSION ANALYZER PROGRAM SCHEDULE

6. CONCLUSIONS

Data gathering and analyses discussed in detail in Sections 3, 4, and 5 have established the feasibility of producing maintenance-oriented systems which will:

1. Eliminate the cost and life threatening potential of catastrophic railroad journal roller bearing failure by any failure mechanism.
2. Detect and/or prevent two of the primary causes of railroad journal roller bearing failure (i.e. inadvertent overlubrication, and progressive mechanical damage to major bearing components) before they progress to the point where catastrophe is imminent.

Discussions with maintenance personnel at various railroads have obtained concurrence with the technical and cost saving goals of the reported and proposed programs.

The relative costs of mass produced "temperature only" and "temperature/strain" Transmitter Bolts are detailed in Section 3-8, wherein it is seen that cost effectiveness is more readily attained with the temperature sensing bolt. The cost of a mass-produced Transmitter Bolt for over-temperature detection will be approximately \$28 per bearing, which is an order of magnitude lower than the "temperature/strain" bolt. By comparison, the consequential costs of an undetected bearing failure causing a dangerous cargo derailment in a heavily populated area, could be enormous.

The cost of an automated ultrasonic test equipment for the prevention of overlubrication is estimated at \$10,000 per unit. The manpower required to operate the ultrasonic inspection equipment is a repair track is estimated to cost \$10,000/yr. Elimination of derailments and hot box setouts, caused by

inadvertent overgreasing, will far outweigh these insignificant initial and operational costs.

Initial and operating costs for the automated Shock Pulse Analyzer are of the same order of magnitude as those of the overlubrication detector. Such a system in use at a wheel shop, where many bearings undergo unnecessary rebuilding, has the potential to save one canvassed railroad \$150,000/year.

7. RECOMMENDATIONS

It is recommended that each of the follow-on programs described in detail in Sections 3, 4, and 5 be instituted because of their cost and lifesaving potential.

Development of the "temperature-sensing" Transmitter Bolt is especially urgent because of its ability to eliminate burnoffs regardless of bearing failure mechanism, and because of the ever-increasing possibility of life-threatening derailments.

8. REFERENCES AND BIBLIOGRAPHY

REFERENCES

- [1] RCA Corporation: "RF/Microwave Devices," 1974.
- [2] Henney, Keith: "Radio Engineering Handbook," McGraw-Hill Book Company, Inc., 1959.
- [3] Belove, Charles and Schilling, Donald L.: "Electronic Circuits: Discrete and Integrated," McGraw-Hill, Inc. 1968.
- [4] Halliday, David and Resnick, Robert: "Physics, Part II," John Wiley and Sons, Inc., 1962.
- [5] Holman, J.P.: "Heat Transfer," McGraw-Hill Book Company, New York, 1963.
- [6] Thermacore, Inc.: "Heat Pipes," Technical Bulletin No. 74-05, May 1974.
- [7] Norfolk and Western Railway Company: "Temperature Sensitive Cap Screws for Journal Roller Bearings", Project 4-69 Roanoke, Virginia 24042
- [8] Breneman, John W.: "Strength of Materials," McGraw-Hill, Inc., 1952.

BIBLIOGRAPHY

- BLH Electronics, Inc.: "SR-4 Strainline Temperature Sensors," Product Data, 206-6, Feb. 1, 1974
- BLH Electronics, Inc.: "Strain Gages," Catalog No. 100, August 1975.
- Interdesign, Inc.: "The Monochip," (undated).
- Machine Design: "Fastener Technology," Sept. 11, 1969.
- Materials Electronics Products Corporation: "Solid State Cooling with Thermoelectrics," Jan. 1974.
- Strainsert Co.: "Bolts and Studs, Custom Load Sensing," Bulletin No. 361-5, 1976.
- Trak Microwave Corp.: "Microwave and RF Components Handbook," Bulletin No. OS100, May 1976.

APPENDIX A
TEST PLAN FOR ON-BOARD
THERMALLY POWERED TRANSMITTER

A.1 INTRODUCTION

The object of the test program described herein is to prove feasibility of remotely detecting extreme temperature and strain excursions in railroad wheel bearings. Two self-contained (in the sense of needing no external power source) prototype transmitters capable of detecting these excursions are being developed. The prototype transmitter will be constructed of components and discrete integrated circuits which are capable of further miniaturization. The prototype will, however, be packaged on standard sized printed circuit boards. Upon successful completion of prototype testing, specific packaging requirements (such as packaging the transmitter within a bolt) can be reviewed. All circuitry involved in transmission and sensing, is being developed to be amendable to small scale integration techniques in the final configurations.


The test program is divided into two separate entities: (1) the development and test of a basic breadboard transmitter and (2) the development and test of prototype transmitter capable of being powered thermally and sensing the required parameters. Table A-1 and Figure A-1 provide graphic display of the schedule and testing programs for easy reference.

A.2 TEST FIXTURES

Two test fixtures will be used in conjunction with the

TABLE A-1. PROGRAM ONE TEST MATRIX

			VERTICALLY POLARIZED	HORIZONTALLY POLARIZED	HORIZONTALLY POLARIZED WHEEL SIMU- LATOR AS GND. PLANE	HORIZONTALLY POLARIZED TRANSMITTER ENCAPSULATED IN WHEEL SIMULATOR
BREAD BOARD TRANSMITTER	BATTERY POWERED UNMODULATED	1	1A	1B	1C	1D
BREAD BOARD TRANSMITTER	BATTERY POWERED MODULATED	2	2A	2B	2C	2D
BREAD BOARD TRANSMITTER	THERMALLY POWERED MODULATED	3	3A	3B	3C	3D
PROTOTYPE BREAD BOARD (TEMP. AND STRAIN SENSING)	BATTERY POWERED MODULATED	4	4A	4B	4C	4D
PROTOTYPE BREAD BOARD (TEMP. AND STRAIN SENSING)	THERMALLY POWERED MODULATED	5	5A	5B	5C	5D
			A	B	C	D

Reproduced from
best available copy. 

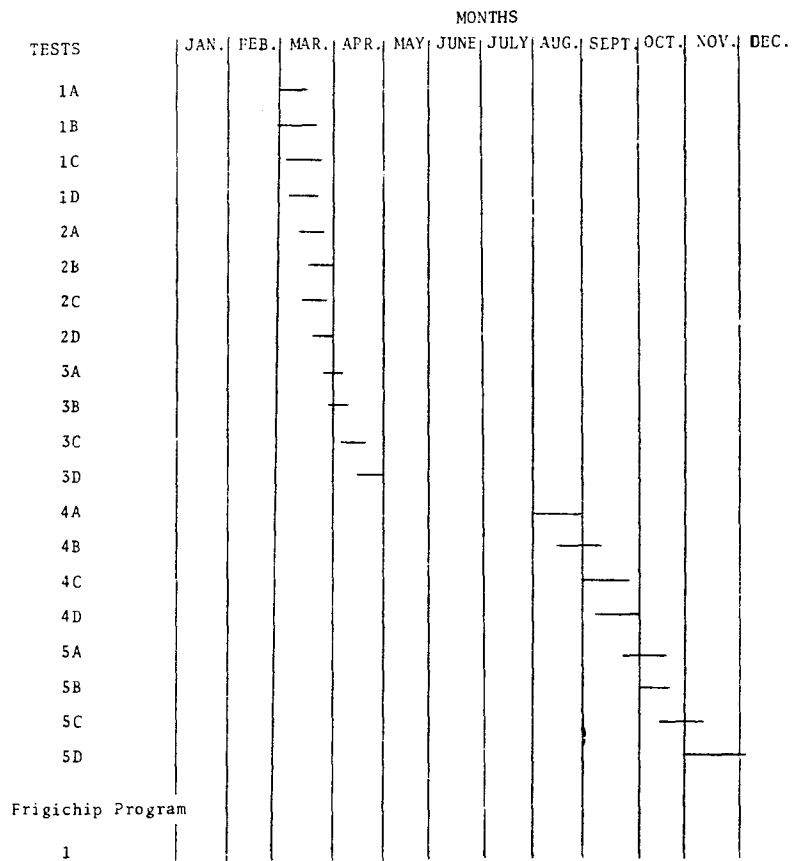


FIGURE A-1. TEST PLAN SCHEDULE

transmitter to simulate actual operating conditions. To determine the effect of a grounded, railroad wheel perpendicular to, and along the same axis as the transmitters antenna, a test fixture simulating the basic RF reflection characteristics of a railroad wheel will be constructed. The test fixture will consist of a metal disc having the same diameter as a railroad wheel. The center of the disc will be drilled out and the transmitter antenna will be placed on this hole perpendicular to the disc so that the antenna is horizontally polarized. Test data will be collected by taking measurements about the locus of a circle whose center is the intersection of the antenna and wheel, and whose plane is horizontal. For each test, the radius of this circle will be enlarged in increments to one mile. The size of these increments will be determined at testing for maximum resolution.

The second test fixture will be used to determine the effect of encapsulating the transmitter in a grounded metal container. This will simulate mounting the transmitter in a standard railroad wheel bolt. Following the same procedure as outlined above, field strength measurements will be taken. Since RF radiation will emanate from only the antenna (the only nonencapsulated section of the transmitter), this test will be used primarily as a tool to improve upon the efficiency of the antenna coupling. Basically, the test fixture is a metal container with a small hole drilled in one end to extend the transmitter's antenna outside the container. The container is grounded to the wheel simulator.

A.3 TEST PROGRAMS AND SCHEDULE

Two test programs will be performed. One, the development of a transmitter capable of detecting strain and temperature excursions, and of being powered by a thermopile, providing sufficient output to be received by a standard UHF communications receiver at a distance of one mile in open terrain from the transmitter. The second program, which is concurrent with test program one, will investigate the feasibility of developing a specific commercially available thermopile in order to provide the necessary power for the transmitter of program one.

A.3.1 Program One

Testing in this program proceeds basically from 1A through 5D in the matrix of Table A-1. As stated in Section I, two basic transmitters will be developed ie. breadboard and prototype. The horizontal parameters are the various test fixtures described in Section A.2 above; (actually "A" and "B" represent the absence of a test fixture). The vertical parameters represent different transmitter configurations. In all tests, transmitted power will be measured at specified angles and distances from the transmitter. In test 1 (i.e. 1A - 1D), the output of a basic unmodulated carrier (battery-powered) transmitter will be assessed. In test 2, the output of the same transmitter, swept or modulated by a relaxation oscillator will be monitored. In test 3, a modulated transmitter, powered by thermopiles will be monitored. In test 4, a battery-powered transmitter whose modulation is switched on by simulated strain and temperature excursions will be tested. In test 5, the same

device as in test 4 will be thermally powered. It is seen that prior to tests 4 and 5, and concurrent with 1 through 3, circuitry for modulating the transmitter carrier will be developed.

A.3.2 Program Two

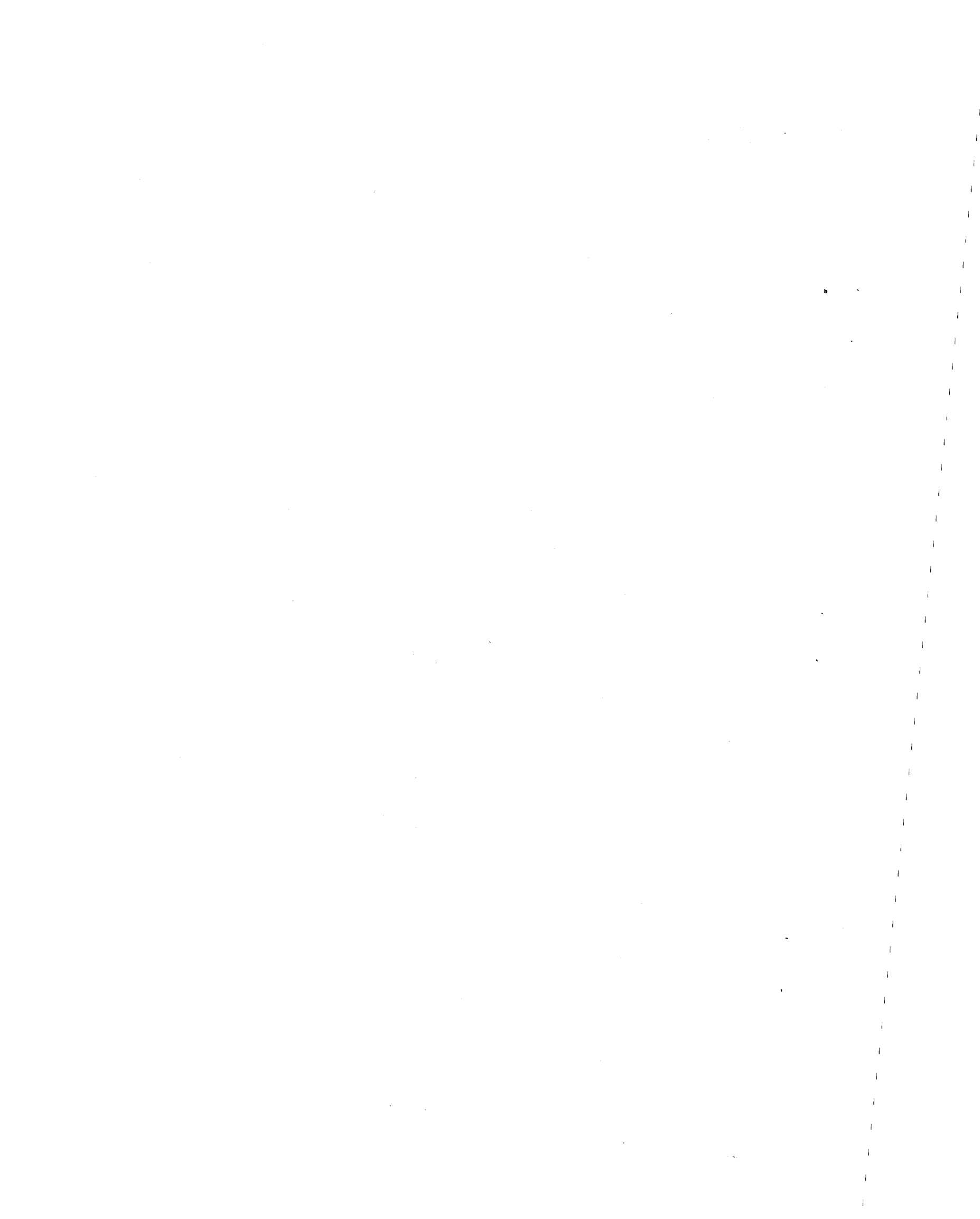
Program two will consist of evaluating candidate thermopile manufacturers to determine capability of meeting the power and sizing demands. Several off the shelf modules, which will approximate the final power output required, will be purchased and "hot plate" will be tested to determine current and voltage capabilities at load against the desired characteristics. These prototypes will be used as the thermal powering units necessary for the completion of tests 3 and 5 in the matrix of program one, and as such, the development stated here will be concurrent with tests 1 and 2 of program one. Timing of programs one and two are seen in Figure A-1.

A.4 DATA FORMAT

It will be noted in the matrix of program one, that two types of transmitter output power sensing are needed, i.e., one for sensing unmodulated carrier power and the second for sensing the (go)-(no-go) chirping of the modulated carrier. Because of this, a field strength meter will be used in tests 1 and 2, and an F.M. or A.M. receiver will be used in tests 2 through 5.

Data will be accumulated in graphic form as polar plots of field strength versus angle from an antenna center line in the horizontal plane. Tests 1 and 2 will provide field strength data as a function of angle and distance (from the transmitter) and tests 2 through 5 will provide yes or no indications as to whether the modulated carrier signal was received. The percent modulation of the received signal will be tabulated.

Conventional laboratory instrumentation will be used to indicate the capabilities of the thermopiles of program two. Measurements of open circuit voltage versus temperature difference across chip, and voltage versus load current at fixed temperature differences across the chip, will be accumulated.



APPENDIX B
TEST PLAN FOR ULTRASONIC OVERLUBRICATION
DETECTOR TEST PROGRAM

B.1 INTRODUCTION

The objective of this test program is to detect excessive lubrication which is a major cause of overheating and subsequent failure of railroad bearings. The pulse echo ultrasonic technique of overlubrication detection will be evaluated.

B.2 TEST EQUIPMENT

When a conventional ultrasonic test unit transducer is coupled to a surface, such as a seal or bearing outer race, the return pattern varies perceptibly with grease layer thickness on the side of the surface opposite the transducer. By selection of one or more gate areas in the return signal and setting of a return signal amplitude limit value, the ultrasonic test technique can effectively serve to indicate the presence or absence of grease, and possibly even the depth of lubricant layer on the inner surface.

The transducer will be applied to the external surface of the bearing via a thin layer of material containing a coupling fluid. The pulser receiver excites the transducer and the return echo pattern is received. The gated areas in the return signal are selected based on the bearing and seal characteristics.

The amplitude of the return signal in the selected gate area is amplified and suitably displayed to the operator. Ultimately, it may be possible to integrate the readings from a predefined sweep pattern to make a single output determination of the relative amount of lubricant in the bearing.

A commercially purchased ultrasonic flaw detector will be used as the pulse-echo ultrasonic analyzer. The unit is a portable industrial instrument consisting of an echo amplitude monitor with a cathode ray tube display and a transducer with attaching cable. The transducer sensor will be coupled to the railroad bearing seal and outer ring by a plexiglas adapter shoe. Locations for transducer monitoring are shown in Figure B-1. The design for a hand held adapter shoe is shown in Figure B-2. The adapter will assure a uniform presentation and orientation of the transducer to the surface each time a test is conducted.

B.3 TEST CONTENT

B.3.1 Static Grease Detection Units

Testing will be accomplished in two areas. First, seals from an 1 in. x 11 in. standard tapered railroad bearing coated with lubricant layers will be statically tested using a 2.5 - 5.0 MHz pulse-echo technique to determine the optimum grease layer detection frequency. In addition, the sensitivity to thickness of the grease layer will be determined along with the selection of gate areas where optimum detection ratio exists. This same static testing will also be conducted on a 6 in. x 11 in. outer ring in the area between the roller tracks and then on assembled bearings mounted on a test machine shaft. In all these tests, the optimum detection frequency and detection gate areas will be determined and recorded.

The lubricant used in these tests is grade B grease and meets AAR specification M-917 for grease type railroad roller bearings.

Reproduced from
best available copy.

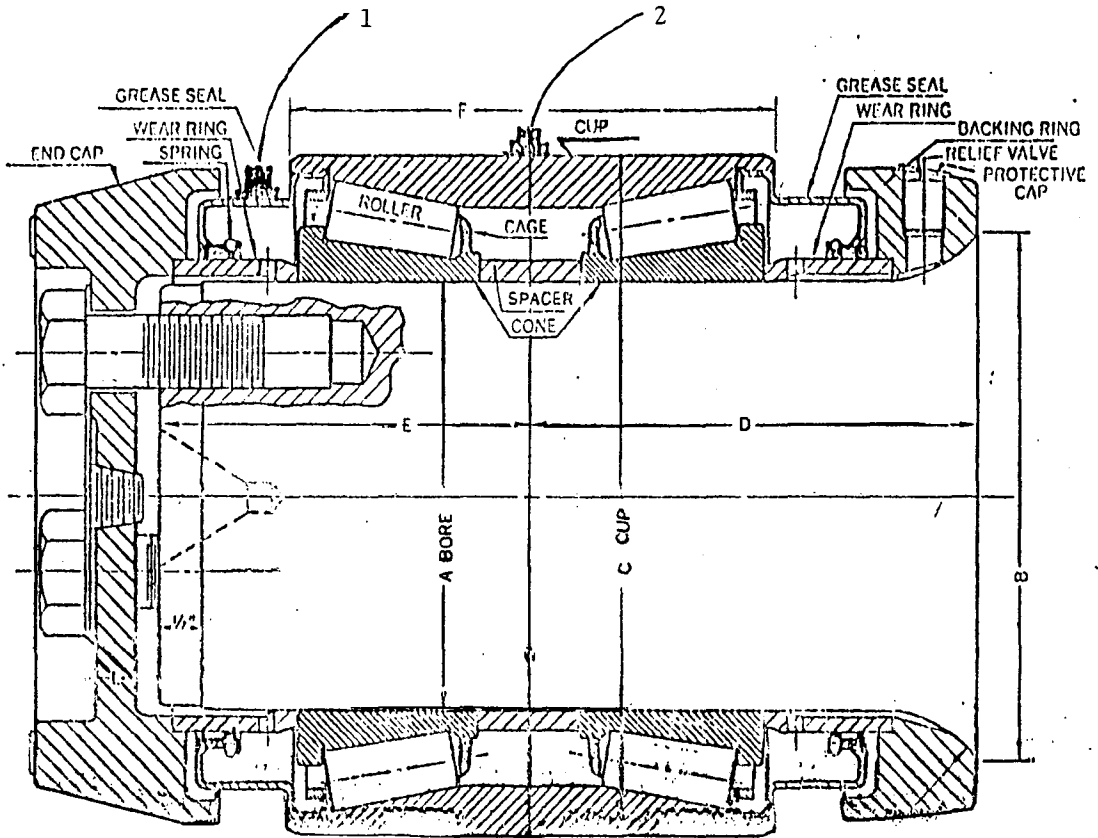


FIGURE B-1. ULTRASONIC GREASE SENSOR DETECTOR LOCATIONS

Reproduced from best available copy.

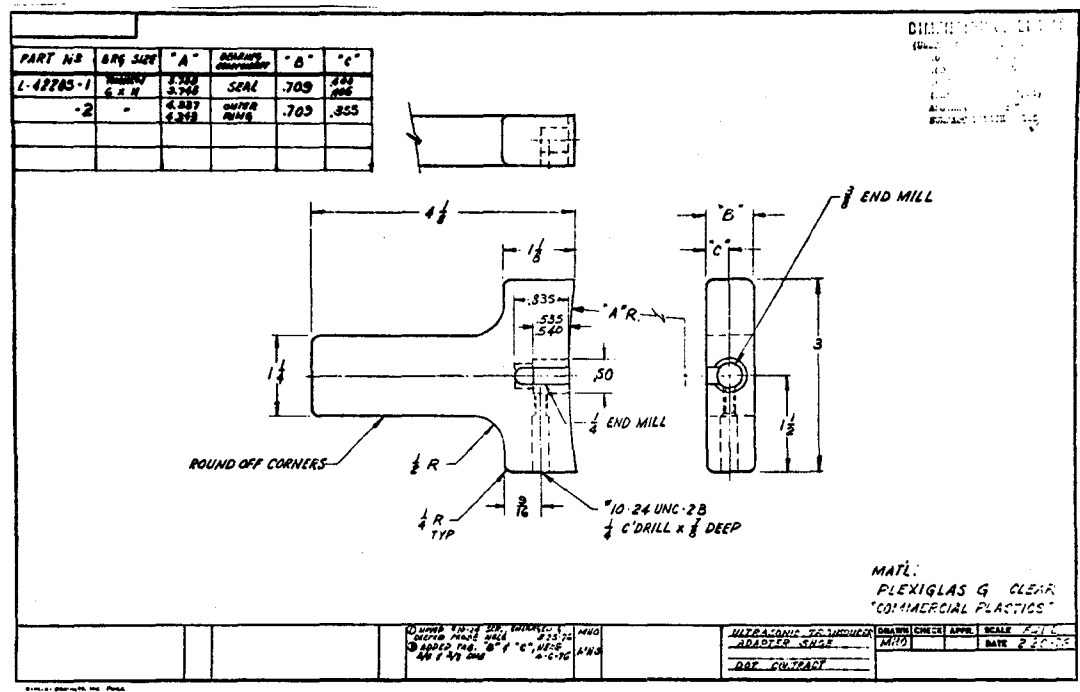


FIGURE B-2. ULTRASONIC TRANSDUCER HOLDER

B.3.2 Grease Migration Test

Secondly, an overgreased bearing grease migration test will be conducted. This test will consist of running two new 6 in. x 11 in. tapered bearings with three different amounts of lubricant for a period of 24 hours. A baseline test will be run first with a AAR normal grease pack of 18 ounces and then additional grease quantities of two and three times the required amount will be added through the grease fitting on the railroad bearing cap. Each test will run for 24 hours at 25,000 lb radial load at an equivalent speed of 60 mph to obtain optimum grease channeling and distribution throughout the bearing. The bearings will be disassembled and inspected visually to determine grease flow patterns. Data will be accumulated after normal greasing and overgreasing occurs to determine the effect of this variable on detection sensitivity, and to determine the minimum degree of overlubrication of the bearing that results in detectable grease pack motion in the available lubricant cavities.

To accomplish this test program, a laboratory railroad bearing test machine setup for a 6 in x 11 in bearings will be utilized. The bearings will be tested under an applied radial load of 25,000 lb and at a speed equivalent to 60 miles per hour train speed. These test conditions should be representative of a freight car bearing load in service. The railroad bearing testing machine was shown in Figure 4-5 of the text and was described in Section 4.3.2 of the text.

The testing program and its monthly milestones are presented in Table B-1.

B.4 DATA FORMAT

Data will be accumulated as return signal amplitude measurements taken from the cathode ray screen of the test equipment. These signals are electrical analogs of energy content of sonic waves rebounding to the transducer during certain chosen time periods after an ultrasonic impulse. The presence or absence, and possibly the thickness of a grease layer will manifest itself as variations in amplitude of appropriately chosen pulse echoes.

The data from the first test will be plotted in graph form: amplitude vs. thickness of grease layer. Data from the second test will also be plotted in graph form: amplitude vs. presence or absence of grease circumferentially plotted around the seals and outer ring.

TABLE B-1. ULTRASONIC OVERLUBRICATION
DETECTOR TEST PROGRAM

Testing and Application of Ultrasonic Test Equipment

Seal

- (1) Develop optimum grease layer detector frequency.
- (2) Select gate areas using a seal separately and then mounted in a bearing.
- (3) Develop sensitivity and establish signal amplitudes in assembled bearings for different thickness layers of grease.

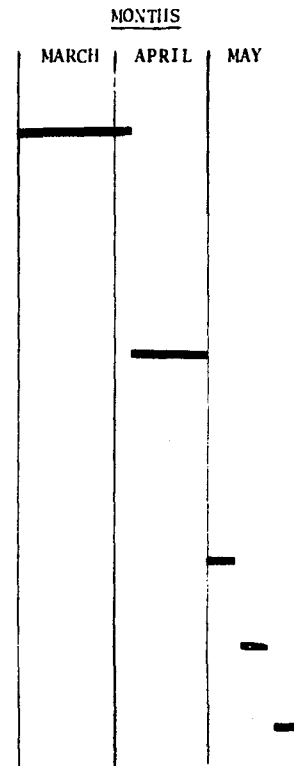
Outer Ring

- (1) Establish the sensitivity to grease in the area between the roller paths.
- (2) Select gate areas using an outer ring separately and then in assembled bearing.
- (3) Develop sensitivity to different thickness layers of grease and establish signal amplitude in assembled bearings for different thickness layers of grease in the area between the roller paths.

Overgreased Bearing Test

- (1) Baseline test - Run two bearings for 24 hours with required amount of grease to determine the grease distribution. (bearing approximately 30% full).
- (2) Run the above baseline test bearings for an additional 24 hours with twice the required grease amount to determine the grease distribution (bearing approximately 60% full).
- (3) Run the above overgreased bearings for an additional 24 hours with three times the required grease amount to determine the grease distribution. (bearing approximately 90% full).

NOTE: (1) Test bearing - 6" x 11" Tapered Roller Bearings.
 (2) Test Machine - Railroad Test Machine
 (3) Test Conditions in overgreased bearing test.
 (a) Fr = 25,000 # , Fa = 0
 (b) Speed - 60 miles/hour



APPENDIX C SHOCK PULSE METER INSTRUMENTATION

C.1 INTRODUCTION

The Shock Pulse Meter is a reliable economical bearing performance diagnostic instrument capable of defining bearing condition in situ with significantly greater clarity than other methods in use.

It is the purpose of this paper to discuss the nature of the phenomenon sensed by the instrument, the processing of the data within the instrument, and the use of the instrument as a diagnostic tool.

C.2 THE NATURE OF THE SENSED CHARACTERISTIC

The dynamics of the rolling element in a bearing due to the transit of discontinuities through the contact ellipse, whether surface discontinuities or particulate matter, gives rise to a discrete emission of energy within the bearing elements. The level of this energy release is a direct function of size of discontinuity and is proportional to the square of the speed of the rolling element at encounter.

Two important reactions to this encounter occur. These are illustrated in Figure C-1.

First, a shock pulse is created, emanating from the point of impact. This pulse is characterized by very sharp rise and very short duration. The pulse travel is governed by the speed of sound in the structure. The pulse is attenuated approximately 14 dB at each mechanical interface, and decays in amplitude in proportion to distance and material damping characteristic.

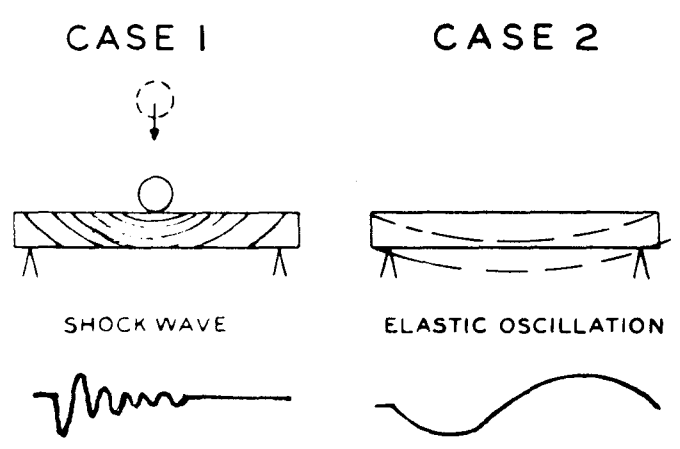


FIGURE C-1. SHOCK PULSE GENERATION

The pulse propagation is independent of bearing or mounting structural resonance and thus is not affected by changes in these with load or wear.

The second reaction is the establishment of elastic resonances within the bearing elements and the surrounding structure. This mode of transfer of mechanical energy is physically governed by bearing and mounting mechanical characteristics and resonances. This elastic resonance so induced is superpositioned on vibration from other sources within the structure. This results in the establishment of the net vibration environment at a given point in the structure. The vibrational envelope, being directly related to structural characteristics reacts differently to bearing originated mechanical energy as load and wear change these characteristics.

Thus, in situ use of vibration measurement to determine bearing condition requires constant attention to the mathematical model used and is confused by dynamic background vibration changes with load and wear within the machine or structure.

In general, the bearing vibration must rise well above the background to be discerned. The remaining time to catastrophic failure may then be quite short.

Some attempts to overcome these classic limitations of vibration measurement involve periodic sampling of the vibration environment, at periods determined by rolling element passage, for example. While these methods are successful for periodic damage so encountered, they tend to miss the same damage if speed and load change and tend to ignore totally the aperiodic type emission coming from rolling element damage or encounters with wear products in the contact area.

In sharp contrast to the use of vibration measurement to determine bearing in situ condition, is the use of shock emission measurement for this determination. The registry of shocks takes advantage of three important characteristics of the shock pulse:

1. It is a sharp rise, short duration pulse of energy related directly to the severity of the contact in the bearing element contact ellipse.
2. It depends for propagation on the speed of sound in the structure and is independent of the spring/mass characteristics of the structure. It is thus not dependent on modeling for data interpretation.
3. It is attenuated markedly (empirical data indicates 14 dB or 80 percent) at mechanical interfaces.

It is upon successful measurement and use of the information contained in these shock emissions that the following thesis is based:

The shock emission envelope of a bearing in situ can readily be used to diagnose and isolate impending bearing failure and diagnose bearing condition.

The shock emission envelope is constructed by measurement of rate of emission of shock pulses versus the level of emitted shock. A typical shock emission envelope comparison of an undamaged and damaged type 6309 ball bearing is shown in Figure C-2

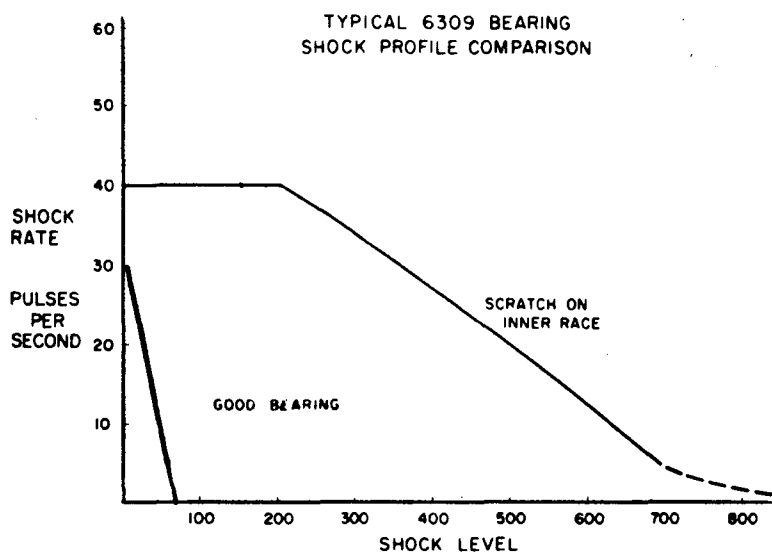


FIGURE C-2. SHOCK EMISSION PROFILE

The change in shock level in relation to time of operation gives the earliest indication of bearing surface damage. The indication is well in advance of a noticeable increase in vibration and may give remaining span time to failure as great as the time preceeding the indications, use conditions remaining the same.

The rate profile of shock emission gives a measure of the extent of damage and may be used to determine the propogation of the damage area.

The shock emission envelope shape is a revealing signature of the bearing and that shape of the envelope is usable to separate damage and undamaged bearings and also indicate installation and lubrication problems.

To successfully determine shock emission envelope requires the measurement of shock amplitude and rate of occurrence of shocks as a function of amplitude. The Shock Pulse Meter was shown in Figure 5-1 of the text.

C.3 OPERATION OF THE SHOCK PULSE METER

The unit used to measure the emitted shock pulses is composed of two distinct parts.

1. An accelerometer having a resonance of about 38 kHz
2. A tuned amplifier and discriminator

The accelerometer and the electronic unit are used in a tuned mode much in the sense that a radio is tuned to a station. The previously described shock pulse resonates the accelerometer as a shock resonates a bell while the amplifier is tuned to the accelerometer resonance. In this way, the background vibration is completely ignored and the results of the impressed shock pulse are passed into the electronic unit.

Within the unit a second unique feature is incorporated. To be of the most analytic use, the device must have a wide dynamic range. In order to avoid the confusion of changing scales, a logarithmic amplification technique is used. In this way, a clear 20,000:1 dynamic range is given for both rate and amplitude measurement. The signal processing is shown in Figure C-3.

The input signal is amplified and then passed to a peak sample-and-hold circuit. The peak determined is used to control the gain of the amplifier and is sent to the rate threshold detector and the meter circuit. In the normal mode, the peak value is displayed on the meter.

The peak sample and hold circuit presents a pulse amplitude proportional to the input signal and is thus a quantization of the shock pulse.

When the unit is commanded into the "Rate" mode, the meter registers pulses per second that are of a magnitude greater than the threshold set on a dial on the front panel of the unit. Setting of this dial and measurement of rate provide the information used to construct the shock emission profile.

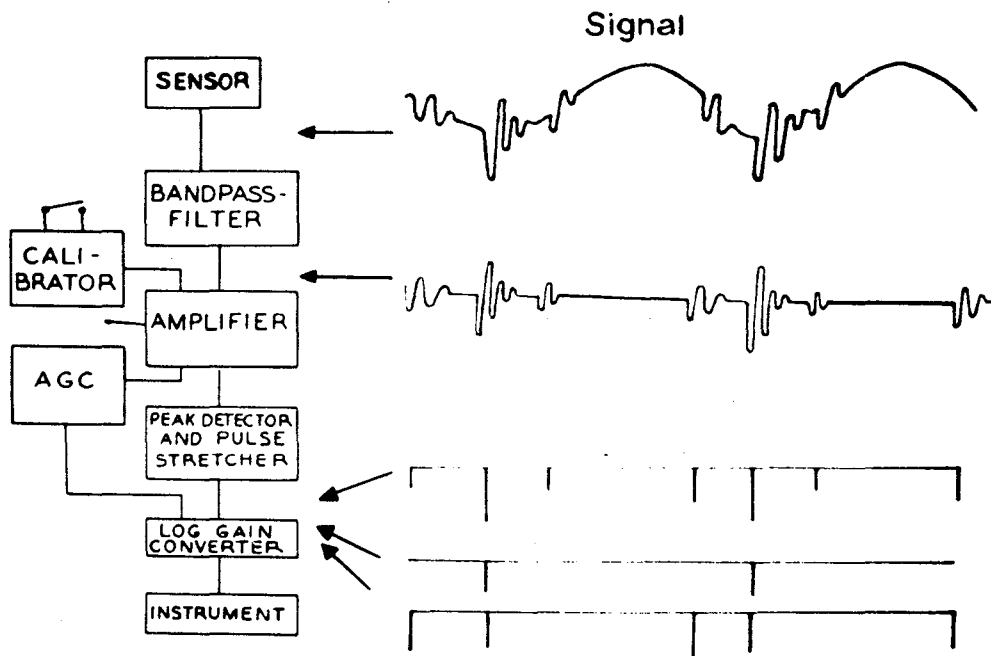


FIGURE C-5. SHOCK PULSE METER SIGNAL PROCESSING FLOW

In addition, a front panel earphone attachment is available so that level discriminated shocks may be listened to in order to determine rhythm. They may also be displayed on an oscilloscope with a shaft revolution marker to determine whether the measured shock is associated with inner ring, outer ring or rolling element damage. A recorder output is provided for long-term monitoring of a shock level as required in unattended measurements.

The unit is portable, about 15 pounds in weight, battery operated by rechargeable NICAD cells and employs integrated circuit electronics in the design for high reliability and dependability.

The unit fully uses the dynamic range in bearing measurement. The high sensitivity of the unit is illustrated by the fact that a typical, inexpensive watch registers one to five on the shock level meter. A quiet bearing is in this region also. A small spall (two square millimeters) may register 80 to 200. A bearing that has significant damage registers several thousand.

C.4 DIAGNOSTIC USES OF THE SHOCK PULSE INSTRUMENTATION

The Shock Pulse Meter is suitable for two categories of use:

1. Use by untrained personnel to measure shock level of bearings in situ and keep records of this data which indicate when a level change occurs that warrants bearing replacement. Unit simplicity and dependability suit it well for this task and it is in wide use in Europe for this task.

2. Use as a diagnostic tool to obtain readily interpreted shock emission profiles for bearing performance analysis.

Signal outputs from the unit are usable in two ways for diagnosis. First, the construction of a plot of shock rate versus shock level is a quite revealing measure of bearing condition. Three example curve shapes are shown in Figure C-4.

Curve A:

Existence of foreign particulate matter in the lubricant is diagnosed from a plot having high rates of very small shock levels but no shocks above a level of three to five.

Curve B:

A curve shape indicating very low rate of very high (hundreds or thousands) shock levels may indicate a dry bearing or rolling element damage.

Curve C:

A curve shape which starts to "fill out," having a significant rate of shocks from .5 to 50 or more, is indicative of damage. The spread in shock level with rate is illustrative of the fact that there is a spread of shock emission level with the way each individual rolling element encounters the damage or wear product.

Once the latter curve shape has been detected, the second diagnostic capability of the instrument may be employed.

Reproduced from
best available copy.

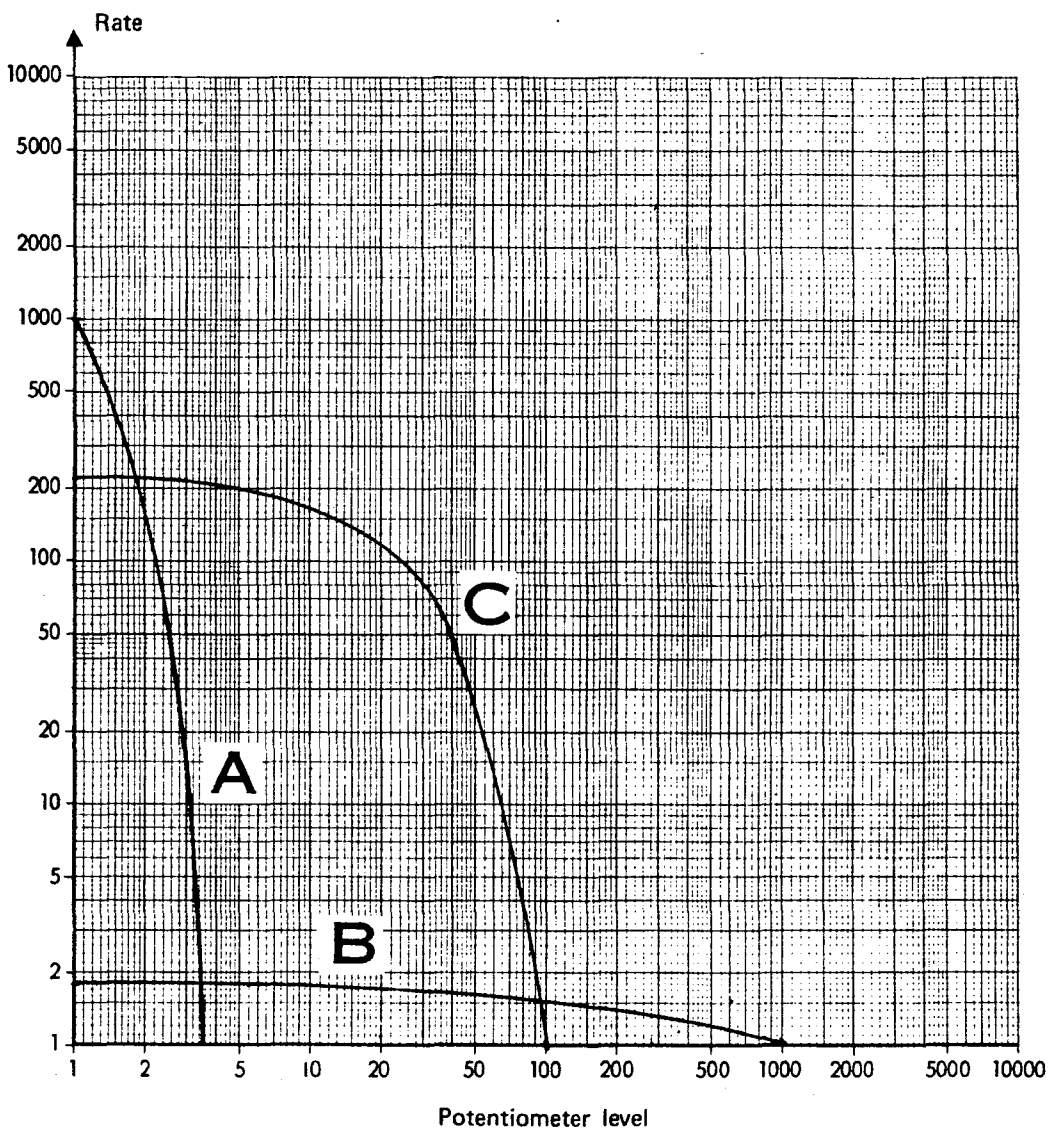


FIGURE C-4. SHOCK EMISSION PROFILE CURVE TYPES

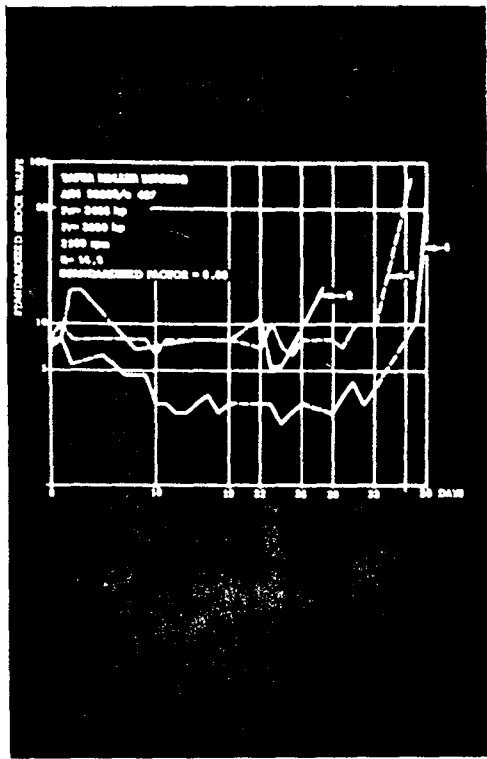
The display of level discriminated shock pulses on an oscilloscope in relation to one shaft revolution will aid in determining location of the most severe (or any other damage selected by level) damage. An inner ring damage will appear stationary with respect to the data frame as it will be encountered once for each passage through the predominate load zone. An outer ring damage will appear to move across the data frame at the inner/outer element relative rate. Rolling element damage will appear as periodic and unrelated to the data frame.

While the preceding illustrations are not meant to be all inclusive, they do attest to the superior capability of this instrument and the clarity of shock pulse signature relative to bearing condition.

Applications of this technique to a vast spectrum from paper mill bearings (450 sample points in one mill) to front wheel bearings have proven the capability for early detection and diagnosis of bearing damage.

Illustrative of this is the taper roller bearing test shown in Figure C-5. In this test the shock level was recorded by unskilled personnel over a period of 38 days of continuous operation. The points where shock level starts to increase markedly (Points of Inflection) give significant lead times notification of the occurrence of damage. On bearing number 6, a 3/4 x 1-mm spall was observed on the cone at six days after the point of inflection or 38 days running time. The shock level had risen from 3 (prior to inflection) to 60 during that six-day period.

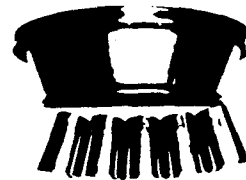
The other two bearings exhibited 4 to 5 days lead times to slightly larger damages on cone and rollers.



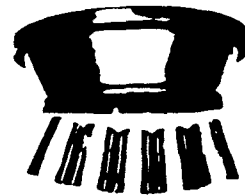
SHOCK LEVEL



STOP AFTER
38 DAYS



STOP AFTER
28 DAYS



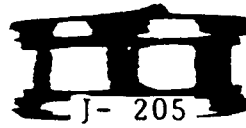
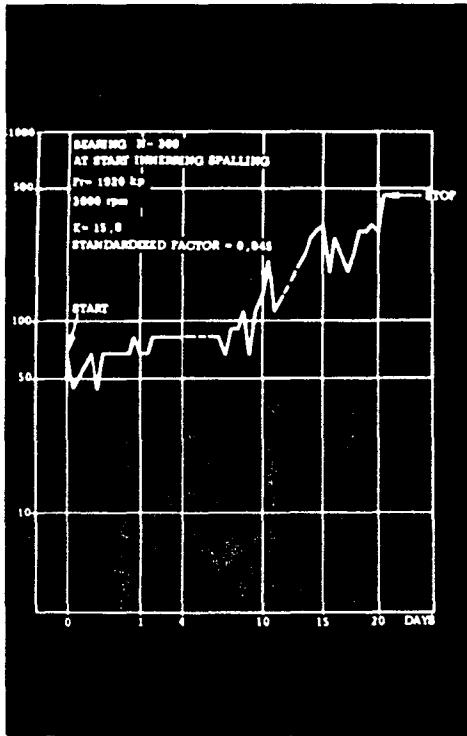
STOP AFTER
36 DAYS

FIGURE C-5. TAPER ROLLER BEARING SHOCK PULSE MEASUREMENT

Figure C-6 illustrates how the Shock Pulse Meter may be used to track the growth of bearing damage. In this test, unskilled personnel recorded the shock level of a cylindrical roller bearing over a period of 20 days. At the start of this test the bearing had, from previous testing, developed a 0.25-mm² spall on the inner element. This registered a shock level of 60 in this test. The shock level increased over the 20 day period to nearly 500 while the spalled area increased to approximately one-half of the inner race area.

Worthy of note is the fact that, while these data were hand recorded (because of the economics of the test), they may also be automatically recorded. A dc voltage proportional to shock level is available at the unit's recorder output connector. Thus, in applications where the economics indicate the desirability of continuous monitoring, the unit has the required output. This same output may be used for shock level limit monitor detection and sounding of an alarm when the present level is exceeded.

The further ability of the method to discriminate between bearings is made possible by the attenuation of shock level by the mechanical interfaces between the bearings. Illustrative of this is a spherical roller bearing test shown in Figure C-7 where a test bearing and a support bearing were located on a common shaft 10 in apart. Separate measurements on the respective bearing housings registered shock levels of 3 to 5 on the support bearing while the test bearing developed damage resulting in shock levels of 200. Thus, the method can discriminate the good bearing (three to five) in proximity to a damage bearing registering shocks nearly two orders of magnitude greater.



AT START



STOP AFTER
20 DAYS



SHOCK LEVEL

FIGURE C-6. SHOCK LEVEL MONITOR OF GROWTH OF DAMAGED AREA

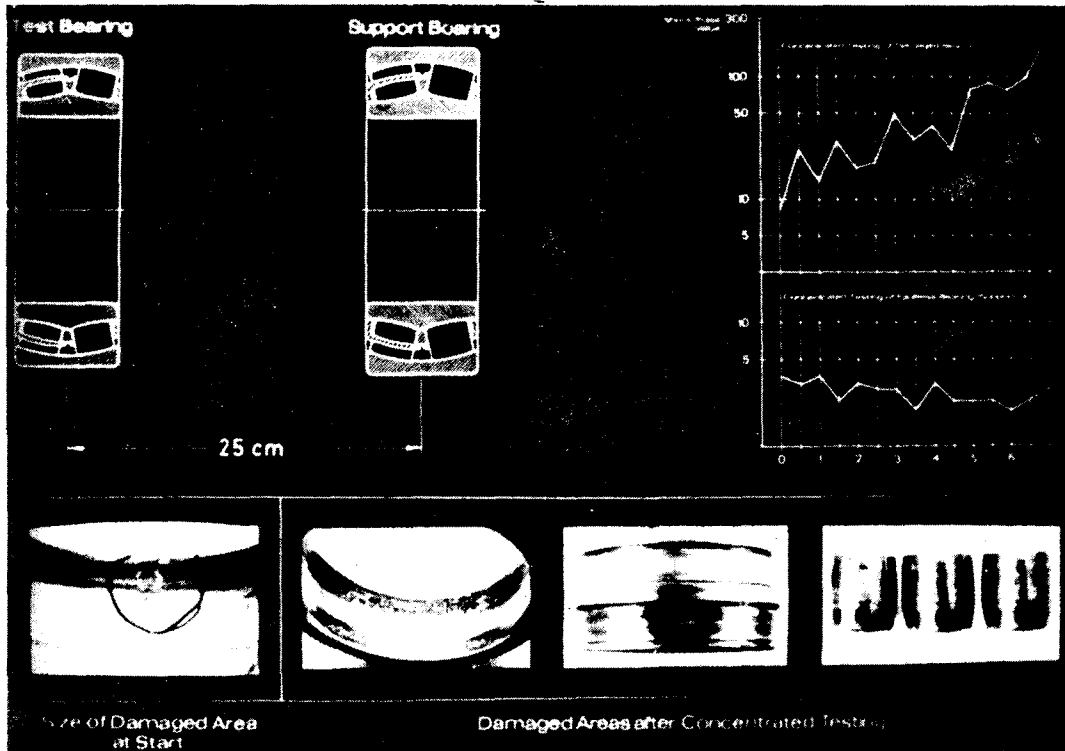


FIGURE C-7. SHOCK PULSE METER ABILITY TO DISTINGUISH SHOCK EMISSIONS OF ADJACENT BEARINGS

C.5 CONCLUSION

The shock pulse method of bearing condition assessment has a superior demonstrated capability to recognize clearly and quite early bearing damage which must propagate significantly to register a change in overall vibration of the bearing.

Note in Figure C-8 the clarity with which inner and outer element damaged bearings (Curve A and Curve B respectively) are discernable from an undamaged bearing (Curve AB) when using Shock Emission Profiles as the measure. The attendant vibration measurement (on the left) is shown for each bearing for comparison.

Reproduced from
best available copy.

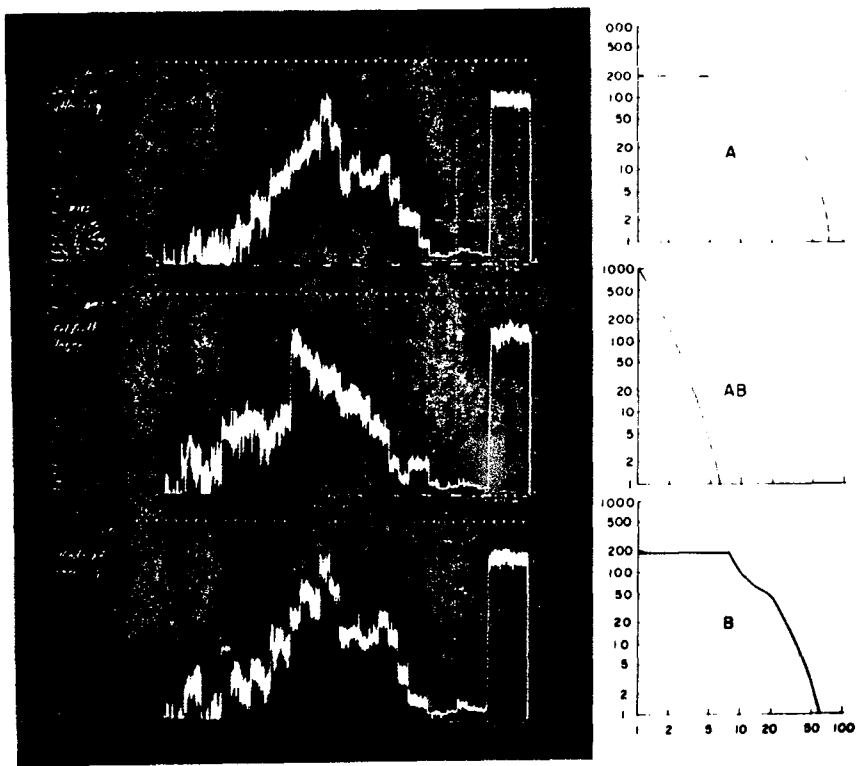


FIGURE C-8. BEARING CONDITION INDICATION BY SHOCK EMISSION AS COMPARED TO VIBRATION

APPENDIX D TEST PLAN FOR SHOCK PULSE BEARING DETECTION PROGRAM

D.1 INTRODUCTION

The object of this program is to evaluate the use of the shock pulse technique to diagnose early failure symptoms in railroad bearings. The capability of early detection of spalling, brinelling and debris-laden lubricant in railroad bearings using the shock pulse technique will be demonstrated during this test program.

D.2 TEST EQUIPMENT

The shock pulse principle of operation is that a damaged bearing in operation generates mechanical shocks at each encounter of a damaged surface with its contacting element. This causes short duration, sharp rise-time pulses of mechanical energy to emanate from the point of impact. The pulse of energy is governed in its travel by the speed of sound in the structural material, and not by the spring mass characteristics of the mounting structure. Therefore, no modeling is required as in vibration analysis systems. It is attenuated at each mechanical interface and decays in amplitude in proportion to the distance travelled and the damping characteristics of the material through which it is travelling. A resonant accelerometer is used as the pulse sensor and its output is fed into an amplifier tuned to the accelerometer's resonant frequency. After signal processing, the output may be analyzed in terms of shock pulse rate of occurrence and amplitude. From this analysis, it will be possible to deter-

mine a quantitative definition of bearing condition, in terms of bearing damage degree and also the extent of lubricant contamination.

A commercially available Shock Pulse Meter will be used as the shock pulse analyzer. The unit is a portable industrial (manually operated) unit consisting of a tuned amplifier and discriminator unit and an accelerometer with attaching cable. The accelerometer sensor will be attached to a railroad bearing adapter which will be in contact with the bearing outer ring load zone. Shock emission data will be compiled for undamaged and damaged bearings tested and summarized to indicate technique sensitivity to and detection threshold for damage.

To accomplish this testing, a test machine setup for railroad bearing testing, with slight modifications, will be employed along with 6 in. by 11 in. tapered railroad bearings. The bearings will be tested under an applied radial load of 1300 lbs. and at speeds of 10 and 20 miles per hour. The light bearing load represents the approximate weight of a railroad wheel set. This will most closely simulate testing in a wheel repair shop where this technique may ultimately be applied.

The railroad bearing test machine, as was shown in Figure 4-5 of the text, consists of two load carrying pillow blocks mounted on a casting frame. These pillow blocks support a rotating shaft which is driven by pulleys and belts from a motor. Both outboard shaft ends are machined and ground to 6 in. x 11 in. axle shaft bearing seat dimensions with the necessary axle cap bolt holes. Test bearings are mounted on the outboard ends of the shaft. Loads are applied to the test bearings using a load beam and yoke type arrangement coupled

coupled to a railroad bearing adapter which rests on the outer ring of the bearing.

The slight modification to the test machine for running these tests consisted of changing the load beam loading system to a dead weight system because of the light test loads.

Standard 6 in. x 11 in. railroad bearings will be used for testing. These bearings will consist of two new bearings and several acquired off-the-road failures. The new bearings will be used as a baseline test simulating unfailed bearings with clean grease. The off-the-road failures will consist of two levels of spalling severity on the rollers only, outer rings only and inner rings only, along with two bearings showing two severity levels of brinelling damage. Also, two bearings used previously for baseline testing will be utilized to detect contaminant in the grease.

D.3 TEST PROCEDURE

Initially, two new bearings will be tested to establish a baseline simulating unfailed bearings with noncontaminated grease. Secondly, a series of tests will be run on off-the-road failures consisting of two severities of spalling on the inner ring only, the rollers only and the outer ring only. A final test will be run consisting of two bearings with two different degrees of particulated contaminant in the grease lubricant. From this test bearing group, damage limits will be established.

The testing program and its monthly milestones are presented in Table D-1.

Data Format

Data from the Shock Pulse Meter will be accumulated for the five different test bearing groups. Each bearing will be tested at two different speeds.

Two different parameters are measurable manually with the Shock Pulse Meter. A peak sample and hold circuit in the meter provides continuous quantization and meter display of the peak impulse level for a given test. These levels will be recorded for each test. In addition, a "rate indicator mode" is available and will be utilized in these tests. In this mode, the front panel meter displays the occurrence rate (pulse/sec) of pulses greater in magnitude than a predetermined dialable level. Using this mode, a graph of shock rate vs shock level will be obtained and plotted for each test.

This is expected to provide a useful measure of bearing condition, since lubricant contamination, spalling, etc., have been easily detected using this technique for essentially similar applications.

TABLE D-1. SHOCK PULSE DAMAGE DETECTION TEST PROGRAM

		MONTHS		
		MARCH	APRIL	MAY
(1)	Baseline test - run 2 new bearings to established baseline simulating unfailed bearings with clean grease.	■		
(2)	Run 2 bearings with inner ring spalling:			
	(a) One bearing minimum failure		■	
	(b) One bearing moderate failure			
(3)	Run 2 bearings with roller spalling:			
	(a) One bearing minimum failure		■	
	(b) One bearing moderate failure			
(4)	Run 2 bearings with outer ring spalling:			
	(a) One bearing minimum failure			■
	(b) One bearing moderate failure		■	
(5)	Run 2 bearings with brinelling:			
	(a) One bearing moderate brinelling			■
	(b) One bearing heavy brinelling			
(6)	Run 2 bearings with particulate contaminant in the grease lubricant.			■

D-5/D-6

- NOTE: (1) Description of failed bearings from off-the-road
- (a). Minimum spalling failure - enough spalling to be removed from service. (2)
 - (b). Moderate spalling failure - approximately twice as much spalling as (a).
 - (c). Moderate brinelling - enough brinelling to be removed from service. (2)
 - (d). Heavy brinelling - possibly starting to show light spalling.
- (2) As Referenced in Association of American Railroad Roller Bearing Manual.
- (3) Test conditions: (a) Test machine modified railroad bearing tester.
 (b) Fr - 1300 lb, Fa = 0 lb
 (c) Speed - 10 and 20 miles/hour

APPENDIX E
GLOSSARY

1. Antenna Resistance - The power supplied to the entire antenna circuit divided by the square of the effective (RMS) antenna current referred to a specified point.
2. Clapp Oscillator - A Colpitts - type oscillator using a series-resonant tank circuit for improved stability.
3. Feedthrough capacitor - A feedthrough insulator that provides a desired value of capacitance between the feedthrough conductor and the metal chassis or panel through which the conductor is passing. Used chiefly for bypass purposes in VHF.
4. Heat pipe - A device used to transfer thermal energy from one point to another. It operates by transferral of energy absorbed by the evaporation of entrapped fluids at one end to its opposite end where the absorbed energy is given up via condensation.
5. Hybrid circuit - A circuit which combines the thin-film and semiconductor technologies. Generally, the passive components are made by the thin-film techniques, and the active components by semiconductor techniques.
6. Hybrid PI - The most useful high-frequency model of the transistor.
7. Radiation resistance - The power radiated by the antenna divided by the square of the effective (RMS) antenna current referred to a specific point.
8. Thermopile - A group of thermocouples connected in series.



APPENDIX F
REPORT OF NEW TECHNOLOGY

As a result of effort expended during performance of Contract DOT-TSC-935.

Invention and/or improvement Highlights

The feasibility of applying the following devices toward improvement of railroad safety has been established as a result of work reported herein:

1. An on-board temperature and strain sensing "Transmitter Bolt" for alerting a train crew in the event of overheating or loosening journal or roller bearings.

2. An on-board temperature sensing "Transmitter Bolt" for alerting a train crew in the event of overheating of journal roller bearings.

3. A maintenance level "Lubrication Detector" for avoiding overgreasing of roller journal bearings in a railroad "repair track."

4. A maintenance level "Shock Analyzer" for detecting certain physical damage to roller journal bearings in a railroad "wheel shop."

110 copies

Preceding page blank

F-1/F-2

B119

12